ASSESSMENT OF PORTLAND-LIMESTONE CEMENT FOR STRUCTURAL APPLICATIONS

A Ph.D. Thesis
Presented to
The Academic Faculty

by

Ahmad Shalan

In Partial Fulfillment
of the Requirements for the Degree
Doctor of Philosophy in the
School of Civil and Environmental Engineering

Georgia Institute of Technology
August 2019

ASSESSMENT OF LIMESTONE-PORTLAND CEMENT FOR STRUCTURAL APPLICATIONS

Approved by:

Dr. Lawrence Kahn, Advisor
School of Civil and Environmental Engineering
Georgia Institute of Technology

Dr. T. Russell Gentry
School of Architecture
Georgia Institute of Technology

Dr. David Scott
School of Civil and Environmental Engineering
Georgia Institute of Technology

Dr. Giovanni Loreto
College of Architecture and Construction Management
Kennesaw State University

Dr. Donald White
School of Civil and Environmental Engineering
Georgia Institute of Technology

Date Approved: May 14, 2019

ACKNOWLEDGEMENTS

This research was a large project and required a lot of time and energy to finish, and I could not have done it without the help and support of many people to whom I am deeply grateful.

I would like to begin by thanking my parents, Abdulkareem and Wafa', for their continuous support throughout my life. You always believed in me and that was a source of strength for me to stay resilient through the difficult times. Thank you for your love and support and I am eternally grateful to you.

I would like to thank my advisor, Dr. Lawrence Kahn for giving me the opportunity to work with him and for his guidance and patience with me. I enjoyed being your student and learning from an expert like yourself. I consider you one of the best educators I met, and I am proud of being your last doctoral student.

I would like to thank my committee, Dr. T. Russell Gentry, Dr. Giovanni Loreto, Dr. David Scott, and Dr. Donald White for their support and guidance. I enjoyed taking your classes and working with you. Thank you for checking my work and for your positivity.

I would like to thank Dr. Leigh Bottomley for her substantial support. Dr. Bottomley, your intervention was critical and was a main factor leading me to the finish line. Thank you very much for your support. I learned a lot from your wisdom and diplomacy in dealing with complications. I could not have done this without your help.

This research was funded by the Georgia Department of Transportation (GDOT) under projects numbers FHWA-GA-17-13-09 and FHWA-GA-17-1433. I would like to thank Supriya Kamatkar and the GDOT Office of Materials and Research for their assistance on this project. I would also like to thank Lehigh Hanson, Argos USA, LafargeHolcim, Cemex for providing us with cements used in this research. I would like to thank Gary Knight and Andy Chafin at the Heidelberg Cement Technology Center for giving me the opportunity to use their Auto Vicat apparatus.

I would like to thank the Fulbright program for awarding me with a scholarship during my PhD program. It was a great opportunity to meet the many intelligent people in this program and to try to build cultural bridges between Americans and my culture. I hope this program continues to grow and succeed in the future.

I would like to thank Dr. Mehdi Rashidi, Dr. Natalia Cardelino, Dr. Alvaro Paul, Dr. La Sasha Walker, and Prasanth Alapati for their assistance throughout my work in Mason building and in the structures lab. I appreciate your positivity and I wish you all the best in your future careers.

I would like to thank Jeremy Mitchell for helping me setup the many tests that I ran in the structures lab. Your practical experience was very useful for the successful completion of my experimental work. Thank you for your positivity and support.

I would like to thank Dr. Kari Watkins and Dr. Michael Rodgers for providing me with the opportunity to assist in teaching the Capstone Design class. Working with you was a pleasure and I enjoyed learning about the various projects that students work on. It was a great experience and I learned a lot.

I would like to thank Dr. James Mulholland for working with me to find solutions to problems that were affecting my progress. Thank you very much for your support which was very useful for the progress towards finishing my program. You are a problem solver and I deeply appreciate your support.

I would like to thank all the undergraduate students who also assisted in my experimental work. Special thanks to John (Zihao) Zhang and Matthew Rash who helped me at a time the physical work at the lab was very demanding and physically exhausting. I appreciate your dedication and intelligence. I wish you the best of luck in your future endeavors.

I would like to thank my siblings, Mona, Dua', Wala', and Mohammed for their love and support. I missed several years of living near you but I am proud to see the successful individuals that you are now.

I would also like to thank Jennifer Davis for her continuous support throughout my work. Thank you for believing in me, for helping me in my work, and for being the great person you are. I admire your intelligence and willingness to help others and I hope the future brings the best it can offer to you.

My PhD experience was not just an academic one, but it was also an experience full of life lessons. To whoever is undergoing difficult times during their PhD program: believe in yourself, do everything you can to succeed, search for help when needed, communicate with trustworthy people, gather opinions to find solutions, and most importantly, never quit. I thank everyone out there that rejects injustice and discrimination, and I hope that more people join this group.

TABLE OF CONTENTS

LIST OF TABLES

LIST OF FIGURES

LIST OF SYMBOLS AND ABBREVIATIONS

AASHTO	American Association of State Highway and Transportation Officials
ACI	American Concrete Institute
ASTM	American Society for Testing and Materials
CSA	Canadian Standards Association
DOT	Department of Transportation
DTG	Thermogravimetric derivative
EPA	United States Environmental Protection Agency
GDOT	Georgia Department of Transportation
pcf	Pound per cubic foot
PSA	Particle size analysis
QXRD	Quantitative X-ray diffraction
SCM	Supplementary cementitious material
SD	Standard deviation
TGA	Thermogravimetric analysis

Cement Chemistry Abbreviations

AFm	Alumina-ferrite-monosulfate
AFt	Alumina-ferrite-trisulfate
C_2S	Dicalcium silicate ($2CaO \cdot SiO_2$)
C_3A	Tricalcium aluminate ($3CaO \cdot Al_2O_3$)
C_3S	Tricalcium silicate ($3CaO \cdot SiO_2$)
C_4AF	Tetracalcium aluminoferrite ($4CaO \cdot Al_2O_3 \cdot Fe_2O_3$)
$C\overline{C}$	Calcium carbonate ($CaCO_3$)

CH	Calcium hydroxide ($Ca(OH)_2$)
C-S-H	Calcium-silicate-hydrate

Symbols

A_v	Area of shear reinforcement within a distance s (in^2)
d_b	Nominal strand dimeter (in.)
d_v	Effective shear depth (in.)
D_{10}	10th percentile particle diameter
$D_{3,2}$	Surface area-weighted mean particle size
$D_{4,3}$	Volume-weighted mean particle size
D_{50}	50th percentile particle diameter
D_{90}	90th percentile particle diameter
D_a	Apparent diffusion coefficient
E	Elastic modulus
L_d	Development length (in.)
f_c'	Concrete compressive strength (psi)
f_{ct}	Concrete splitting tensile strength (psi) in ACI 318-95
f_{pe}	effective stress in the prestressing steel after losses (ksi)
f_{pc}	Compressive stress in concrete (after allowance for all prestresss losses) at centroid of cross section resisting externally applied loads or at junction of web and flange when the centroid lies within the flange (ksi). In a composite member, f_{pc} is the resultant compressive stress at the centroid of the composite section, or at junction of web and flange, due to both prestresss and moments resisted by precast member acting alone.
f_{ps}	average stress in prestressing steel at the time for which the nominal resistance of the member is calculated (ksi)
f_{pu}	Tensile strength of prestressing strand

f_r concrete modulus of rupture

f_{sp} Concrete splitting tensile strength (psi) in ACI 363R-10 [1]

f_y Specified minimum yield strength of reinforcing bars (ksi);

L_d *Development length of prestressing strand (in.)*

L_t *Transfer length of prestressing strand (in.)*

M_{cre} Moment causing flexural cracking at section due to externally applied loads (kip-in)

M_{max} Maximum moment at section due to externally applied loads (kip-in)

s Spacing of transverse reinforcement measured in a direction parallel to the longitudinal reinforcement (in.)

SSA Specific surface area

SG Specific gravity

T Temperature

V_d Shear force at section due to unfactored dead load (kip)

V_i Shear force at section due to externally applied loads occurring simultaneously with M_{max} (kip)

w_c unit weight (pcf)

w/c Water-to-cement mass ratio

w/b Water-to-cementitious material mass ratio, where the "cementitious materials" includes the cement, limestone, and any supplementary cementitious materials

κ Multiplier for strand development length:

= 1.6 for pretensioned members with a depth greater 24 in.

= 1.0 for pretensioned members with a depth of less than or equal to 24.0 in.

SUMMARY

This research assessed the applicability of Type IL cements satisfying AASHTO M 240 specifications for use in structural applications in place of Type I/II cements which satisfy AASHTO M 85 specifications for construction of transportation structures. Type I/II and Type IL cements from five producers were investigated where Type IL cements included up to 15% calcite by mass. The cements and both mortars and concretes made with these cements were studied to determine material properties including setting time and hydration kinetics; mechanical properties including strength development, elastic modulus, and tensile strength; dimensional stability properties including drying shrinkage and creep; and structural properties for precast prestressed concrete including Mostafa strand pull-out strength, transfer length, development length, and beam flexural strength. The results showed that the performance of concrete made with Type IL cement was primarily affected by the cement fineness which increased strength and drying shrinkage. The structural properties of concrete made with Type IL cement showed similar performance to concrete made with Type I/II cement. Type IL cement may be used in place of Type I/II cement when fineness values are specified.

CHAPTER 1: INTRODUCTION

This research investigated the use of Type IL cement as a replacement of Type I/II cement in concretes for structural applications. Five cement producers provided Type I/II and Type IL cements. Concretes were produced from each cement source and samples were tested for mechanical properties, durability properties, and dimensional stability properties. Prestressed concrete structural properties were also investigated where 30-ft long beams were produced and tested.

Blending cements with limestone filler is becoming a more common practice. Cement production is the most energy intensive part of concrete production. Blending cement with limestone filler reduces the amount of cement used in concrete and therefore lowers the cost and the carbon footprint of concrete production. Concrete with low water/binder ratio (*w/b*) (such as high performance concrete) contain unhydrated cement that can reach 35% by mass [2]. The unhydrated cement acts as unreacted filler which is wasteful. Therefore, the unhydrated cement may be replaced with limestone filler which is less costly and much lower energy intensive. However, the effects of blending cement with limestone changes the hydration of cement, the mechanical properties (such as compressive strength), and durability of concrete [3]. The effect varies with different clinker chemical composition, limestone chemical composition, limestone fineness and size distribution, curing method, sulfates and chlorides presence, and temperature [4].

Several of countries in Europe permitted blending limestone with portland cement. It was reported that Heidelberg Cement produced cements with up to 20% limestone

since 1965 [4]. Limestone blended portland cement up to 10% was allowed by the Spanish standards since 1960 and was raised to 35% in 1975 [5]. French standards permitted up to 35% limestone in 1979 [5].

The European standard EN 197-1 [6] allows Portland cement (CEM I) to contain up to 5% of other minor constituents such as limestone. The standard also contains specifications for several blends of Portland-limestone cement with 6% to 20% limestone (for CEM II/A-L and CEM II/A-LL) and 21% to 35% limestone (for CEM II/B-L and CEM II/B-L) as well as specifications on limestone quality.

Canadian standards permitted the use of limestone in Portland cement since the 1980s. CSA A3001-08 [7] permits 5% to 15% limestone in Portland-limestone cement and may be used for general use (GUL), moderate heat of hydration (MHL), high early strength (HEL) and low heat of hydration (LHL).

In the United States, ASTM C150 (2004) [8] and AASHTO M85 (2009) [9] allow up to 5% limestone in Portland cement. The limestone must contain at least 70% by mass calcium carbonate. In 2012, ASTM C595 [10] and AASHTO M240 permit 5% to 15% limestone.

1.1 Purpose and objectives

Using higher percentages by mass of limestone in Portland-limestone cements could lower the cost of production and the carbon footprint. As discussed in the background, past research results indicated that limestone filler effects on cement were of physical nature such as better grading and decreased permeability while others argued

that limestone filler had chemical effects on the properties of cement. Research findings have some contradicting recommendations on the optimum limits of limestone content. The optimum amounts must consider mechanical as well as durability properties in the resulting concrete.

The purpose of this research was to investigate the effect of increased limestone replacement up to 15% by mass in Type IL cement on the performance of concrete for structural applications, particularly bridge components. The objectives included assessment of key material properties such as particle size analysis, phase analysis, hydration kinetics, strength development, drying shrinkage, and creep. The final objective was to assess the structural performance of concrete made with Type IL cement compared to those made with Type I/II cement. Full-scale prestressed beams were constructed and tested to determine prestress losses, prestressing strand bond, transfer length, development length, and flexural strength. These properties were compared with AASHTO LRFD bridge design standards.

The specific objectives were:

1. Compare Type IL cements from several regional producers in terms of the particle size analysis and chemical composition.
2. Examine the effect of the limestone content on properties such as setting time, concrete mechanical properties, and dimensional stability.

3. Examine the effect of temperature on properties such as hydration kinetics, setting time, concrete mechanical properties, and dimensional stability when using Type IL cement.
4. Examine the effect of water/binder ratio and cement factor on concrete mechanical and durability properties when using Type IL cement.
5. Examine the effect of combining Type IL cement with supplementary cementitious materials such as fly ash (15% replacement) and slag (50% replacement) on properties such as hydration kinetics, setting time, concrete mechanical properties, and dimensional stability.
6. Assess and compare the structural properties of concrete made with Type IL cement to concrete made with Type I/II cement.

1.2 Research motivation

As shown in Figure 1.1, portland cement production contributes to about 5% of anthropogenic CO_2 emissions each year [11]. About half the emitted CO_2 from cement production is due to the conversion of the raw materials (calcination) while the other half is due to fuel combustion [12]. Figure 1.2 shows that cement production increased 67 times since 1926 [13]. Global trends in cement production are expected to continue to increase in the future [14], which in return would increase CO_2 emissions.

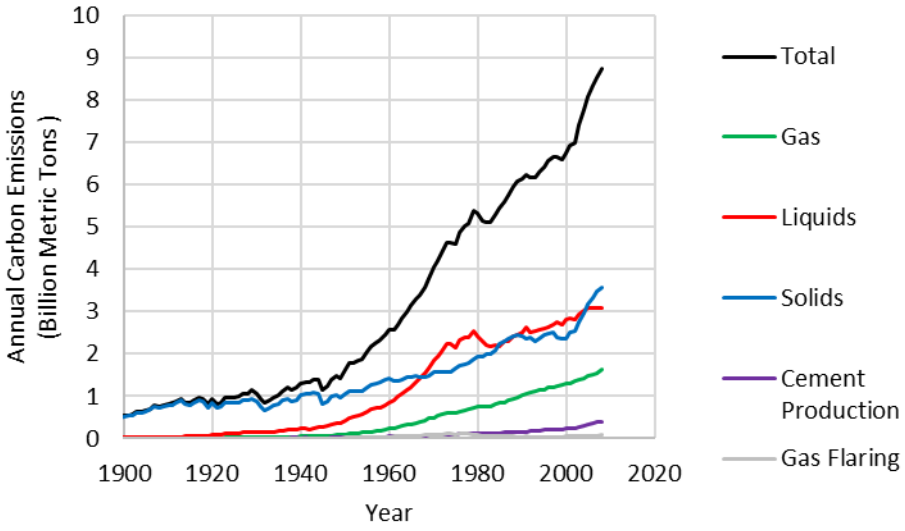

Figure 1.1: Annual Global Fossil-Fuel Carbon Emissions [11]

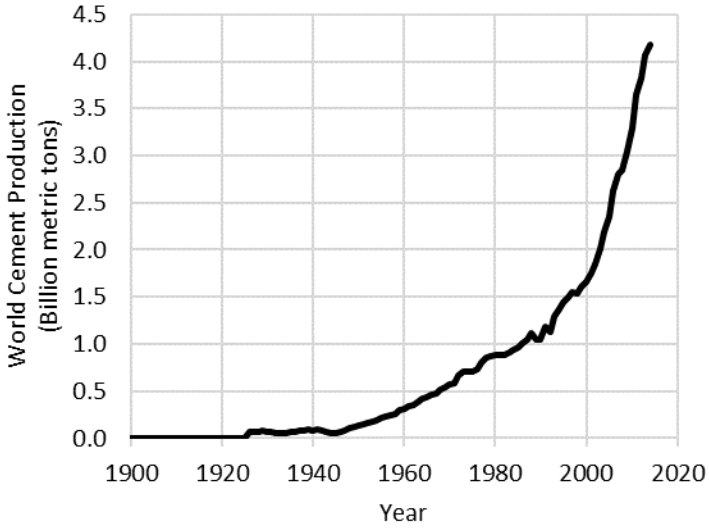

Figure 1.2: World cement production over time [13]

Solutions are needed to reduce the carbon wastes for improved environmental quality. Some of the solutions available to the cement industry are energy efficiency improvement, replacing high-carbon fuels with low-carbon fuels, blended cements, and

removing carbon dioxide from the atmosphere [12]. These solutions affect the carbon intensity of carbon emissions in cement production. Figure 1.3 shows the carbon intensity of cement production in different regions. Even though China is the largest carbon emitter (in total amount), India has the largest carbon emissions per ton of cement (253 kg Carbon/ton), followed by North America (242 kg Carbon/ton), and then China (240 kg Carbon/ton); while western Europe has the lowest carbon emissions per ton of cement [12].

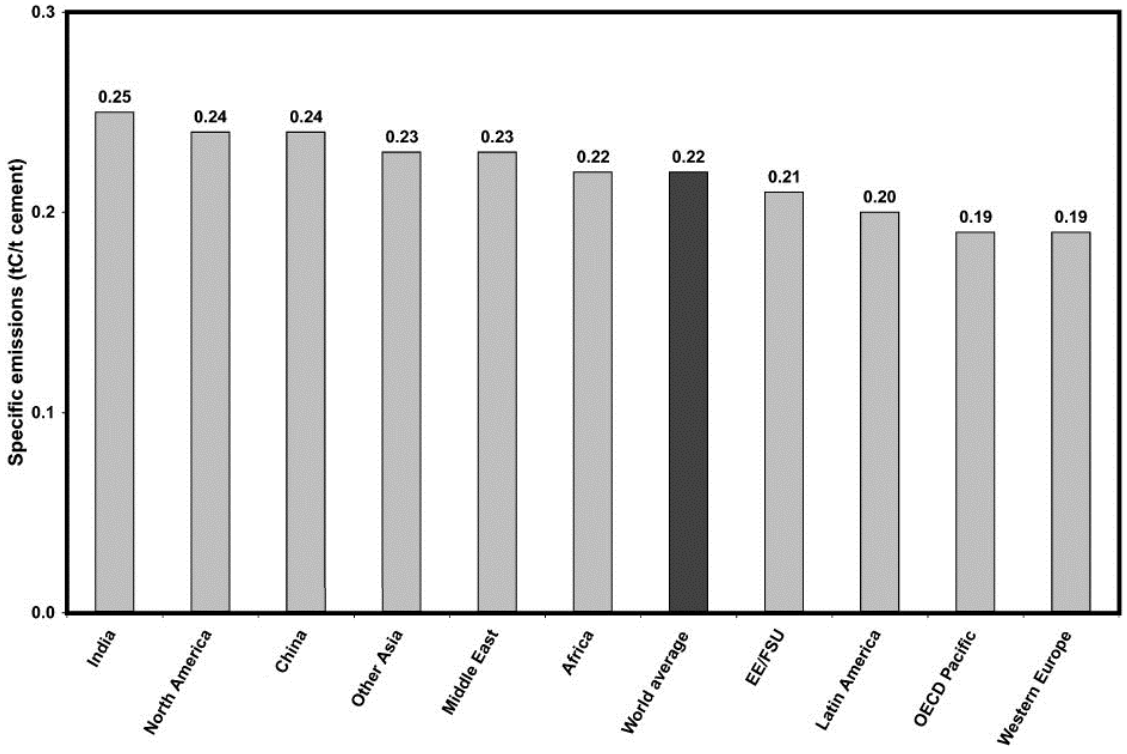

Figure 1.3: Carbon intensity of cement production in different regions (tons of carbon per tons of cement)
[12].

In cement production, clinker manufacturing is the most energy-intensive process, and, therefore, the largest source of CO_2 emissions. In blended cements, a portion of the clinker is replaced with other products that have a lower carbon footprint such as limestone. Replacing part of the clinker portion of cement with a more sustainable material would therefore reduce the embodied energy in cement. Limestone is a widely available raw material of low cost and low energy-demand to collect. In this research, limestone-blended portland cement, with clinker replacement by limestone of up to 15% (by mass), was investigated and assessed for use in structural applications.

1.3 Scope

This research investigated eleven cements, portland Type I/II and Type IL cements with up to 15% interground limestone from five producers.

Material studies included investigation of curing at standard, room temperature conditions (73°F), curing at low temperature conditions (40 ºF) to simulate cold weather conditions, curing at high temperature conditions (90 ºF) to simulate hot weather conditions, and curing at elevated temperature (140 °F) to simulate steam curing conditions used for some precast concrete bridge girders.

Two 30-ft long rectangular beams each were constructed using concrete made with Type I/II cement and using Type IL cement. The four beams were tested to compare strand transfer and development length as well as beam flexural strength between the two types of concretes.

CHAPTER 2: LITERATURE REVIEW

2.1 Introduction

Limestone replacement in portland cement has been used since the 1960's. The effect on cement hydration can be advantageous or disadvantageous depending on the amount of replacement, the quality of the limestone, the quality of the clinker, fineness, and the method of curing. Some researchers optimized the replacement so that the effect can be negligible when compared to unblended portland cement. In summary, adding limestone filler increased workability and reduced water demand, but it can be detrimental when high slump values are required. Higher limestone replacement increased the susceptibility to thaumasite formation of sulfate attack and rebar corrosion, however that depended on the permeability which can be mitigated by particle size distribution as well as curing method which can passivate the rebars. Optimum amount of limestone replacement should be determined based on the required use and environmental conditions.

2.2 Influence of limestone on the hydration of portland cements

Limestone filler was initially thought of an inert filler and an expert committee appointed by the Norwegian government in 1948 concluded that "nothing in the test data indicates that any chemical reaction takes place between the cement paste and calcite" [15]. The assumption that limestone was an inert filler that has no influence on cement hydration needed to be investigated. Feldman et al. [16] indicated that calcium carbonate interacted with C_3A and affected its hydration. The results showed that adding $CaCO_3$

suppresses the hydration reaction of C_3A (depending on the percentage) and that is due to the formation of low form of calcium carboaluminate on the surface of the C_3A grains. A study of the reaction at 50% humidity led to the conclusion that C_3A reacts with $CaCO_3$ by a direct or solid-state direct mechanism where the solid reactants are converted to solid products without the going into intermediate solution mixing. Only one or two molecular layers of water are absorbed to the solid surface. The choice of 50% humidity rather than 100% was to rule out the solution mechanism. Figure 2.1 shows the rapid expansion of C_3A and C_3A-$CaCO_3$ exposed to 50% relative humidity.

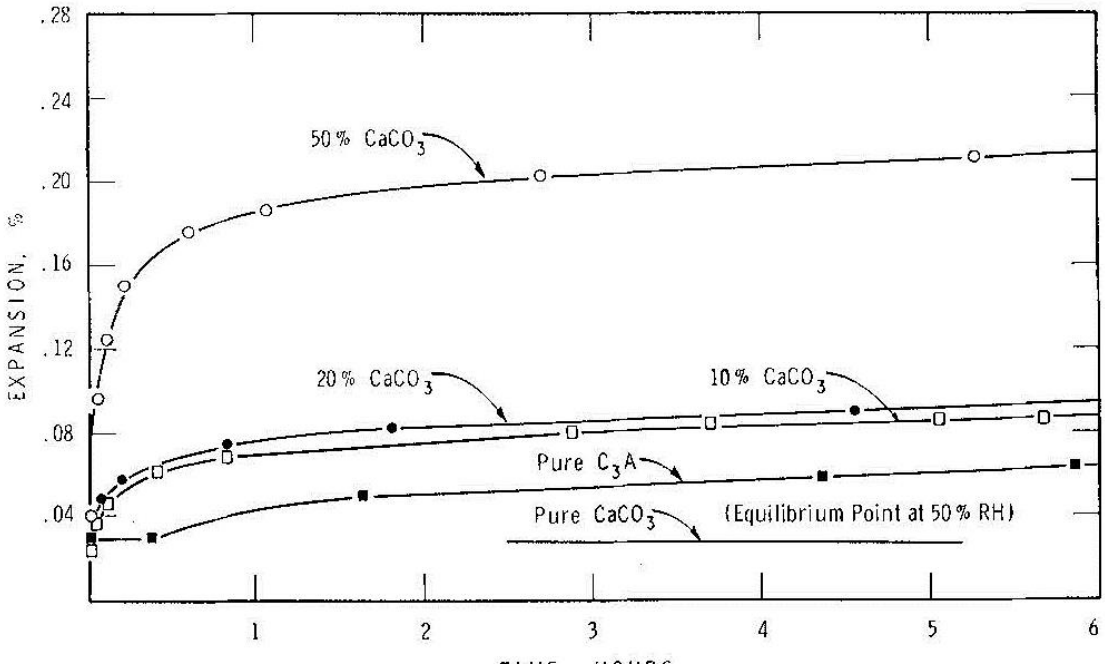

Figure 2.1: Expansion of C_3A and C_3A-$CaCO_3$ mixtures on exposure to 50% relative humidity [16]

Soroka and Stern [15] found that calcareous fillers affected the compressive strength due to accelerated hydration. Using calcareous filler provided similar results of

compressive strength regardless of the specific chemical composition of the fillers which lead to the conclusion that the fillers effect was only related to accelerated rate on cement hydration. Experimental results suggested the formation of calcium carboaluminate, however, it was concluded that it had a negligible effect the compressive strength. Soroka and Setter [17] indicated that as the limestone became finer, it has a larger influence on the hydration reactions of portland cement regarding degree of hydration and the gel/(space + air) ratio, (Table 2.1).

Table 2.1: Effect of 30% limestone filler on degree of hydration and Gel/(space + air) ratio [17]

Age, Days	Property	Reference Mortar (No Filler)	Fineness of Filler Specific surface - sq.cm per g			
			1,150	3,600	6,700	10,300
3	Combined water, per cent	8.52	9.12	9.66	10.26	9.95
	Degree of hydration	0.371	0.397	0.420	0.477	0.388
	Air content, lit. per cu.m	28	24	18	13	7
	Gel/(space + air) ratio	0.273	0.293	0.311	0.331	0.299
	Compr.strength, kg per sq.cm	121	136	151	172	180
7	Combined water, per cent	10.15	11.08	11.10	11.44	10.98
	Degree of hydration	0.441	0.481	0.485	0.497	0.477
	Air content, lit. per cu.m	28	24	18	13	7
	Gel/(space + air) ratio	0.317	0.345	0.351	0.362	0.356
	Compr.strength, kg per sq.cm	164	196	204	238	245
28	Combined water, per cent	13.38	13.92	13.57	14.40	13.02
	Degree of hydration	0.582	0.605	0.590	0.626	0.566
	Air content, lit. per cu.m	28	24	18	13	17
	Gel/(space + air) ratio	0.398	0.415	0.412	0.436	0.409
	Compr.strength, kg per sq.cm	245	285	296	335	341

On the other hand, Matschei at al. [18] indicated that calcite reacts to form several carboaluminate phases and that the sulfate content in the paste affects the limestone reactivity. Figure 2.2 shows the phase equilibrium of limestone in cement paste.

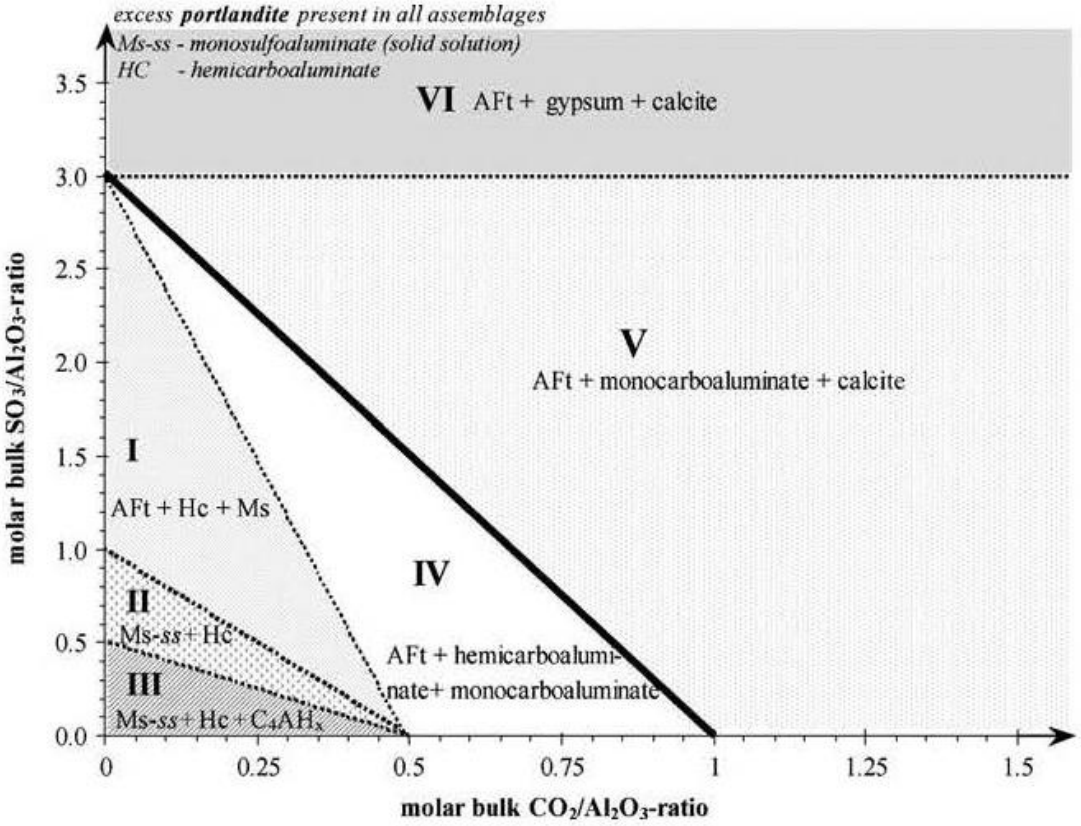

Figure 2.2: Phase equilibrium of limestone in cement paste [18]

Lothenbach et al. [19] investigated the effect of blending 4% limestone with portland cement on the hydration reactions of portland cements. They used that low value of limestone filler to limit the negative effects on concrete properties such as compressive strength, drying shrinkage, durability (with respect to sulfate attack, chloride attack, and carbonation), freeze and thaw behavior, and ASR; when more than 5% filler is used as

reported by Hawkins et al. [3]. Experimental results were compared to those of thermodynamic models coupled with kinetic equations of clinker dissolution as a function of time. The model provided detailed explanation on the formation of hydrates with and without the addition of limestone filler. The model showed similar phases with and without limestone filler for the first week of hydration. Then, the stable phase assemblages varied considerably. Significantly more ettringite was predicted with limestone filler. Also, in the presence of limestone filler, monocarbonate rather than monosulfate was stable during hydration. The predicted volume of hydrating cement was slightly higher with limestone filler leading to less porosity. Regarding the pore solution, the model predicted lower aluminum and higher sulfate and carbonate concentrations for specimens with limestone filler since ettringite and monocarbonate were calculated to be present.

Limestone accelerates hydration by providing nucleating sites [19]. However, the total amount of heat evolved does not vary, assuming same amount of cement was hydrated. Comparing experimental results with modeled results (thermodynamic modeling coupled with kinetic equations) explained the dominating processes of cement hydration.

Ramachandran [20] compared hydrated cements components with limestone filler of 5% to 50% and analyzed their chemical composition. He concluded that $CaCO_3$ was incorporated in the C-S-H phase of C_3S and that ettringite transformation was not affected. However, Kakali et al. [21] tested specimens containing 0% to 35% limestone filler and found that the transformation of ettringite to monosulfate was delayed in the

presence of limestone filler and that calcium aluminate monocarbonate formation was favorable to monosulfate formation. Ramachandran [20] relied on thermal analysis while Kakali et al. [21] performed XRD analysis which is more accurate. The conclusion that limestone filler presence affects ettringite transformation is more accurate.

However, Figure 2.3 shows that the expansion of cement mortar with dolomitic limestone was lower than cement mortar with calcitic limestone at lower C_3A content (7.54%) leading to the conclusion that dolomitic limestone has lower reactivity than calcitic limestone with clinker having lower C_3A content, but negligible difference was observed with clinker having higher C_3A content (11.74%). They also found that although portland-limestone was finer than unblended cement, the water demand (quantity of water required to prepare cement paste of standard consistency) was lower by about 25% when using 10% limestone and that cement with lower C_3A had higher water demand.

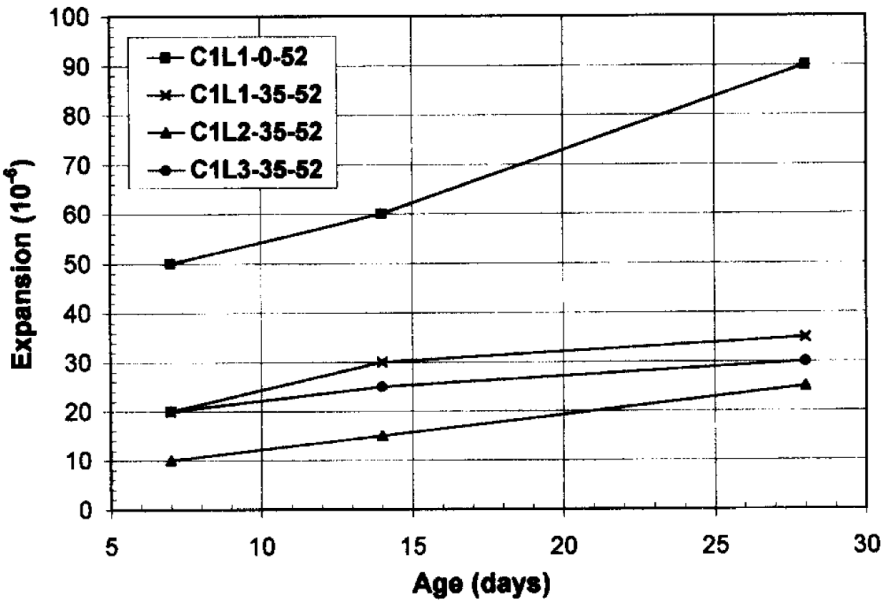

Figure 2.3: Linear expansion of cement mortar made from clinker with lower C_3A (7.54%) in relation to the curing age and the limestone quality (L1: high calcite, L2: high dolomite, L3: high quartz/clay) [22]

Carbonate source may be limestone and/or dolomite filler. It can be of coarse or fine size, and of different percentages of replacement of cement. Nocun´-Wczelik et al. [23] performed calorimetry to evaluate the heat evolution of specimens with various carbonate sources and fineness. They also found the conductivity of the hydration suspension, and rheological properties as functions of time. They concluded that using fine carbonate additives increases the rate of hydration (nucleation) and adds an additional peak on the calorimetric curve (Figure 2.4) due to the formation of calcium aluminate hydrate phase and calcium carboaluminate. Dolomite filler gives similar heat evolution curves as coarse limestone, but dolomite better enhances early hydration product precipitation. Using coarse limestone reduces the chemical shrinkage to values similar to samples made from unblended cement. Higher percentage addition of fine limestone causes higher chemical shrinkage but is limited by diffusion control. Carbonate

filler changes the rheological properties of the paste where it increases yield stress, plastic viscosity, and thixotropy (in the case of using dolomite, Table 2.2). Strong thixotropy of pastes when using dolomite filler can be beneficial in geotechnical applications. Regarding volume stability, shrinkage decreased with higher limestone content (Table 2.3). However, Figure 2.5 shows that using coarse limestone filler (1500 cm^2/g) lead to lower shrinkage than using fine limestone filler (14500 cm^2/g).

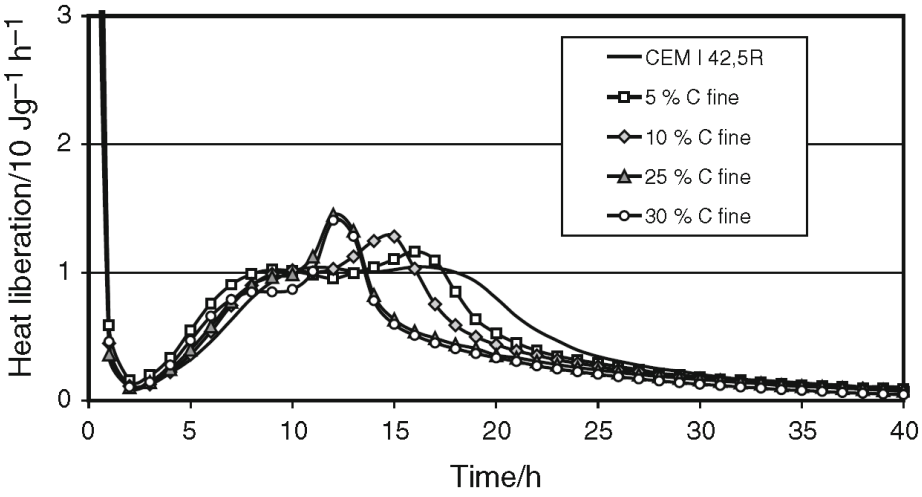

Figure 2.4: Heat evolution of cement with fine limestone powder additive [23]

Table 2.2: Rheological parameters of hydrating cement–dolomite pastes [23]

Samples	*w/c*	η/Pa s	T_y/Pa	T_{max}/Pa
CEM I 42,5R	0.4	5.4	11.8	16.1
CEM I + 5 % $CaMg[CO_3]_2$	0.4	13.4	42.7	68.9
CEM I + 20 % $CaMg[CO_3]_2$	0.4	16.5	45.1	71.5

η viscosity, T_y yield stress, T_{max} rigidity of thixotropic structure

Table 2.3: Creep and Shrinkage Results for Concrete with *w/b* = 0.60 after 90 days [24]

	Limestone Content,%				
	0	15	25	35	45
Cube strength (MPa)	41.0	36.5	30.5	23.5	17.0
Creep (μm/m)	790	780	775	770	760
Drying shrinkage (μm/m)	680	630	605	590	575

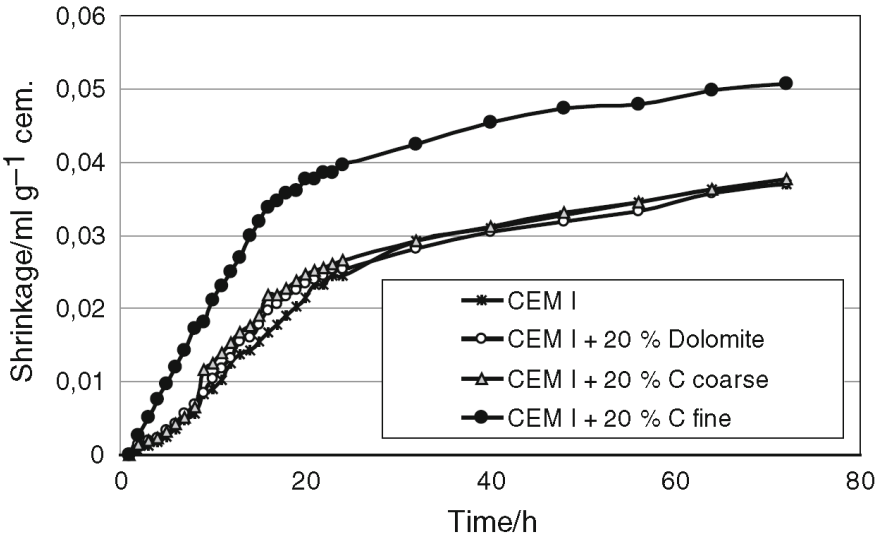

Figure 2.5: Chemical shrinkage of pastes [23]

Bonavetti et al. [2] studied the effect of using up to 20% limestone filler in low *w/b* concrete. The use of filler and finer clinker (due to intergrinding process) leads to higher hydration at early ages and to higher early strength. When using 0.5 *w/b*, the degree of hydration is similar between unblended cements and blended cements of 10% and 20% limestone. Since lower *w/b* leads to higher unhydrated cement, the max allowable percentage of filler increases with lower *w/b* to obtain similar volume of hydration products (i.e. similar quality which is related to gel-space ratio). For example, it is possible to use 15% filler for typical high-performance-concrete with 0.3 to 0.35 *w/b*, but only 5% for typical concrete with 0.50 *w/b* (Figure 2.6).

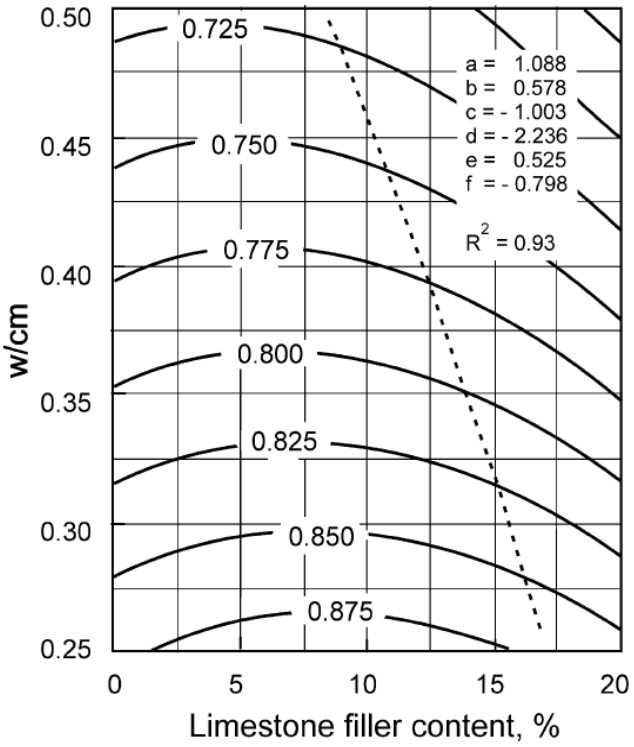

Figure 2.6: Influence of limestone filler content and *w/b* on the gel–space ratio of cement paste at 28 days [2]

In summary, the above findings agree on the fact that the presence of limestone affects hydration of cement especially in accelerating the rate of hydration as well as the fact that limestone reacts with C_3A to form carboaluminates. The difference in opinion on the effect on properties of concrete arise from the difference in the calcium carbonate source (calcite or dolomite), quality (% $CaCO_3$), size distribution, method of mixing (blending vs. intergrinding), and C_3A content of the clinker.

2.3 Setting time

Setting time was lower for all samples containing limestone filler when compared to unblended samples [23]. However, El-Didamony et al. [25] found that the setting time was higher with 5% limestone and got lower with higher filler content when compared to unblended cement (Figure 2.7). The difference in values when compared to those of Tsivilis et al. is most probably from the fact that different fineness that El-Didamony et al. used (3000 ±50 cm^2/g) compared to that of Tsivilis et al. (3800 to 4300 cm^2/g). Other factors may include the C_3A content of clinker and the chemical composition of limestone (high calcite, dolomite, or quartz/clay).

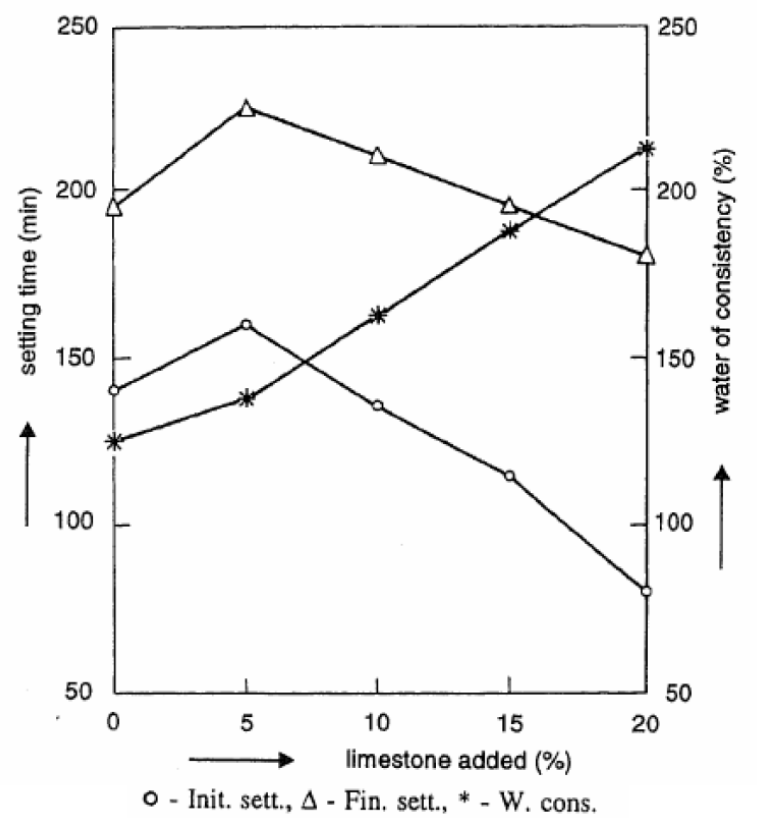

Figure 2.7: Setting time and water demand of portland-limestone cement pastes [25]

2.4 Mechanical properties

Tsivilis et al. [22] compared the compressive strength of pure samples with ones having limestone filler content ranging from 5% to 35% and interground to varying fineness with clinker of two chemical compositions (Figure 2.8).

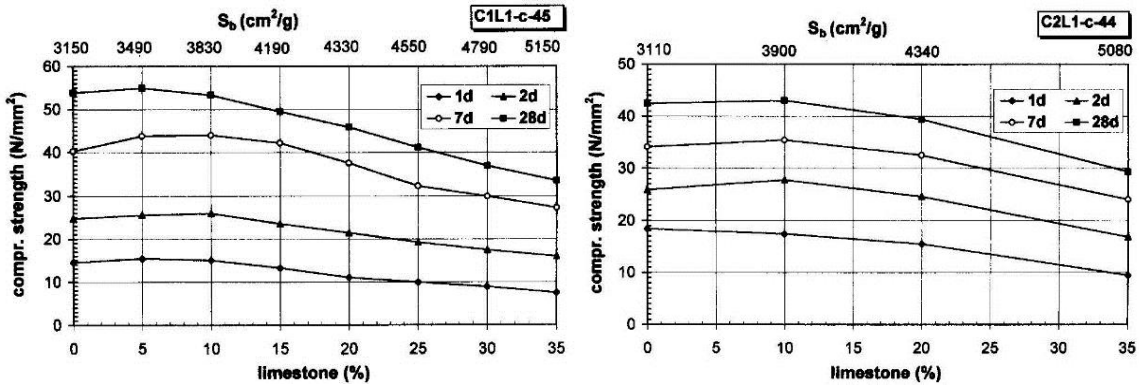

A) C_3S=65%, C_2S=13%, C_3A=8%, C_4AF=11%

B) C_3S=58%, C_2S=19%, C_3A=12%, C_4AF=6%

Figure 2.8: Influence of limestone content on strength development [22]

The results showed that limestone was more reactive with clinker having higher C_3A content, and that fineness has an optimum value to produce higher compressive strength.

Hydrated cementing materials content in concrete depends on cement content and the degree of hydration. Compressive strength of concrete with filler is less at later stages than concrete without filler since less hydrated cementing materials are produced and higher effective *w/b* due to cement replacement with filler (Figure 2.9). Gel-space ratio measures the combined effects of addition of limestone: acceleration of hydration, dilution, and higher effective *w/b*. the higher the gel-space ratio, the higher the

compressive strength of the concrete (Figure 2.10). Optimum value of limestone filler content can be estimated using the gel-space ratio concept.

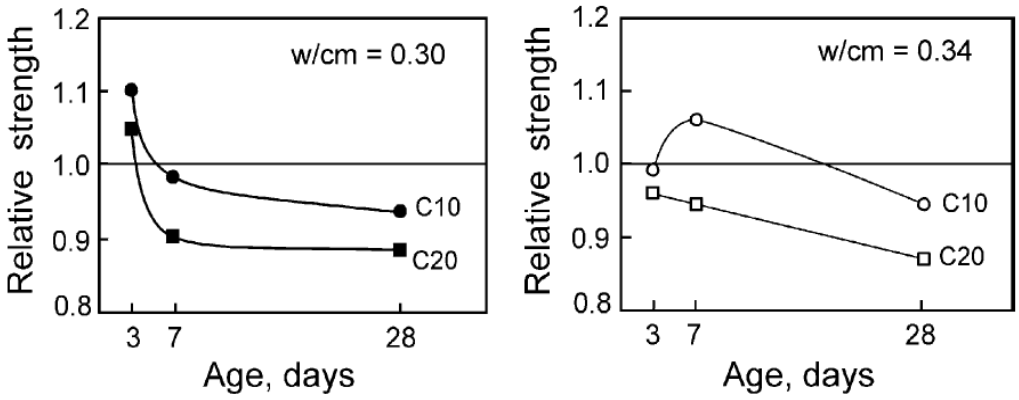

Figure 2.9: Relative compressive strength of concrete [2]

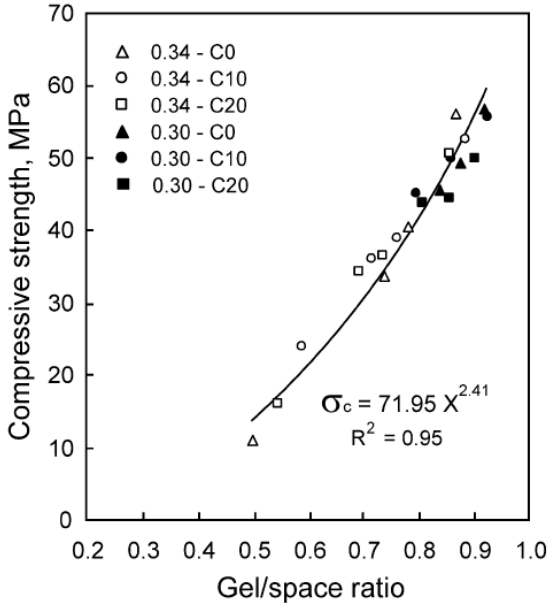

Figure 2.10: Compressive strength of concrete as function of the gel/space ratio (Bonavetti et al, 2003) [2]

2.5 Drying shrinkage and creep

Dhir et al. [24] measured the effect of increasing limestone content from 0% to 45% on the creep and drying shrinkage of concrete. They found that the higher the limestone content, the lower the creep and the drying shrinkage as shown in Table 2.4. The creep results were within the precision of the test and therefore the effect of limestone filler was negligible. They concluded that both properties depend on the restraining effects of aggregates and that the limestone filler resulted in similar or reduced volume when compared to portland cement.

Table 2.4: Comparison of 90 day deformation properties of concrete made with portland cement and limestone-blended portland cement [24]

Property	Concrete type				
	PC	PLC			
		LS15	LS25	LS35	LS45
Cube strength[a], N/mm^2	41.0	36.5	30.5	23.5	17.0
Creep[b], $\times 10^{-6}$	790	780	775	770	760
Drying shrinkage[c], $\times 10^{-6}$	680	630	605	590	575

[a]28 days, 20°C water cured

[b]Creep loading at 28 days, $0.40f_{cu}$

[c]Shrinkage at 20°C, 55% RH

Adams et al. [26] discussed the effect of limestone on the drying shrinkage of cement mortar. They concluded that drying shrinkage increased as the surface area (fineness increased). They also recommended that shrinkage had a better correlation Southwestern fineness factor (SFF) than with Blaine surface area, where the SFF is the ratio of the Blaine surface area (m^2/kg) to the percent passing No. 325 sieve. The SFF

ratio gives a bigger contribution to the very fine fraction which has a significant effect on shrinkage.

Bentz et al. [27] conducted restrained shrinkage tests on mortar rings made with cements without limestone and with cements with 10% limestone that was ground at three fineness levels (fine, intermediate, and coarse). The results, shown in FFF, showed that finer limestone resulted in higher tensile stresses due to shrinkage than the coarsest limestone.

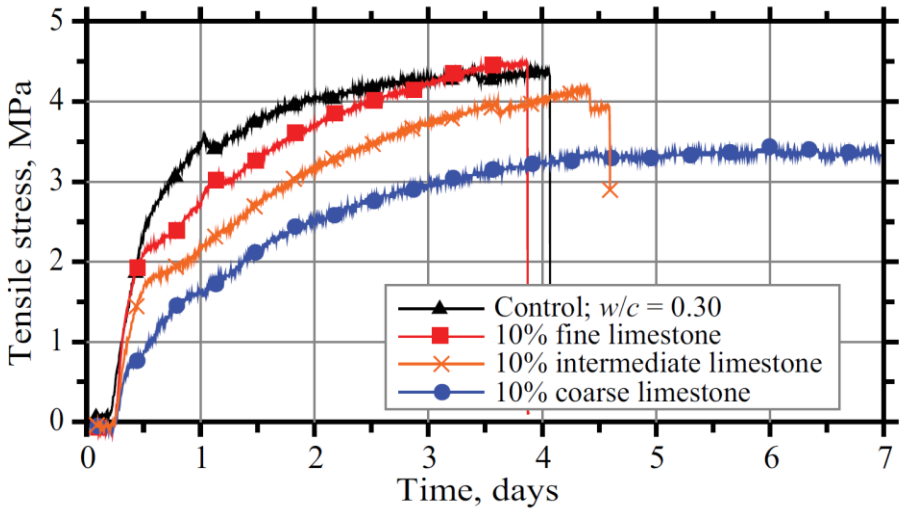

Figure 2.11: Stress development versus time of plain mortar rings and mortar rings containing 10% replacement by mass of different fineness limestone powders [27].

Alunno-Rosseti and Curcio [28] compared drying shrinkage of concretes made with cements with and without 20% limestone from two plant sources. Their results showed increased shrinkage with higher cement content but the difference between concretes made with and without limestone was negligible (Table 2.5).

Table 2.5: One-Year Drying Shrinkage (UNI Standard 6555) of Concretes Made With Cements With or Without 20% Limestone [28]

	Plant B				Plant G			
Cement content, kg/m^3	270		330		270		330	
Limestone content of cement, % by mass	0	20	0	20	0	20	0	20
Shrinkage, μm/m	635	640	680	690	540	560	615	595

Detwiler [29] measured the drying shrinkage according to ASTM C157 [30] of concrete made without and with 2.5% limestone, as well as mixes with Class C fly ash. The results showed that 2.5% limestone did not affect the shrinkage of mixes with or without fly ash (Table 2.6).

Table 2.6: Drying shrinkage (ASTM C157 [30]) of concrete mixes with and without 2.5% limestone and with and without Class C fly ash [29]

Mix	4 days	7 days	14 days	28 days	8 weeks	16 weeks	32 weeks
Type I (control)	0.002	0.009	0.015	0.025	0.039	0.044	0.049
LS	0.003	0.008	0.017	0.025	0.038	0.046	0.051
Type I with 15% C-ash	0.004	0.019	0.019	0.02	0.023	0.046	0.061
LS with 15% C-ash	0.003	0.011	0.022	0.026	0.029	0.046	0.058

2.6 Sulfate and chloride resistance

Gonzalez and Irasser [31] studied the effect of sulfate attack on concrete with portland-limestone cement. Table 2.7 shows the results of ASTM C 1012 [32] tests on various types of cement with various amount of limestone replacement. Two forms of sulfate attack occur in concrete made with blended cement: ettringite form (the classical

form) and thaumasite form. Ettringite form of sulfate attack depends on the C_3A content. It can be mitigated by reducing C_3A content and reducing the permeability by reducing *w/b* and well compacting. Some data show that limestone content improves classical sulfate resistance because limestone leads to lower expansion while others show that there is no relation and that sulfate attack resistance relies solely on C_3A content.

Higher limestone content changes the mode of sulfate attack to thaumasite formation. Thaumasite attack is enhanced in the presence of sulfates, water, carbonates, and low temperatures. The rate of expansion is directly proportional to limestone content while time to failure is inversely proportional to limestone content.

Table 2.7: Sulfate Resistance of Limestone Mixtures [31]

Cement	Type V			Type V			Type II		
C3A content, % mass C3S content, % by mass	0 40			1 74			6 51		
Limestone replacement	0	10	20	0	10	20	0	10	20
Time to 0.10% Expansion, days	1260	857	208	148	164	92	165	209	108
Reduction in compressive strength (1 year in sulfate solution, %)	3	4	5	29	17	50	8	25	40

Limestone filler slightly reduces the permeability of concrete (due to stabilization of ettringite as discussed earlier) and lowers pH of cement paste. Batic et al. [33] found that adding limestone filler of up to 5% decreases chloride penetration of concrete while higher percentages of filler slightly increase chloride penetration. Figure 2.12 shows the rebar corrosion rate in different electrolytes. In the figure, “N” stands for unblended portland cement, “F” for cement with limestone filler, “1” for *w/b* of 0.5, “2” for *w/b* of 0.65, “A” for air curing, and “C” for curing in lime water.

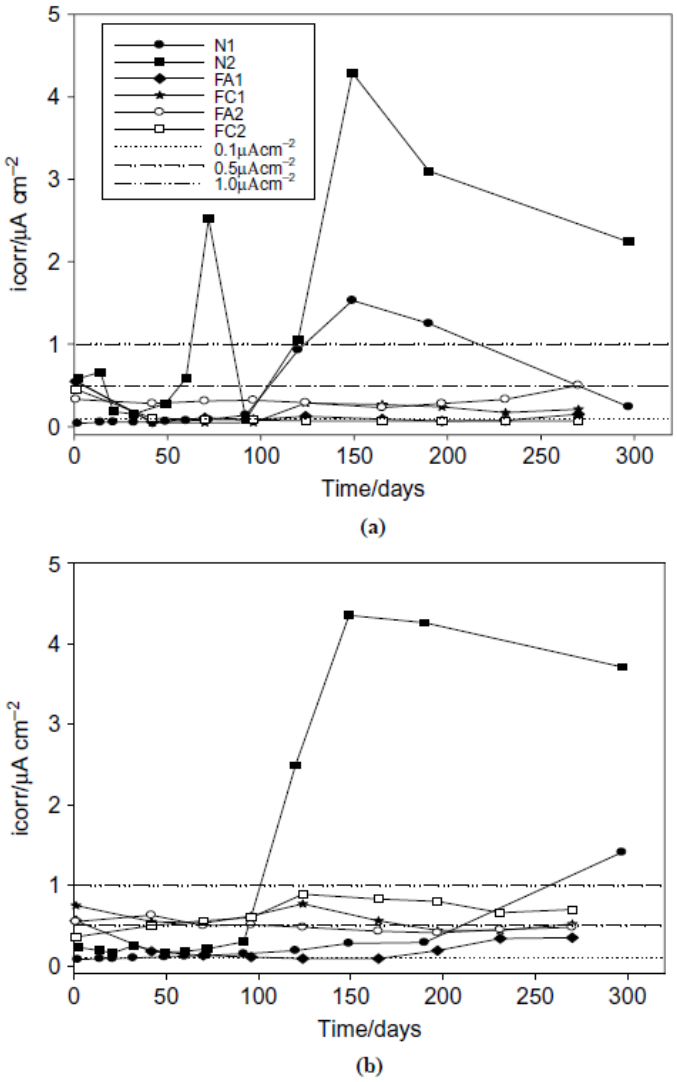

Figure 2.12: Rebar corrosion rate in different electrolytes. (a) Tap water, (b) 3% NaCl [33]

Limestone-filler's influence on rebar corrosion depends on *w/b*, curing, and chloride presence. Higher *w/b* increases corrosion but minimizes the difference in corrosion rate between concrete with and without limestone-blended cements. Limestone addition changes the rebar surfaces by replacing the hydraulic compounds (SiO_2 and CaO) with carbonated iron oxyhydroxides.

Carbonates change the nature of the protective layer on rebars and reduce the protective properties of mortar in the presence of chlorides. However, carbonates passivate rebars in concrete with high *w/b* and cured in lime water. This is because in the presence of limestone filler, curing in limewater favors the growth of hydrated calcium silicate and crystalline calcium hydroxide on rebar surface. Passivation of rebars due to carbonate anions counterbalances the effect of lower pH due to limestone addition. Limestone filler slightly decreases the conductivity (Figure 2.13), i.e. increases the electrical resistivity of concrete (probably due to the higher volume of the hydrated cement products and lower porosity due to ettringite stabilization as discussed earlier) but changes corrosion from localized to more uniform since the tendency for repassivation became higher, making rebar more susceptible to chloride attack.

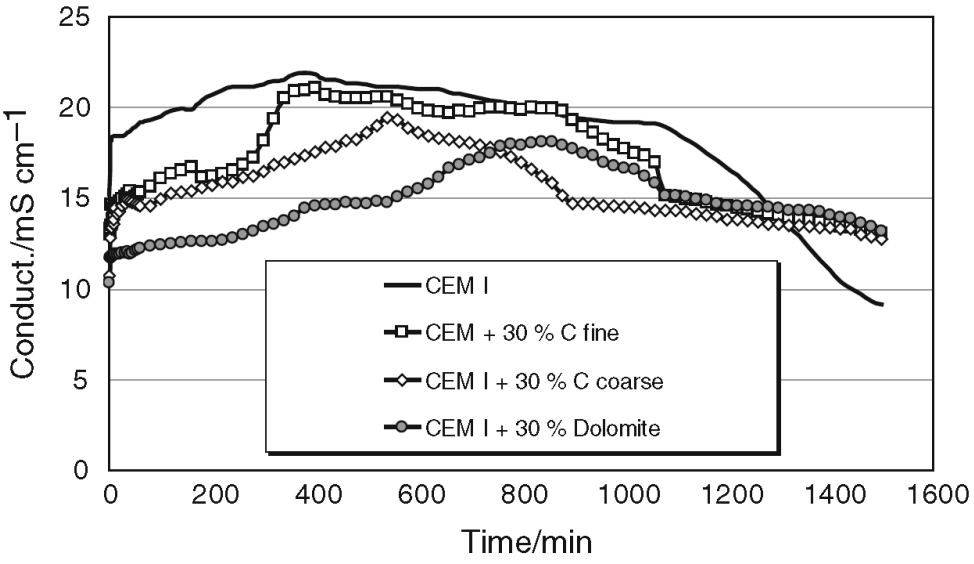

Figure 2.13: Conductivity of cement suspensions [23]

CHAPTER 3: EXPERIMENTAL PROGRAM

3.1 Experimental objectives

The first objective was materials characterization. Materials characterization included QXRD analysis to identify the phase composition of all cements used in this study, isothermal calorimetry to identify the hydration kinetics of cement and cementitious materials, particle size analysis to find effect of particle size on the performance of Type IL cement, and Vicat time of setting to identify differences in setting time between Type I/II cement and Type IL cements.

The second objective was to evaluate the performance of Type IL cement in concrete. Concrete assessment included mechanical properties, drying shrinkage, and creep. The mechanical properties investigated were compressive strength development over time, elastic modulus, and tensile strength.

The third objective was to investigate the effect of curing temperature on the performance of Type IL cement in concrete and cement paste. The target was to find the effect of low and high temperatures on hydration, setting time, and concrete mechanical properties.

The forth objective was to examine the effect of supplementary cementitious materials (SCMs) on the performance of Type IL cement in concrete and cement paste. The target was to investigate the applicability of using fly ash and slag cement with Type

IL cement and to examine the synergistic effects for enhancing the performance of Type IL cement.

The fifth objective was to evaluate the performance of Type IL cement in prestressed concrete beams. The target was to check the bond capacity of prestressing strands with concrete made with Type IL cement, the strand transfer and development lengths, plus the beam flexural capacity, and to compare the results with those from beams made with Type I/II cement.

The experimental work is classified into four main categories based on the primary type of material investigated: Solids, cement paste, concrete, and prestressed concrete structures. Figure 3.1 shows a schematic of the test methods used in this research. To provide a broader view of the larger project investigating Type IL cement, Figure 3.2 shows the test methods completing the larger study. Each test method is discussed in more details in subsequent chapters.

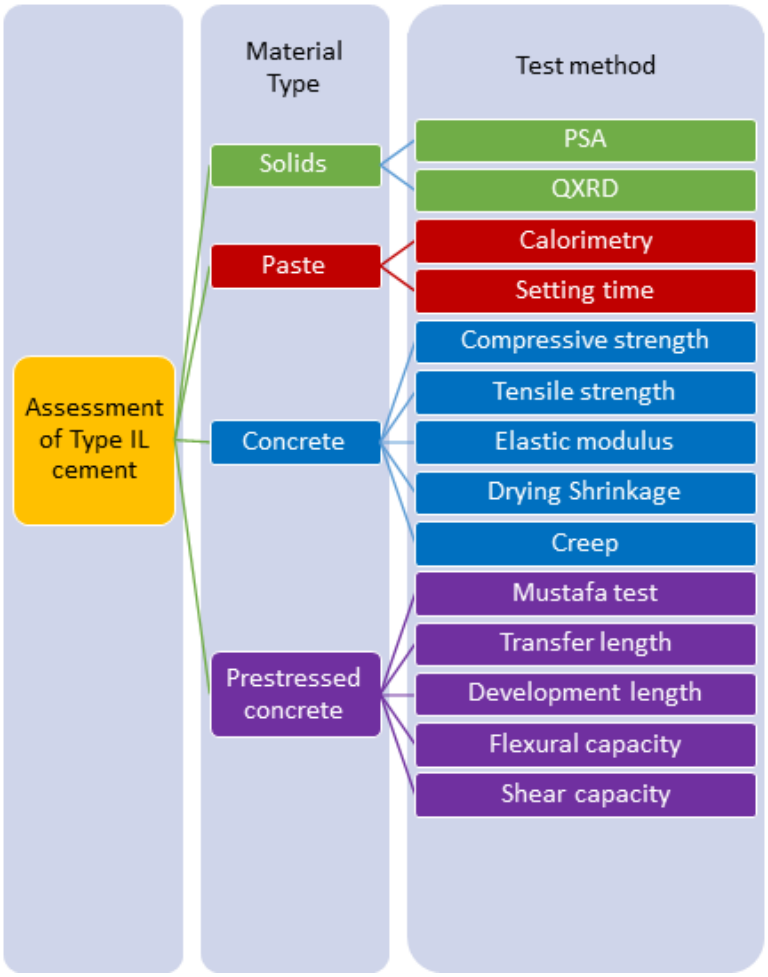

Figure 3.1: Schematic of the test methods used in this research

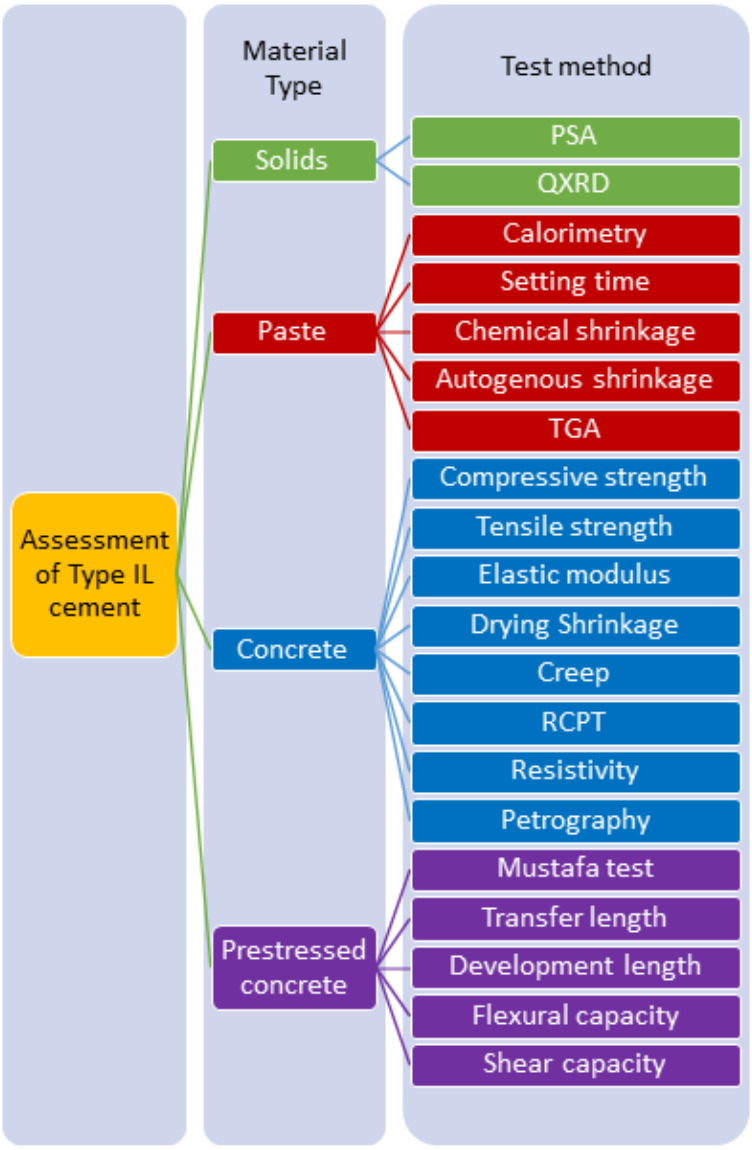

Figure 3.2: Schematic of the test methods used in the broader project examining Type IL cement

3.2 Materials

3.2.1 Cement

Cements were received from 5 cement plants. Each plant provided Type I/II cement and Type IL cement. Plant E provided two Type IL cements, one with a fine grind and one with a coarse grind. Table 3.1 summarizes the sources of the materials and the cement characteristics.

Table 3.1. Cements used for this research

Producer	Location	Cement characteristics
(A)	Calera, AL	Limestone source (dolomite) LS replacement rate (14-15%)
(B)	Clinchfield, GA	Softer limestone source Georgia source
(C)	Holly Hill, SC	Limestone source (marl) Geography (SC source)
(D)	Theodore, AL	Softer limestone source
(E)	Leeds, AL	Type IL with fine and coarse ground limestone

3.2.2 Aggregates

Coarse granite gneiss aggregates were obtained from Vulcan Materials quarry at Lithia Springs, GA. Fine aggregates (natural alluvial sand) were obtained from Sand Rock Transit at Atlanta, GA, and the source was from Shorter, AL. Table 3.1 and

Table 3.2 show the aggregates properties. Figure 3 shows the grain size distribution of the fine aggregates along with ASTM C33 [34] limits.

Table 3.1: Properties of coarse aggregates

Dry rodded unit weight (lb/ft^3)	98
Bulk specific gravity (SSD)	2.609
Absorption capacity	0.58%
Maximum size of aggregate (in)	0.75

Table 3.2: Properties of fine aggregates

Fineness modulus	2.4
Bulk specific gravity (SSD)	2.630
Absorption capacity	0.40%

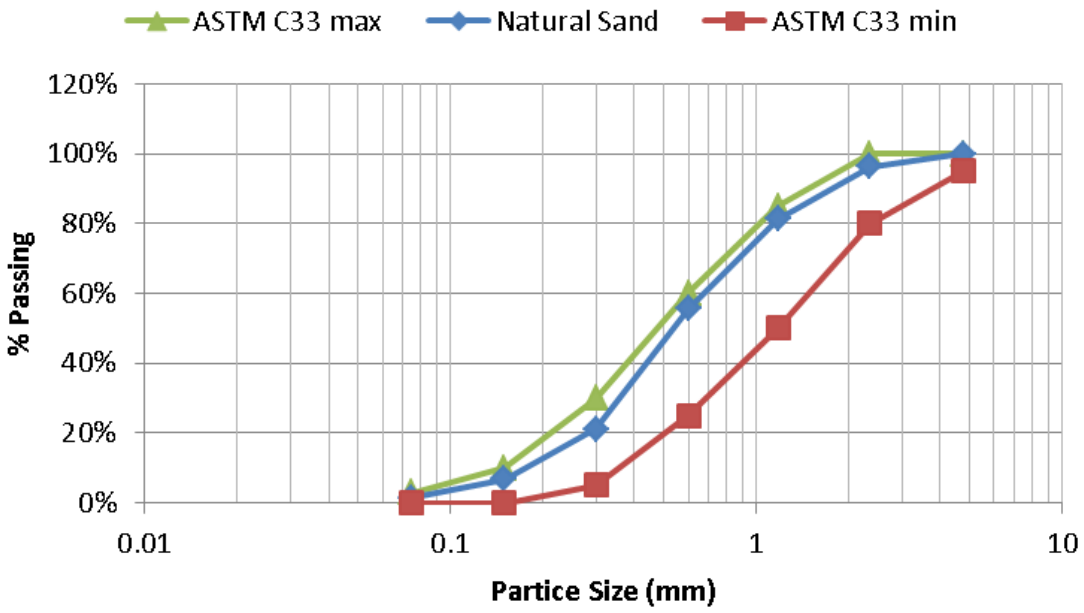

Figure 3.3: Grain size distribution of fine aggregates

3.2.3 Concrete mix design

The concrete mix designs were developed based on Georgia Department of Transportation (GDOT) Section 500 specifications [35]. Three Classes of concrete - A, AA, and AAA - were cast with the *w/b* ratios of 0.490, 0.445, and 0.320, respectively, which satisfy the requirements of the GDOT specifications as given in Table 3.3.

Table 3.3: Concrete mix requirements from GDOT specification section 500

Class of Concrete	Coarse Aggregate Size No.	Min. Cement Factor lb/yd^3	Max. *w/b*	Slump acceptance Limits (in) Lower-Upper	Entrained Air Acceptance Limits (%) Lower-Upper	Minimum Compressive Strength at 28 days (psi)
A	56, 57, 67	611	0.490	2-4”	2.5-3	3000
AA	56, 57, 67	635	0.445	2-4”	3.5-7	3500
AAA	67,68	675	0.440	2-4”	2.5-6	5000

Eleven concrete mixtures were prepared using the Type I/II cements from sources A to E, along with their companion Type IL cements. Mixtures were designed to meet the highest *w/b* ratio and the minimum total cementitious materials content for each GDOT Class (Table 3.3). Crushed granite coarse aggregates (Lithia Springs, GA; #67 stone, dry-rodded unit weight = 98 lb/ft^3, SG = 2.61) and natural sand fine aggregates (Byron, GA; fineness modulus = 2.4, SG = 2.65) were proportioned at 1889 lb/yd^3 (1120 kg/m^3) and 1260 lb/yd^3 (750 kg/m^3), respectively, for each of the 11 mixtures. A mid-range water reducer (Sika SikaPlast-300GP) was used for Class A and AA, and a high range water reducer (Sika Viscocrete 2100) was used for AAA concrete to ensure adequate workability. The dosages of admixtures were adjusted to achieve the slump in the range

of 2-4 inches required by GDOT section 500 (Table 3.3). The concrete mix design for the three concrete Classes are shown in Table 3.4.

Table 3.4: Concrete mix designs for Class A, AA and AAA concretes

Material	Weight (pcy)		
	Class A	Class AA	Class AAA
Cement	611	635	800
Water	299	283	256
Coarse Aggregate (#67 granite)	1890	1890	1890
Fine Aggregate (natural sand)	1230	1253	1096
Water reducer	Mid-range WR (SikaPlast -300GP) 2 fl. oz/100 lb cement	Mid-range WR (SikaPlast -300GP) 8-12 fl. oz/100 lb cement	High-range WR (Sika Viscocrete 2100) 4 fl. oz./ 100 lb cement

The raw materials were mixed in 5 ft^3 batches in a 9 ft^3 rotating drum mixer, following ASTM standard practices [36]. Cylindrical specimens were cast in cylinders measuring 4-in. (diameter) by 8-in. (length) for compressive and tensile strength testing and 6 in (diameter) by 12-in. (length) for elastic modulus measurements. Concrete prisms 3-in. square cross-section and approximately 11 ¼ in. long were cast for drying shrinkage tests according to ASTM C157 [30]. Specimens were removed from their molds 24 hours after casting and cured in a saturated calcium hydroxide (limewater) solution at 70 ± 3°F until testing. Other concrete mixes were cured at 40 ºF and at 90 ºF in temperature-controlled curing boxes.

3.2.4 Water reducers

Based on trial batches of concrete, SikaPlast-300GP, a mid-range water reducer, was selected to be used for Class A and Class AA concretes. For Class AAA concrete, high range water reducer was needed to achieve the required slump and was obtained from Sika (Sika Viscocrete 2100).

3.2.5 Supplementary cementations materials

Fly Ash [37] (Class F and Class C) was provided by Boral Materials - USA. The Class F fly ash was from Cartersville, GA and the Class C fly ash was from Juliette, GA. Slag was provided by Holcim (US) Inc.

3.2.6 Prestressed concrete beams

After contacting ready-mixed concrete producers in Atlanta and considering the availability of Type IL cement in Georgia for precast construction, producer "C" was selected for the construction of the four prestressed beams at Tindal Corporation, Conley, GA.

3.3 Curing conditions

3.3.1 Cement paste

Cement paste was used for isothermal calorimetry and Vicat time of setting. Isothermal calorimetry was conducted at room temperature (73 ºF) and at 140 ºF to

simulate high temperature curing, which is commonly used in precast concrete construction to accelerate strength development. Vicat time of setting tests were conducted at 40 ºF, 73 ºF, 90 ºF, and 140 ºF.

3.3.2 Concrete mechanical properties

Four curing conditions were used for concrete cylinders: Room temperature (73 °F, according to ASTM 192 [36]), low temperature conditions (40 ºF) to simulate cold weather, high temperature conditions (90 ºF) to simulate hot weather, and elevated temperature (140 °F) to simulate steam curing conditions used for some precast concrete bridge girders. Figure 3.4 shows the saturated lime-water baths used for curing samples at room temperature. Figure 3.5 shows the curing box used for low and for high temperature curing.

Figure 3.4: Saturated lime-water baths for curing at room temperature

Figure 3.5: Intellicure temperature-controlled curing box for low and high temperature curing

3.3.3 Concrete drying shrinkage (ASTM C157 vs ALABAMA Specs)

Drying shrinkage samples were cured until 28 days of age (ASTM C157 [30]) in lime-water baths at the four temperatures mentioned above. Drying then initiated at 73 ºF and 50 % relative humidity for all samples.

Another group of samples were only water bath cured for 7 days (Alabama DOT Standard Specifications for Highway Construction, Section 501 [38]), and then drying was at 73 ºF and 50 % relative humidity.

3.3.4 Concrete creep

Creep samples were cured until 3 days of age in lime-water baths at 73 ºF, and then loaded at age of 3 days at 40% of their compressive strength. Loading at 3 days of age was selected to simulate the maturity of concrete at which precast beams are prestressed.

3.4 Cement characterization

The first step to identify key differences between Type I/II and Type IL cement was to compare their physical and chemical properties in terms of particle size, hydration kinetics, and chemical phases present in each type of cement. The methods used were particle size analysis, isothermal calorimetry, and quantitative X-ray diffraction analysis (QXRD).

3.4.1 Particle size analysis

Particle size analysis was conducted on all cements to investigate the effect of fineness of cement and ground limestone on concrete performance. The instrumentation used was Malvern Mastersizer 3000 (Figure 3.3) which is a laser diffraction particle size analyzer. Ethanol was used as a solvent instead of water to prevent cement hydration while conducting the measurements.

Figure 3.6: Malvern Mastersizer 3000

3.4.2 Isothermal Calorimetry

Isothermal calorimetry was conducted using a TAM Air Isothermal Calorimeter (Figure 3.7) for all cements at room temperature (73 °F) and at 140 °F to compare the hydration kinetics of limestone cements to Type I/II cements. The temperature of 140 °F was selected to simulate high temperature accelerated curing of precast concrete. Samples were made with all cements and tested at both temperatures. Also, samples were made with all cements and SCMs combined, and also tested at both temperatures. Sand was used for the reference ampoules at high temperature after it showed better performance than empty ampules since sand is an inert material with approximately the same heat capacity as the sample in the reference. All samples were made with a *w/b* ratio of 0.44. For the samples with SCMs, fly ash replacements were 15% by mass and slag replacements were 50% by mass. Figure 3.8 shows a schematic of the test matrix.

Figure 3.7: TAM Air Isothermal Calorimeter

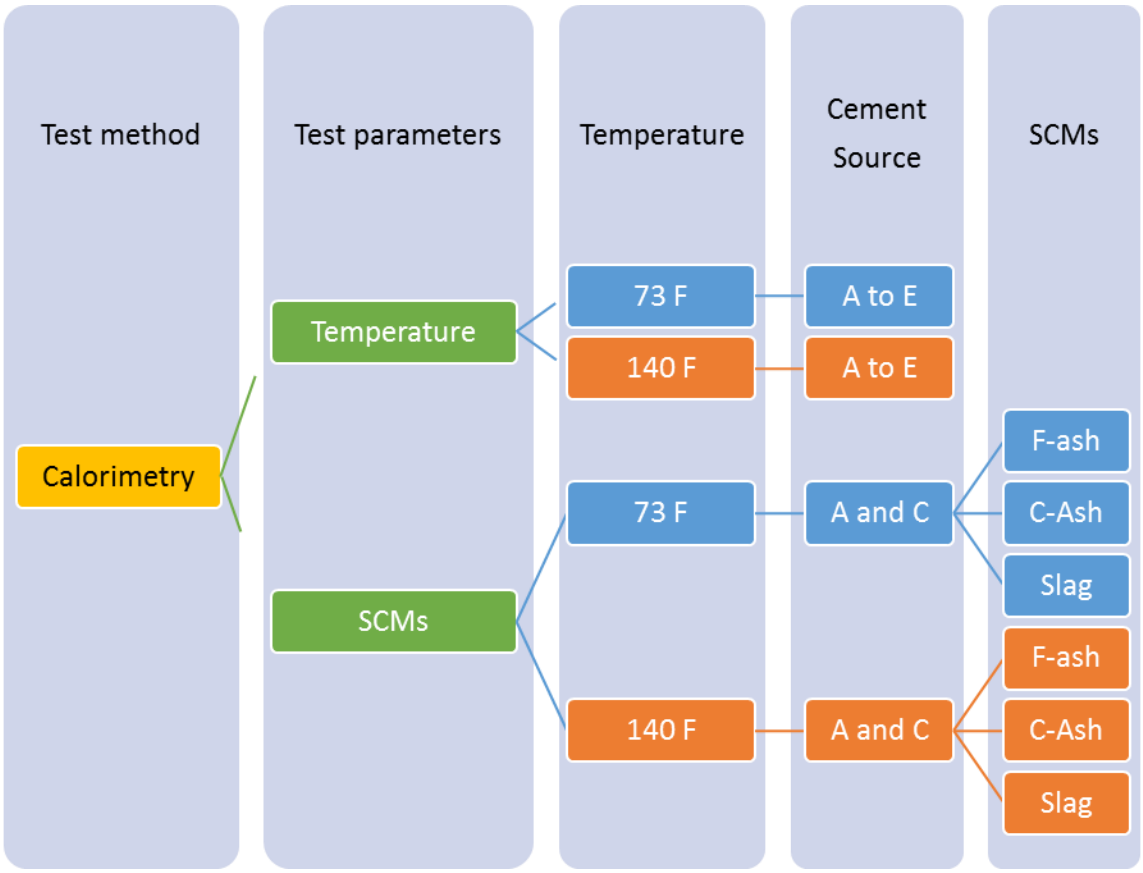

Figure 3.8: Schematic of the test matrix for isothermal calorimetry

3.4.3 Quantitative X-ray diffraction analysis (QXRD)

QXRD was conducted to compare the phases present in samples of the cements received. Samples were sent to Heidelberg Technology Center in Atlanta were QXRD was performed at their facilities.

3.5 Time of setting

Vicat time of setting (ASTM C191 [39]) was conducted for all cements at 40 °F, 73 °F, and 90 °F to compare the initial and final setting times of limestone cements to Type

I/II cements at different temperatures. In addition to that, the effect of blending secondary cementitious materials (SCMs) was examined at 73 °F, where 15% Class F fly ash, 15% Class C fly ash, and 50% slag replaced the cement (by weight) for each sample. Three samples were made for each variable and the average values were reported.

The instrument used was ToniSET (Figure 3.9) which is an automatic Vicat needle instrument at Heidelberg Technology Center. In the testing protocol, a penetration of 25 mm was defined as the initial time of setting, and a penetration of 2 mm was defined as the final time of setting.

Figure 3.9: ToniSET automatic Vicat instrument

A *w/b* ratio of 0.31 was used for samples. This was based on the *w/b* needed to achieve normal consistency for cement C and was close to the normal consistency of

several of the cement samples from sources A to E. Using one specific *w/b* was used to allow comparing different cement sources with each other. Three samples per cement source were prepared. The rest of the procedure followed ASTM C191.

The test matrix was designed to investigate the effect of temperature and the effect of SCMs on the setting time of Type I/II and Type IL cements. In order to achieve that, the test matrix consisted of four main groups. The first group consisted of plain mixes (i.e. cement paste without SCMs) where samples from sources A to E were prepared and tested at 73 °F. The second group consisted of plain mixes from sources A to E and tested at 90 °F. The third group consisted of plain mixes from sources A to E and tested at 40 °F. The forth group consisted of cements from sources A to E blended with SCMs. The SCMs used were fly ash (class F and class C) and slag. The SCMs replacements were 15% by mass for the fly ash and 50% by mass for slag. The SCMs were added to the cement and dry blended before mixing with water. Figure 3.10 shows a schematic of the test matrix.

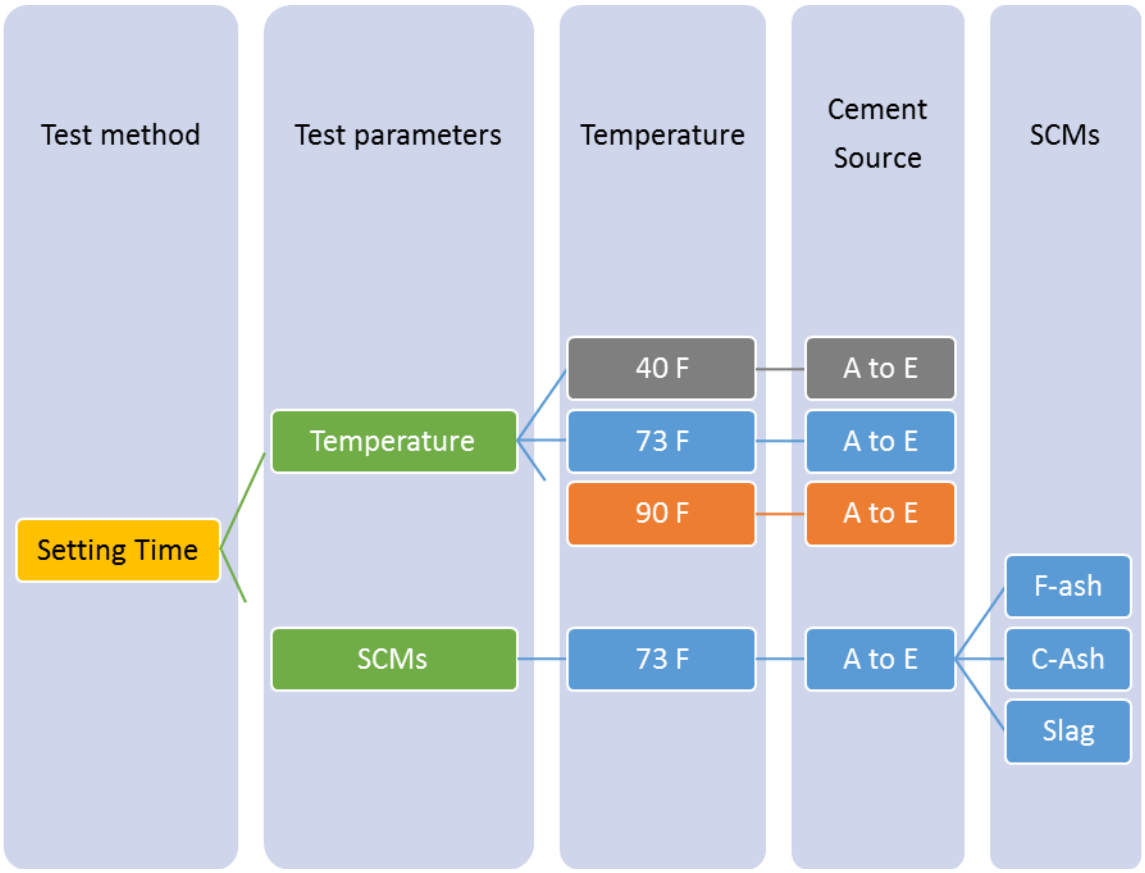

Figure 3.10: Schematic of the test matrix for Vicat tie of set

The time at which the first measurement for the tests done at 73 °F was taken at 30 minutes. However, for the tests at 40 °F, the first measurement was taken at 120 minutes. This was done since there are limited number of testing points available on the surface of the specimen (ASTM C191 requires a minimum spacing of 5 mm between previous penetrations) and to prevent depleting those testing points on the sample surface by the time an initial set and a final set has been reached. Subsequent measurements were taken at a 10 minutes increment for all tests.

3.6 Concrete mix design

Concrete mix design has been developed for class A, AA, AAA concretes in accordance with GDOT Section 500 [40]. For class A, and AA concrete, SikaPlast-300GP, a mid-range water reducer, was selected to be used based on trial batches of concrete.

For class AAA, several concrete producers in the State of Georgia were consulted for concrete mix designs for high strength concrete. The target strength was 8 ksi at 28 days which is a typical value used for prestressed concrete in bridge applications. All the requirements of GDOT Specification 500 and Specification 865 for Class AAA concrete and prestressed concrete needed to be met as well. Therefore, trial batches were produced and high range water reducer was needed to achieve the required slump and was obtained from Sika (Sika Viscocrete 2100). Class AAA concrete mixes were produced using cement from producers A and C. Batch quantities for Class A, AA, and AAA mixes are shown in Table 3.5. Concrete batching was performed at room temperature (73-75 °F).

Table 3.5: Concrete mix design

Material	Class A (lb/yd3)	Class AA (lb/yd^3)	Class AAA (lb/yd^3)
Cement	611	635	800
Water	299	282	256
Coarse Aggregates	1890	1890	1890
Fine Aggregates	1229	1253	1096
w/b (water-cement ratio)	0.489	0.445	0.320
Mininum Required 28-day strength (psi)	3000	3500	5000

3.7 Concrete assessment

In this research, the assessment of concrete was organized into two main categories: mechanical properties, and long-term effects. These will be discussed in more details in subsequent sections. Figure 3.11 shows a schematic of the test program for concrete assessment.

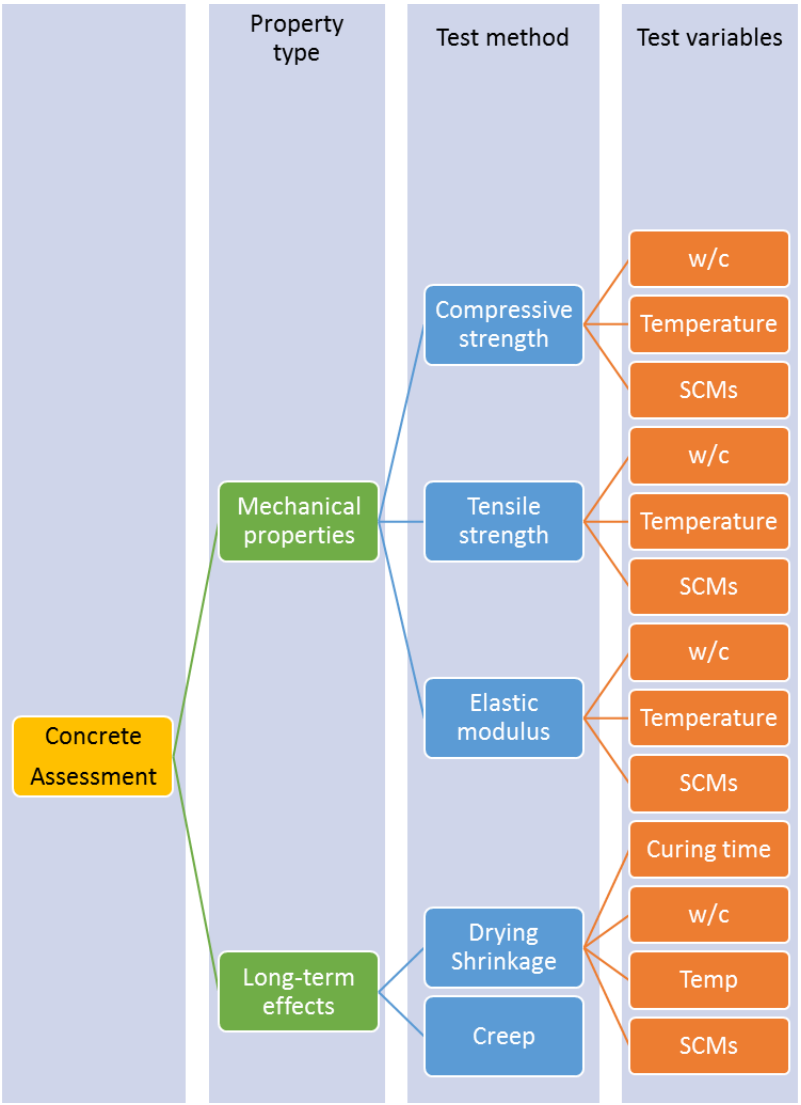

Figure 3.11: schematic of the test program for concrete assessment

3.7.1 Mechanical properties

The mechanical properties tested are compressive strength (ASTM C39 [41] and AASHTO T 22-14 [42]), elastic modulus (ASTM C469 [43]), and splitting tensile strength (ASTM C496 [44] and AASHTO T 198-15 [45]). Each test method is discussed in more details in subsequent sections.

3.7.1.1 Compressive strength

Compressive strength of concrete cylinders (4 in. x 8 in.) was measured for class A. AA, and AAA concrete at 1 day, 7 days, 28 days, 56 days, 90 days, and 1 year according to ASTM C39 [41].

Class AA concrete was made using cement from all the five cement producers. After examining the properties and performance of all cements, it was found that cement fineness had significant effects on the performance of concrete. Cement producer "A" had finer Type IL cement while producer "C" had Type IL cement with a fineness similar to that of the Type I/II cement. Cements from producers A and C became the representative types for further tests. Those cements were selected for producing the samples of Class A and Class AAA concretes. Figure 3.12 shows the experimental program for the compressive strength tests.

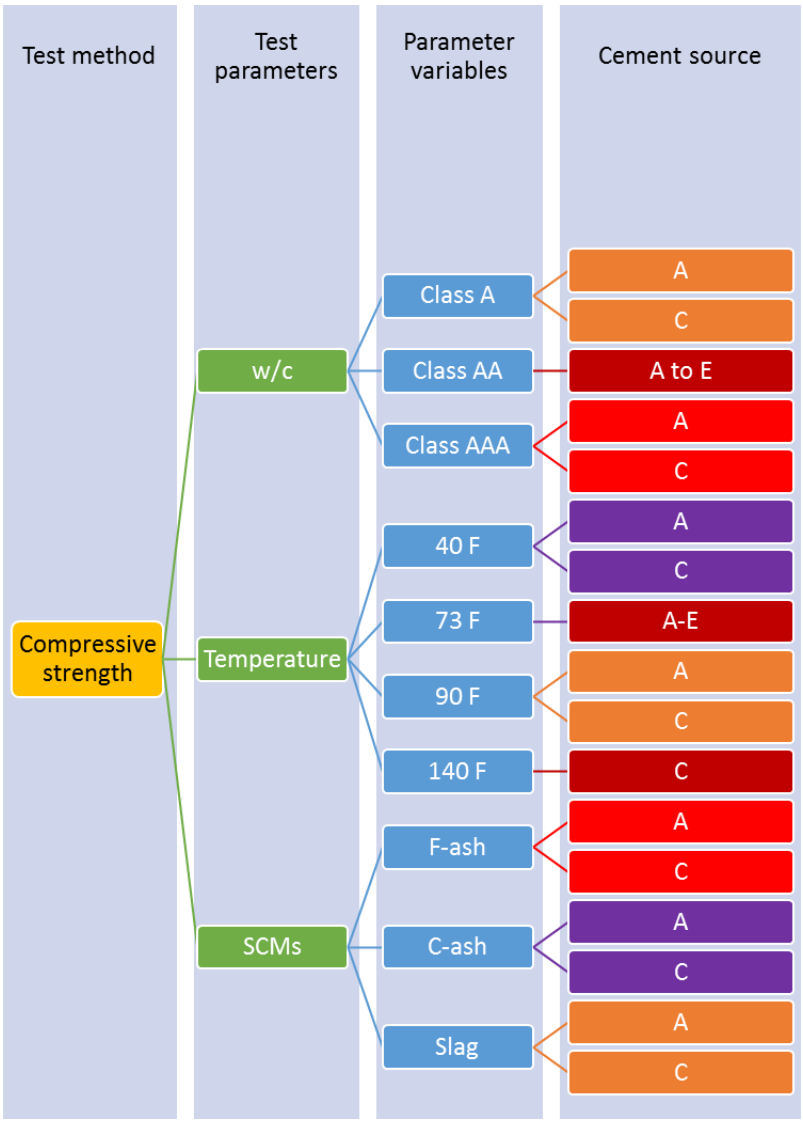

Figure 3.12: Experimental program of the compressive strength of concrete

3.7.1.2 Elastic modulus

Elastic modulus (ASTM C469 [43]) was measured using concrete cylinders (6 in. x 12 in.) at 28 days of age. Figure 3.13 shows the experimental program for the elastic modulus tests.

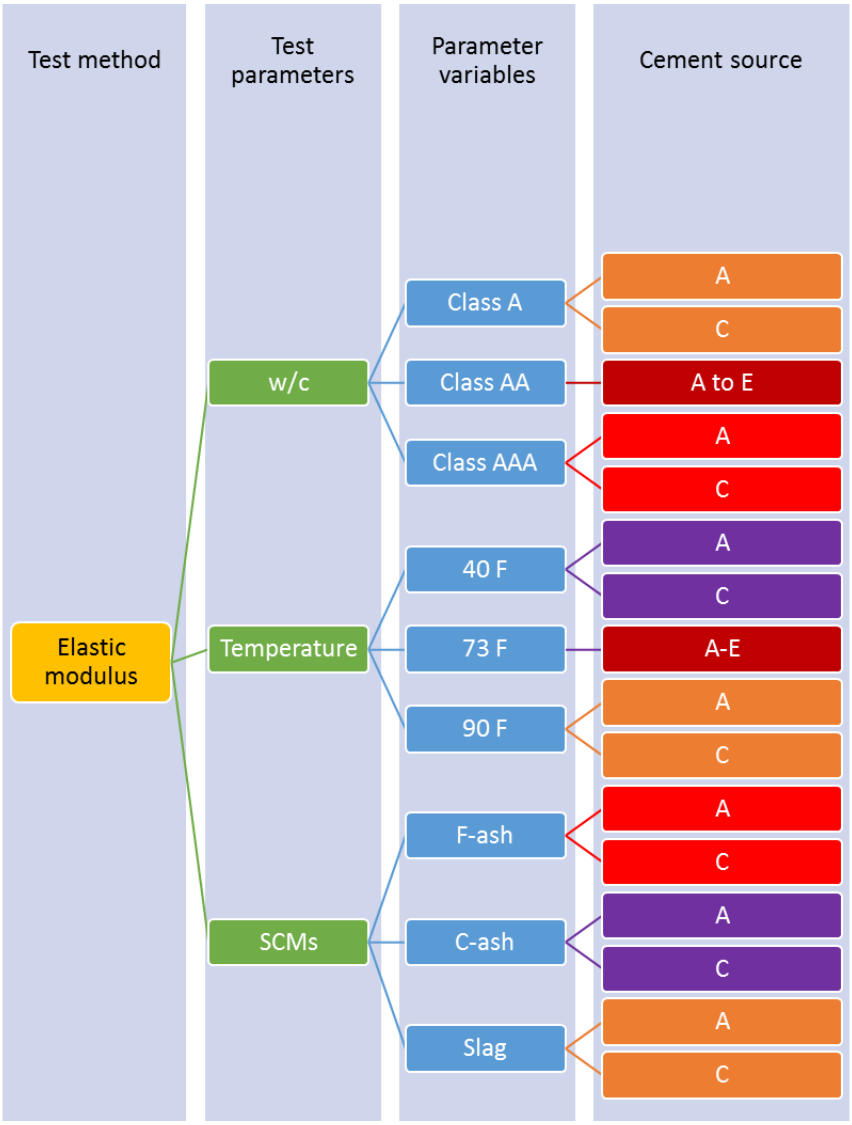

Figure 3.13: Experimental program for the elastic modulus of concrete

3.7.1.3 Splitting tensile strength

Splitting tensile strength (ASTM C496 [44]) was measured using concrete samples (4 in. x 8 in.) at 28 days of age. Figure 3.14 shows the experimental program for the splitting tensile strength tests.

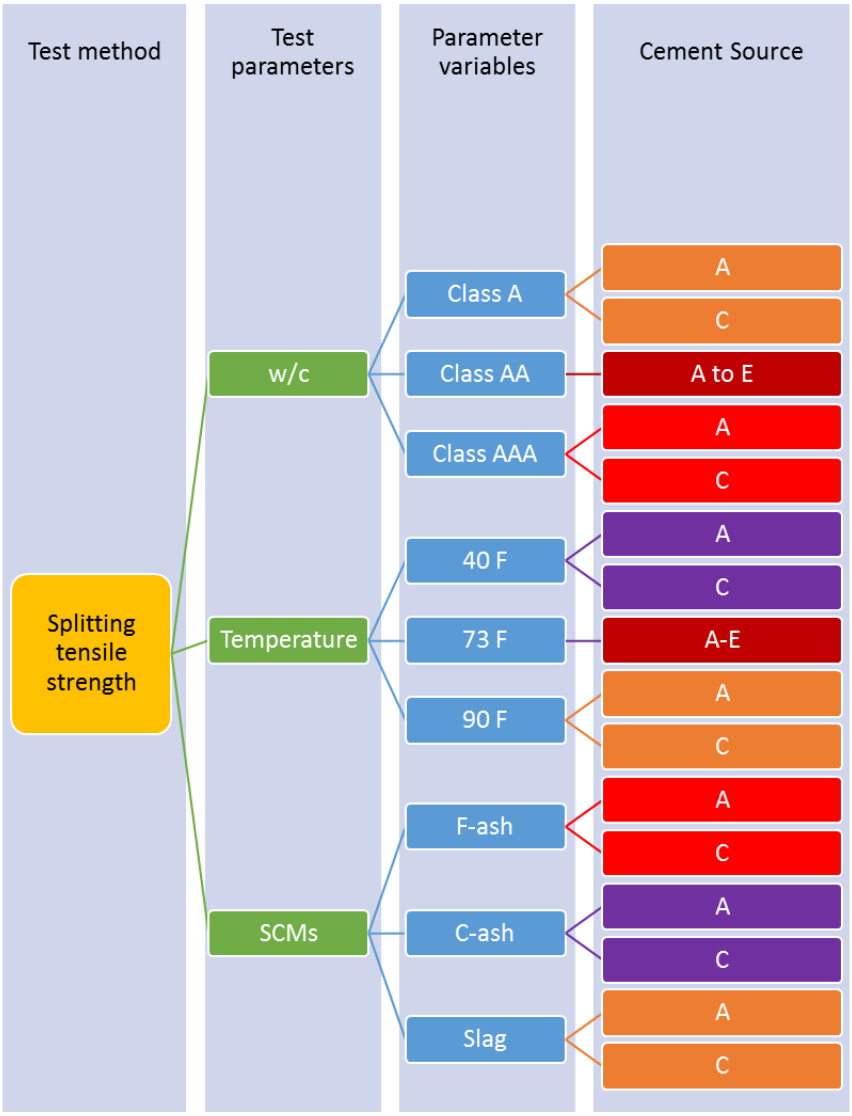

Figure 3.14: Experimental program for the splitting tensile strength of concrete

3.7.2 Drying shrinkage

Drying shrinkage prisms (3 in. x 3 in. x 10 in.) were cured in lime-saturated water for 28 days (ASTM C157 [30] and AASHTO T 160-09 [46]), and then drying initiated at standard room temperature and humidity. Measurements were then taken at 4 days, 7,

days, 14 days, 4 weeks, 8 weeks, 16 weeks, and 32 weeks using a length comparator (Figure 3.15).

A second group of samples were only cured for 7 days as discussed in Section 3.3.3. Figure 3.16 shows the experimental program for the drying shrinkage tests.

Figure 3.15: Drying shrinkage sample with length comparator

Figure 3.16: Experimental program for the drying shrinkage of concrete

3.7.3 Creep

Creep (ASTM C512 [47]) samples were made using 4-in. diameter cylinders, 15-in. long molds as shown in Figure 3.17. Steel circular plates were placed at the two ends of the molds and were permanently attached to the cylinders. Two cylinders were stacked

in each loading frame as shown in Figure 3.18. The circular end plates for each cylinder had pins or holes at their centers. This was used to reduce the eccentricity between the stacked cylinders.

The samples were cured identically to compression test samples for 3 days. They were then loaded to 40% of their compressive strength. Loading at 3 days of age was selected to simulate the maturity of the concrete at which time prestressing is applied. A detachable mechanical multi-length strain gage (Figure 3.19) was used to measure the creep strain while a load cell was used to measure the load applied.

Figure 3.17: Mold used for creep specimens with embedded nuts for DEMEC measurements

Figure 3.18: Creep frames

Figure 3.19: Detachable mechanical strain gage (DEMEC).

3.8 Effect of concrete class (*w/b* and cement factor)

As mentioned in the concrete mix design section, three concrete classes were produced according to GDOT Section 500 [40]. The *w/b* ratios were 0.489 for Class A, 0.445 for Class AA, and 0.320 for Class AAA. The cement factor used were 611 lb/yd^3 for Class A, 635 lb/yd^3 for Class AA, and 800 lb/yd^3 for Class AAA.

3.9 Effect of curing temperature

As mentioned in the curing conditions section (Section 3.3), concrete samples were cured at 4 temperatures: at 40 ºF, 73 ºF, 90 ºF, and 140 ºF.

3.10 Effect of SCMs

As mentioned in the "Materials" section (Section 3.2), the effect of replacing cement with SCMs was investigated. The SCM replacements are detailed in section 3.2.5.

3.11 Structural concrete properties

This study also compared the performance of Type I/II and Type IL cements in prestressed concrete beam applications.

Mustafa test-blocks [48] were constructed to investigate adequacy of bond between prestressing strand and the two concrete types. Prestressed beams were constructed to measure prestress losses, strand transfer length, strand development length, and beam flexural strength. Each test is discussed with more details in subsequent sections. Figure 3.20 shows the experimental program for prestressed concrete.

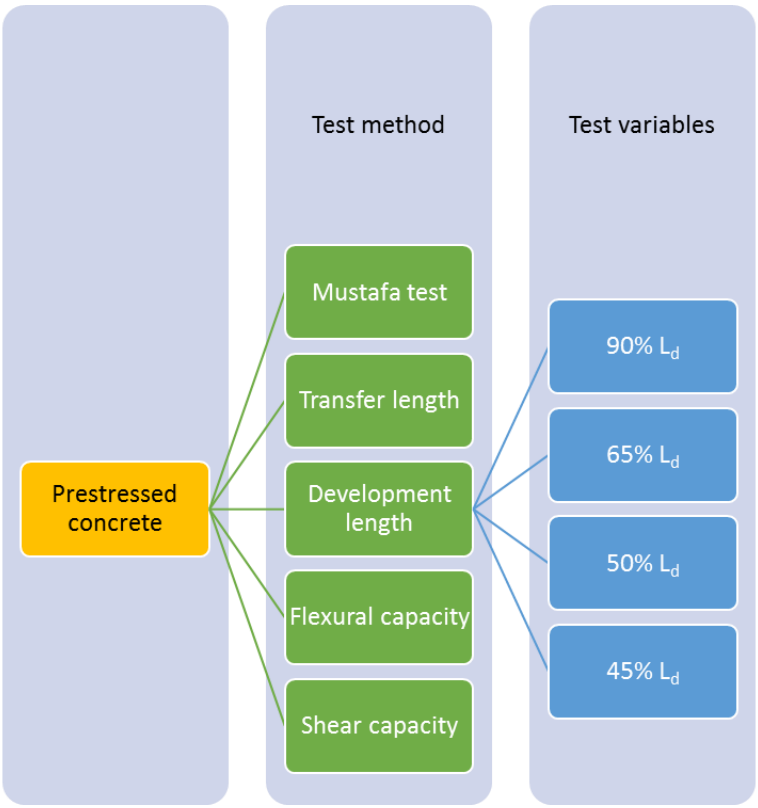

Figure 3.20: Experimental program for prestressed concrete

3.11.1 Beam design

The beams were designed according to the standards in AASHTO LRFD Bridge Design Specifications [49]. The beam span was designed to accommodate testing the development length which was calculated using AASHTO equation 5.11.4.2-1:

$$L_d \geq \kappa \left(f_{ps} - \frac{2}{3} f_{pe} \right) d_b \qquad \text{Equation 3.1}$$

where:

L_d = development length (in.)

d_b = nominal strand dimeter (in.)

f_{ps} = average stress in prestressing steel at the time for which the nominal resistance of the member is calculated (ksi)

f_{pe} = effective stress in the prestressing steel after losses (ksi)

κ = 1.6 for pretensioned members with a depth greater 24 in.

Figure 3.21 shows the beam design. A depth of 25 in. was selected to satisfy the condition for using κ = 1.6 which more accurately represents prestressed concrete beams in bridge applications. Two ½-in. diameter steel strands 270 ksi 7-wire low relaxation strands were used. Beams were designed to assure flexural failure prior to shear failure. A width of 10 in. was selected to satisfy the spacing requirements between two steel strands, plus welded-wire fabric shear reinforcement, and concrete cover. The design of the concrete mix design was identical to the concrete produced at the lab.

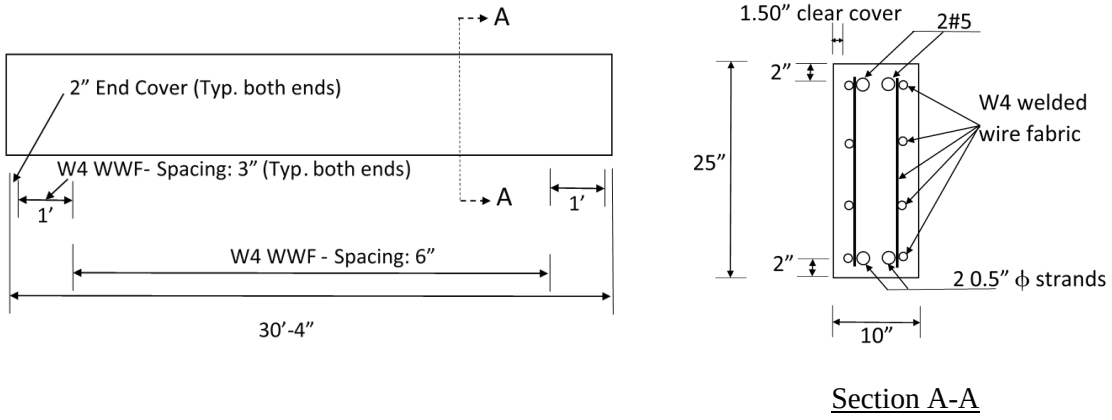

Figure 3.21: Prestressed beam design

A total of four beams were produced: two made with Type I/II cement while the other two were made with Type IL cement. Figure 3.22 shows one prestressed beam prior to testing.

Figure 3.22: Prestressed beam prior to testing

3.11.2 Beam construction

Four beams were produced at Tindall Corporation using class AAA concrete provided by Thomas Concrete with cement from plant C. Two beams were produced using Type I/II cement, while two other beams were produced using Type IL cement.

Figure 3.23 and Figure 3.24 show formwork and prestressing anchorage, and concrete placement and finish, respectively. To minimize the cost of construction, the beams were cast on their side. Fresh concrete properties were tested on site as shown in

Figure 3.25. Figure 3.26 shows samples of concrete cylinders that were also produced to measure their mechanical properties.

Figure 3.23: Formwork, welded-wire fabric, and prestressing

Figure 3.24: Placing concrete and finishing the surface for the beams

Figure 3.25: Measurement of fresh concrete properties

Figure 3.26: Preparation of concrete cylinders for mechanical testing

3.11.3 Structural properties

To investigate the performance of limestone cement concretes in prestressed beams applications, four prestressed beams were produced at Tindal Corporation and trucked to the Structures and Materials Laboratory at Georgia Tech (Figure 3.27). Two beams were made with Type I/II cement concrete and the other two with Type IL cement concrete.

The beams were used to measure prestress losses, strand transfer length, strand development length, and beam flexural strength. Three bending tests were performed on each beam: two for development length and the third for flexural capacity. The layout of each test was designed to prevent excessive damage in areas of the beam used for each subsequent test.

Figure 3.27: Delivery of the prestressed beams from Tindal Corporation to Georgia Tech.

3.11.3.1 Strand bond, Mustafa test for direct pull-out

Mustafa test for strand direct pull-out was performed to compare the non-prestressed bond strength of prestressing strands with concretes made with Type I/II and Type IL cement. The specimen design and test procedure followed the specifications given by Logan [48].

One concrete block was made with Type I/II cement while the other was made with Type IL cement. Six strands were placed in each block. The strands were identical to the ones used for the beams (½-in. diameter steel strands 270 ksi 7-wire low relaxation strands). Each strand was 60 in. long. The blocks were 24 in x 36 in. x 24 in. The strands were embedded to a depth of 19 in. under the top surface with PVC tubes placed at the top 2 in. to act as bond breakers. Figure 3.28 shows the design of the blocks for Mustafa tests; Figure 3.29 shows the formwork; and Figure 3.30 shows concrete placement. Figure 3.31 shows the specimen and Figure 3.32 shows the instrumentation used for the test. The load was measured using a load cell. The deflection was measured using a linear variable differential transformer (LVDT).

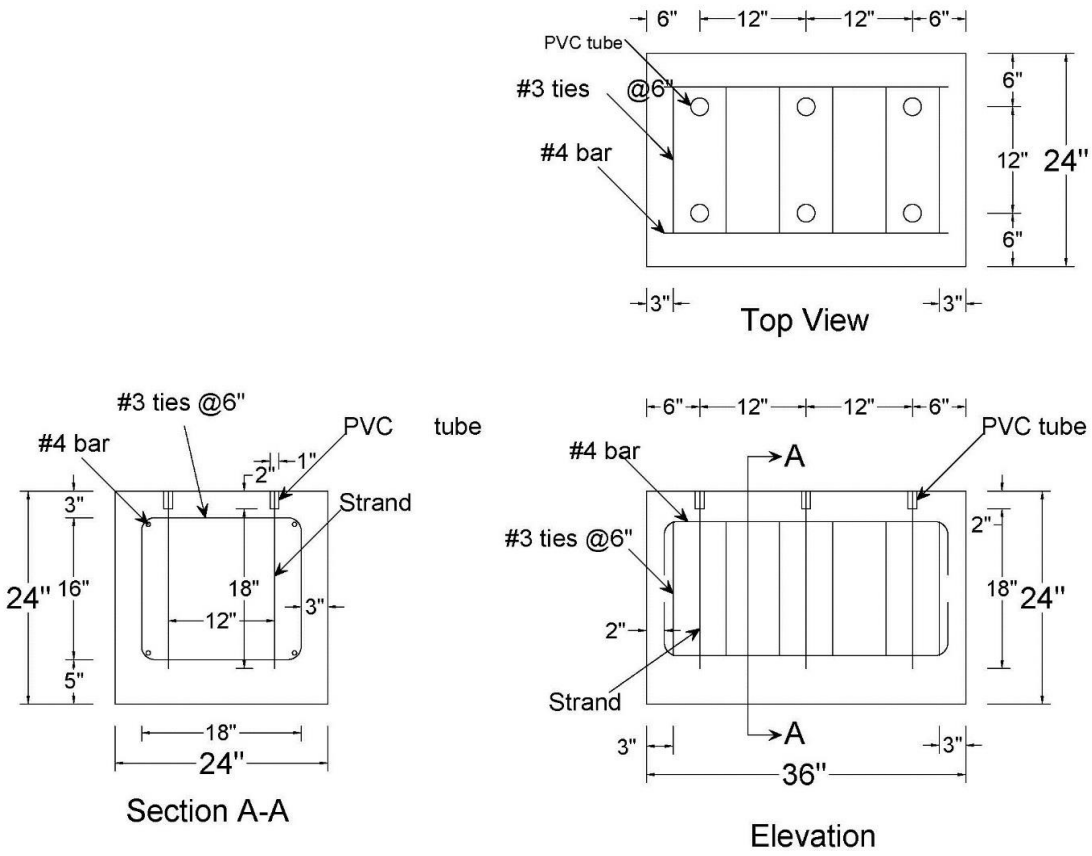

Figure 3.28: Design of concrete blocks for Mustafa test.

Figure 3.29: Formwork for Mustafa test specimens.

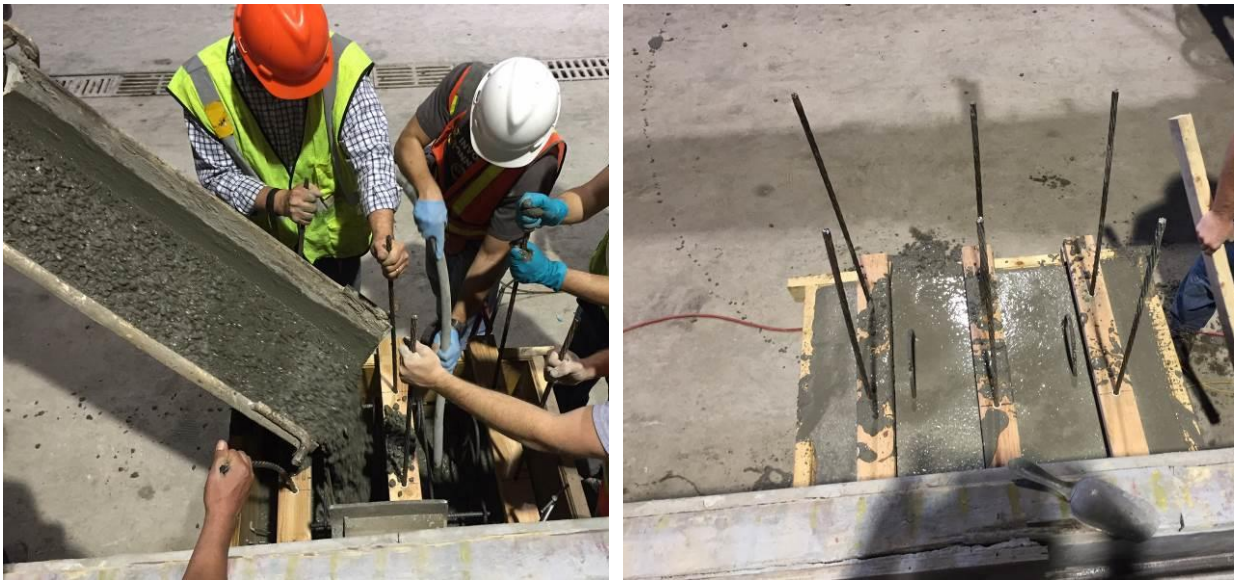

Figure 3.30: Placing concrete for Mostafa Pull-out test

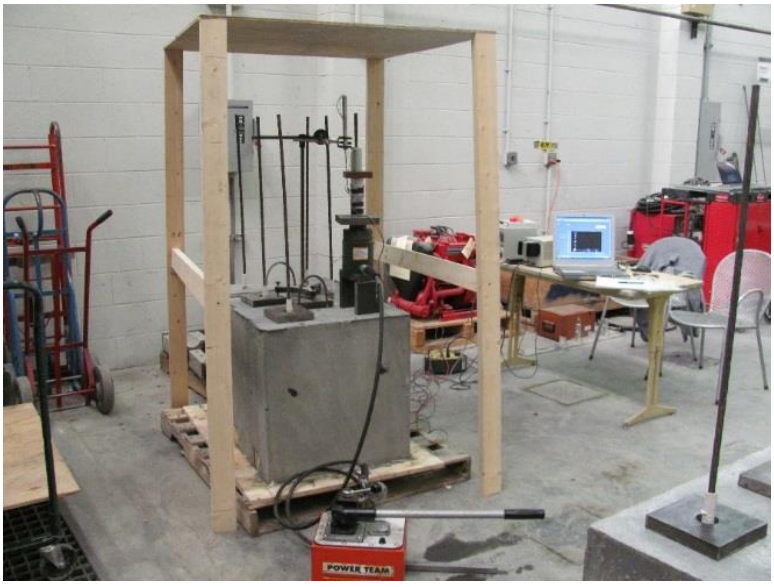

Figure 3.31: Specimen for the Mustafa test.

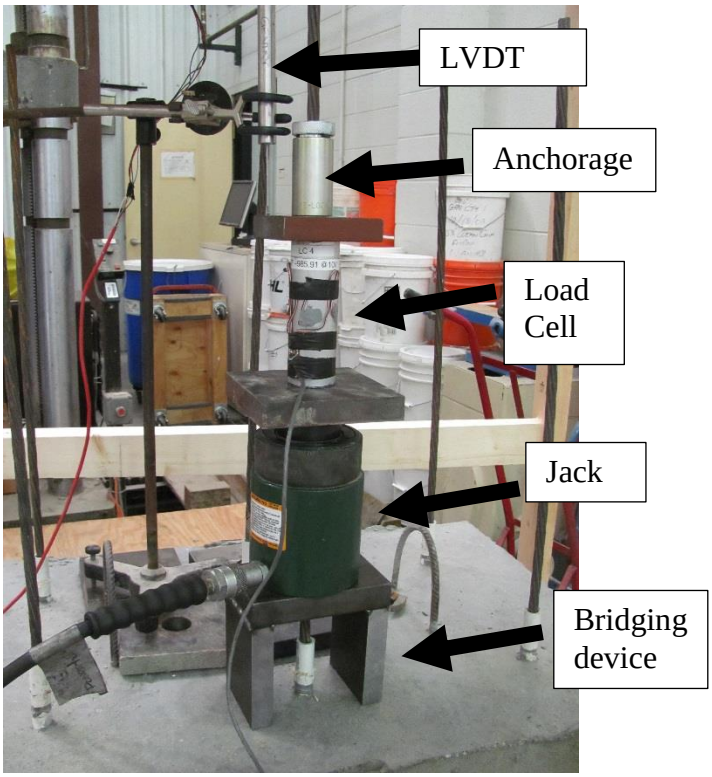

Figure 3.32: Instrumentation for the Mustafa test

3.11.3.2 Prestress losses in precast beams

Prestress losses were measured using vibrating wire strain gages that were embedded at midspan of each beam at the level of the prestressing strands (Figure 3.33). The strain measurements were taken beginning 3 hours after concrete placement and periodically until development length testing, between 128 and 152 days after stressing. The vibrating wire strain gages were model 4200 from Geokon. A portable handheld readout unit (Model GK-404) was used to read the strain and concrete temperature (Figure 3.34).

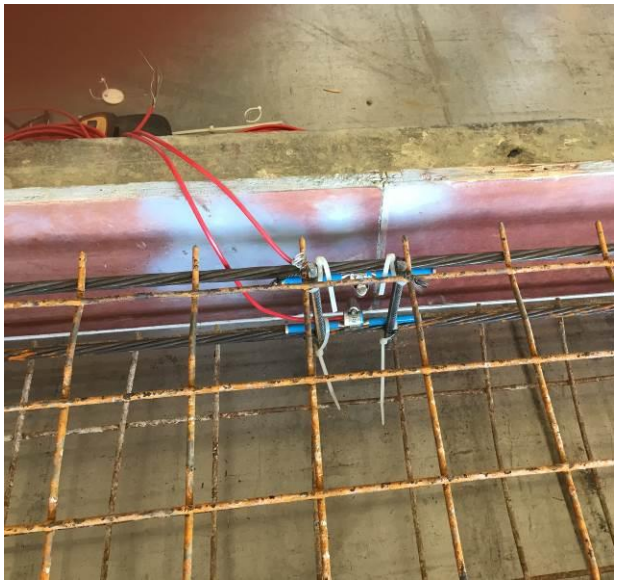

Figure 3.33: Installing vibrating-wire strain gages at midspan next to prestressing strands

Figure 3.34: Vibrating wire strain gage and readout unit from Geokon

The prestress force in each beam was designed to provide 70% of the tensile strength of the strand (f_{pu}) after anchorage set, as long as it did not exceed 40% of the concrete compressive strength at the level of the strand. Therefore, the initial jacking force in the prestressing was 31 kips.

3.11.3.3 Transfer length

Transfer length was measured using a detachable mechanical strain gage (DEMEC). Readings were taken at the level of the prestressing strands. DEMEC points were steel T-nuts embedded in the side of each beam and were spaced 2–in. on center (Figure 3.35). The gage length used with the DEMEC gage was 8 in. The beams were cast on their side; so, the forms which held the DEMEC points in correct position were on the top of the sections being cast as shown in Figure 3.36.

Figure 3.35: Metal nuts for transfer length measurements

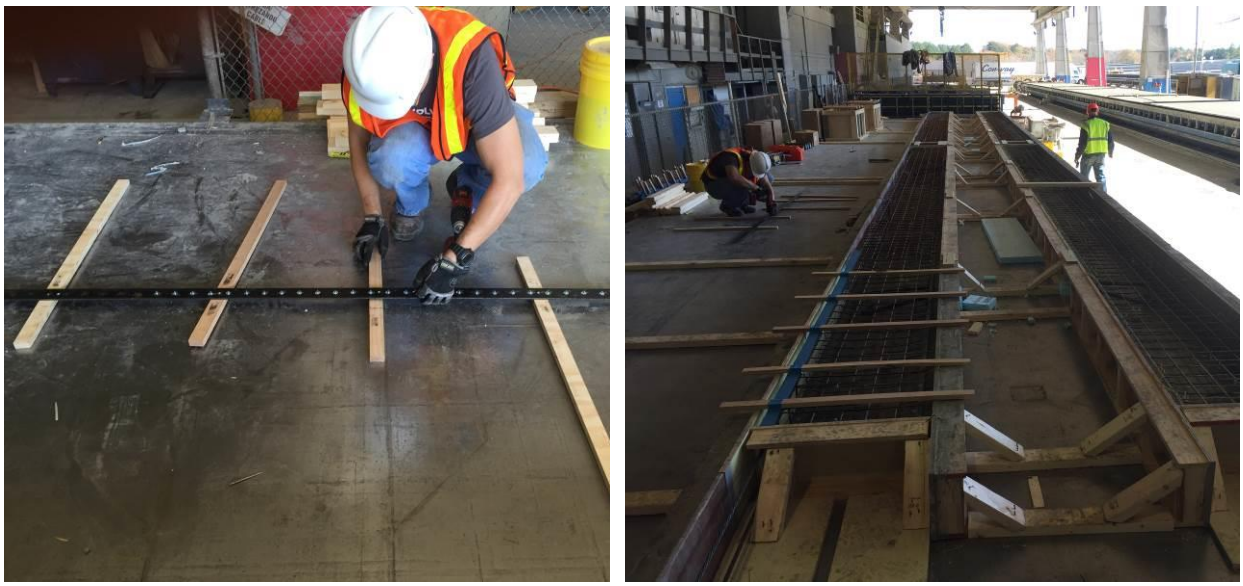

Figure 3.36: Placement of embedded nuts located in steel spacer bar for transfer length measurements.

3.11.3.4 Development length

For the development length test, loads were applied at various distances from the end of the beam based on theoretical AASHTO LRFD [49] development length (L_d) values (Equation 3.1). The ratio of the end distances ranged from 90% of L_d to 45% of L_d.

Two development length tests were performed on each beam by applying a concentrated load at a specific distance from one of the supports as illustrated in Figure 3.37. The first test applied the concentrated load at 90% of L_d. If no strand slip was measured, the second test applied the concentrated load at 65% of L_d (using the other end of the beam). If no strand slip was measured, the second beam was used for the third test where the concentrated load was applied at 50% of L_d (on a second beam). Finally, if

no strand slip was measured in the third test, the forth test applied the concentrated load at 45% of L_d (on the other end of the second beam).

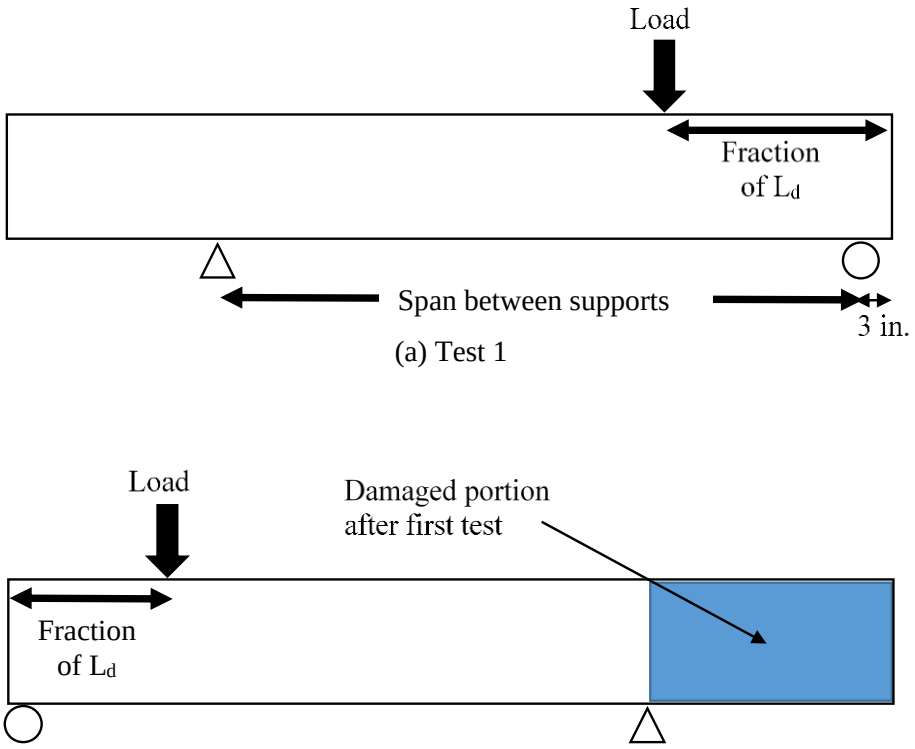

Figure 3.37: Development length tests sequence each beam

Since each beam was tested more than once, a beam testing sequence was developed to run three bending tests on each beam while avoiding damaged areas from previous tests as shown in Figure 3.37. For the first test, the beam was supported over about two thirds of its length. The center of one support was located 3-in. from the right end, while the second support location was 22 ft. from the first support, leaving an 8-ft

cantilever. Load was applied at 90% of the AASHTO LRFD [49] design development length (Equation 3.1). from the right end for the first test.

For the second test, the beam was again supported over about two-thirds of its length so that the undamaged zone from the first test was now subject to the load. The load was applied at 65% of the AASHTO [49] design development length (Equation 3.1) from the undamaged end.

The same sequence was applied again for the second beam but with 50% and 45% of the AASHTO [49] design development length (Equation 3.1) used instead of the 90% and 65%, respectively. To prevent a compression strut from forming, the shear span was kept greater than twice the depth of the beam. This is why the value of 45% of the AASHTO [49] design development length was the minimum distance from the support to the applied load. Table 3.6 summarizes the distance from the end to the load point and the span lengths for the development length tests.

Table 3.6: Summary of testing protocol for development length tests

Cement Type	Beam number	Distance between load application and beam end		Span between supports (in.)
		Relative to AASHTO development length (L_d)	Actual Value (in.)	
Type I/II	B2	90%	111	261
	B2	65%	80	209
	B1	50%	62	264
	B1	45%	56	264
Type IL	B4	90%	111	261
	B4	65%	80	209
	B3	50%	62	264
	B3	45%	56	264

To measure strand slip, gages were fixed to the end of the prestressing strands to measure any slip of the strands relative to the concrete surface as shown in Figure 3.38. The gages were attached to the prestressing strands that protruded from the edge of the beam and measured any relative slip with reference to the end surface of the beam.

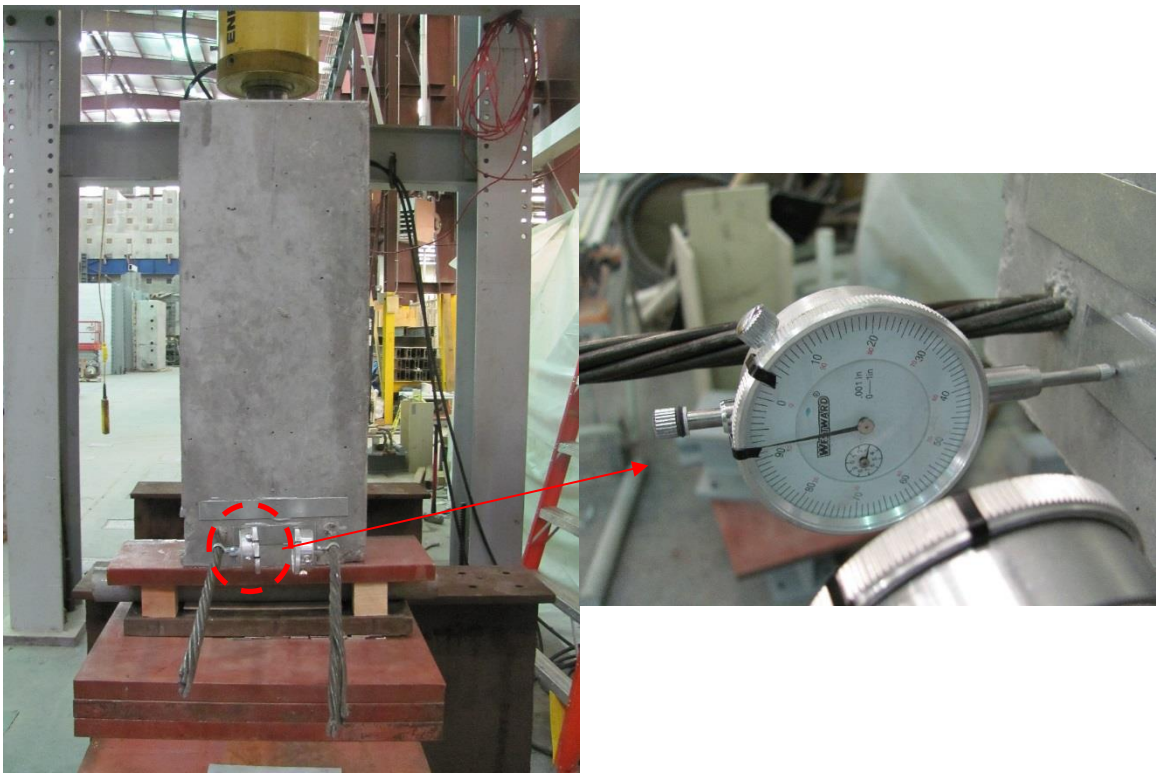

Figure 3.38: Gages used for measuring strand slip in the development length test

3.11.3.5 Flexural capacity

The third test of each beam was conducted to compare the flexural capacity of beams made with Type I/II cement to beams made with Type IL cement. For the third test, the beam was loaded at midspan, and the supports were moved inward and placed at

114 in. from each end the damaged areas from the previous two tests out of the tested segment, as shown in Figure 3.39.

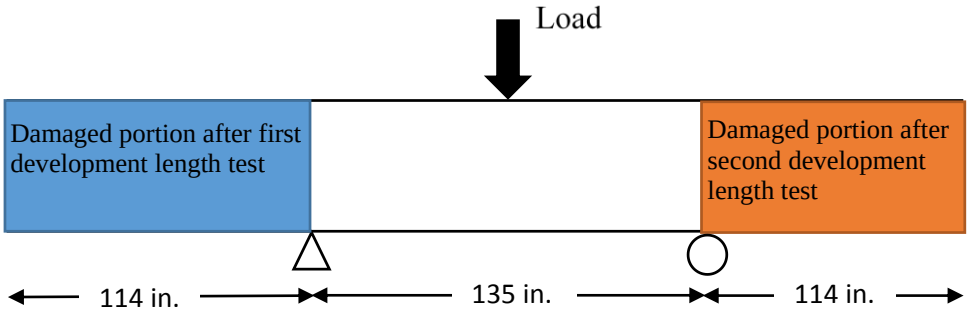

Figure 3.39: Flexural strength test schematic

CHAPTER 4: CEMENT CHARACTERIZATION

4.1 Quantitative X-ray diffraction

Table 4.1 shows the results of the quantitative X-ray diffraction (QXRD) analysis for Type I/II and Type IL cements from plants A – E. The chemical compositions of all Type I/II cements followed the specifications of ASTM C 150. Plant E had the highest amount of C_3S which contributed to early age microstructural and strength development. Plants A and B had more C_2S which contributed to later microstructural and strength development. Plant D had the highest percentage of C_3A and Plant B had the most C_4AF.

Table 4.1: QXRD analysis results (%)

Phase Name	Cement Source										
	A	AL	B	BL	C	CL	D	DL	E	EL C	ELF
C_3S	52.1	50.8	55.9	54.3	60.9	52.7	55.5	53.5	64.3	61.9	54.4
C_2S	24.2	17.3	21.6	15.3	16.4	17.9	17.4	15.3	13.1	7.6	14.7
C_3A cubic	2.95	3.27	2.78	2.1	1.9	1.54	4.22	4.1	4.23	3.83	3.3
C_3A orthorhombic	0.01	0	0.19	0.49	0	0	0.73	0.55	0	0.07	0.14
C_3A TOTAL	2.96	3.27	2.97	2.59	1.9	1.54	4.95	4.65	4.23	3.9	3.44
C_4AF	10.3	9.3	12.9	13.5	12.2	12.1	10.8	9.9	10.6	10.3	10.3
Lime	0.26	0.1	0.34	0.16	0.25	0.19	0.42	0.27	0.28	0.04	0
Periclase	3.11	2.23	0.19	0.26	0.81	0.48	0.33	0.14	0.98	1.39	1.73
Quartz	0.03	0.1	0.07	0.32	0.23	0.3	0.45	0.83	0.06	0.18	0.31
Arcanite	0.26	1.09	0.32	1.26	0.01	0.15	0.29	0.41	1.1	1.76	2.16
Gypsum	0.25	0.75	0	0.01	0.01	0.01	0.01	0.01	0.03	0.02	0.1
Bassanite / Plaster	1.99	1.6	3.19	3.32	2.45	2.99	3.86	2.94	1.62	1.05	0.28
Anhydrite	0.06	0.12	1.55	0.87	0.06	0.01	0.07	0.04	0.17	2.34	1.77
Calcite	3.24	12.2	1.07	7.9	4.22	10.8	4.15	10.5	2.39	8.28	9.78
Portlandite	1.29	1.18	0	0.21	0.63	0.82	1.74	1.52	1.17	1.32	1.12

4.2 Particle size analysis

Particle size analysis was performed on cements from all 5 plants and is shown in Table 4.2 and Figure 4.1. The results show that there were two groups of Type IL cements: Type IL with finer particle size than Type I/II and Type IL with similar particle size to Type I/II. It was observed that particle size was an important factor in predicting hydration, early-age shrinkage, and strength development rates. The Type IL cements from sources A, D, and E had finer particle size distributions compared to their Type I/II counterparts, but the Type IL cements from sources B and C were found to be more similar in gradation to the Type I/II cement. Coarse gradations for Type IL cements have been found in previous studies to correlate with slower rates of hydration, reduced early-age shrinkage, and slower rates of compressive strength development.

Table 4.2: Particle size summary for cements A-E [50]

Cement	D_{10} [μm]	D_{50} [μm]	D_{90} [μm]	Surface weighted mean ($D_{3,2}$) [μm]	Volume weighted mean ($D_{4,3}$) [μm]	SSA [m^2/kg]	Blaine [m^2/kg]	SG
A	2.77	10.0	30.2	6.28	14.1	288	448	3.08
AL	2.29	7.5	21.8	5.09	10.2	356	597	3.05
B	3.17	10.4	31.9	6.71	15.1	282	416	3.17
BL	2.41	10.1	32.1	5.83	14.3	326	600	3.11
C	3.03	10.1	34.1	6.53	15.1	278	465	3.04
CL	2.25	10.2	33.6	5.60	14.6	324	606	3.01
D	2.45	11.9	34.0	6.19	15.5	293	460	3.10
DL	2.37	9.5	28.6	5.66	12.9	321	574	3.07
E	3.15	11.8	36.2	7.07	16.8	257	428	3.10
EL (CG)	2.99	10.8	32.8	6.69	14.9	271	511	3.05
EL (FG)	2.54	8.9	25.4	5.72	11.8	317	553	3.10

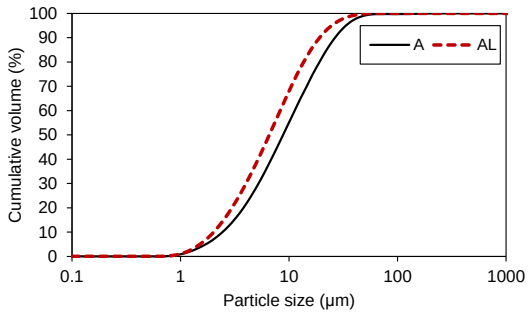

(a) Plant A

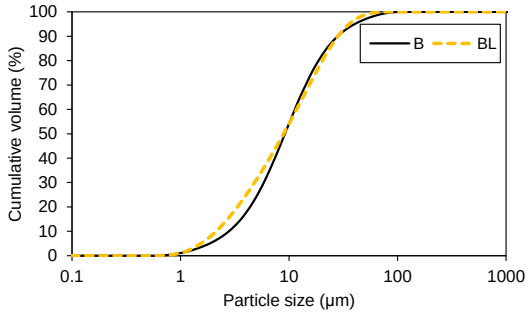

(b) Plant B

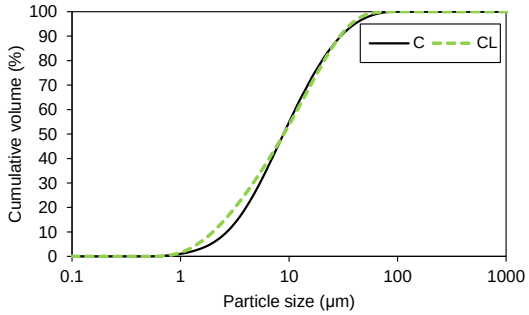

(c) Plant C

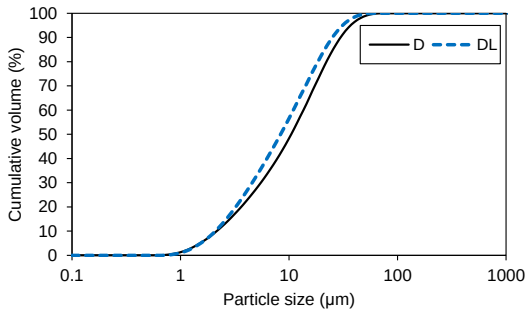

(d) Plant D

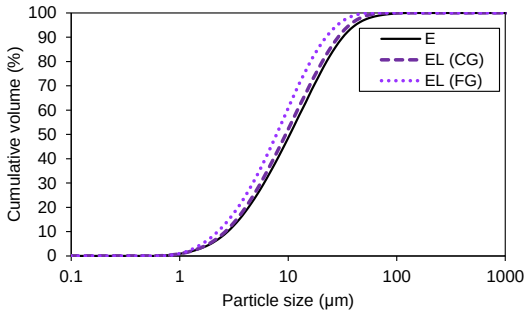

(e) Plant E

Figure 4.1: Cumulative particle size distribution for cements A to E

4.3 Calorimetry

4.3.1 Cements without SCMs

Isothermal calorimetry was performed on cement pastes at 140 °F for Cements A-E. Pastes were prepared at a *w/b* = 0.44 which is the maximum *w/b* specified for class AAA concrete in GDOT Section 500 [40]. The results are shown in Figure 4.2.

Finer Type IL cements (AL, DL, ELC, and ELF) showed an accelerated hydration reaction compared to the companion Type I/II cement pastes, as indicated by the left shift of the heat release (measured as power) curves. The total cumulative heat converged with the companion Type I/II for these finer Type IL cements. On the other hand, the coarser Type IL cements (BL and CL) showed slower hydration and less cumulative heat than their companion Type I/II cements, indicating less total hydration.

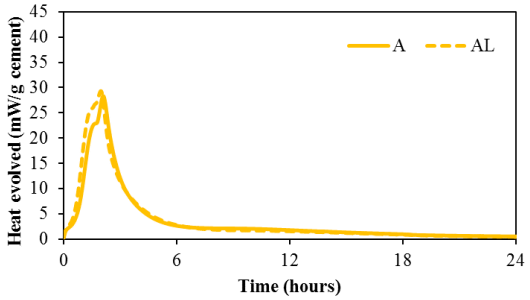

(a) Plant A (heat evolved)

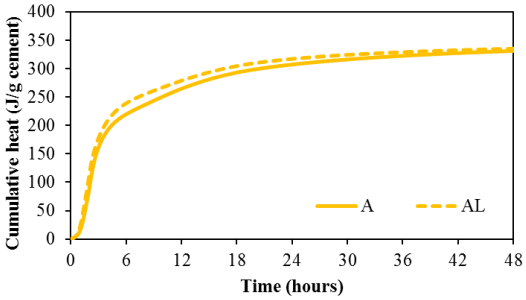

(b) Plant A (cumulative heat)

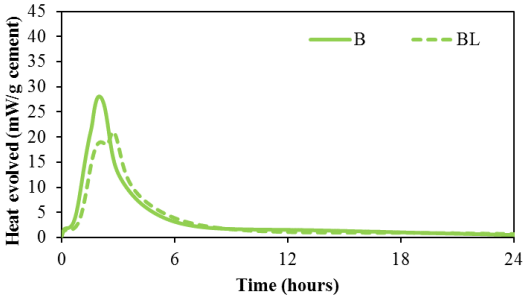

(c) Plant B (heat evolved)

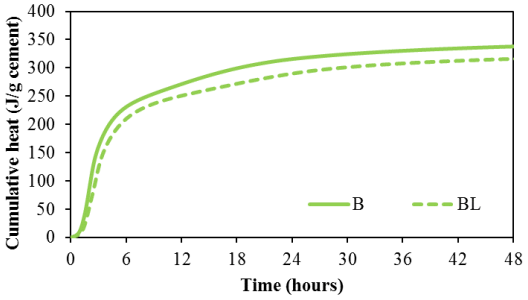

(d) Plant B (cumulative heat)

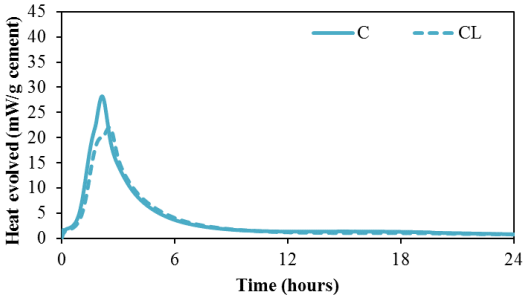

(e) Plant C (heat evolved)

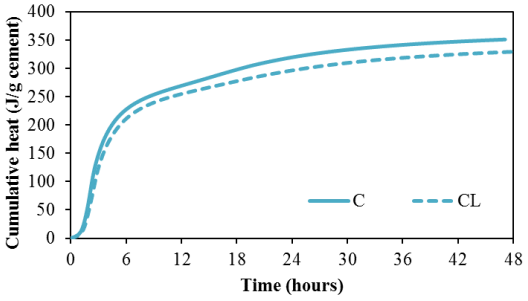

(f) Plant C (cumulative heat)

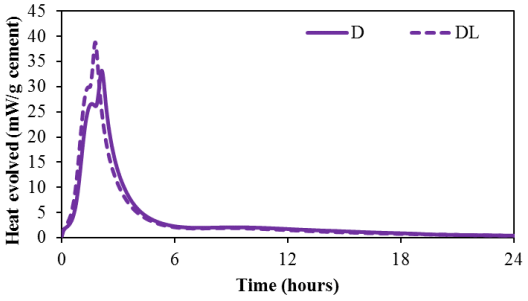

(g) Plant D (heat evolved)

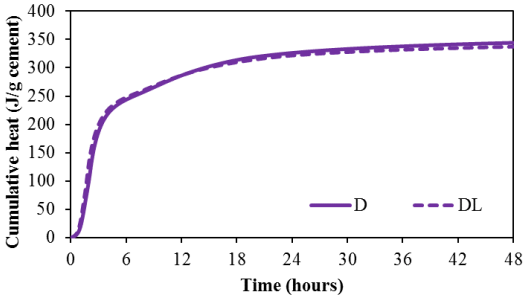

(h) Plant D (cumulative heat)

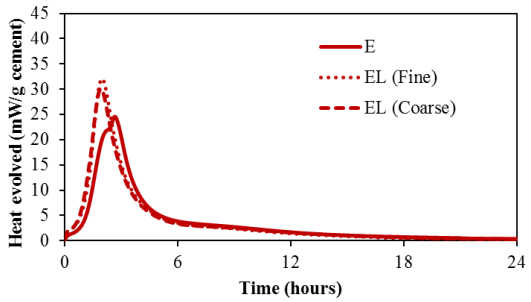

(i) Plant E (heat evolved)

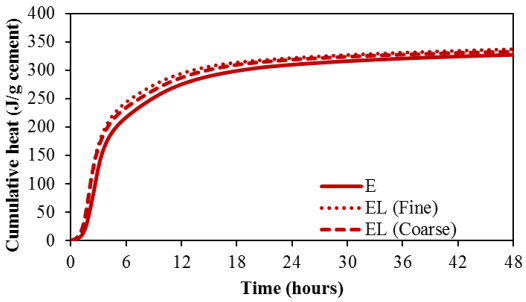

(j) Plant E (cumulative heat)

Figure 4.2: Calorimetry results (power and cumulative heat of hydration) for cements A to E at 140 °F

When compared to results of calorimetry performed at 73 °F [50], similar trends with cement fineness were observed. Figure 4.3 shows a comparison of the calorimetry results of cements from plants A and C at 73 °F and 140°F.

For the finer Type IL cement (AL), Type IL cement produced higher cumulative heat than Type I/II cement at 73 °F, while the cumulative heat converged at 140°F.

On the other hand, the coarser Type IL cement (CL) produced similar cumulative heat to Type I/II cement at 73 °F, while Type IL cement produced lower cumulative heat than Type I/II cement at 140 °F. These results suggest that early age strength development may be slightly delayed in precast concrete utilizing Type IL cements with similar fineness to Type I cements.

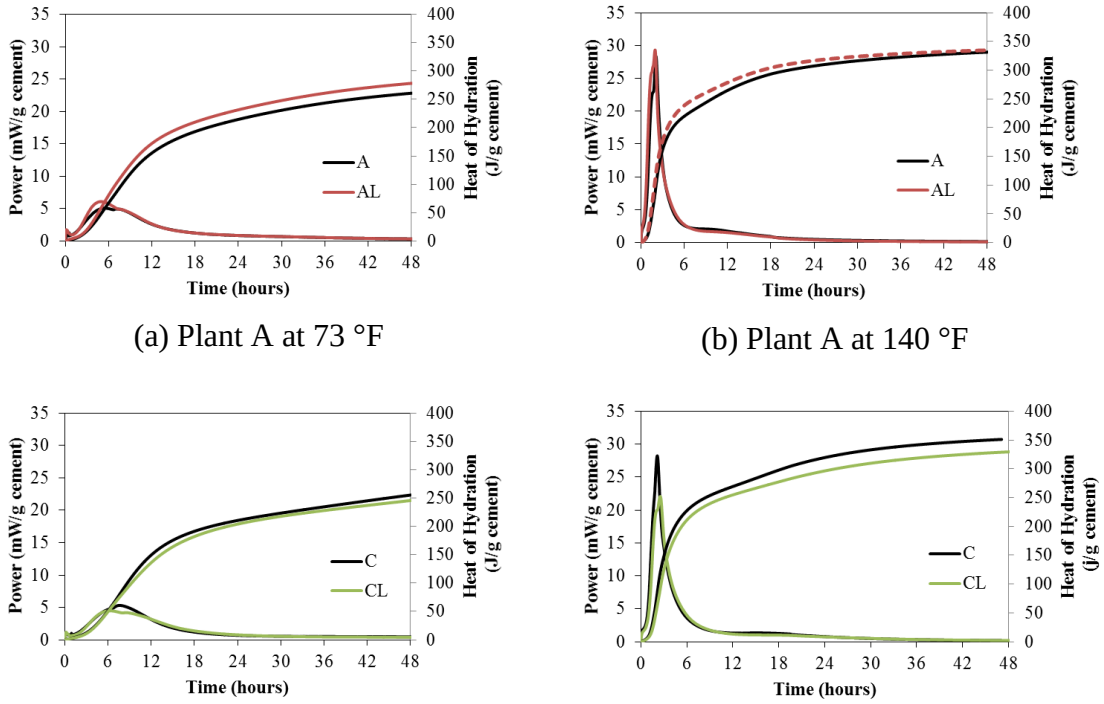

(a) Plant A at 73 °F

(b) Plant A at 140 °F

(c) Plant C at 73 °F

(d) Plant C at 140 °F

Figure 4.3: Isothermal Calorimetry of cements from plants A and C at 73°F and 140 °F

4.3.2 Cements with SCMs

Isothermal calorimetry was also performed on cement pastes from plant A and plant C at 140 °F with the following secondary cementitious materials (SCMs): 50% slag and 15% fly ash (Class C and Class F). Pastes were prepared at a *w/b* = 0.44 which is the maximum *w/b* specified for class AAA concrete in GDOT Section 500.

Figure 4.4 shows the isothermal calorimetry heat evolution curves of cements from plants A and C with SCMs. For the finer Type IL cement (AL), Type IL cement showed an accelerated hydration reaction with all SCMs when compared to the companion Type I/II cement with SCMs, as indicated by the left shift of the heat release

(power) curves. Additionally, the peaks of power evolution were higher for Type IL cements when compared to their companion Type I/II cements. This results in faster hydration kinetics which may result in greater early strength. On the other hand, the coarser Type IL cement (CL) showed slower hydration with all SCMs with lower peaks of power evolution when compared to the companion Type I/II cement with SCMs. This indicates slower hydration reaction kinetics and therefore suggest slower early strength gain.

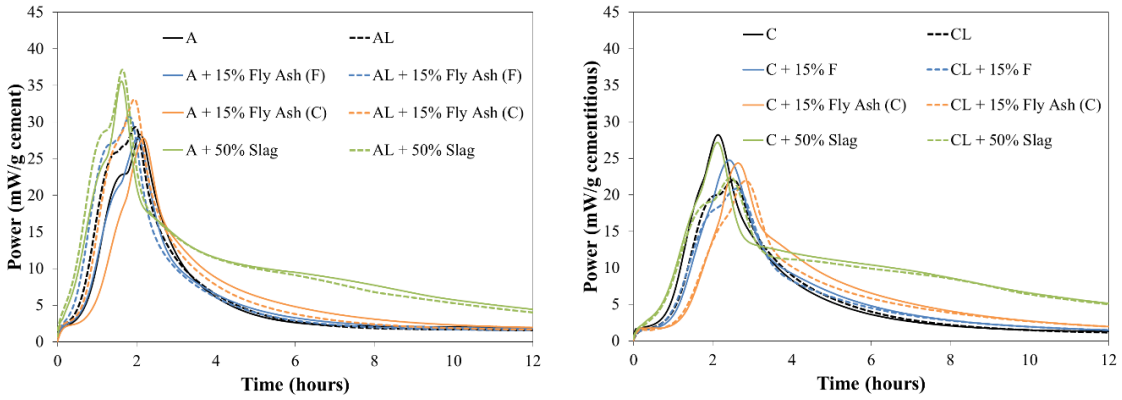

(a) Plant A (b) Plant C

Figure 4.4: Isothermal calorimetry heat evolution curves for cements from plants A and C with secondary cementitious materials (SCMs)

Figure 4.5 shows the cumulative heat of hydration curves for cements from plants A and C with SCMs. For the finer Type IL cement (AL), Type IL cement with SCMs showed similar cumulative heat of hydration to the companion Type I/II cement with SCMs. This may indicate similar quantity hydration microstructure which may result in equivalent strength values on the long term. On the other hand, the coarser Type IL cement (CL) showed ~5% lower cumulative heat of hydration with all SCMs than Type

I/II cement. This may indicate that lower quantity of hydration microstructure which may result in lower strength values in the long term.

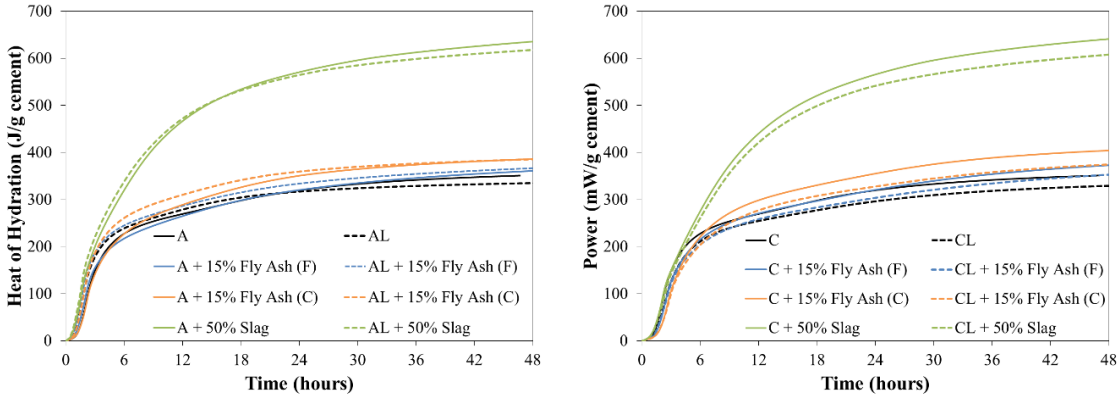

(a) Plant A (b) Plant C

Figure 4.5: Cumulative heat of hydration curves for cements from plants A and C with secondary cementitious materials (SCMs)

CHAPTER 5: TIME OF SETTING

5.1 Group 1: Plain mixes at 73 °F

Figure 5.1 shows the results of the time of setting for the group of samples from sources A to E and tested at 73 °F.

The results show that Type IL cement showed faster setting time (10% to 20%) for finer limestone cements (such as AL and ELF) and similar setting time for the coarser ones (CL). Higher fineness provides more nucleation sites and therefore increase the rate of hydration which explains the faster setting.

In contrast to the trends related to cement fineness, cement BL showed faster setting time than cement B (~25%) although cements B and BL were of similar fineness. Also, cement D and DL showed similar setting times although cement DL was finer. An aluminate-to-sulfate imbalance can result in slower or faster set [51]. QXRD analysis showed that Cements B, BL, D, and DL had higher orthorhombic C_3A than the rest of the cement sources.

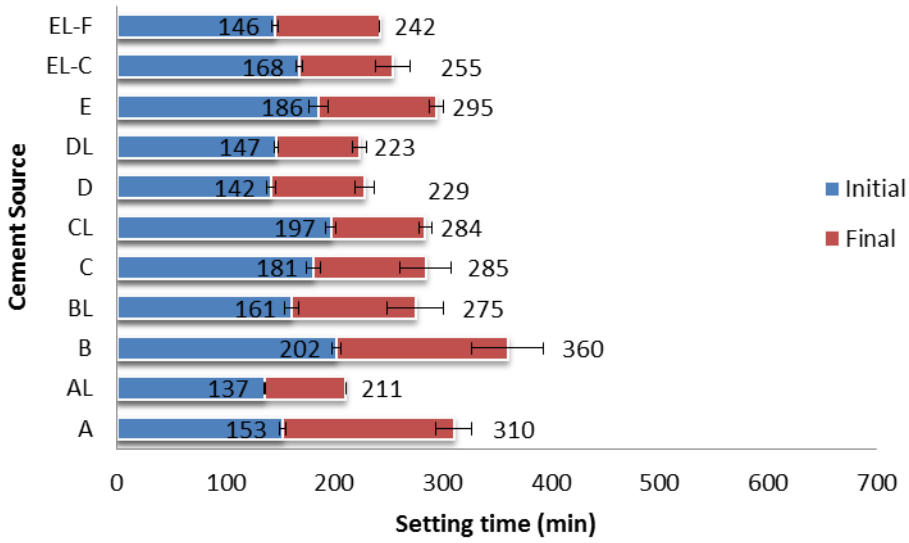

Figure 5.1: Time of setting of cements A to E at 73 °F

The data in Figure 5.1 was then used with the QXRD results to create Figure 5.2 which shows a scatter plot of the relation between calcite content and setting time together with linear regression best fit lines. The results show that the setting time decreased with higher calcite content. The slope of the linear best fit line for the final setting was steeper than the one for the initial setting, indicating a higher effect of the calcite content on the final setting time.

The author included coefficient of determination (R^2) values in the plot to indicate the variance of errors when using a linear fit between the independent and dependent variables, such as calcite content vs setting time. This value is a good indicator for further research. The R^2 value depends on several factors including correlation model used, sample size (epistemic uncertainty), and the standard errors in the independent variables

[52]. Epistemic uncertainty can be reduced by a larger sample size. Therefore, a low R^2 value does not indicate no relation between the dependent and independent variables. The dependent variables that are discussed in this thesis depend on many independent variables. For example, setting time depends on the fineness, the proportioning of the main cement phases (i.e. chemical composition), aluminate-to-sulfate balance, calcite content, temperature, consistency (normal consistency was not achieved in all samples to keep a constant *w/b* among the samples), and others. In an ideal comparison, all these independent variables except for one need to be kept constant to observe the effect of changing that one independent parameter. That was not possible in this research since the cement samples were collected from regional cement producers with varying cement compositions and properties.

Another significant factor that lead to low R^2 values in this research is that the sample size was small in most cases. The author investigated many different performance-related variables, but the sample size in each of these tested performance variables was limited to a maximum of eleven cement types, i.e. a maximum of eleven points in the scatter plot. That number is relatively low and further research with larger sample size is recommended.

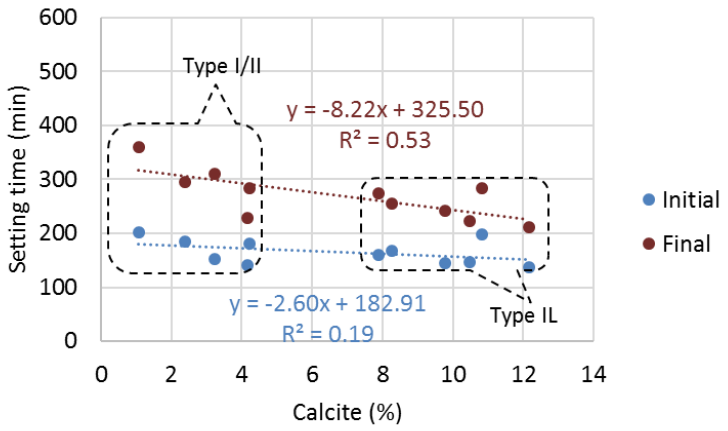

Figure 5.2: Effect of calcite content on setting time at 73 °F

Figure 5.3 shows the effect of the particle size on the setting time at 73 ºF. The results show that larger particle size led to slower setting time. When the data for Type I/II and Type IL cements were separated, as shown in Figure 5.4, the results showed that the particle size had a more significant effect on Type IL cements than Type I/II cements.

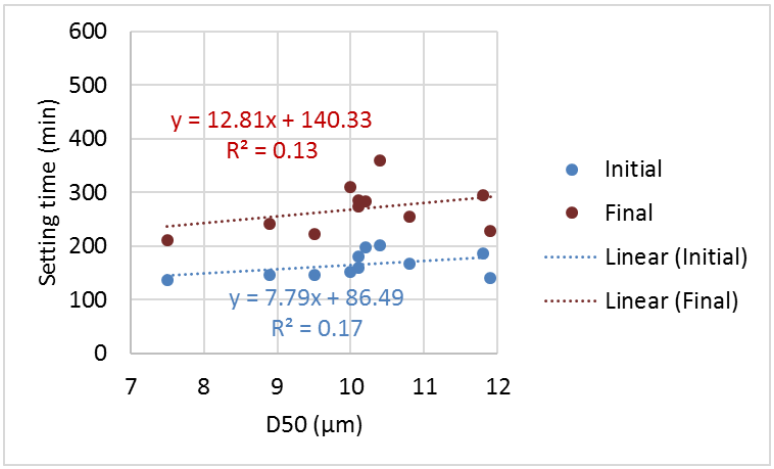

Figure 5.3: Effect of particle size on the setting time at 73 ºF

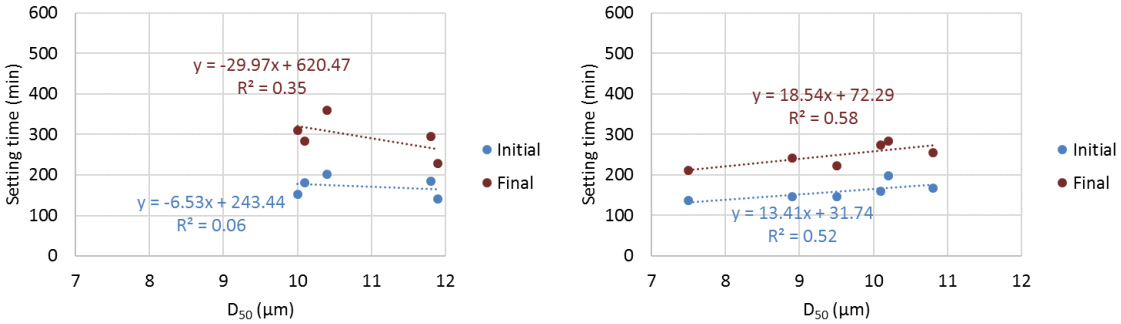

(a) Type I/II (a) Type IL

Figure 5.4: Effect of particle size of Type I/II and Type IL cements on the setting time at 73 ºF

In general, the values of the setting times are relatively close to those reported in the literature (but with lower limestone replacements). Table 5.1 and Table 5.2 show the results reported by Hooton [53] and [3]

Table 5.1: Vicat setting times for ASTM and CSA Cements [53]

Cement label	CaCO3, % (TGA)	Initial Set (min)	Final Set (min)
1 (10.3% C_3A)	0.3	175	355
1c	4.1	167	323
2 (9.1% C_3A)	0.8	134	283
2c	4.7	119	224
3 (8.3% C_3A)	0.3	153	294
3c	2.6	170	340

Table 5.2: Vicat Setting Times for interground Cements at Constant Blaine [3]

% Limestone by mass of total cement	Initial Set (min)	Final Set (min)
0	160	300
3	170	300
5.5	170	295
8	165	290

5.2 Group 2: Plain mixes at 90 °F

Figure 5.5 shows the results of the time of setting for the group of samples from sources A to E and tested at 90 °F.

The results show that Type IL cement showed faster setting time (7% to 25%). The exception was cement D and DL where the setting time was relatively similar (within the standard deviation).

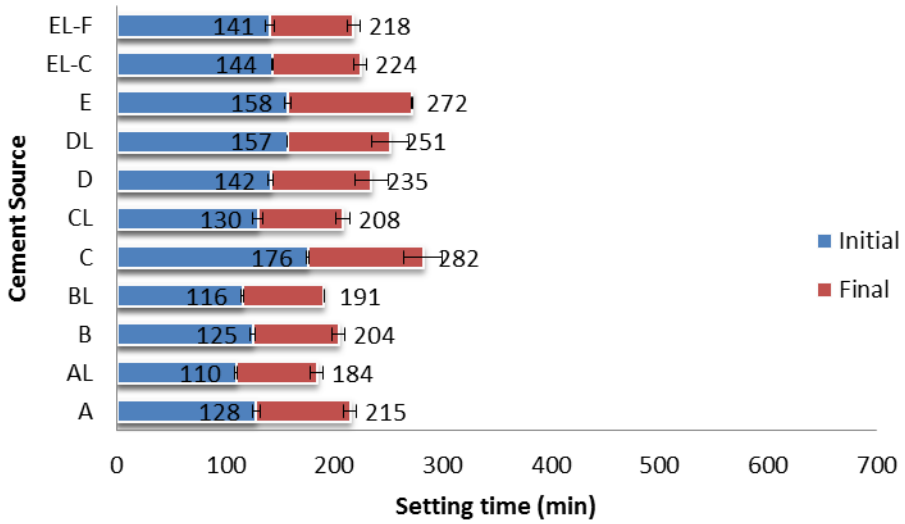

Figure 5.5: Time of setting of cements A to E at 90 °F

Figure 5.6 shows a comparison of the setting time at 90 °F and 73 °F for Type I/II cements and Type IL cements. The results show that the higher temperature caused a larger difference of the setting time of Type I/II cement than Type IL cement. For example, the higher temperature decreased the setting time of cement A by 31% where it

decreased the setting time of cement AL by 13%. This indicated that the dilution effect of limestone replacement of clinker was more dominant at higher temperatures.

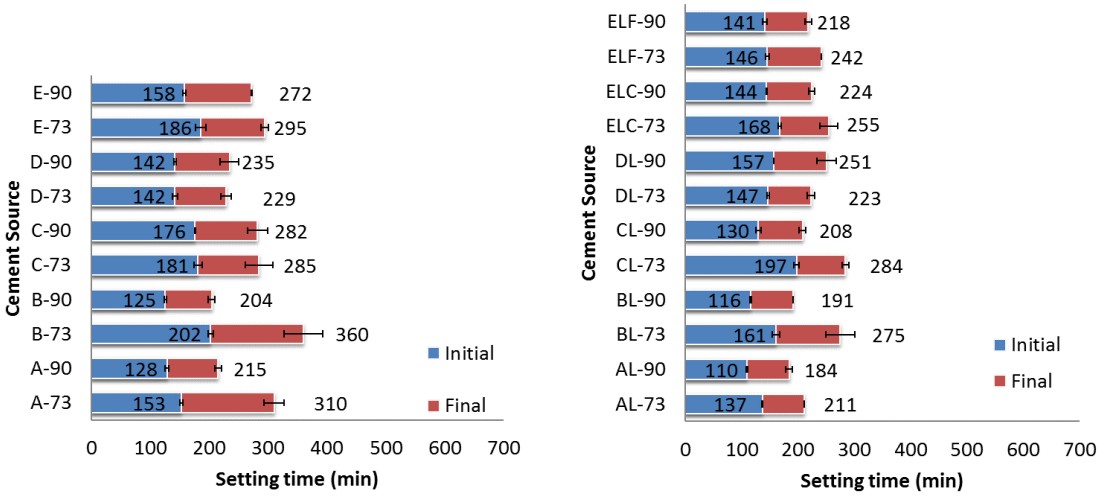

(a) Type I/II (b) Type IL

Figure 5.6: Time of setting of Type I/II cements (a) and Type IL cements (b) at 73 °F and at 90 °F

It should be noted that this effect was not observed for cements C and D. The QXRD analysis showed that cement C had ~15% more C_3S than cement CL while the amount of C_2S was relatively similar in both. Cement D had ~4% more of C_3S but ~12% more of C_2S than cement DL. This may have affected the rate of hydration at higher temperature. The lack of consistency in the C_3S and C_2S in Type I/II and Type IL from sources C and D affected the trends observed for the setting time at higher temperature.

Figure 5.7 shows the scatter plot of the relation between calcite content and setting time at 90 °F. The results show that the setting time decreased with higher calcite content. The data in Figure 5.7 was separated to produce separate scatter plots for Type I/II and Type IL, as shown in Figure 5.8, which shows a conflicting behavior of Type I/II

and Type IL cements at 90 ºF. For Type I/II, higher calcite content led to a slower setting time. However, for Type IL, higher calcite content led to faster setting time.

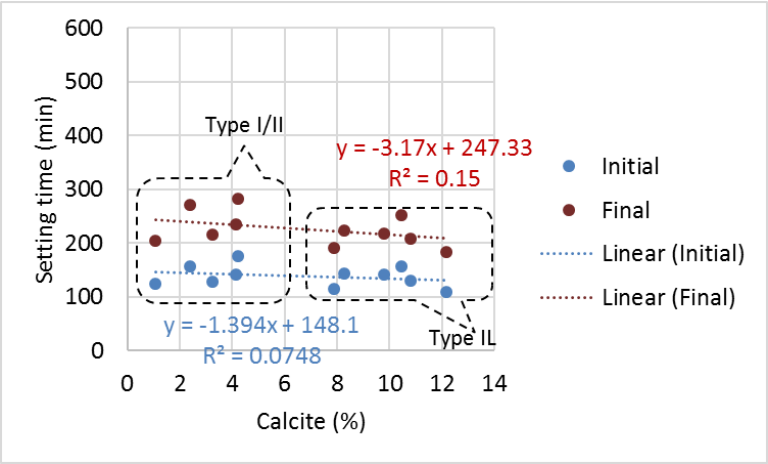

Figure 5.7: Effect of calcite content on setting time at 90 °F

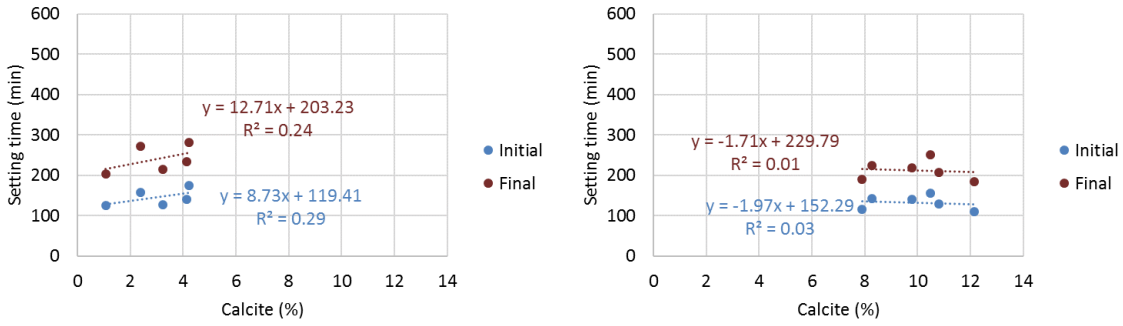

(a) Type I/II (b) Type IL

Figure 5.8: Effect of calcite content on setting time of Type I/II and Type IL cements at 90 °F

Figure 5.9 shows the scatter plots of the relation between the setting time and the C_3A content for Type I/II and Type IL cements at 90 ºF. For Type I/II cement, higher

C_3A content led to faster setting time. However, for Type IL cement, higher C_3A content led to slower setting time, indicating an interference of limestone with the hydration of C_3A phase at 90 ºF (which was not observed at 73 ºF).

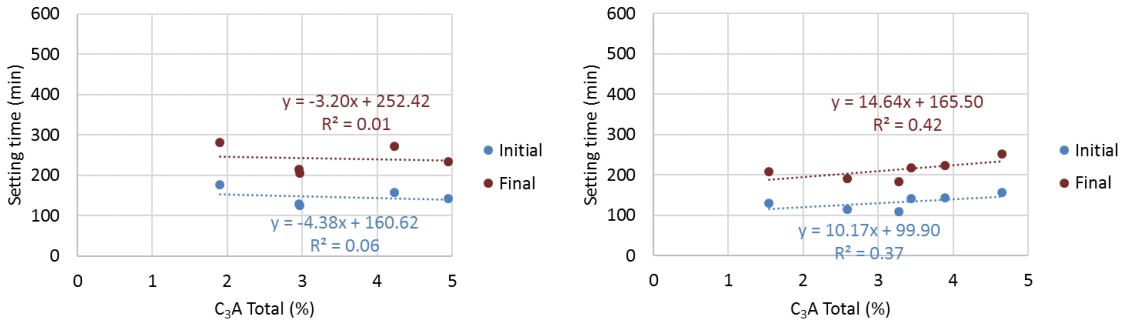

(a) Type I/II (b) Type IL

Figure 5.9: Effect of C_3A content on setting time of Type I/II and Type IL cements at 90 °F

5.3 Group 3: Plain mixes at 40 °F

Figure 5.10 shows the results of the time of setting for the group of samples from sources A to E and tested at 40 °F.

The results show that Type IL cements experienced faster setting time (~10% to ~40%) than their companion Type I/II cements. The exception was cement DL where the setting time was larger (~10%).

As described for the higher temperature, cement D had ~4% more of C_3S but ~12% more of C_2S than cement DL. This may have affected the rate of hydration at lower temperature.

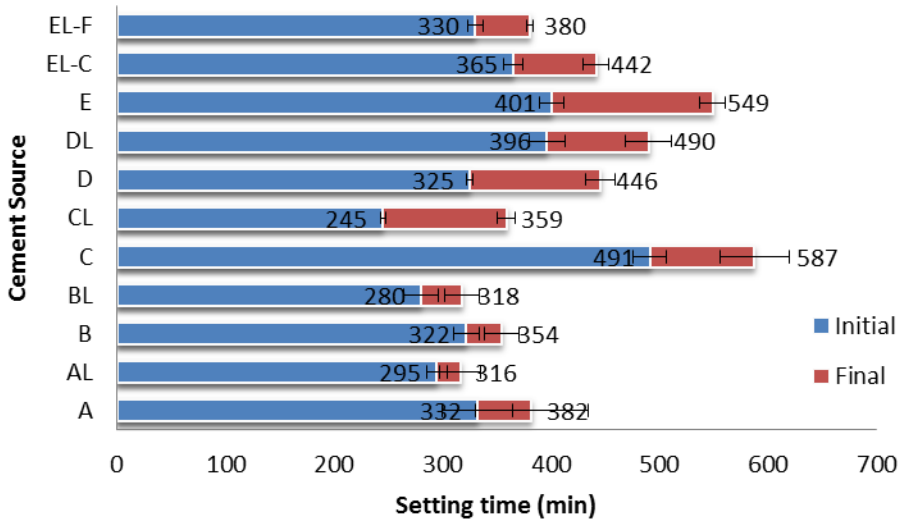

Figure 5.10: Time of setting of cements A to E at 40 °F

Figure 5.11 shows a comparison of the setting time at 40 °F and 73 °F for Type I/II cements and Type IL cements. The results show that the lower temperature caused a larger difference of the setting time of Type IL cement than Type I/II cement. For example, the lower temperature increased the setting time of cement A by 23% where it increased the setting time of cement AL by 50%. This indicated that the nucleation effect of limestone replacement of clinker was more dominant at lower temperatures.

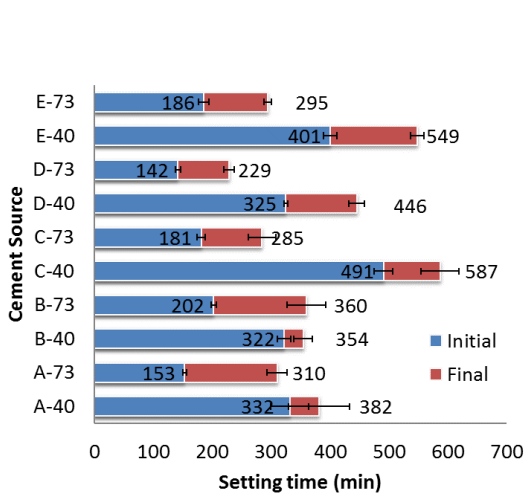

(a) Type I/II

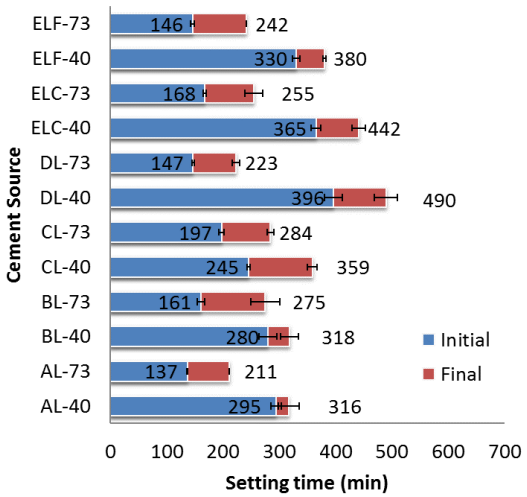

(b) Type IL

Figure 5.11: Time of setting of Type I/II cements (a) and Type IL cements (b) at 40 °F and at 73 °F

Figure 5.12 shows scatter plots of the relation between calcite content and setting time for Type I/II and Type IL cements at 40 ºF. For Type I/II, the higher calcite content led to slower setting time. However, for Type IL, higher calcite content led to faster setting time.

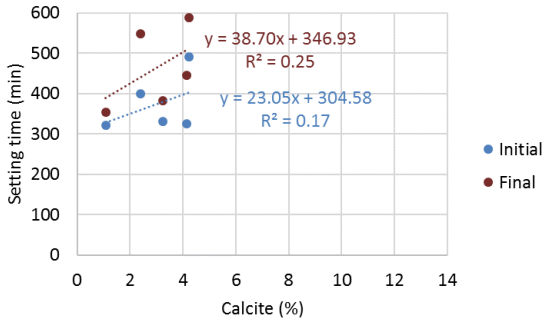

(a) Type I/II

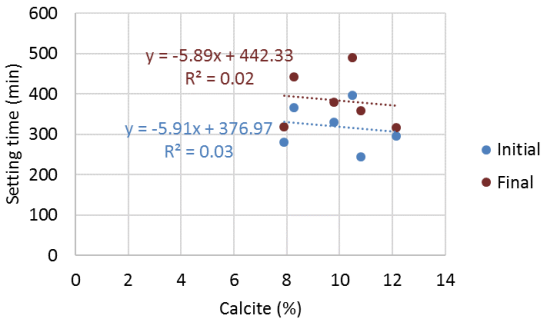

(b) Type IL

Figure 5.12: Effect of calcite content on setting time of Type I/II and Type IL cements at 40 °F

Figure 5.13 shows scatter plots of the relation between C_3A content and setting time for Type I/II and Type IL cements at 40 ºF. For Type I/II, the higher C_3A content led to faster setting time. However, for Type IL, higher C_3A content led to slower setting time, indicating an interference of limestone with the hydration of C_3A phase at 40 ºF (which was not observed at 73 ºF).

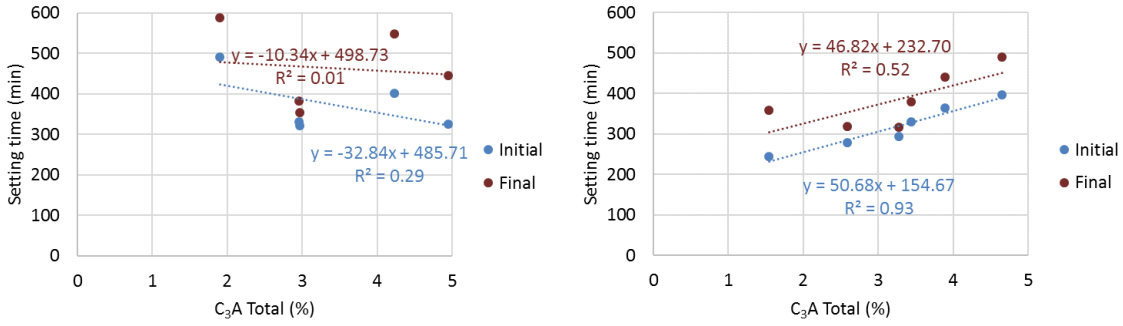

(a) Type I/II (b) Type IL

Figure 5.13: Effect of C_3A content on setting time of Type I/II and Type IL cements at 40 °F

5.4 Group 4: SCM mixes at 73 °F

5.4.1 Fly ash

Figure 5.14 and Figure 5.15 show the results of the time of setting for the group of samples with 15% fly ash Class F and Class C, respectively, from sources A to E were tested at 73 °F.

For class F ash, the results show that Type IL cement showed faster setting time (~6% to ~25%) for sources A, D, and E which was the group of Type IL cements with higher fineness. Type I/II and IL from sources B and C showed similar times of setting

and that was the group of Type IL cements with similar particle sizes to their companion Type I/II cement.

For class C ash, the results show that Type IL cement showed faster setting time (~7% to ~10%) for sources A, B, C, and E. Type I/II and IL from source D showed faster setting than Type IL.

In general, class F showed faster setting than class C (~14% average). This is due to the higher fineness of class F fly ash.

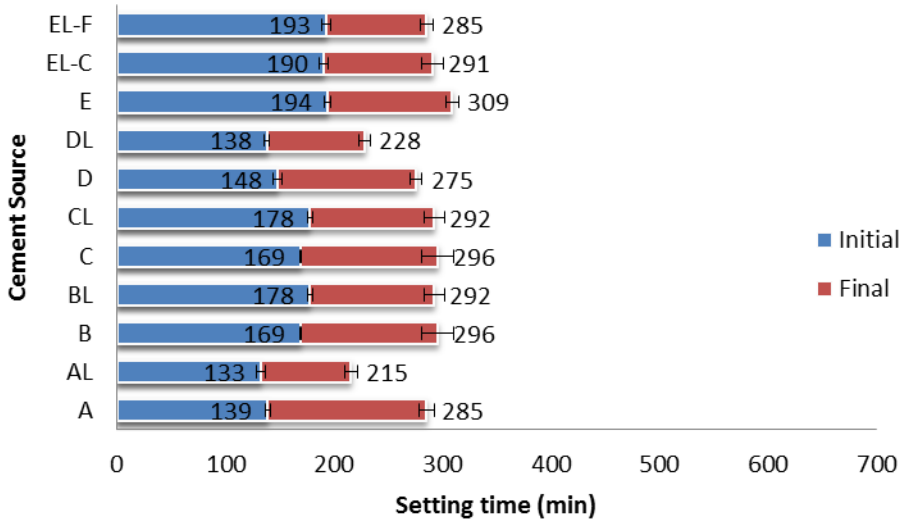

Figure 5.14: Time of setting of cements A to E with 15% fly ash Class F at 73 °F

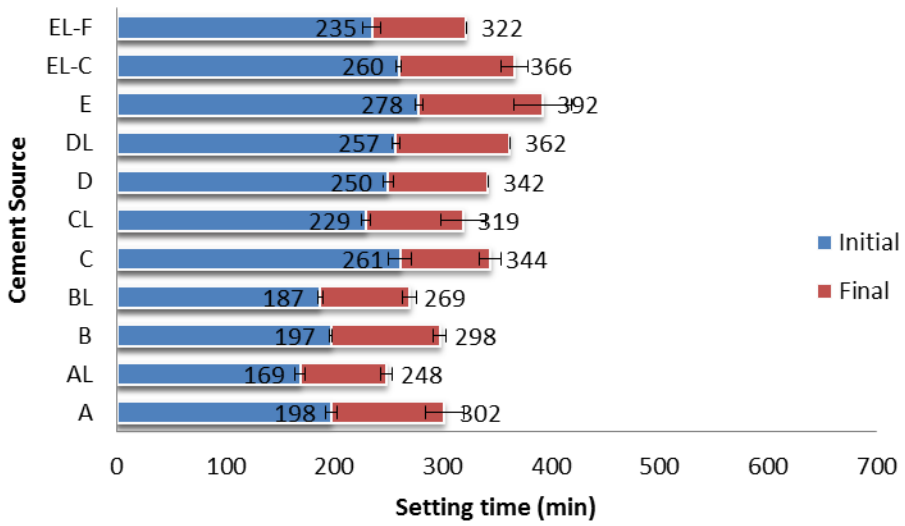

Figure 5.15: Time of setting of cements A to E with 15% fly ash Class C at 73 °F

Figure 5.16 and Figure 5.17 show the effect of calcite content on the setting time of pastes of pastes with 15% replacement by weight of cement with fly ash. The results show that higher calcite content led to faster setting time for both classes of fly ash.

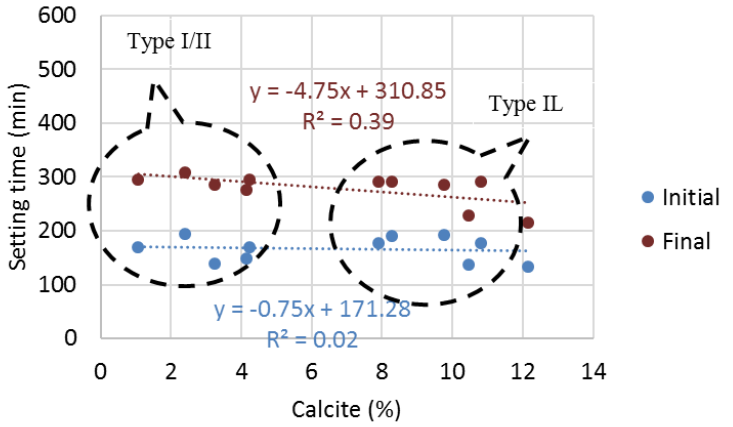

Figure 5.16: Effect of calcite content on the setting time of pastes with 15% Class F fly ash

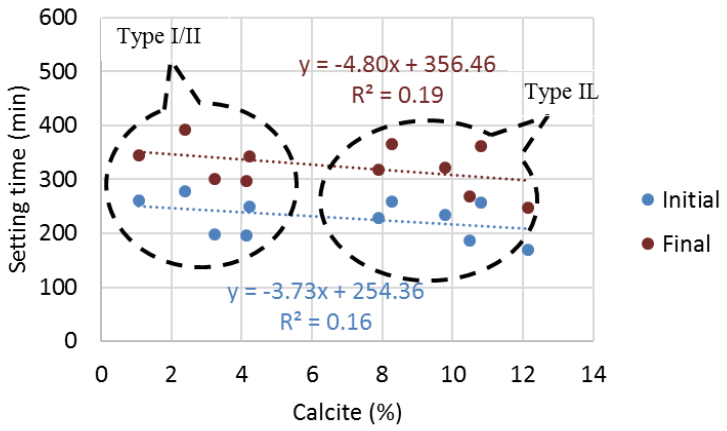

Figure 5.17: Effect of calcite content on the setting time of pastes with 15% Class C fly ash

5.4.2 Slag

Figure 5.18 shows the results of the time of setting for the group of samples with 50% slag from sources A to E were tested at 73 °F.

The results show that Type IL cement showed relative similar setting times of Type I/II and Type IL cements (with one standard deviation). Slag was finer than all the cements which had a dominant effect over the limestone replacement.

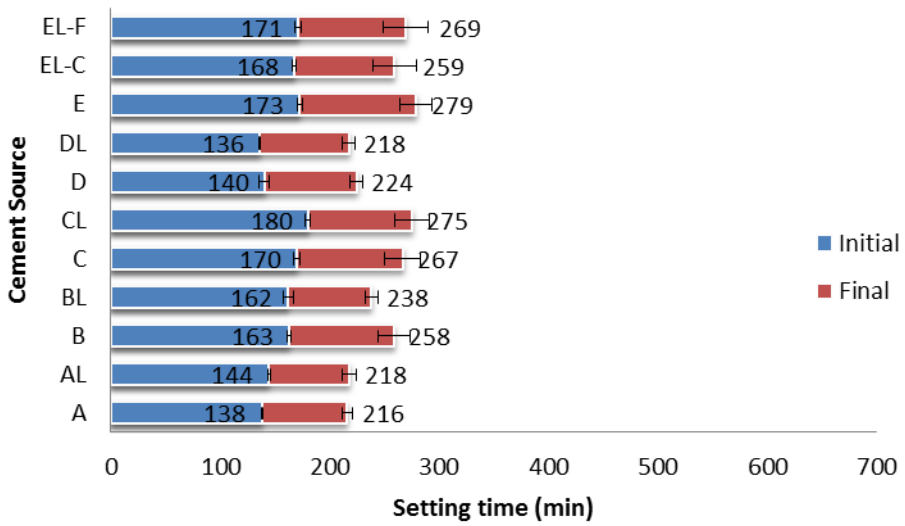

Figure 5.18: Time of setting of cements A to E with 50% slag at 73 °F

Figure 5.19 shows the effect of calcite content on the setting time of pastes with 50% replacement by weight of cement with slag. The results show that the calcite content had no significant effect on the setting time.

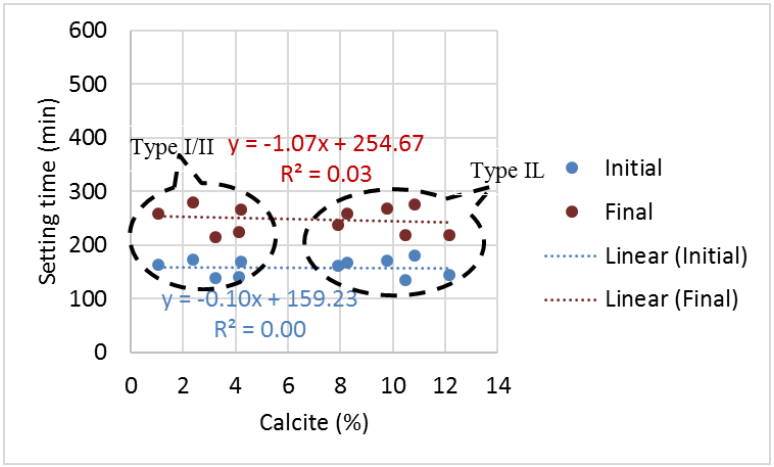

Figure 5.19: Effect of calcite content on setting time of cement pastes with 50% slag replacement

5.5 Chapter discussion and conclusions

The trends shown in the previous section showed that calcite content affects the setting time. The scatter plots showed that higher content of calcite reduced the setting time for Type IL cement at 40 ºF, 73 ºF, and 90 ºF. These results agree with the results of El- Didamony et al. [25] shown in Figure 2.7 (shown again below for ease of the reader) that showed faster setting with higher limestone added (when above 5% as in Type IL cements). The results also showed that Type IL cement is more sensitive to lower temperature. For example, when comparing the setting times at 40 °F and at 73 °F, the lower temperature increased the setting time of cement A by 23% where it increased the setting time of cement AL by 50%. This indicated that the nucleation effect of limestone replacement of clinker was more dominant at lower temperatures.

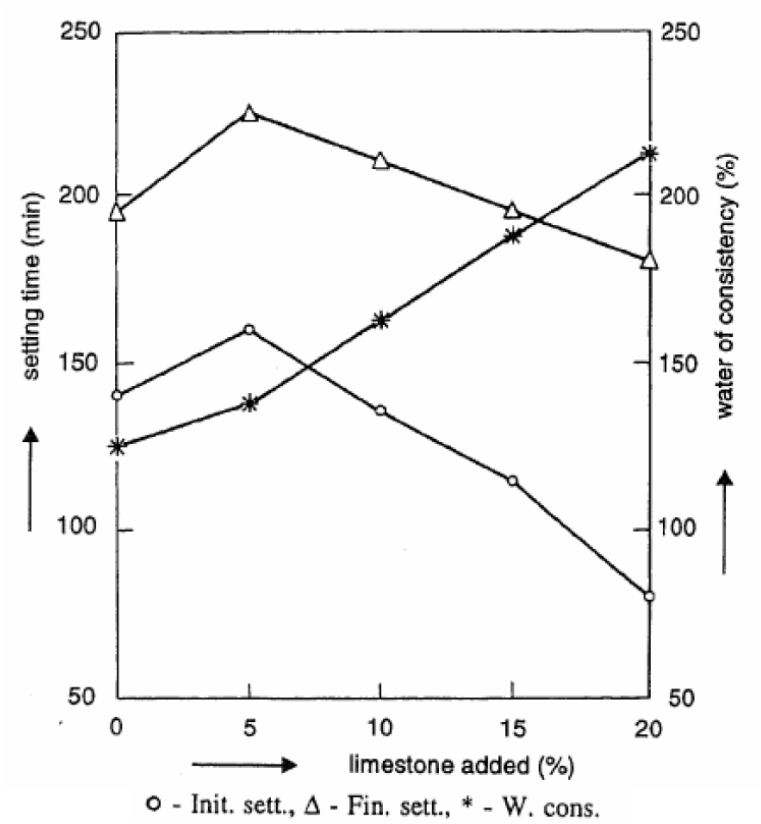

Figure 2.7: Setting time and water demand of portland-limestone content pastes [25]

Larger particle size increased the setting time for Type IL cement. The same conclusion could not be made for Type I/II due to the lack of variation of mean particle size of the Type I/II samples.

Higher C_3A content increased the setting time of Type IL cement at 40 ºF and 90 ºF, while it higher C_3A content decreased the setting time at 73 °F; suggesting an interaction of limestone with C_3A at 40 ºF and 90 ºF.

For the SCM mixes, higher calcite content resulted in lower setting time when blended with fly ash, while the calcite content did not show a significant effect on setting time when blended with slag.

The coefficient of determination was generally low but that can be attributed to factors discussed in section 5.1 including small sample size (epistemic uncertainty), standard errors in the independent variables (aleatoric variability), and the model used. Equally important, setting time depends on several other factors such as fineness, the proportioning of the main cement phases (i.e. chemical composition), aluminate-to-sulfate balance, calcite content, temperature, consistency (normal consistency was not achieved in all samples to keep a constant *w/b* among the samples). These factors were not constant and have therefore interfered with the results.

Despite the fact that the R^2 values were low, the results show trends that are a good starting point for further research. The author recommends further research with larger sample size for the effect of calcite content, the C_3A content (especially at low temperature), and particle size on setting time at various temperatures. The author also include recommends a parametric study of the effect of each of the cement and SCM phases on the setting time.

CHAPTER 6: EFFECT OF *W/B* AND CEMENT FACTOR ON MECHANICAL PROPERTIES AND DRYING SHRINKAGE OF CONCRETE

This chapter discusses the effect of *w/b* and cement factor (amount of cement per cubic yard of concrete) on the mechanical properties and drying shrinkage of concrete. Three different groups of concretes were produced based on the mix designs mentioned in Section 3.6, where the *w/b* was 0.489, 0.445, and 0.320 and were labelled Class A, AA, and AAA, respectively following the labels used in Georgia Department of Transportations (GDOT) Section 500 [40].

Throughout chapters 6 to 9, each concrete mix was labelled using a three-part label. The first part referred to the cement source used (as per Section 3.2.1). The second part of the label refers to the concrete class (Section 3.6), and the third part referred to the curing temperature. For this chapter, all the samples were cured at 73 °F. For example, BL-AA-73 referred to class AA concrete (*w/b* = 0.445 and cement factor = 635 lb/yd^3) made with Type IL cement from source "B".

6.1 Compressive strength

6.1.1 Class AA concrete (w/b = 0.445, cf = 635 lb/yd^3)

Initially, all of the cement sources (A to E) were used to produce Class AA concrete. Figure 6.1 shows the compressive strength values (up to 1 year) of Class AA concrete made with Type I/II and Type IL cements from plants A to E. The Class AA

specimens were cured in saturated lime-water baths at room temperature (73 ºF) until testing. Other samples were cured at 40 ºF and at 90 ºF as discussed in Chapter 7.

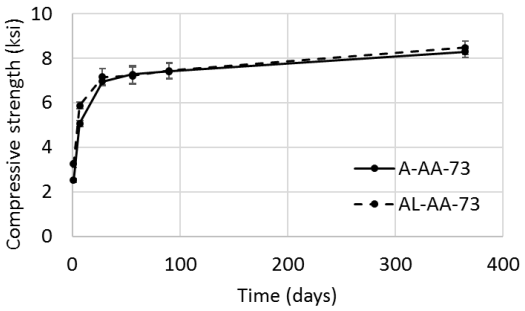

(a) Plant A

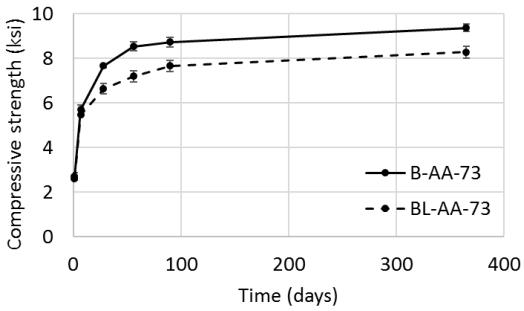

(b) Plant B

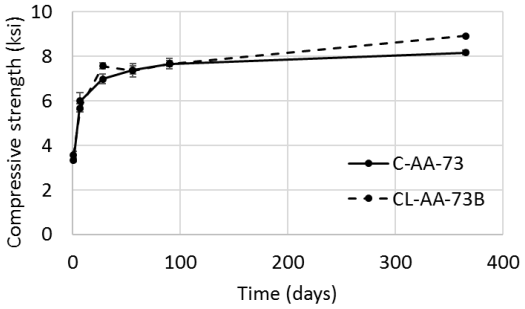

(c) Plant C

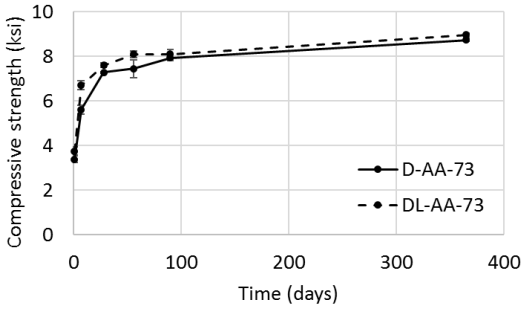

(d) Plant D

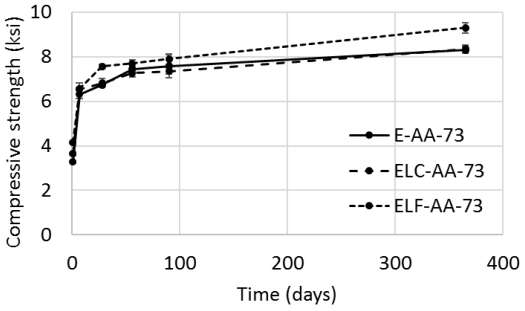

(e) Plant E

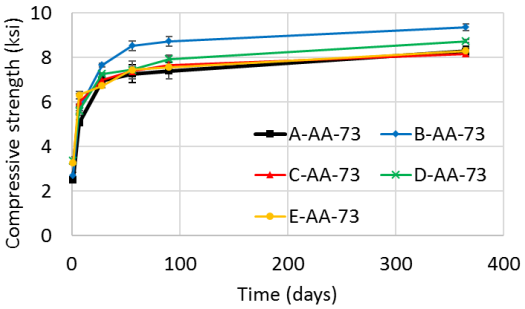

(f) Concrete made with Type I/II

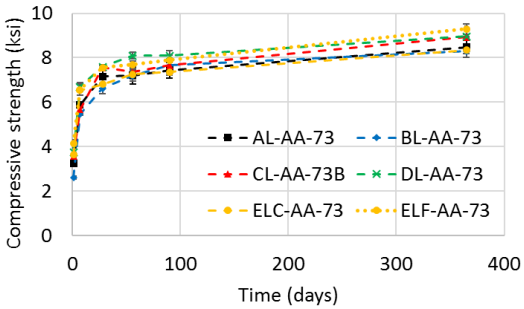

(g) Concrete made with Type IL

Figure 6.1: Compressive strength of Class AA concrete.

At one day, concretes made with the finer Type IL cements (AL, DL, ELC, and ELF) showed 10% to 35% higher compressive strength than concretes made with their companion Type I/II cement. The coarser Type IL cements showed values closer to Type I/II cement (~3% higher for CL). The author hypothesizes that the finer limestone cements provided additional nucleation sites which resulted in faster hydration and higher strength at early age.

At one year, all Type IL cements showed either equal or up to 20% higher strength when compared to their companion Type I/II cement. This indicated that the dilution effect had a negligible effect on the long-term strength of Type IL cement.

The calcite content, the average particle size, and the percentage of cement phases (C_3S, C_2S, C_3A, and C_4AF), were investigated for their effects on the compressive strength.

Figure 6.2 shows a scatter plot of calcite content vs. the compressive strength of class AA concrete at 1 day, 28 days, and 1 year. After applying a linear regression best fit

line, it can be seen that the higher the calcite content, the greater the compressive strength, however the effect of calcite content diminishes for strength at 1 year. The data also suggest that for Type IL cement, about 10% calcite content produces a maximum strength for all ages.

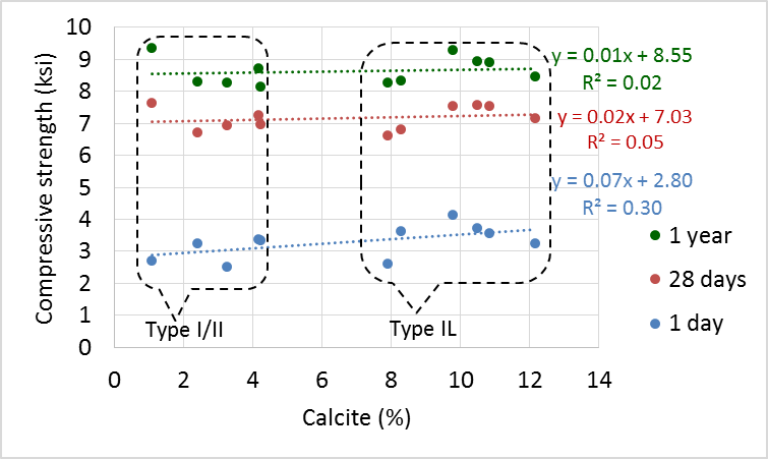

Figure 6.2: Effect of calcite content on compressive strength of class AA concrete

Analysis of variance (ANOVA) was conducted to investigate the statistical significance of the difference in values of the compressive strength of concretes made with Type I/II or Type IL cement of each plant. The null (no difference) hypothesis was that average strength of Type I/II and Type IL are similar ($\mu 1=\mu 2$). A summary of the results for class AA concrete is shown in Table 6.1. If the p-value was lower than 0.05, the null hypothesis was rejected and the difference in the average strength values were considered statistically significant. If the p-value was higher than 0.05, the differences were considered statistically insignificant. If the differences were statistically significant,

the percentage difference is shown. A positive percentage difference indicates concrete with Type IL showed a higher value than concrete made with Type I/II cement.

Table 6.1: ANOVA results for comparing Type I/II and Type IL from each plant for the compressive strength of Class AA concrete

Time	Cement source					
	A/AL	B/BL	C/CL	D/DL	E/ELC	E/ELF
7 days	+3%	Similar	Similar	+19%	Similar	Similar
28 days	Similar	-14	+8%	Similar	Similar	+12%
1 year	Similar	-12%	+9%	Similar	Similar	+12%

The results showed that the fine-grade Type IL cement from plant E showed statistically significant different results when compared to Type I/II from the same plant, while there was no statistical significance in the difference between the strength of the coarse grade Type IL cement and Type I/II from plant E.

The author hypothesized that there are more differences between plant producers than there are between Type I/II and Type IL from the same plant. Table 6.2 shows the ANOVA results of comparing the compressive strength of class AA concrete among all five different plants.

Table 6.2: ANOVA results for comparing the differences between plants for the compressive strength of class AA concrete

Time	Cement Source	
	Type I/II	Type IL
7 days	Different	Different
28 days	Different	Different
1 year	Different	Similar

The results show that difference in strength between plants was statistically significant in all cases except the 1-year strength of Type IL cement. This indicates that the difference between plants has a more significant effect on strength than the difference between Type I/II and Type IL. The results also show that there is no statistical significance difference of the strengths of Type IL cements from different producers at 1 year.

Referring to the literature review discussed earlier, the trends seen here were that the higher calcite content increased early-age strength of concrete agreed with the results reported by Hooton et al. [4] and Tsivilis et al. [22], where higher limestone content (up to 10%) resulted in higher 1, 2, and 7 days strength, as shown in Figure 2.8 (copied here for ease of the reader). Differences in cement chemistry, particle size distributions, concrete mix proportions, limestone material properties, among other factors can and have affected the results. Nevertheless, the trends seen in the research reported herein indicate relationships between strength, calcite content, and fineness which need further analyses with larger sample sizes.

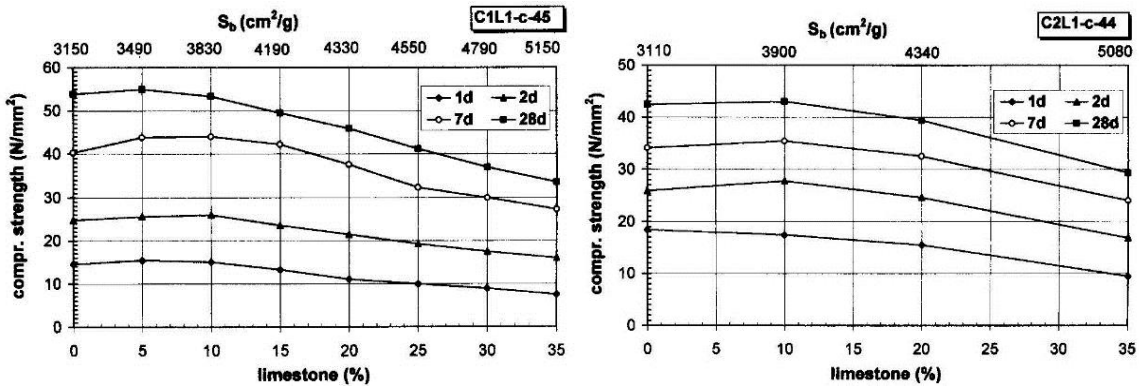

A) C_3S=65%, C_2S=13%, C_3A=8%, C_4AF=11%

B) C_3S=58%, C_2S=19%, C_3A=12%, C_4AF=6%

Figure 2.8: Influence of limestone content on strength development [22]

6.1.2 Class AAA concrete (w/b = 0.320, cf = 800 lb/yd^3)

After examining the properties and performance of Class AA concrete made with all cements, it was found that cement fineness had significant effects on the performance of concrete. Cement producer "A" had finer Type IL cement while producer "C" had Type IL cement with a fineness more similar to that of the Type I/II cement. Based on that, cement from producers "A" and "C" were selected for the class AAA study. Figure 6.3 shows the compressive strength of Class AAA concrete from plants A and C. The concrete was cured at room temperature (73 °F) in a lime-saturated water bath until testing.

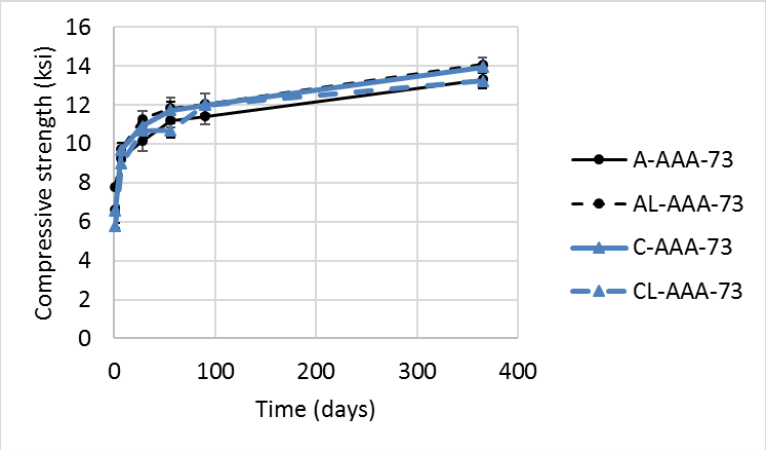

Figure 6.3: Compressive strength of Class AAA concrete from Plants A and C

When comparing the effect of Type I/II and Type IL cements in class AAA concrete, cement AL resulted in higher concrete strength than cement A at all ages. However, cement CL resulted in lower concrete strength than cement C at all ages up to 90 days where the strength converged with concrete made with cement C. Fineness had a significant effect for class AAA concrete. The finer Type IL cement (cement AL) resulted in higher concrete strength while the coarser Type IL (cement CL) resulted in a lower concrete strength. The strength of concrete made with cement CL later converged with that of concrete made with cement C indicating negligible significance of the dilution effect at later ages. Another point to note is that the difference in strength of concretes made with cements A and AL of class AAA concrete was higher than the difference between concretes made with cement A and AL of class AA concrete.

Class AAA concrete showed higher strength than class AA concrete for both plants. When comparing each cement of class AAA concrete with the same one from class AA concrete, the difference was about 60% for all cements at 90 days. However, at

one day, there was a larger variability. Cement A and AL of class AAA concrete showed a relatively larger difference than cements A and AL of class AA (~160% and 140%, respectively). Cement C and CL of class AAA concrete showed a relatively smaller difference than cements C and CL of class AA concrete (~100% and ~60%, respectively). This implies that the effect of fineness is more significant at early ages.

Figure 6.4 shows a scatter plot of calcite content vs. the compressive strength of concrete class AAA, at 1 day, 28 days, and 1 year. The higher the calcite content, the greater the compressive strength. This indicates that the nucleation effect was significant.

The author included coefficient of determination (R^2) values in the plot to indicate the variance of errors when using a linear fit between the independent and dependent variables, such as calcite content vs compressive strength. This value is a good indicator for further research. The R^2 value depends on several factors including correlation model used, sample size (epistemic uncertainty), and the standard errors in the independent variables [52]. Epistemic uncertainty can be reduced by a larger sample size. Therefore, a low R^2 value does not indicate no relation between the dependent and independent variables. The dependent variables that are discussed in this thesis depend on many independent variables. For example, compressive strength depends on the fineness, the proportioning of the main cement phases (i.e. chemical composition), calcite content, the moisture content of the coarse and fine aggregates, and others. In an ideal comparison, all these independent variables except for one need to be kept constant to observe the effect of changing that one independent parameter. That was not possible in this research since

the cement samples were collected from regional cement producers with varying cement compositions and properties.

Another significant factor that lead to low R^2 values in this research is that the sample size was small in most cases. The author investigated many different performance-related variables, but the sample size in each of these tested performance variables for Class AAA concrete was limited to a maximum of four cement types, i.e. a maximum of four points in the scatter plot. That number is relatively low and further research with larger sample size is recommended.

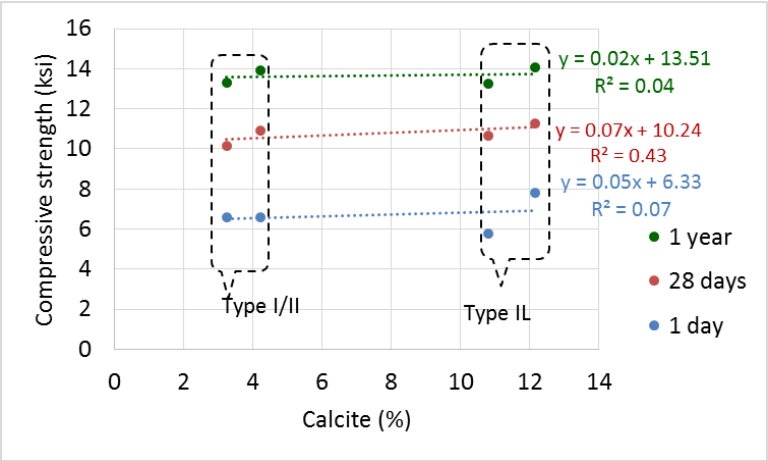

Figure 6.4: Effect of calcite content on the compressive strength of class AAA concrete

Analysis of variance (ANOVA) was conducted to investigate the statistical significance of the difference in values of the compressive strength of Type I/II and Type IL cement of plants A and C. A summary of the results for class AAA concrete is shown in Table 6.3. A positive percentage difference indicates concrete with Type IL showed a higher value than concrete made with Type I/II cement.

Table 6.3: ANOVA results for comparing Type I/II and Type IL from each plant for the compressive strength of Class AAA concrete

Time	Cement source	
	A/AL	C/CL
7 days	Similar	-7%
28 days	+11%	Similar
1 year	Similar	-5%

The results showed that the difference in concrete strength between C and CL were statistically significant. Cement CL had a similar fineness to cement C but had a lower strength (dilution effect). Cement AL was finer and that increased the strength which also decreased the difference between A and AL leading to statistically insignificant differences between A and AL. In addition to that, the author investigated the effect of different cement source on the strength of Type I/II and Type IL cements. Table 6.4 shows the ANOVA results of comparing the compressive strength of class AAA concrete among plants A and C.

Table 6.4: ANOVA results for comparing the differences between plants for the compressive strength of class AAA concrete

Time	Cement Source	
	Type I/II	Type IL
7 days	Similar	AL > CL by 8%
28 days	Similar	Similar
1 year	Similar	AL > CL by 6%

The results show that difference in strength between plants was not statistically significant for Type I/II cement but was statistically significant for Type IL cement. This indicates that for class AAA concrete, the difference in the cement source has a significant effect on strength of Type IL cement but not on Type I/II cement for class AAA concrete (due to the difference of fineness of cements AL and CL).

6.1.3 Class A concrete (w/b = 0.49, cf = 611 lb/yd^3)

Cement producers A and C were selected to produce Class A concrete for the same reasons mentioned for class AAA concrete. Figure 6.5 shows the compressive strength of class A concrete from plants A and C.

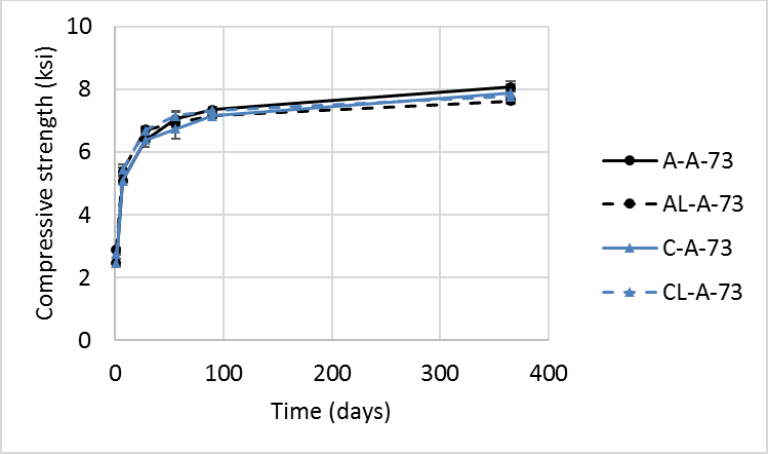

Figure 6.5: Compressive strength of class A concrete from Plants A and C

The general trend observed was that at higher *w/b*, the difference in concrete strength when using Type I/II or Type IL cements were relatively smaller due to the higher dilution effect. When comparing Type I/II and Type IL cements of class A concrete, cements AL and CL showed slightly lower strength than cement A and C,

respectively, at all ages (~3% at 90 days). This indicates that at this higher *w/b* ratio, the dilution effect was more significant than at lower *w/b* ratios. At early age, the difference was larger for cement CL (~20%) than cement AL (~10%), indicating that the nucleation effect due to fineness is more significant at early ages. Class A concrete showed slightly lower strength than class AA concrete for both plants. When comparing each cement of class A concrete with the same one from class AA concrete, the difference at 90 days was relatively low (~1% to 7%). However, at one day, there was a larger variability. Cement A and AL of class A concrete showed a relatively lower difference than cements A and AL of class AA (~1% and 11%, respectively). Cement C and CL of class A concrete showed a relatively larger difference than cements C and CL of class AA concrete (~25%). This implies that the effect of fineness is more significant at early ages.

Figure 6.6 shows a scatter plot of calcite content vs. the compressive strength of concrete class A, at 1 day, 28 days, and 1 year. For 1-day and 28-days values, the higher the calcite content, the greater the compressive strength. This indicates that the nucleation effect was significant. The only exception was the 1-year strength values of class A concrete, where the higher the calcite content, the lower the compressive strength, indicating that the dilution effect was significant at later age.

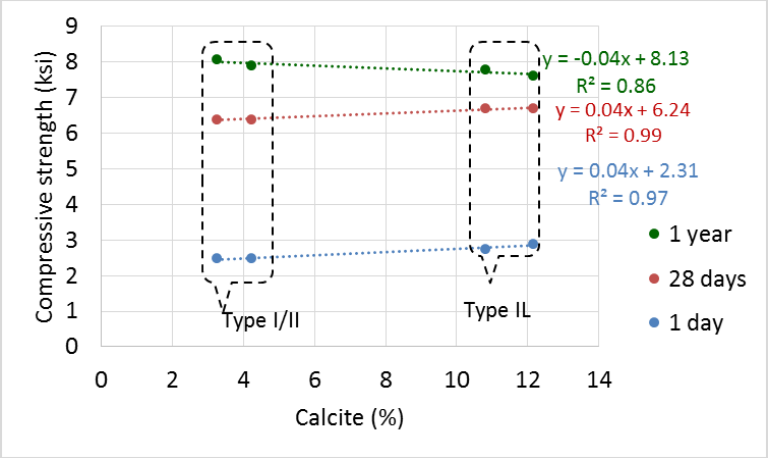

Figure 6.6: Effect of calcite content on the compressive strength of class A concrete

Analysis of variance (ANOVA) was conducted to investigate the statistical significance of the difference in values of the compressive strength of Type I/II and Type IL cement of plants A and C. A summary of the results for class A concrete is shown in Table 6.5. A positive percentage difference indicates concrete with Type IL showed a higher value than concrete made with Type I/II cement.

Table 6.5: ANOVA results for comparing Type I/II and Type IL from each plant for the compressive strength of Class A concrete

Time	Cement source	
	A/AL	C/CL
7 days	Similar	+11%
28 days	Similar	Similar
1 year	-6%	Similar

The results showed that for class A concrete, the difference in strength between Type I/II and Type IL was not statistically significant except for plant A at 1 year and

plant C and 7 days. The author hypothesizes that at this high *w/b* ratio and low cement factor, the effect of limestone replacement on the compressive strength diminishes.

In addition to that, the authors investigated the effect of different cement source on the strength of Type I/II and Type IL cements. Table 6.6 shows the ANOVA results of comparing the compressive strength of class A concrete among plants A and C.

Table 6.6: ANOVA results for comparing the differences between plants for the compressive strength of class A concrete

Time	Cement Source	
	Type I/II	Type IL
7 days	Similar	Similar
28 days	Similar	Similar
1 year	"A" > "C" by 6%	Similar

The results in Table 6.6 show that difference in strength between plants was not statistically significant for Type I/II and Type IL cements, except for the 1-year strength of Type I/II cement. This indicates that for class A concrete, cement source has little effect on the compressive strength.

6.2 Elastic modulus

Elastic modulus was measured for concrete cylinders (6 in. x 12 in.) at 28 days of age. Figure 6.7 shows the elastic moduli [43] for class AA concrete measured at 28 days, along with theoretical values computed using ACI 318-14 [54] section 19.2.2.1:

$$E_c = w_c{}^{1.5} 33 \sqrt{f'_c} \qquad \text{Equation 6.1}$$

where:

- E: modulus of elasticity (psi)
- w_c: unit weight (pcf)
- f_c': compressive strength (psi)

Carrasquillo [55] showed that the ACI equation for predicting the modulus of elasticity over-predicted the values when the concrete compressive strength exceeded 6 ksi, and therefore concluded that a better equation is given by:

$$E = 40000 \sqrt{f'_c} + 10^6 \qquad \text{Equation 6.2}$$

where:

- E: modulus of elasticity (psi)
- f_c': compressive strength (psi)

The above equation is also adopted in ACI 363R-10 [1] (Equation 6-1 in ACI 363R-10) for high strength concrete and provides a better estimate for the measured values of the elastic moduli of all the samples mentioned in this report. Figure 6.7 shows the values calculated with Equation 6.2 which shows better prediction than Equation 6.1.

For class AA concrete, the average elastic moduli of all Type IL samples varied from -5% to +18% compared to the companion Type I/II cement. The largest difference was between Type I/II cement from plant E and the fine-grade Type IL cement from that plant. This indicated that higher fineness increases the elastic modulus due to the formation of more hydrated microstructure. The calculated values obtained using Equation 6.1 over-estimated the values for all cements by an average of 24% for Type I/II and 18% for Type IL mixes. However, the calculated values obtained using Equation 6.2 over-estimated the values for all cements by an average of 7% for Type I/II and 3% for Type IL mixes.

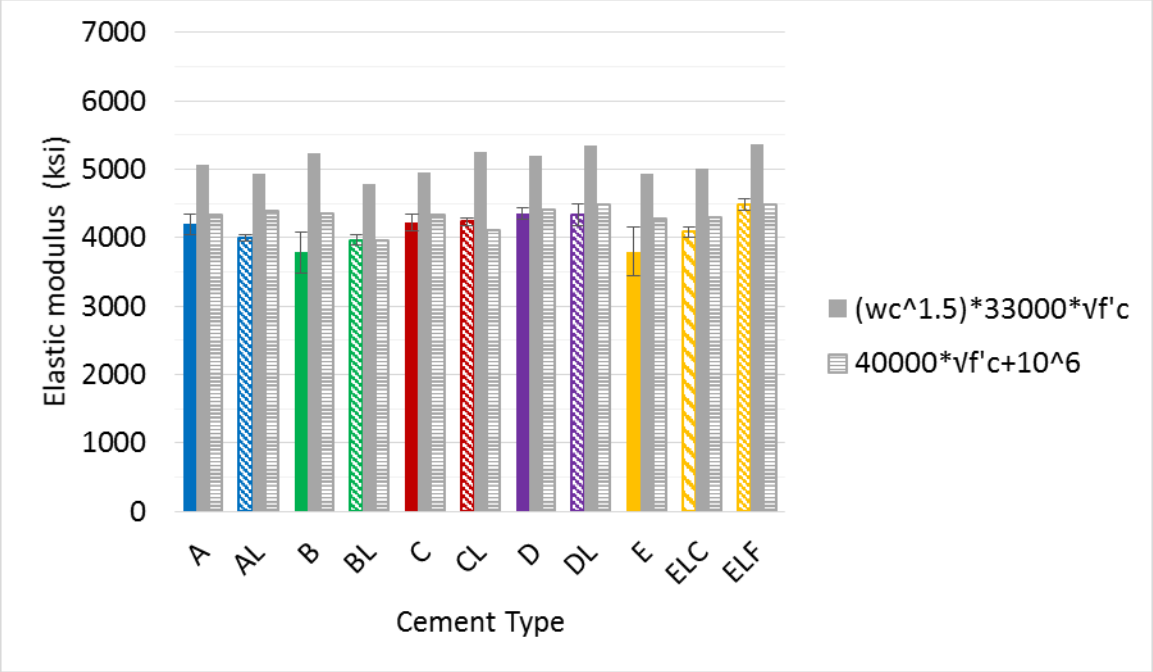

Figure 6.7: Elastic modulus of class AA concrete

Figure 6.8 shows a scatter plot of calcite content vs. the elastic modulus of class AA concrete at 28 days. After applying a linear regression best fit line, it can be seen that the higher the calcite content, the higher the elastic modulus. This indicates that the nucleation effect was significant for the elastic modulus, where a higher calcite content led to a more developed microstructure.

The author included coefficient of determination (R^2) values in the plot to indicate the variance of errors when using a linear fit between the independent and dependent variables, such as calcite content vs the elastic modulus. This value is a good indicator for further research. The R^2 value depends on several factors including correlation model used, sample size (epistemic uncertainty), and the standard errors in the independent variables [52]. Epistemic uncertainty can be reduced by a larger sample size. Therefore, a low R^2 value does not indicate no relation between the dependent and independent variables. The dependent variables that are discussed in this thesis depend on many independent variables. For example, the elastic modulus depends on the fineness, the proportioning of the main cement phases (i.e. chemical composition), calcite content, the moisture content of the coarse and fine aggregates, and others. In an ideal comparison, all these independent variables except for one need to be kept constant to observe the effect of changing that one independent parameter. That was not possible in this research since the cement samples were collected from regional cement producers with varying cement compositions and properties.

Another significant factor that lead to low R^2 values in this research is that the sample size was small in most cases. The author investigated many different

performance-related variables, but the sample size in each of these tested performance variables for Class AA concrete was limited to a maximum of eleven cement types, i.e. a maximum of eleven points in the scatter plot. That number is relatively low and further research with larger sample size is recommended.

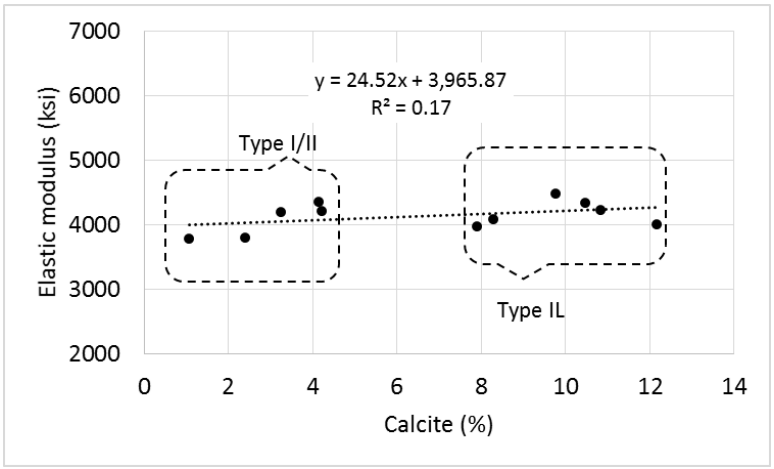

Figure 6.8: Effect of calcite content on elastic modulus of class AA concrete

Figure 6.9 shows the effect of average particle size of cement on the elastic modulus of class AA concrete. The results show low correlation between the average particle size and the elastic modulus.

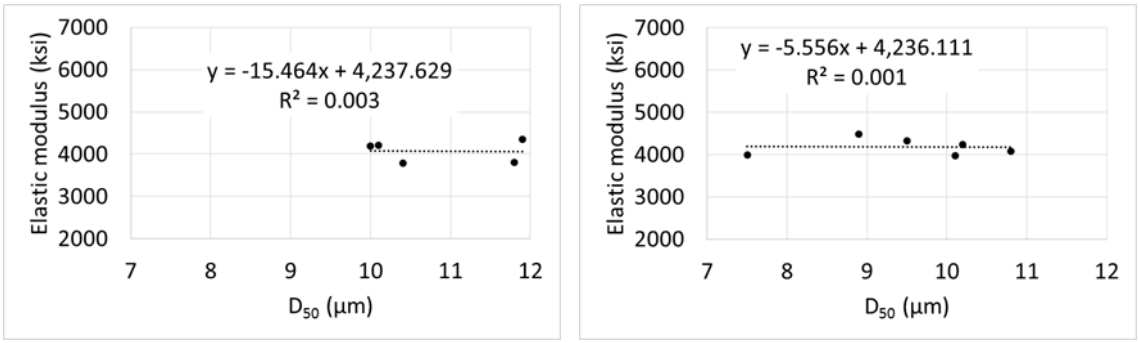

(a) Type I/II (b) Type IL

Figure 6.9: Effect of average particle size of cement on the elastic modulus of class AA concrete

Analysis of variance (ANOVA) was conducted to investigate the statistical significance of the difference in values of the elastic modulus of Type I/II and Type IL cement from each plant. A summary of the results for class AA concrete is shown in Table 6.7. A positive percentage difference indicates concrete with Type IL showed a higher value than concrete made with Type I/II cement.

Table 6.7: ANOVA results for comparing the elastic modulus of Type I/II and Type IL from each plant of Class AA concrete

Cement Source					
A/AL	B/BL	C/CL	D/DL	E/ELC	E/ELF
Similar	+5%	-15%	Similar	Similar	+18%

The results showed that the fine-grade Type IL cement from plant E showed statistically significant results when compared to Type I/II from the same plant, while there was no statistical significance in the difference between the strength of the coarse grade Type IL cement and Type I/II from plant E. In addition to that, the authors

hypothesized that there are more differences between Plant producers than there are between Type I/II and Type IL from the same plant.

Table 6.8 shows the ANOVA results of comparing the elastic modulus of class AA concrete among different plants. The results show that difference in elastic modulus between plants was statistically significant for Type I/II but not statistically significant for Type IL. This indicates that the difference between plants has a more significant effect on the elastic modulus of Type I/II cement.

Table 6.8: ANOVA results for comparing the differences between plants for the elastic modulus of class AA concrete

Cement Source	
Type I/II	Type IL
"A" > "C" by 9%	Similar

Figure 6.10 and Figure 6.11 show the elastic moduli using cements from plants A and C for class AAA and class A concrete, respectively. For class AAA concrete, Type IL showed 1% to 5% lower values (indicating that the dilution effect was significant in class AA concrete. The finer particle size of cement AL reduced the difference to only 1 %. For class A concrete, the results were relatively similar (differences were not statistically significant). Equation 6.2 was used for the theoretical values since it can be used for concretes with compressive strength ranging from 3 ksi to 12 ksi which was the case for all concretes at 28 days.

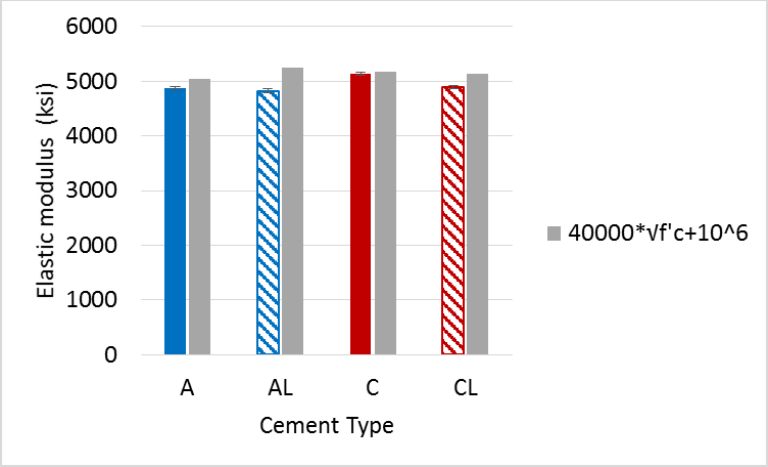

Figure 6.10: Elastic modulus of class AAA concrete

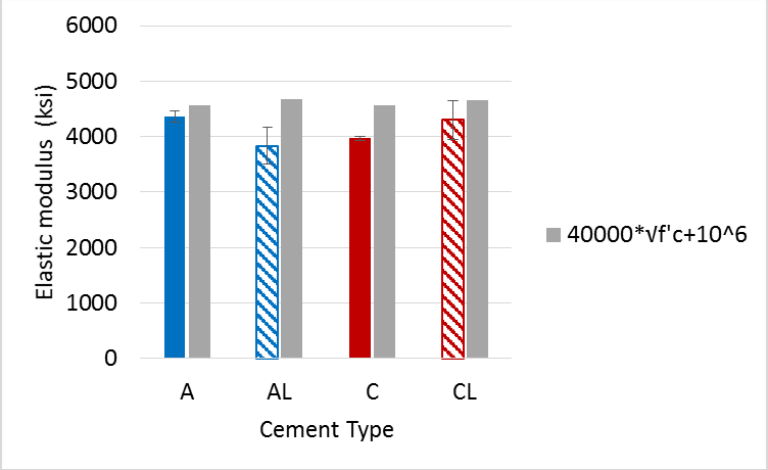

Figure 6.11: Elastic modulus of class A concrete

Figure 6.12 and Figure 6.13 show scatter plots of calcite content vs. the elastic modulus of concrete classes AAA and A, respectively, tested at 28 days. After applying a linear regression best fit line, it can be seen that the higher the calcite content, the lower the elastic modulus.

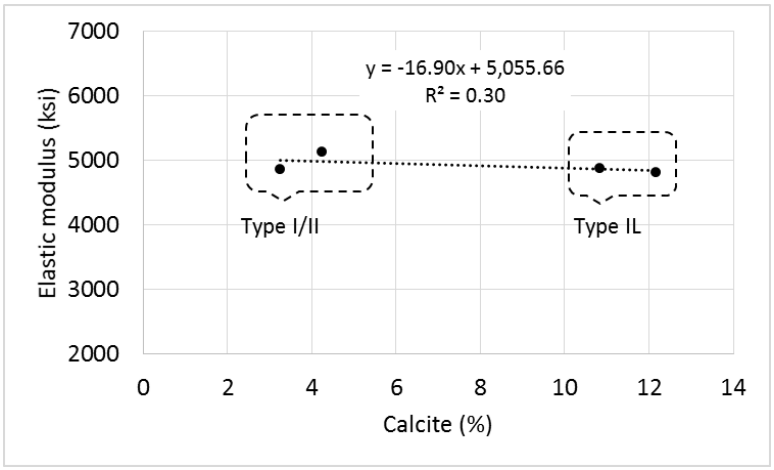

Figure 6.12: Effect of calcite content on elastic modulus of class AAA concrete

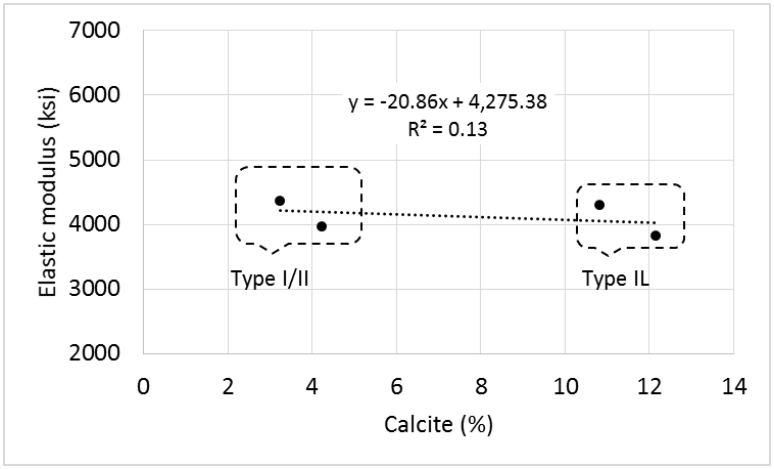

Figure 6.13: Effect of calcite content on elastic modulus of class A concrete

Table 6.9 shows ANOVA results for all three concrete classes. The results show that the differences between Type I/II and Type IL from plant A were not statistically significant. The differences between cement C and CL were statistically significant for classes AAA and AA, but not for class A. For Classes AA and AAA concrete, Type IL cement showed lower elastic modulus values when of similar fineness to Type I/II (plant

C). The finer Type IL cement, AL, reduced the differences between Type I/II and Type IL leading to no significant differences. The differences were not statistically significant for class A concrete due to the low cement factor.

Table 6.9: ANOVA results for comparing the elastic modulus of Type I/II and Type IL from each plant of classes A, AA, and AAA concrete

Concrete class	Cement Source	
	A/AL	C/CL
AAA	Similar	-5%
AA	Similar	-15%
A	Similar	Similar

Table 6.10 shows the ANOVA results of comparing the elastic modulus of classes A, AA, and AAA concrete between plants A and C. For classes A and AAA, the results show that difference in strength between plants was statistically significant for Type I/II but not statistically significant for Type IL. This indicates that for classes A and AAA concrete, the difference between plants had a more significant effect on the elastic modulus of Type I/II cement than Type IL.

Table 6.10: ANOVA results for comparing the differences between plants A and C for the elastic modulus of classes A, AA, and AAA concrete

Concrete class	Cement Type	
	Type I/II	Type IL
AAA	Similar	"AL" > "CL" by 7%
AA	Similar	"AL" > "CL" by 10%
A	"A" > "C" by 9%	Similar

6.3 Splitting tensile strength

Splitting tensile strength [ASTM C496, AASHTO T 198] was measured for concrete samples (4 in. x 8 in.) at 28 days of age. Figure 6.14 shows splitting tensile strength values for class AA concrete, along with calculated values computed using ACI 363R-10 (equation 6-13 in ACI 363R-10 section 6.6):

$$f_{sp} = 7.4\sqrt{f'_c} \qquad \text{Equation 6.3}$$

where:

f_{sp} = splitting tensile strength (psi)

f_c' = compressive strength (psi)

The splitting tensile strength, f_{ct}, was related to the modulus of rupture, f_r, in ACI 318-95 with the following statement: "f_r shall be modified by substituting $f_{ct}/6.7$ *for* $\sqrt{f_c'}$ ". That same relation for splitting tensile strength is given in ACI 318-14 section 19.2.4. That substitution results in the following, traditional relation for the splitting tensile strength:

$$f_{ct} = 6.7\sqrt{f_c'}$$

The AASHTO LRFD 7th Ed. (2016) relates the splitting tensile strength, f_{ct}, to the modulus of rupture in section C5.4.2.7 by substituting $f_{ct}/0.96$ *for* $\sqrt{f_c'}$. That substitution results in the following relation for splitting tensile strength in psi units:

$$f_{ct} = 7.3\sqrt{f_c'}$$

Oluokun et al. (1991) researched "Splitting Tensile Strength and Compressive Strength Relationship at Early Ages"; they recommend that f_{ct} equal $0.584*(f_c')^{0.79}$ for f_c' greater than 6000 psi, which applies to AA and AAA concrete in this current research. Results showed that the Oluokun et al. relation gave calculated results about equal to $7.4\sqrt{f_c'}$.

Because the current AASHTO Bridge Design Specifications (2016), and recent research suggested tensile strength be about $7.4\sqrt{f_c'}$, that relation was used for comparison to experimentally determined spilt tensile strengths (Figure 6.14).

No statistically significant differences were observed between Type I/II and Type IL cements for class AA concrete.

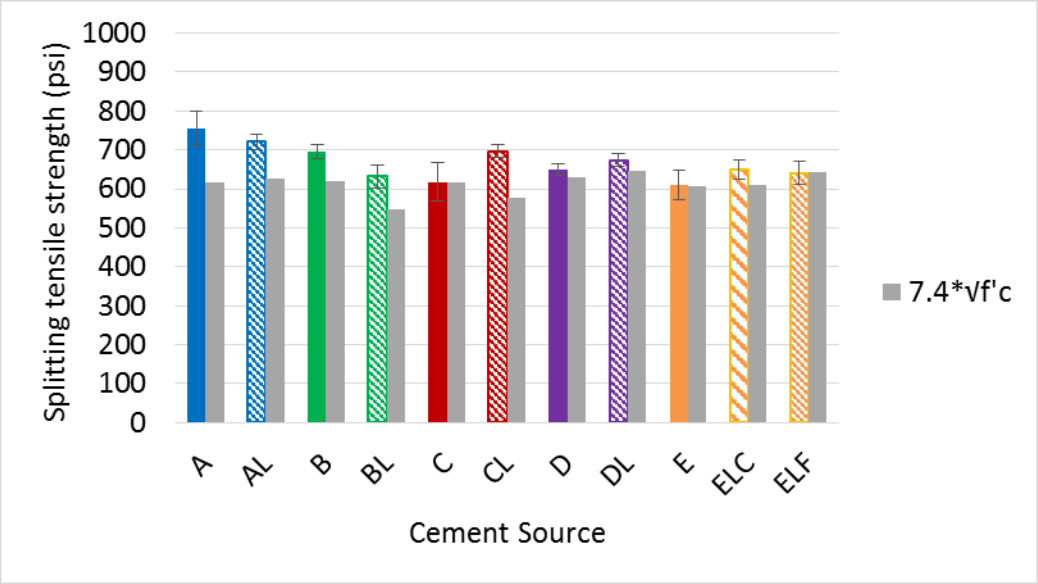

Figure 6.14: Splitting tensile strength of class AA concrete

Figure 6.15 shows a scatter plot of calcite content vs. the splitting tensile strength of class AA concrete at 28 days. After applying a linear regression best fit line, there was very low correlation between the calcite content and the splitting tensile strength. The calculated values obtained using ACI's equation under-estimated the values for concretes made with Type I/II by an average of 8% and for concretes made with Type Il cement by an average of 10%.

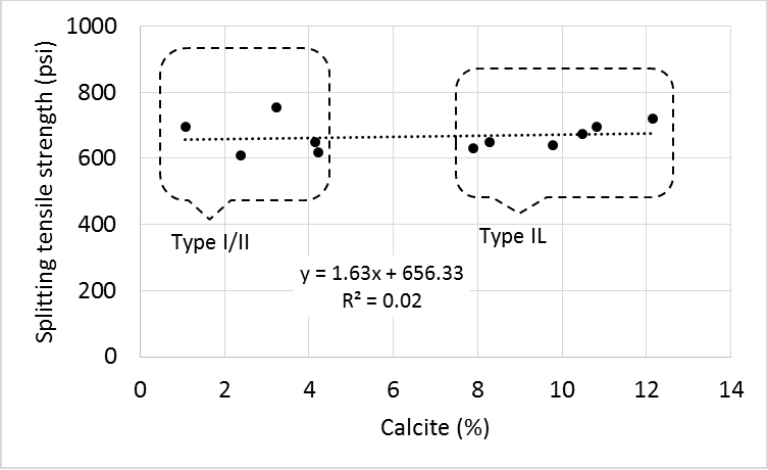

Figure 6.15: Effect of calcite content on the splitting tensile strength of class AA concrete

Figure 6.16 shows the effect of average particle size of cement on the splitting tensile strength of class AA concrete. The results show that larger particle size (i.e., lower fineness) leads to lower splitting tensile strength for Type I/II and Type IL cements. The slope of Type I/II cement is 115% steeper than that of Type IL cement, indicating a more significant effect of particle size on the splitting tensile strength of Type I/II cement. The

author suggests further research in this trend with larger sample sizes and maintain other variables constant (such as calcite content and chemical composition).

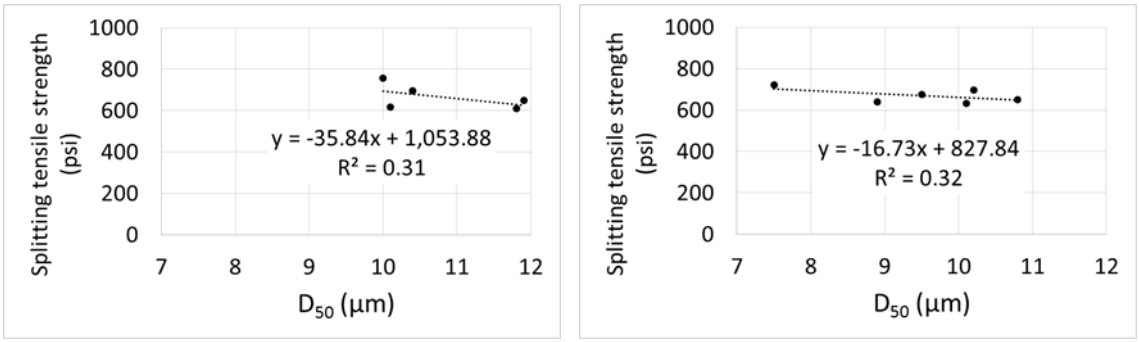

(a) Type I/II (b) Type IL

Figure 6.16: Effect of average particle size of cement on the splitting tensile strength of class AA concrete

Analysis of variance (ANOVA) was conducted to investigate the statistical significance of the difference in values of the tensile strength of Type I/II and Type IL cement from each plant. A summary of the results for class AA concrete is shown in Table 6.11. A positive percentage difference indicates concrete with Type IL showed a higher value than concrete made with Type I/II cement.

Table 6.11: ANOVA results for comparing Type I/II and Type IL from each plant for the tensile strength of Class AA concrete

Cement Source					
A/AL	B/BL	C/CL	D/DL	E/ELC	E/ELF
Similar	-9%	Similar	Similar	Similar	Similar

The results showed that there was no statistical difference between the tensile strength of Type I/II cement and Type IL from most plants. In addition to that, the authors hypothesized that there are more differences between Plant producers than there are between Type I/II and Type IL from the same plant.

Table 6.12 shows the ANOVA results of comparing the splitting tensile strength values of class AA concrete among different plants. The results show that difference in tensile strength between plants was statistically significant for Type I/II and Type IL cement. This indicates that the source of the cement has a more significant effect on the splitting tensile strength than the type of cement.

Table 6.12: ANOVA results for comparing the differences between plants for the tensile strength of class AA concrete

Cement Source	
Type I/II	Type IL
Different	Different

Figure 6.17 and Figure 6.18 show the splitting tensile strength using cements from plants A and C for class AAA and class A concrete, respectively. The results show that Type I/II and Type IL showed relatively similar values for both concrete classes.

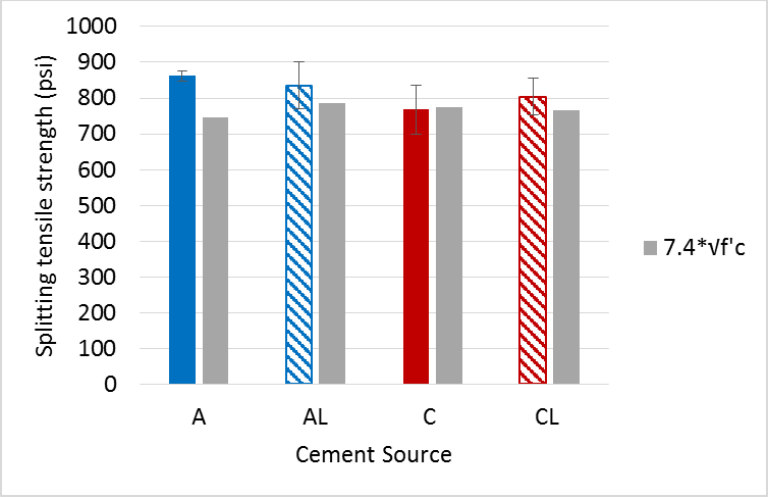

Figure 6.17: Splitting tensile strength of class AAA concrete

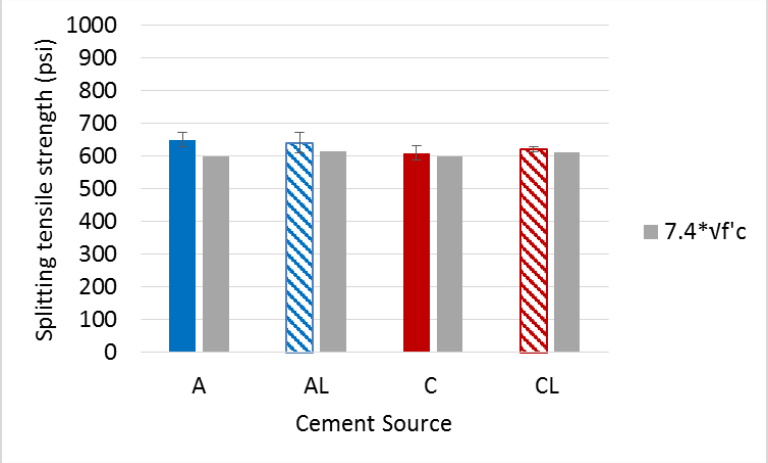

Figure 6.18: Splitting tensile strength of class A concrete

Figure 6.19 and Figure 6.20 show scatter plots of calcite content vs. the tensile strength of concrete classes AAA and A, respectively, tested at 28 days. After applying a linear regression best fit line, it can be seen that there was no correlation between the calcite content and the splitting tensile strength.

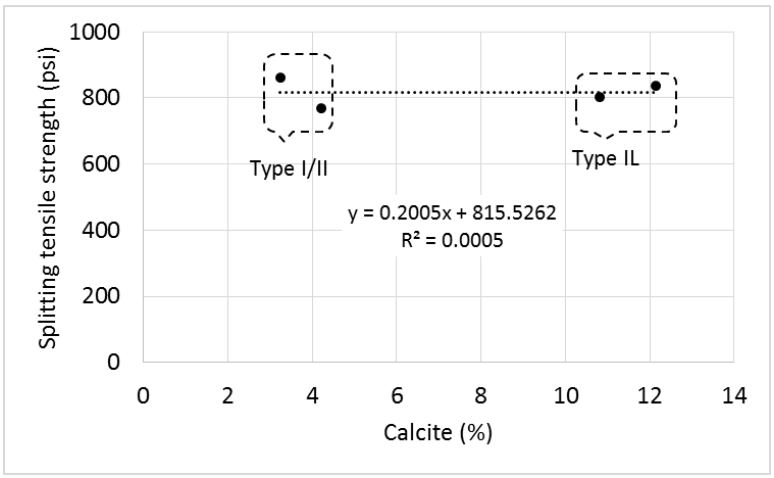

Figure 6.19: Effect of calcite content on splitting tensile strength of class AAA concrete

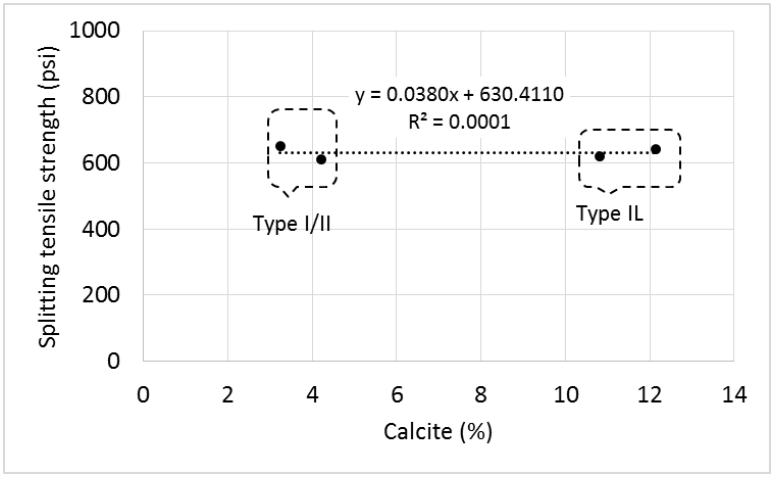

Figure 6.20: Effect of calcite content on splitting tensile strength of class A concrete

Table 6.13 shows ANOVA results for all three concrete classes. The results show that the differences between Type I/II and Type IL were not statistically significant for all concrete classes.

Table 6.13: ANOVA results for comparing tensile strength of Type I/II and Type IL from each plant of classes A, AA, and AAA concrete

Concrete class	Cement Source	
	A/AL	C/CL
AAA	Similar	Similar
AA	Similar	Similar
A	Similar	Similar

Table 6.14 shows the ANOVA results of comparing the splitting tensile strength of classes A, AA, and AAA concrete among different plants. For classes A and AAA, the results show that difference in strength between plants were not statistically significant.

Table 6.14: ANOVA results for comparing the differences between plants for the splitting tensile strength of classes A, AA, and AAA concrete

Concrete class	Cement Type	
	Type I/II	Type IL
AAA	Similar	Similar
AA	Different	Different
A	Similar	Similar

6.4 Drying shrinkage

Drying shrinkage prisms (ASTM C157 [30]) were water bath cured for 28 days, and then drying was initiated; shrinkage was measured at 4 days, 7, days, 14 days, 4 weeks, 8 weeks, 16 weeks, 32 weeks, and 1 year. Another group of samples were only water bath cured for 7 days, and then drying was measured at the same drying times

mentioned before (Alabama DOT Standard Specifications for Highway Construction, Section 501).

The results show that higher calcite content and higher fineness of the cement resulted in higher shrinkage values. The results also showed that the shorter period of curing lead to higher drying shrinkage with the finer limestone cements.

The magnitudes of drying shrinkage were different for the three different classes of concretes studied: classes A, AA, and AAA. Extensive measurements were made using class AA concrete while more cursory studies were conducted using classes A and AAA.

6.4.1 Class AA concrete

Drying shrinkage was measured for class AA concrete mixes made with Type I/II and Type IL cements from plant A to E.

Figure 6.21 shows the drying shrinkage values (ASTM C157) of Class AA concrete made with Type I/II and Type IL cements from Plants A to E and cured at 73 ºF.

The results show that the finer Type IL cements, i.e. from plants A, D and E, show relatively higher drying shrinkage after 1 year (~5% to ~15%) than Type I/II cement. The coarser Type IL cements, i.e. from plants B and C, show equivalent or lower drying shrinkage than Type I/II cement (~15% for plant B).

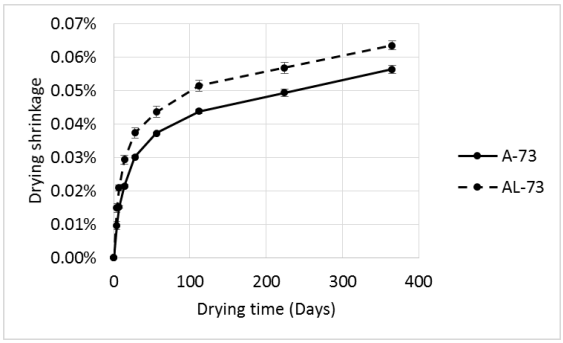

(a) Plant A

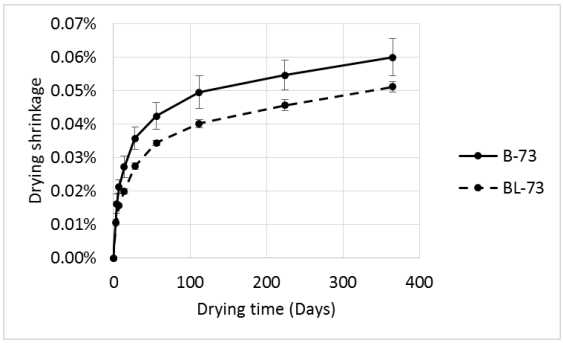

(b) Plant B

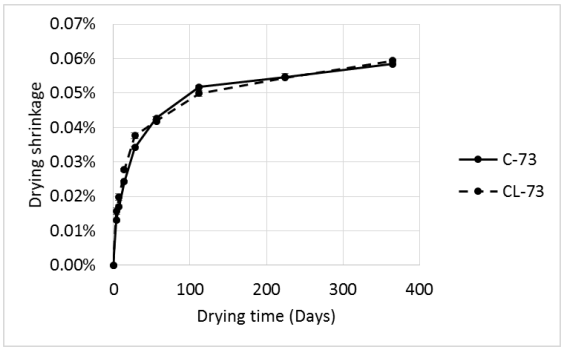

(c) Plant C

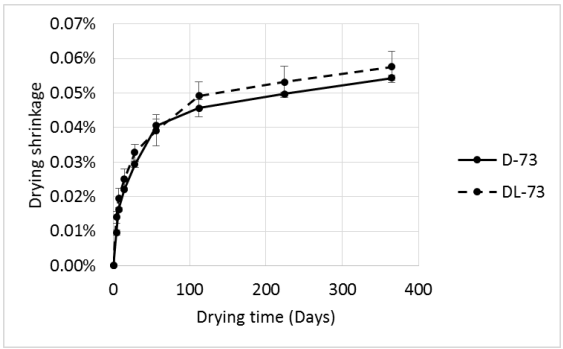

(d) Plant D

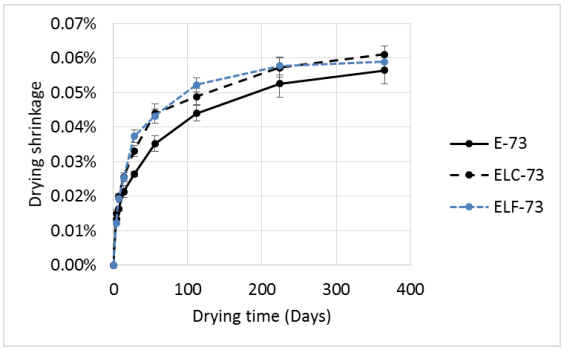

(e) Plant E

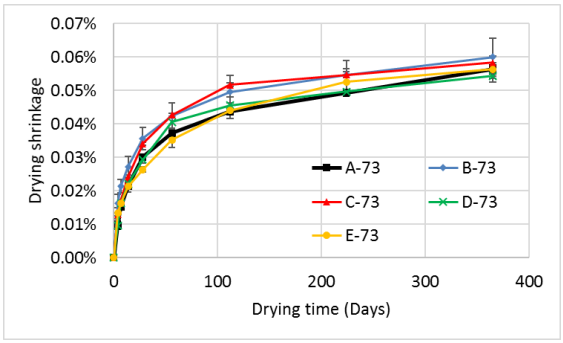

(f) Concrete made with Type I/II

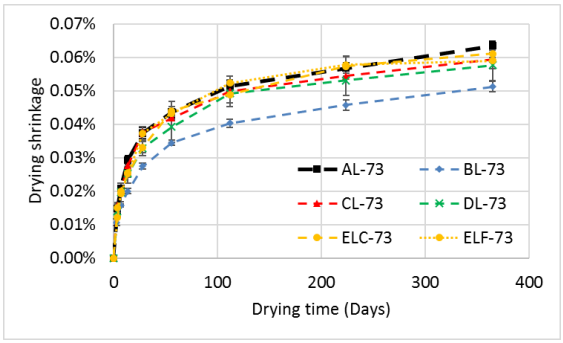

(g) Concrete made with Type IL

Figure 6.21: Drying shrinkage [ASTM C157] of Class AA concrete using Type I/II and Type IL cement from plants A to E and cured at 73 ºF

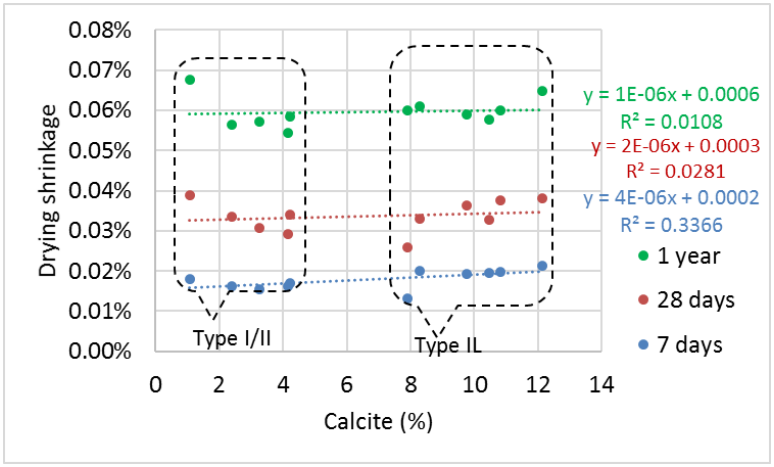

Figure 6.22 shows a scatter plot of calcite content vs. the drying shrinkage of class AA concrete at 7 days, 28 days, and 1 year. After applying a linear regression best fit line, it can be seen that the higher the calcite content, the larger the drying shrinkage. This indicates that the dilution effect due to limestone replacement is more significant on the drying shrinkage since it leaves a larger amount of free water that is able to escape through drying.

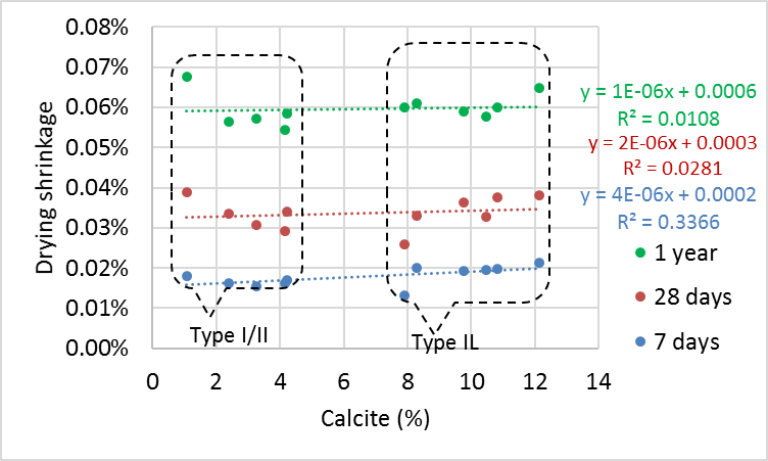

Figure 6.22: Effect of calcite content on drying shrinkage of class AA concrete

Previous research also showed that limestone additions resulted in increases in drying shrinkage, as shown in Table 6.15 and Table 6.16 from Hawkins et al. [3].

Table 6.15: Effect of Blended Limestone on Type I Cement (11.4% C_3A, 339 m^2/kg) [56]

Time (Days)	Drying Shrinkage (ASTM C 596)	
	Control (0% Limestone)	5% Limestone
4	0.044	0.050
11	0.063	0.071
18	0.070	0.079
25	0.072	0.082

Table 6.16: Effect of Blended Limestone on Type II Cement (6.4% C_3A, 400 m^2/kg) [56]

Time (Days)	Drying Shrinkage (ASTM C 596)		
	Control (0% Limestone)	3% Limestone	5% Limestone
4	0.046	0.049	0.050
11	0.064	0.067	0.068
18	0.075	0.077	0.079
25	0.081	0.085	0.085

Figure 6.23 and Figure 6.24 show scatter plots of the average particle size vs. the drying shrinkage of concrete class AA at 1 day, 28 days, and 1 year for Type I/II and Type IL cements, respectively.

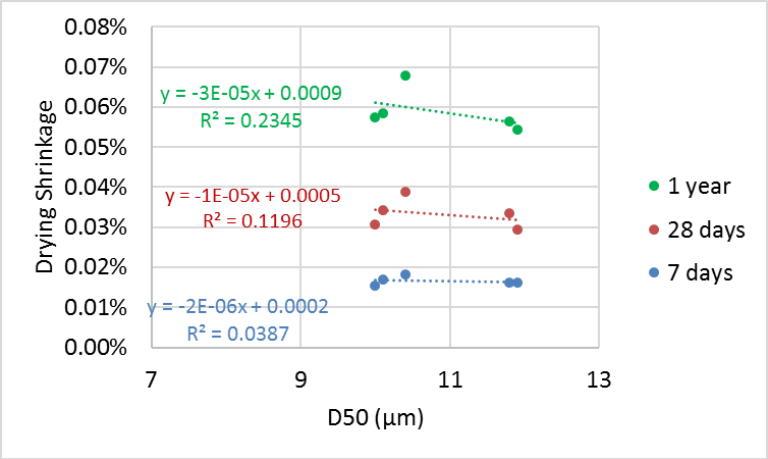

Figure 6.23: Effect of particle size on the drying shrinkage of class AA concrete using Type I/II cement

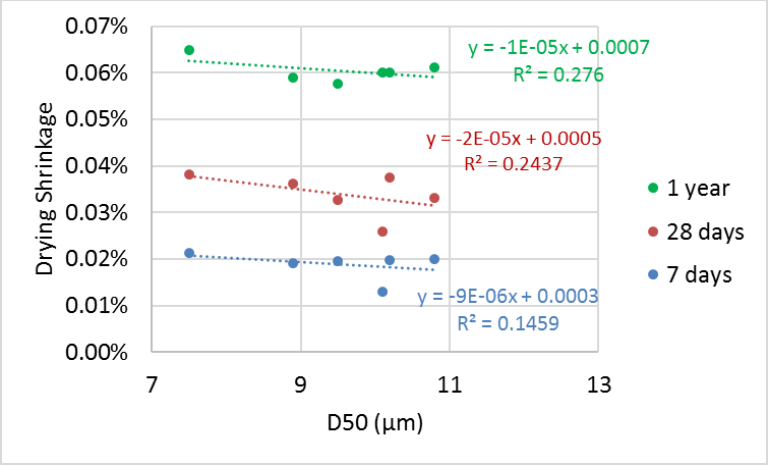

Figure 6.24: Effect of particle size on the drying shrinkage of class AA concrete using Type IL cement

The effect of curing concrete for 28 days (per ASTM C157) on drying shrinkage was compared to curing concrete for only 7 days before start of drying at 73 ºF (Alabama Specifications – Section 501). Figure 6.25 shows the effect of curing time on the drying shrinkage of Type IL and Type I/II cements from plant E.

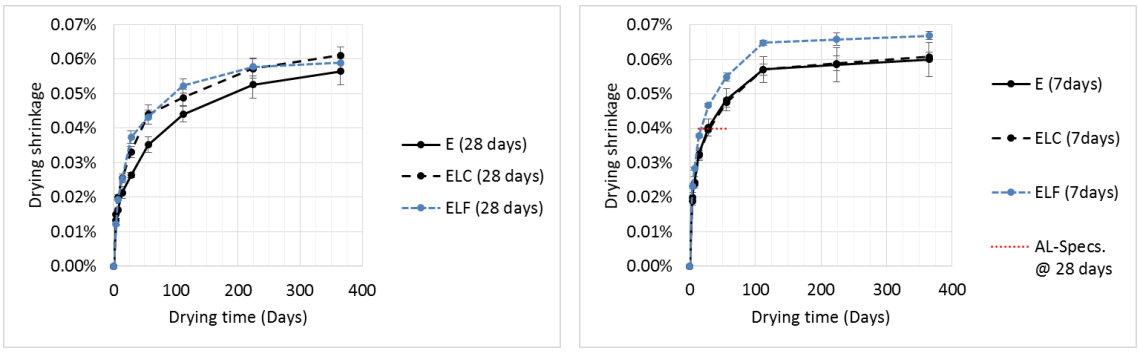

(a) 28 days curing (b) 7 days curing

Figure 6.25: Effect of curing time on the drying shrinkage of Type I/II and Type IL cements (fine and coarse grade) from Plant E

The results show that when cured for just 7 days, the finer grade Type IL cement showed higher drying shrinkage (~10%) than Type I/II and the coarse grade Type IL cement. The coarse grade Type IL cement showed similar drying shrinkage values to Type I/II cement when cured for just 7 days. Alabama specifications for Class B concrete specifies a maximum drying shrinkage of 0.04%. The fine-grade Type IL cement (ELF) cured for 7 days did not exceed that maximum allowable shrinkage of Alabama specifications.

Note, Class B concrete in Alabama specifications is approximately equivalent to Class AA in GDOT Section 500 where Class B has a *w/b* = 0.45 and min. strength of 4

ksi at 28 days compared to a *w/b* of 0.445 and 3.5 ksi strength at 28 days for GDOT's Class AA concrete.

Analysis of variance (ANOVA) was conducted to investigate the statistical significance of the difference in values of the drying shrinkage of Type I/II and Type IL cement of each plant. A summary of the results for class AA concrete is shown in Table 6.17. A positive percentage difference indicates concrete with Type IL showed a higher value than concrete made with Type I/II cement.

Table 6.17: ANOVA results for comparing Type I/II and Type IL from each plant for the drying shrinkage of Class AA concrete

Time	Cement Source					
	A/AL	B/BL	C/CL	D/DL	E/ELC	E/ELF
7 days	+37%	-26%	+16%	Similar	+23%	+18%
28 days	+24%	-23%	+10%	Similar	+25%	+41%
1 year	+13%	Similar	+2%	Similar	Similar	Similar

The results showed that Type IL cements from all plants (except plant D) showed statistically significant different results when compared to Type I/II from the same plant. Plant D showed similar shrinkage results for Type I/II and Type IL.

6.4.2 Class AAA concrete

Drying shrinkage was measured for class AAA concrete mixes made with Type I/II and Type IL cements from plant A and plant C. Samples were cured for 28 days in a

saturated lime-saturated water bath [ASTM C157]. After that, the concrete prisms were taken out to dry at 73 °F.

Figure 6.26 shows the drying shrinkage results for Type I/II and Type IL cement from plant A (Cement A and AL) and plant C (cement C and CL) cured at 73 °F for Class AAA concrete. Shrinkage values for Class AA concrete are shown for comparison.

For class AAA concrete, cement AL (higher fineness) showed lower drying shrinkage than cement A (~10% at 1 year). For cements C and CL (similar fineness), cement C and CL showed similar shrinkage values at 1 year.

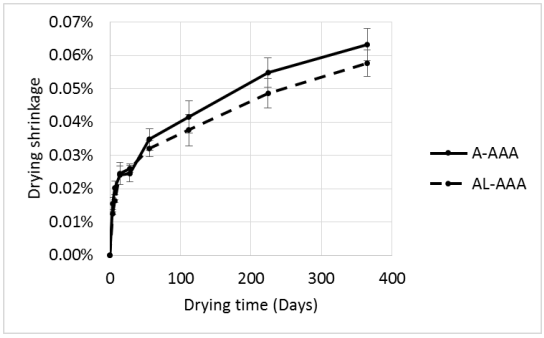

(a) Cement A/AL

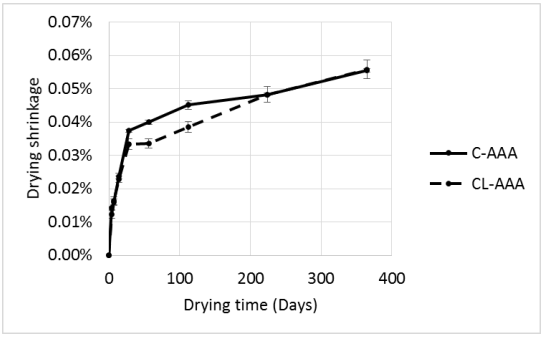

(b) Cement C/CL

Figure 6.26: Drying shrinkage [ASTM C157] of Type I/II and Type IL cement from plants A and C with Class AAA concrete

A second group of Class AAA concrete prisms was cured for only 7 days in a lime- saturated water bath to show the effect of curing time on drying shrinkage. After curing, the concrete prisms were taken out to dry at 73 °F. Figure 6.27 shows the drying shrinkage results for concrete made with cement A/AL and C/CL and cured at 73 °F for 7 days as well as those cured for 28 days.

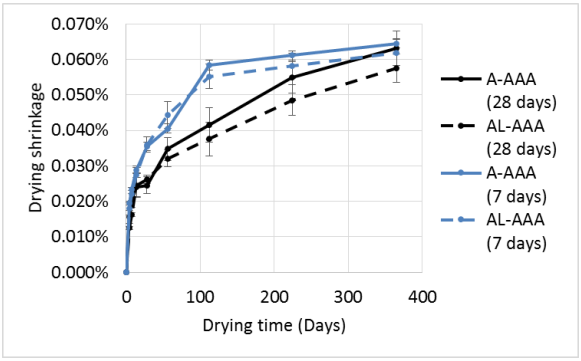

(a) Cement A/AL

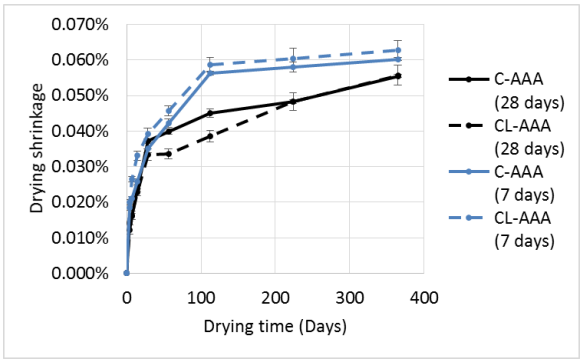

(b) Cement C/CL

Figure 6.27: Drying shrinkage of Type I/II and Type IL cement from plants A and C cured for 7 days and 28 days with class AAA concrete

For cements A and AL, the samples cured for 7 days showed higher drying shrinkage than samples cured for 28 days (~40% for Type I/II and ~45% for Type IL at 112 days). At one year, the difference became smaller (2% for Type I/II and 7% for Type IL). The drying shrinkage values of A and AL cured for 7 days differed by less than 5%.

For cements C and CL, the samples cured for 7 days also showed higher drying shrinkage than samples cured for 28 days (~25% for Type I/II and ~50% for Type IL at 112 days). At one year, the difference became smaller (9% for Type I/II and 12% for Type IL). The drying shrinkage values of C and CL cured for 7 days differed by less than 4%.

Analysis of variance (ANOVA) was conducted to investigate the statistical significance of the difference in values of the drying shrinkage of Type I/II and Type IL cement of plants A and C. A summary of the results for class AAA concrete is shown in

Table 6.18. A positive percentage difference indicates concrete with Type IL showed a higher value than concrete made with Type I/II cement.

Table 6.18: ANOVA results for comparing Type I/II and Type IL from each plant for the drying shrinkage of Class AAA concrete

Time	Cement source	
	A/AL	C/CL
7 days	-20%	Similar
28 days	Similar	-11%
1 year	Similar	Similar

For 7 days of drying, the results showed that the difference in drying shrinkage between A and AL (finer Type IL) were statistically significant. Cements and C and CL had a similar fineness and the differences in shrinkage were not statistically significant. However, at one year, both plants showed that the differences between Type I/II and Type IL cements were not statistically significant.

6.4.3 Class A concrete

Drying shrinkage was measured for class A concrete mixes made with Type I/II and Type IL cements from plant A and plant C. Samples were cured for 28 days in a lime-saturated water bath [ASTM C157]. After that, the concrete prisms were taken out to dry at 73 °F.

Figure 6.28 shows the drying shrinkage results for Type I/II and Type IL cement from plant A (Cement A and AL) and plant C (cement C and CL) cured at 73 °F for Class AAA. Shrinkage values for Class AA concrete are shown for comparison.

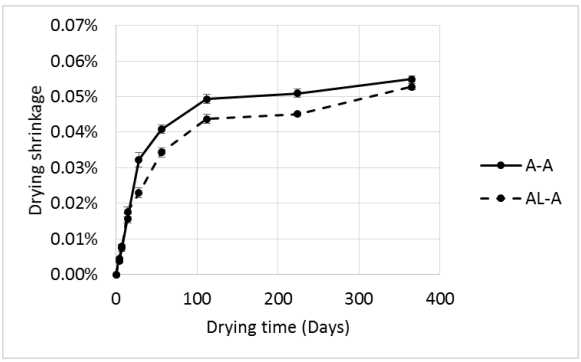

(a) Cement A/AL

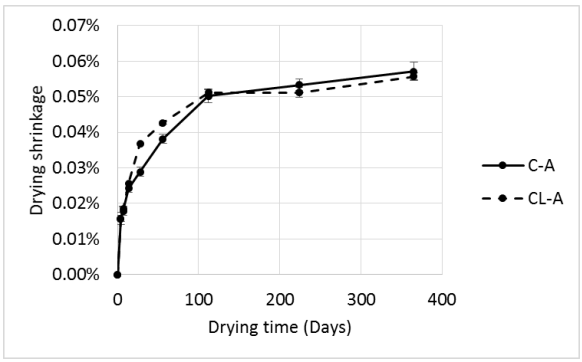

(b) Cement C/CL

Figure 6.28: Drying shrinkage [ASTM C157] of Type I/II and Type IL cement from plants A and C with class A concrete

For class A concrete, cement AL showed lower drying shrinkage than cement A (5% at 1 year). Cements C and CL showed relatively similar values at most ages including one year. C and CL showed similar values at 4 days and 7 days, but CL showed higher values (10% at 56 days) from 14 days until 16 weeks (112 days), when the values converged with those of C.

A second group of Class A concrete prisms was cured for only 7 days in a lime-saturated water bath to show the effect of curing time on drying shrinkage. After curing, the concrete prisms were taken out to dry at 73 °F. Figure 6.27 shows the drying shrinkage results for concrete made with cement A/AL and C/CL and cured at 73 °F for 7 days as well as those cured for 28 days.

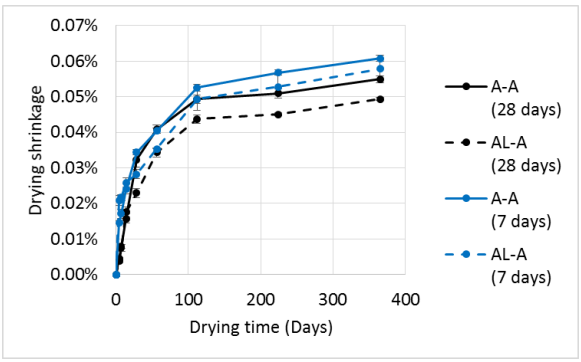

(a) Cement A/AL

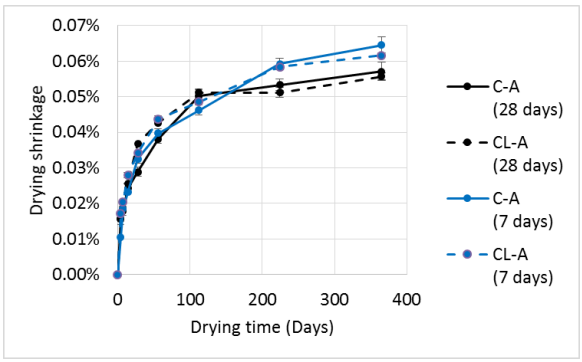

(b) Cement C/CL

Figure 6.29: Drying shrinkage of Type I/II and Type IL cement from plants A and C cured for 7 days and 28 days with class A concrete

For cements A and AL, the samples cured for 7 days showed higher drying shrinkage than samples cured for 28 days (10% at 1 year). The drying shrinkage values of A and AL cured for 7 days differed by 5% at 1 year.

For cements C and CL, the samples cured for 7 days showed higher drying shrinkage than samples cured for 28 days (12% at 1 year). The drying shrinkage values of C and CL cured for 7 days differed by 5% at 1 year. This indicates that shorter curing time results in higher drying shrinkage for this class of concrete, but the trends between A and Al and C and CL were similar regardless of the curing time.

Analysis of variance (ANOVA) was conducted to investigate the statistical significance of the difference in values of the drying shrinkage of Type I/II and Type IL cement of plants A and C. A summary of the results for class AAA concrete is shown in Table 6.19. A positive percentage difference indicates concrete with Type IL showed a higher value than concrete made with Type I/II cement.

Table 6.19: ANOVA results for comparing Type I/II and Type IL from each plant for the drying shrinkage of Class A concrete

Time	Cement source	
	A/AL	C/CL
7 days	Similar	Similar
28 days	-29%	+27%
1 year	-4%	Similar

For 7 days of drying, the results showed that the difference in drying shrinkage between Type I/II and Type IL cements from both plants were not statistically significant. However, at one year, cement A and AL showed statistically significant differences while cement C and CL showed differences that were not statistically significant. This indicates that finer limestone cement has a more significant effect on the long-term drying shrinkage of concrete with higher *w/b* (i.e. class A).

Figure 6.32 and Figure 6.33 show scatter plots of the *w/b* vs. the drying shrinkage of concrete at 1 day, 28 days, and 1 year for Type I/II and Type IL cements, respectively.

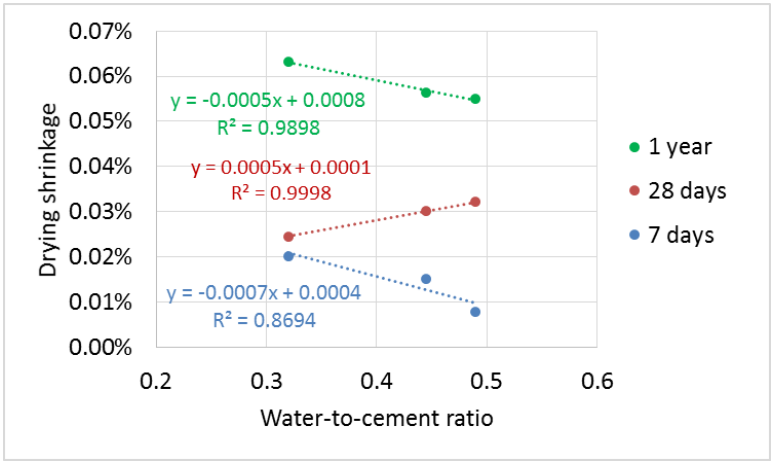

Figure 6.30: Effect of *w/b* on drying shrinkage of concrete using Type I/II cement

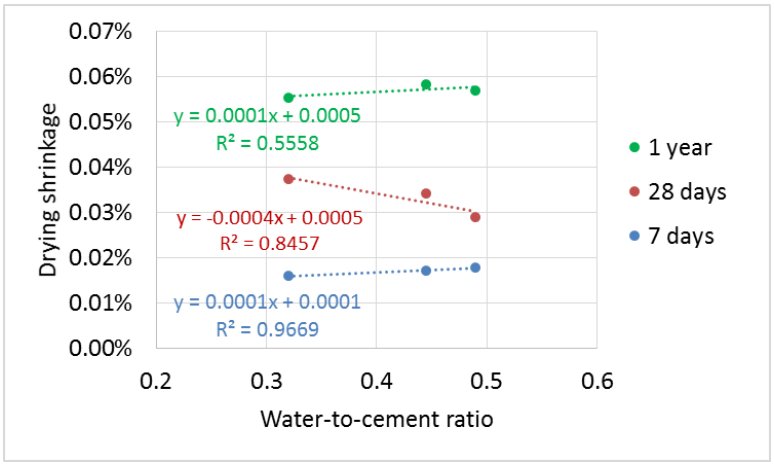

Figure 6.31: Effect of *w/b* on drying shrinkage of concrete using Type IL cement

The results show different behavior between Type I/II and Type IL cements. Higher values of *w/b* of concrete made with Type I/II cement resulted in higher drying shrinkage at 28 days but lower shrinkage values at 7 days and at 1 year. However, higher values of *w/b* of concrete made with Type IL cement resulted in lower drying shrinkage at 28 days but higher shrinkage values at 7 days and at 1 year. These conflicting results may be a result of the combined effects of other parameters on the drying shrinkage such as calcite content and the average particle size.

6.5 Chapter discussion and conclusions

6.5.1 Effect of w/b on mechanical properties

Figure 6.32 and Figure 6.33 summarize the compressive strength values of classes A, AA, and AA concrete, for plants A and C, respectively.

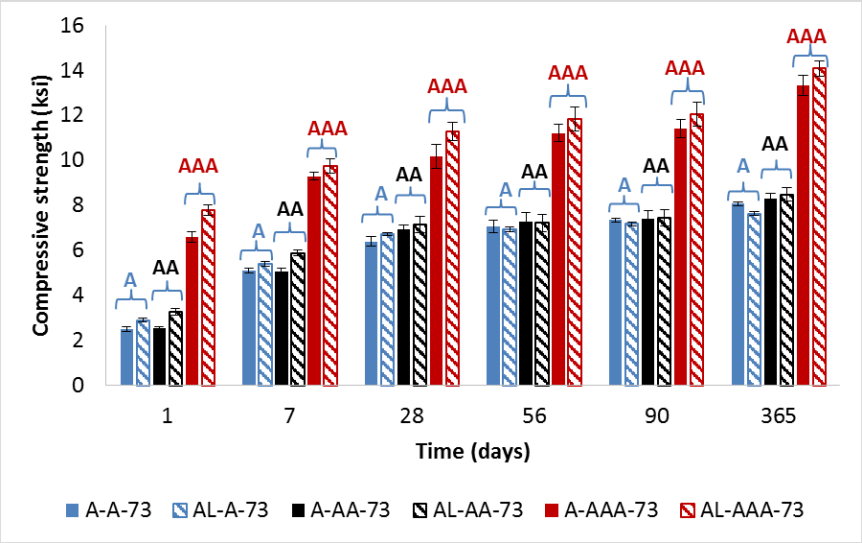

Figure 6.32: Compressive strength of Classes A, AA, and AAA concrete using Type I/II and Type IL cements from Plant A

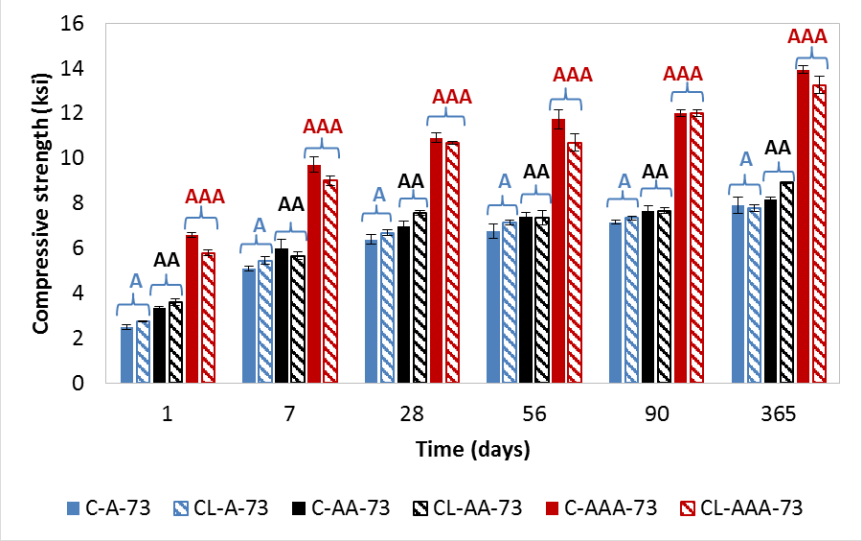

Figure 6.33: Compressive strength of Classes A, AA, and AAA concrete using Type I/II and Type IL cements from Plant C

The effects of several parameters on the compressive strength were investigated. Despite the variability in cement chemistry and physical properties, a general trend was found that the higher calcite content, the greater the compressive strength. Some exceptions to this occurred when Type IL cement was of lower fineness (such as "CL-AAA-73"), and this suggests that several factors affect the performance simultaneously. Therefore, further research into each of these parameters separately (while keeping the other parameters constant) is recommended. Also, it was found that higher fineness of Type IL cement led to greater strength.

Previous researchers [22, 57, 58] reported similar trends in compressive strength relationship with calcite content and fineness. Cement chemistry also played a role. The results reported by Tsivilis et al. [22] Figure 2.8 (shown below for ease of the reader) shows that compressive strength increased with higher limestone content (before the strength decreased again with higher limestone percentages). The data also showed that in addition to limestone content, fineness and cement chemistry affected the strength, which agree with the results of the research current research.

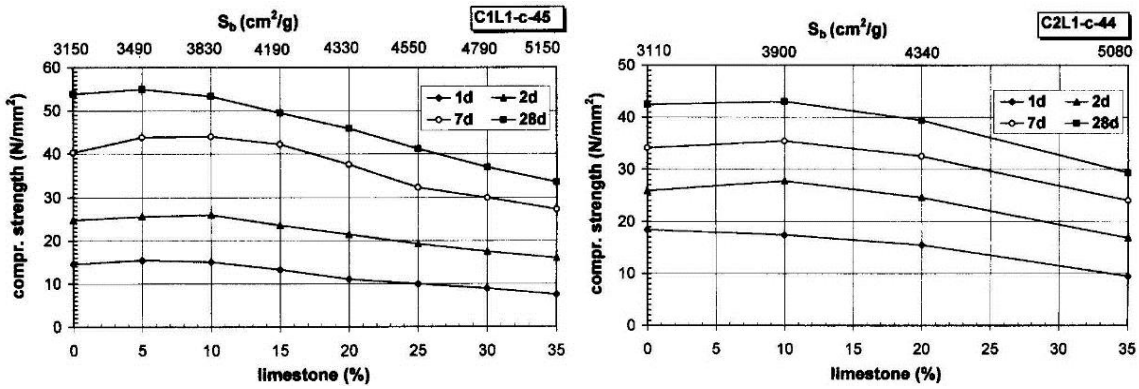

A) C_3S=65%, C_2S=13%, C_3A=8%, C_4AF=11%

B) C_3S=58%, C_2S=19%, C_3A=12%, C_4AF=6%

Figure 2.8: Influence of limestone content on strength development [22]

The effect of Type IL cement on the strength varied in different concrete classes. It was found that the higher the concrete class (i.e., higher cement factor and lower *w/b* ratio), the greater the effect of Type IL cement on the strength.

For class A concrete, no statistically significant differences were found between use of Type I/II and Type IL cements. Also, for class A concrete, the difference in strength among cement producers was not statistically significant.

For class AA concrete, the difference in strength resulting of using fine-grade Type IL cement or Type I/II cement was significant while the difference in concrete strength as a result of using coarse-grade Type IL cement or Type I/II was not significant. Also, for class AA concrete, the difference in strength among cement producers was statistically significant.

For class AAA concrete, the effect of Type IL cement was more significant than the other two classes. Type IL cement led to lower strength when the limestone had

similar fineness to Type I/II. Higher fineness of Type IL cement increased the strength and resulted in statistically insignificant differences with Type I/II cement.

Figure 6.34 shows a comparison of the elastic modulus values of classes A, AA, and AAA measured at 28 days.

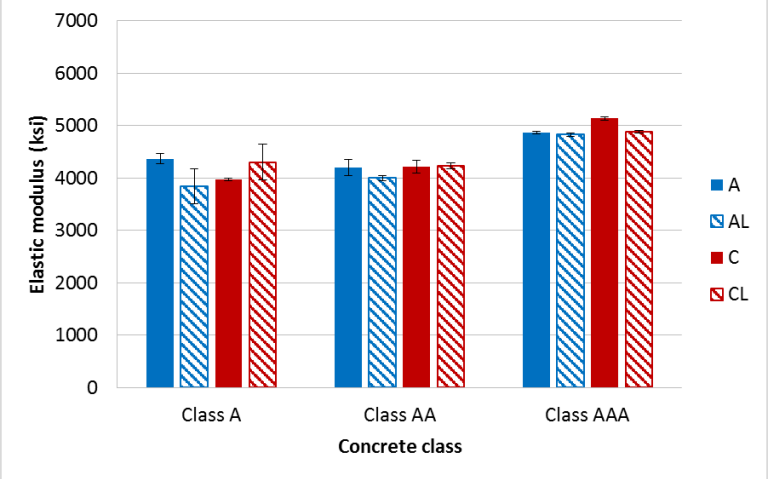

Figure 6.34: Elastic modulus values of classes A, AA, and AAA concrete

The effect of several parameters on the elastic modulus was investigated. For class AA concrete, it was found that the higher the calcite content, the higher the elastic modulus. However, for classes A and AAA concrete, it was found that the higher calcite content, the lower the elastic modulus. Also, a general trend was observed where concretes with higher fineness of Type IL cement showed greater elastic modulus. In general, the elastic modulus followed the trends of the compressive strength, but further research with larger sample sizes and control over different parameters such as cement chemistry and fineness is recommended.

The effect of Type IL cement on the elastic modulus varied in different concrete classes. For the finer Type IL cement (AL), the elastic modulus was similar for all three concrete classes. However, for plant C (where the average particle size of Type I/II and Type IL were similar), cement CL resulted in a lower elastic modulus than C for class AAA concrete while cement CL resulted in a higher elastic modulus for class A concrete. The effect of nucleation was more dominant for class A (lower cement factor and higher *w/b* ratio) while the dilution effect was more dominant for class AAA concrete (higher cement factor and lower *w/b*).

For class AA concrete, finer Type IL cement (ELF) resulted in higher elastic modulus values than Type I/II (E) and the coarser Type IL from the same source (ELC). Also, the variation in results showed that the source of the cement had a more significant effect on the elastic modulus than the type of cement for this class of concrete.

Regarding tensile strength, Figure 6.35 shows a comparison of the splitting tensile strength values of classes A, AA, and AAA.

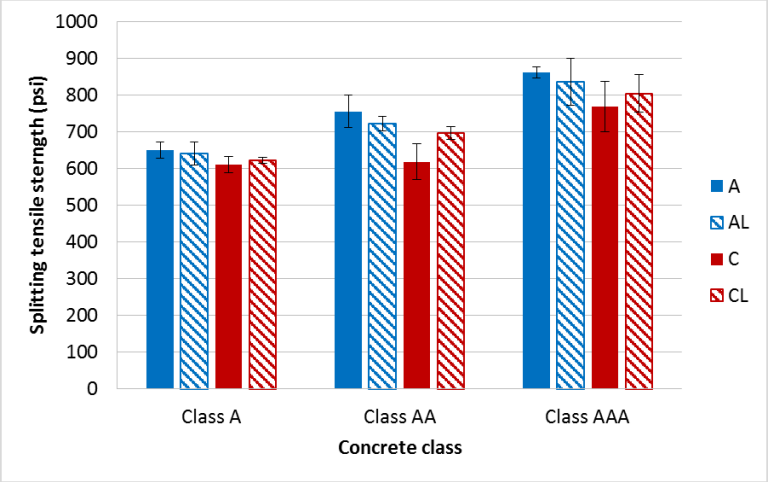

Figure 6.35: Splitting tensile strength values of classes A, AA, and AAA concrete

The effect of several parameters on the splitting tensile strength was investigated. It was found that as the calcite content showed low correlation with the splitting tensile strength. However, it was found that higher fineness of Type IL cement led to greater splitting tensile strength.

The effect of Type IL cement on the strength was similar in different concrete classes. It was found that the effect of Type IL cement on the splitting tensile strength was not statistically significant for class A, AA, and AAA concretes.

For class AA concrete, the difference in splitting tensile strength values of Type IL cement among cement producers was statistically significant, indicating the source of the Type IL cement had a more significant effect on the splitting tensile strength values than the type of cement.

A general conclusion is that the behavior of Type IL cement differs in different *w/b* and cement content. As was discussed earlier, the difference was enhanced with low *w/b* and high cement factor.

6.5.2 Drying shrinkage

To summarize the drying shrinkage values of classes A, AA, and AA concrete, Figure 6.32 and Figure 6.33 show the values for plants A and C, respectively.

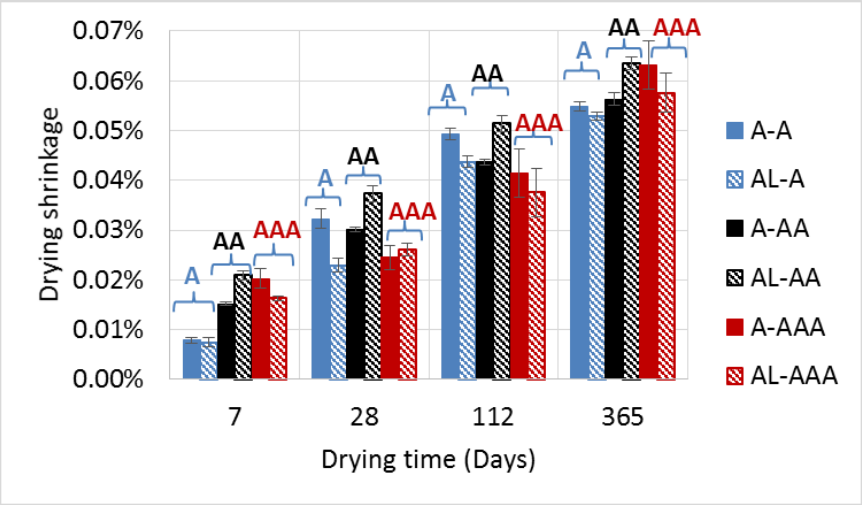

Figure 6.36: Drying shrinkage (ASTM C157 [30]) of Classes A, AA, and AAA concrete using Type I/II and Type IL cements from Plant A

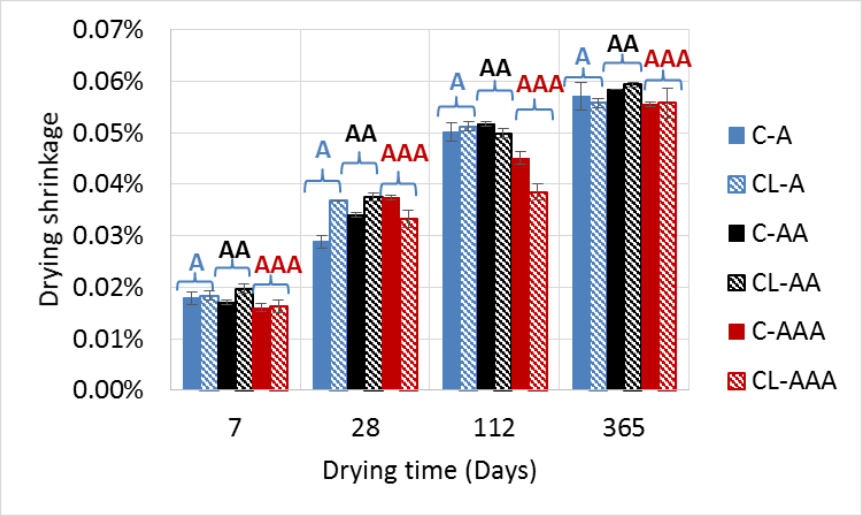

Figure 6.37: Drying shrinkage (ASTM C157 [30]) of Classes A, AA, and AAA concrete using Type I/II and Type IL cements from Plant C

The effect of several parameters on the drying shrinkage was investigated. It was found that the higher calcite content, the greater the drying shrinkage. Also, it was found that higher fineness of Type IL cement led to greater shrinkage. At early age, Type I/II and Type IL cements showed conflicting relationships with the average particle size where finer Type I/II cements resulted in lower shrinkage while finer Type IL cements showed higher shrinkage values. Previous research also showed that limestone additions resulted in increases in drying shrinkage, as shown in Table 6.15 and Table 6.16.

The effect of Type IL cement on the drying shrinkage varied in different concrete classes. Type IL cement in class AAA concrete showed lower shrinkage than Type IL in class AA concrete.

For class A concrete (i.e. higher *w/b*), no statistically significant differences in shrinkage were found between Type I/II and Type IL cement at 7 days. However, finer

limestone cement (AL) decreased the long-term drying shrinkage of this class of concrete.

For class AAA concrete (i.e. lower *w/b*), no statistically significant differences in shrinkage were found between Type I/II and Type IL cement at 1 year. However, finer limestone cement decreased the early age drying shrinkage of this class of concrete.

CHAPTER 7: CONCRETE CURING TEMPERATURE

7.1 Compressive strength

Class AA concrete mixtures were prepared using Type I/II and Type IL from sources A and C, and were cured at room temperature (73 °F), 90 °F, and 40 °F until the time of testing.

Figure 7.1 and Figure 7.2 show the compressive strength results for Type I/II and Type IL cement from sources A and C, respectively. The numerical value in the legend indicates the curing temperature in ºF. Log scale was used for "Time" to show difference in early-age behavior.

The results in Figure 7.1 (Cement A/AL) showed that Type IL cement resulted in relatively higher 1-day compressive strength than Type I/II cured at all curing temperatures. At 28 days, Cement AL cured at 90 °F showed significant increase (~30%) in compressive strength when compared to cement A cured at 90 °F. However, the difference in strength between A and AL was smaller for other curing temperatures (~3% for 73 °F curing, and ~7% for 40 °F curing). At 1 year, cement AL cured at 90 °F showed about 40% higher strength than cement A cured at 90 °F. Also, at 1 year, cement AL cured at 40 °F showed slightly lower strength (~4%) than cement A cured at 40 °F.

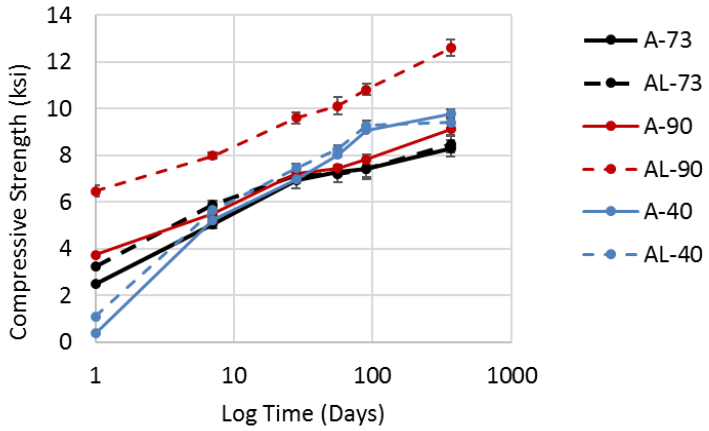

Figure 7.1: Concrete compressive strength of Type I/II and Type IL cement from **Plant A** cured at 73 ºF, 90 ºF, and 40 ºF

The results in Figure 7.2 (Cement C/CL) showed that at 1 day, Type IL cement resulted in slightly higher (~7%) compressive strength than Type I/II when cured at 73 ºF. The difference between Type I/II and Type IL was higher (~35%) for the mixes cured and 40 ºF, while Type IL cement showed slightly lower (3%) 1-day compressive strength than Type I/II when cured at 90 ºF.

At 28 days, Type IL cement showed similar compressive strength to Type I/II for the mixes cured at 90 ºF and 40 ºF, while Type IL showed slightly higher (~9%) compressive strength than Type I/II for the mixes cured at 73 ºF.

At 1 year, Type IL cement showed similar compressive strength to Type I/II for the mixes cured at 90 ºF and 40 ºF, while Type IL showed slightly higher (~9%) compressive strength than Type I/II for the mixes cured at 73 ºF.

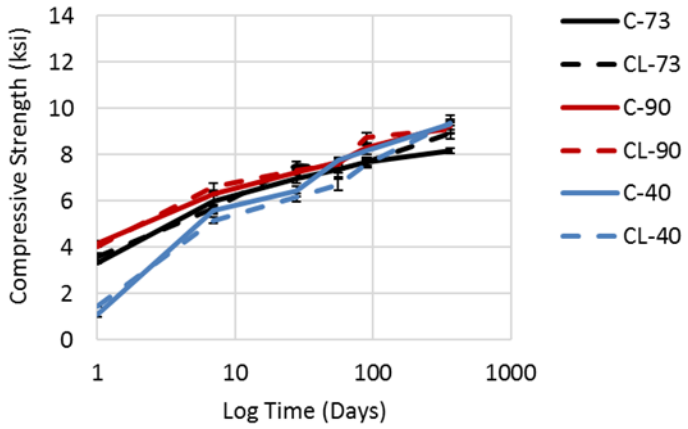

Figure 7.2: Concrete compressive strength of Type I/II and Type IL cement from **Plant C** cured at 73 ºF, 90 ºF, and 40 ºF

The particle size analysis of Type I/II and Type IL cements from plant A and C are summarized in Table 7.1. The median particle size of cement AL is about 25% lower than cement A (7.5 µm and 10 µm respectively). This smaller particle size provides more nucleation sites for cement hydration and therefore increase the rate of hydration leading to faster strength development. The smaller particle size also improves the particle packing which may also increase the compressive strength. The higher temperature (90 ºF) seems to have enhanced the difference in the rate of hydration significantly as seen in the strength development of cement AL at 90 ºF in Figure 7.1. However, cement C and CL had a relatively similar median particle size, which explains the similar rate of strength development shown in Figure 7.2.

Table 7.1: Particle size summary for cements from Plant A and C

Cement	Surface mean [μm]	Volume mean [μm]	D_{10} [μm]	D_{50} [μm]	D_{90} [μm]
A	6.28	14.1	2.77	10.0	30.2
AL	5.09	10.2	2.29	7.5	21.8
C	6.53	15.1	3.03	10.1	34.1
CL	5.60	14.6	2.25	10.2	33.6

Figure 7.3 and Figure 7.4 show scatter plots of calcite content vs. the compressive strength of concrete at 1 day, 28 days, and 1 year for concrete cured at 90 ºF and 40 ºF, respectively. After applying a linear regression best fit line, it can be seen that when curing at 90 ºF, the higher the calcite content, the larger the compressive strength at all ages. However, for the concrete cured at 40 ºF, neither the calcite content nor the limestone fineness seemed to have a significant effect on the compressive strength. Table 7.2 shows the calcite content of Type I/II and Type IL cements from plant A and C.

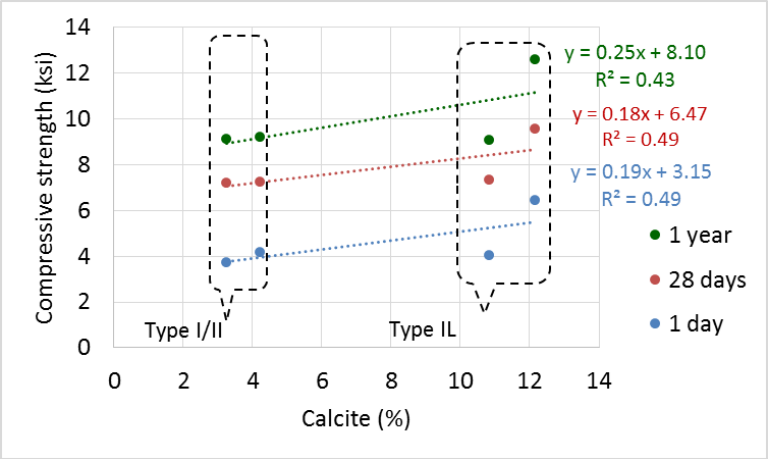

Figure 7.3: Effect of calcite content on compressive strength of concrete cured at 90 ºF

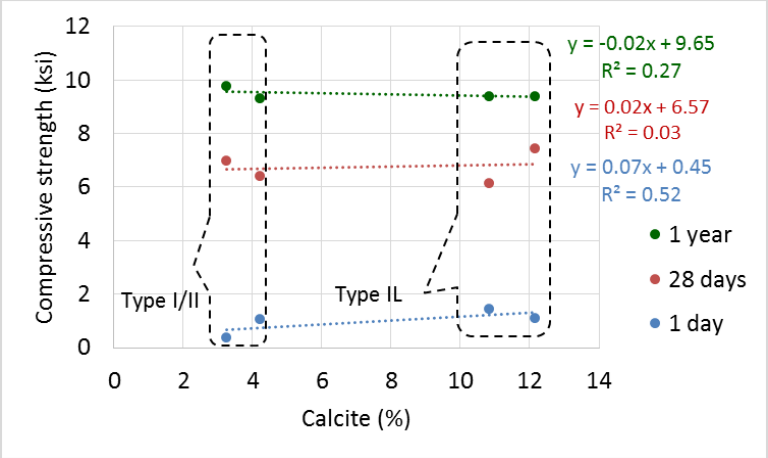

Figure 7.4: Effect of calcite content on compressive strength of concrete cured at 40 ºF

Table 7.2: Summary of calcite content if cements from plants A and C

Cement Type	Cement Source	
	Plant A	Plant C
Type I/II	3.2%	4.2%
Type IL	12.2%	10.8%

Analysis of variance (ANOVA) was conducted to investigate the statistical significance of the difference in values of the compressive strength of concrete made with Type I/II and Type IL cement of plants A and C. The null (no difference) hypothesis was that average strength of Type I/II and Type IL are similar (μ1=μ2). A summary of the results for the 90 ºF mixes is shown in Table 7.3, and for the 40 ºF mixes in Table 7.4, and the values for the base mixes (73 ºF) are shown in both tables. If the p-value was lower than 0.05, the null hypothesis was rejected and the difference in the average strength values were considered statistically significant. If the p-value was higher than 0.05, the differences were considered statistically insignificant. If the differences were

statistically significant, the percentage difference is shown. A positive percentage difference indicates concrete with Type IL showed a higher value than concrete made with Type I/II cement.

Table 7.3: ANOVA results for comparing Type I/II and Type IL from each plant for the compressive strength of the 90 ºF mixes

Time	Cement source			
	A/AL (73 ºF)	A/AL (90 ºF)	C/CL (73 ºF)	C/CL (90 ºF)
7 days	+3%	+45%	Similar	+5%
28 days	Similar	+33%	+8%	+1%
1 year	Similar	+38%	+9%	Similar

Table 7.4: ANOVA results for comparing Type I/II and Type IL from each plant for the compressive strength of the 40 ºF mixes

Time	Cement source			
	A/AL (73 ºF)	A/AL (40 ºF)	C/CL (73 ºF)	C/CL (40 ºF)
7 days	+3%	+8%	Similar	-8%
28 days	Similar	Similar	+8%	Similar
1 year	Similar	Similar	+9%	Similar

For the mixes cured at 90 ºF, the results showed that the differences between the compressive strength of concrete made with Type I/II and Type IL cements were significant for both plants A and C, except for the one-year strength of plant C mixes. This indicates that limestone has a statistically significant effect on the compressive strength when curing at high temperature. The finer Type IL (AL) resulted in 38% higher

concrete compressive strength than Type I/II (A) while the coarser Type IL (CL) resulted in similar values at one year, indicating that Type IL cement fineness has a significant effect on the long-term strength of mixes cured at high temperature.

For the mixes cured at 40 ºF, the results showed that the differences between the compressive strength of concrete made with Type I/II and Type IL cements were not significant for both plants A and C, except for the 7 days strength. This indicates that limestone has a statistically significant effect on early age compressive when curing at low temperature, but does not have a significant effect on later ages.

7.2 Elastic modulus

Elastic modulus was measured for concrete cylinders (6 in. x 12 in.) at 28 days of age (ASTM C469). Figure 7.5 and Figure 7.6 show the effect of curing temperature on the elastic moduli of concrete made with cements from plant A and plant C, respectively. All mixes showed relatively similar values to the base mixes. The figures also show the elastic moduli compared to the values calculated using Equation 6.2 (from ACI 363R-10 section 6.3).

$$E_c = 40000\sqrt{f'_c} + 10^6 \qquad \text{Equation 6.2}$$

where:

E_c: Modulus of elasticity (psi)

f_c': specified compressive strength of concrete (psi)

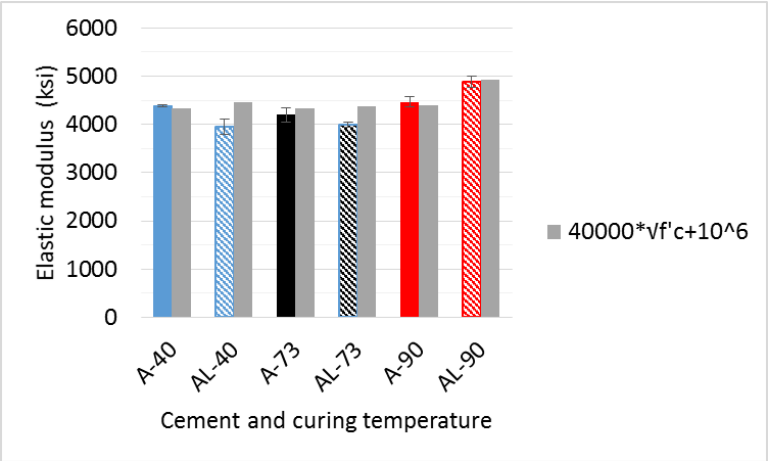

Figure 7.5: Elastic modulus of Class AA concrete made with Type I/II and Type IL cements from plant A cured at 40, 73, and 90 ºF

For concrete made with cements from Plant A, curing at 40 ºF resulted in 10% lower elastic modulus of Type IL (AL-40) than Type I/II (A-40) which followed the trend previously discussed for the 73 ºF mix. On the other hand, curing at 90 ºF resulted in 10% higher elastic modulus of concrete made with cement AL-90. ACI 363R-10's equation overestimated (13%) the elastic modulus value for AL-40 indicating the equation is not accurate for cold temperature curing. For the 90 ºF mixes, the equation predicted relatively close values to the measured ones.

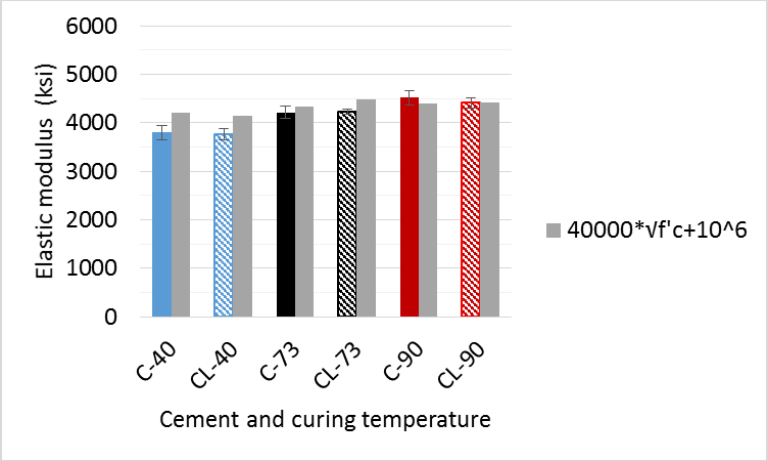

Figure 7.6: Elastic modulus of Class AA concrete made with Type I/II and Type IL cements from plant C cured at 40, 73, and 90 ºF

For concrete made with cements from Plant C, curing at 40 ºF resulted in statistically similar elastic modulus of Type I/II (C-40) and Type IL (CL-40) which followed the trend previously discussed for the 73 ºF mix. Statistically similar values were obtained for the C-90 and CL-90 mixes. ACI 363R-10's equation overestimated (10%) the elastic modulus value for both C-40 and CL-40 mixes, indicating that the equation is not accurate for cold temperature curing. For the 90 ºF mixes, the equation predicted relatively close values to the measured ones.

The above results followed the same trends observed for the compressive strength. Figure 7.7 shows the compressive strength values of concretes made with Type I/II and Type IL cements from plants A and C and cured at 40, 73, and 90 ºF. Figure 7.8 shows the elastic modulus values of concretes made with Type I/II and Type IL cements from plants A and C and cured at 40, 73, and 90 ºF. The trends seen for the elastic modulus values followed the trends seen for the compressive strength.

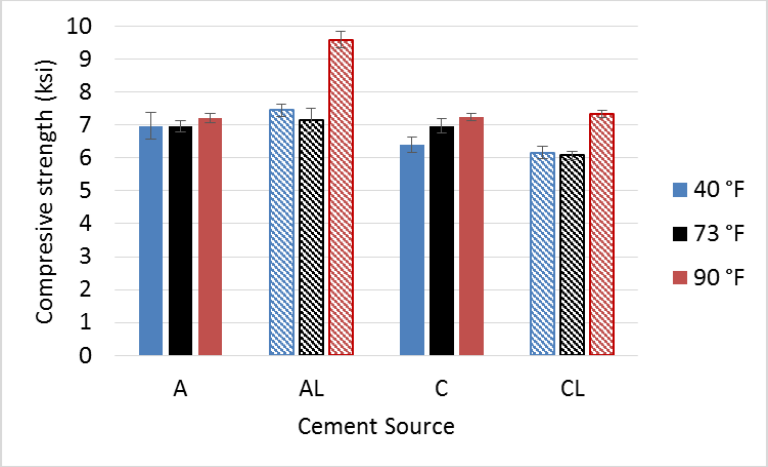

Figure 7.7: Compressive strength values of concretes made with Type I/II and Type IL cements from plants A and C and cured at 40, 73, and 90 ºF

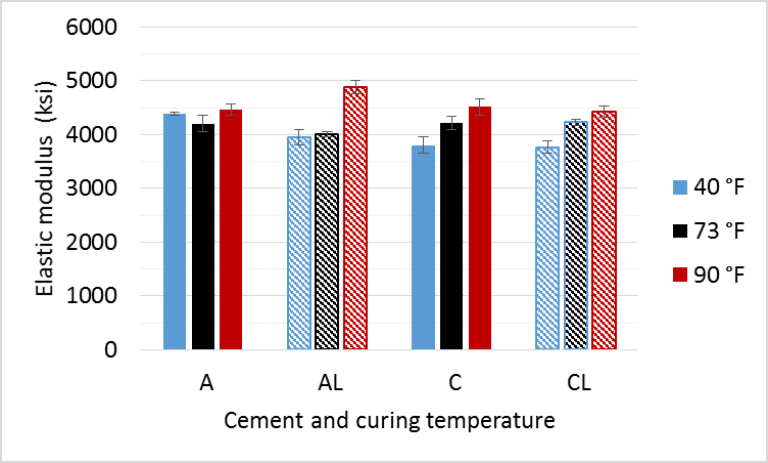

Figure 7.8: Elastic modulus values of concretes made with Type I/II and Type IL cements from plants A and C and cured at 40, 73, and 90 ºF.

Figure 7.9 shows a scatter plot of calcite content vs. the elastic modulus of concretes using cements from plants A and C and cured at 40, 73, and 90 ºF. After applying a linear regression best fit line, the general trend seen is that the higher the calcite content, the lower the elastic modulus for the mixes cured at 40 ºF. However, for

the concrete mixes cured at 90 ºF, higher calcite content resulted in larger elastic modulus values. This indicates that higher calcite content has an adverse effect on the stiffness of concrete at cold temperature curing.

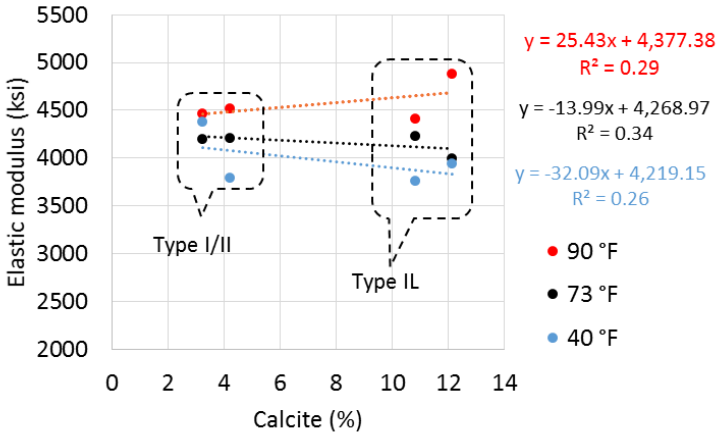

Figure 7.9: Effect of calcite content on elastic modulus of concrete with SCMs

7.3 Splitting tensile strength

Splitting tensile strength [ASTM C496, AASHTO T 198] was measured for Class AA concrete samples (4 in. x 8 in.) at 28 days of age. Figure 7.10 and Figure 7.11 show the effect of curing temperature on the splitting tensile strength values of concrete made with cements from plant A and plant C, cured at 40, 73, and 90 ºF. The figures also show the calculated values computed using ACI 363R-10 (equation 6-13 in ACI 363R-10 section 6.6) which was discussed in Chapter 6:

$$f_r = 7.4\sqrt{f'_c} \qquad \text{Equation 6.3}$$

where:

- f_{sp} = splitting tensile strength (psi)
- f_c' = compressive strength (psi)

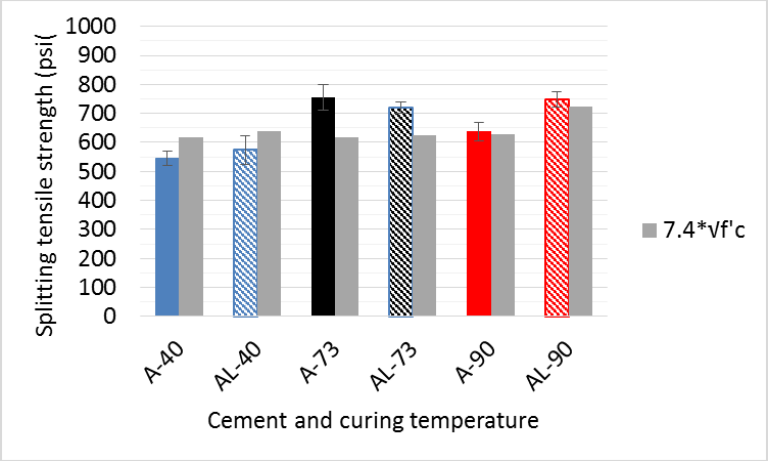

Figure 7.10: Splitting Tensile strength of concrete made with Type I/II and Type IL cements from plant A cured at 40, 73, and 90 ºF

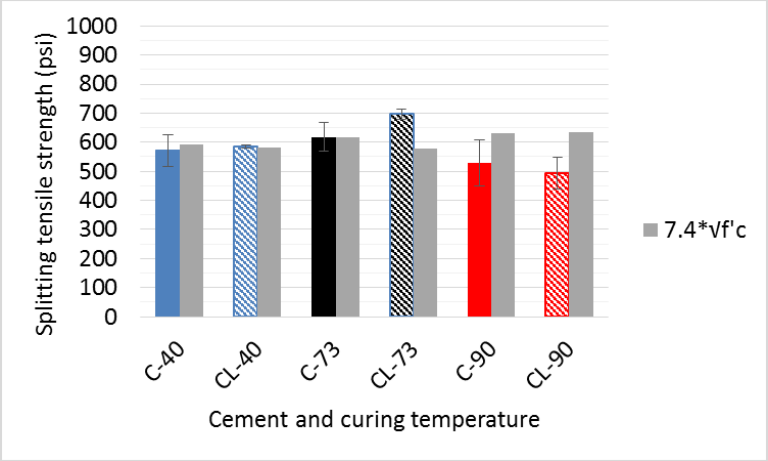

Figure 7.11: Splitting Tensile strength of concrete made with Type I/II and Type IL cements from plant C cured at 40, 73, and 90 ºF

For plant A (Figure 7.10), curing at 90 ºF resulted in 17% higher value of the mix made with AL, while the curing at 40 ºF resulted no statistically significant difference between A and AL. For plant C (Figure 7.11), curing and high and low temperature did not yield statistically significant differences between C and CL. This indicates that the finer Type cement AL has a significant effect on the results when cured at high temperature.

Figure 7.12 shows a scatter plot of calcite content vs. the splitting tensile strength of the concretes made with cements from plants A and C and cured at 40, 73, and 90 ºF. After applying a linear regression best fit line, it can be seen that the higher the calcite content, the higher the splitting tensile strength, but the slope of the regression line was highest for the mixes cured 90 ºF indicating that high temperature enhances the effect of limestone of the tensile strength of concrete.

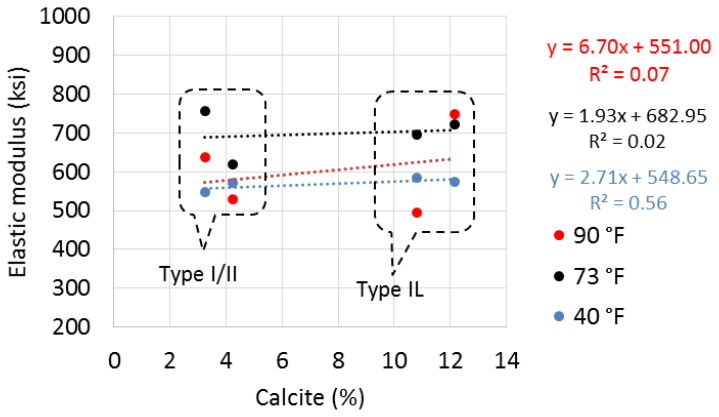

Figure 7.12: Effect of calcite content on the splitting tensile strength of concrete cured at 40, 73, and 90 ºF

Figure 7.13 shows a scatter plot of the average particle size (D_{50}) on the splitting tensile strength of concretes made with cements from plants A and C and cured at 40, 73, and 90 ºF. After applying a linear regression best fit line, it can be seen all best fit lines had negative slopes indicating a lower splitting tensile strength with larger particle size. The best fit line for values obtained at 90 °F showed the highest negative slope and the highest R^2 value, indicating a significant effect of particle size on the splitting tensile strength at high temperature (90 °F).

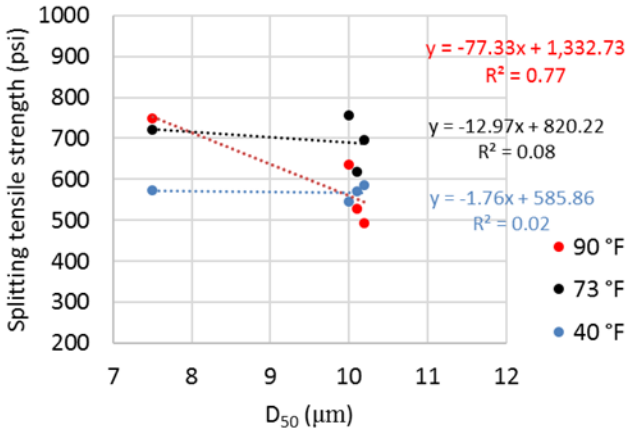

Figure 7.13: Effect of particle size on the splitting tensile strength of concrete cured at 40, 73, and 90 ºF

7.4 Drying shrinkage

Figure 7.14 and Figure 7.15 show the drying shrinkage values of class AA concrete made with Type I/II and Type IL cements from plants A and C cured at 90 ºF, 73 ºF, and 40 ºF (for 28 days). After curing, drying was done at 73 ºF for all samples.

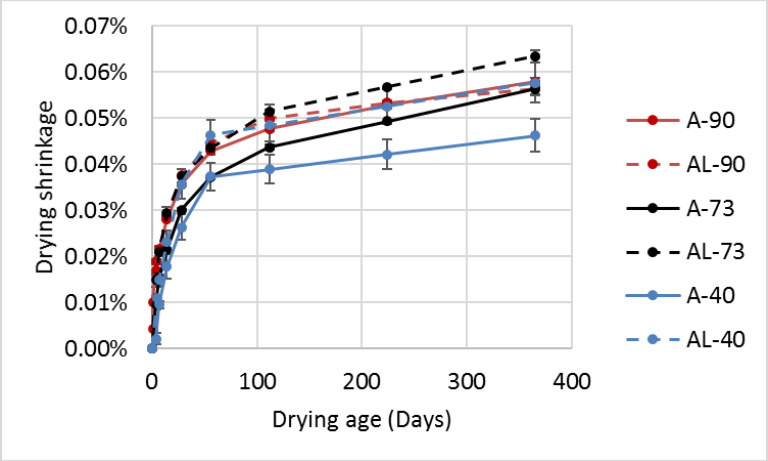

Figure 7.14: Drying shrinkage concrete using Type I/II and Type IL cements from plant A cured at 90 ºF, 73 ºF, and 40°F

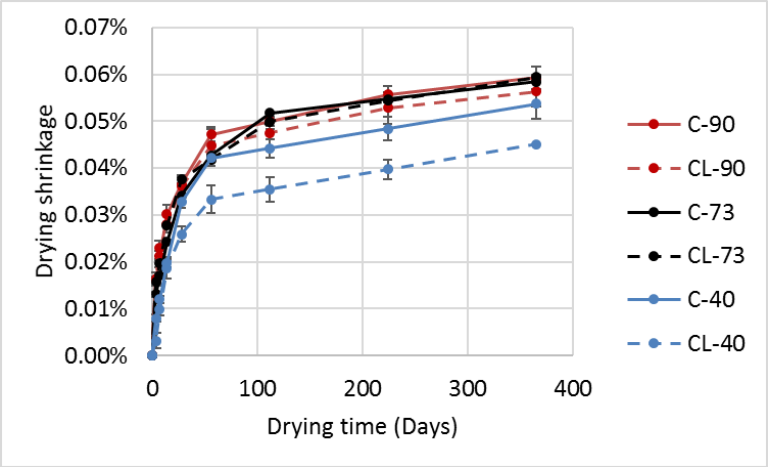

Figure 7.15: Drying shrinkage concrete using Type I/II and Type IL cements from plant C cured at 90 ºF, 73 ºF, and 40ºF

For plant A, curing at 90 ºF resulted in similar drying shrinkage values of Type I/II and Type IL cement. When compared to the base mixes (i.e. cured at 73 ºF), Type IL showed lower values (~10%), while Type I/II showed similar values.

For plant C, curing at 90 ºF resulted in similar drying shrinkage values of Type I/II and Type IL cement at both curing temperatures.

For plant A, curing at 40 ºF resulted in significantly larger drying shrinkage values (~25%) of Type IL cement than Type I/II cement. When compared to the base mixes (i.e. cured at 73 ºF), Type I/II and Type IL cements cured at 40 ºF showed lower values (~20% and ~10% respectively) than the base mixes.

For plant C, curing at 40 ºF resulted in lower drying shrinkage values (~15%) of Type IL cement than Type I/II cement. When compared to the base mixes (i.e. cured at 73 ºF), Type I/II and Type IL cements cured at 40 ºF showed lower values (~10% and ~25% respectively) than the base mixes.

The Federal Highway Administration (FHWA) Section 718-47 [59] specifies maximum drying shrinkage of 0.06% at 56 days which all the above mixes have successfully met.

Figure 7.16 and Figure 7.17 show scatter plots of calcite content vs. the splitting tensile strength of the concretes made with cements from plants A and C and cured at 90 ºF and 40 ºF, respectively. After applying a linear regression best fit line, it can be seen that higher the calcite content decreases the one-year shrinkage of the concretes cured at 90 ºF. However, for the concretes cured at 40 ºF, higher calcite content resulted in higher drying shrinkage.

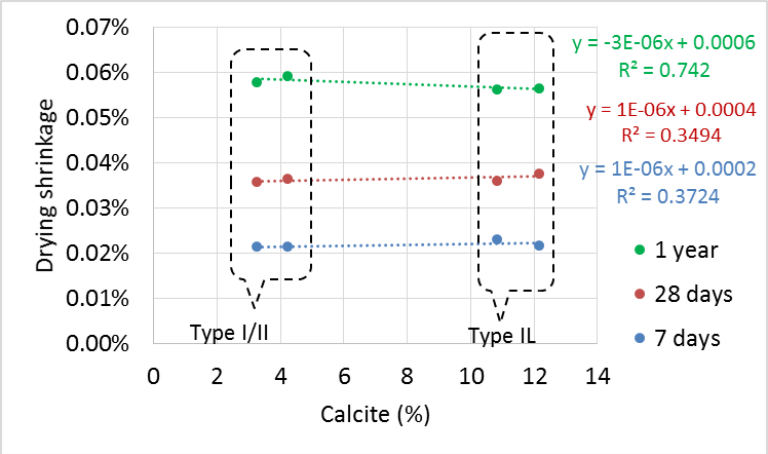

Figure 7.16: Effect of calcite content on the drying shrinkage of concrete cured at 90 ºF

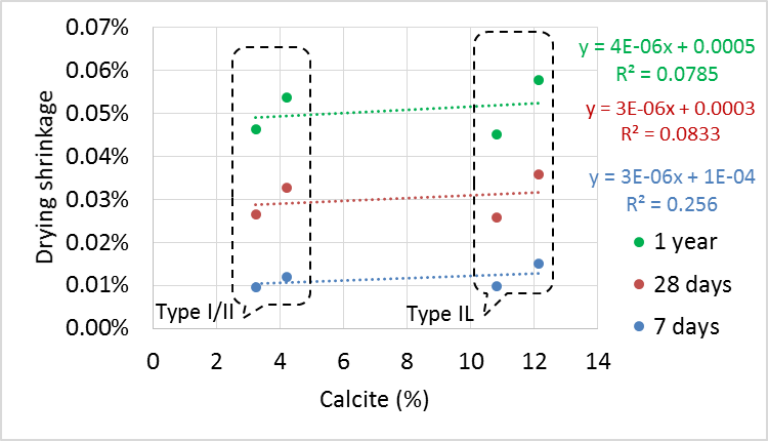

Figure 7.17: Effect of calcite content on the drying shrinkage of concrete cured at 40 ºF

7.5 Chapter discussion and conclusions

The results showed that the finer Type IL cement are more sensitive to higher curing temperature. When curing at 90 °F, the finer Type IL cement (AL) showed significant (30%) increase in compressive strength development at early age as well as 1 year when compared with Type I/II cement (A). When curing at 40 °F, finer Type IL

cement (AL) showed higher early strength but similar strength at later age. Limestone particles increased the nucleation sites and particle packing and therefore increased the early-age strength at low temperature. Similar trends were observed for the elastic modulus and splitting tensile strength. Cement "AL" resulted in 10% higher concrete elastic modulus and 17% higher concrete splitting tensile strength than cement "A" when curing at 90 °F.

In the case of Type IL (CL) and Type I/II (C) cements of similar fineness, curing at 90 °F showed similar concrete compressive strength. When curing at 40 °F, Type IL cement (CL) showed higher early age compressive strength but similar strength at 1 year. The higher early-age strength when using cement CL at low temperature can be attributed to the increased nucleation sites and particle packing due to limestone particles.

For the drying shrinkage, curing at 90 °F resulted in similar values for A and AL, while AL showed higher drying shrinkage values than A when cured at 40 °F. The author hypothesizes that higher temperature together with the finer Type IL cement (AL) resulted in a stiffer (higher elastic modulus) and more developed microstructure than concrete made with cement A at early ages, and the greater modulus resisted shrinkage strains. However, when cured at 40 °F, "AL" resulted in higher drying shrinkage than "A" just as observed for samples cured at room temperature. For plant C, curing at 90 °F resulted in similar shrinkage values when using cement "C" or "CL", while curing at 40 °F showed lower shrinkage when using "CL" than "C". The author hypothesizes that the samples made with coarser Type IL cement "CL" and cured at 40 °F resulted in more water to bleed out of the concrete, reducing the *w/b* and therefore decreasing the drying

shrinkage. Higginson [60] showed that coarser cement resulted in higher water bleed from the concrete before it hardened. Figure 7.18 shows the effect of cement fineness on bleeding of concrete [60] Further research with larger sample sizes is recommended to study that effect.

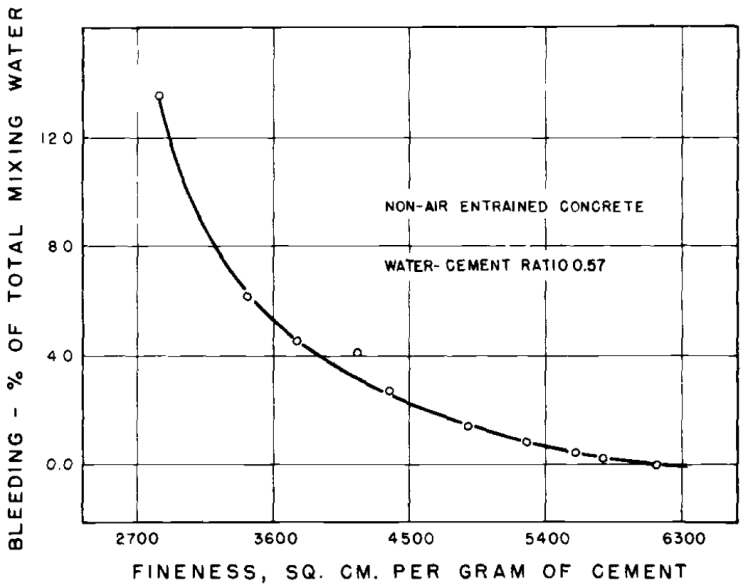

Figure 7.18: Effect of cement fineness on bleeding of concrete [60]

CHAPTER 8: INTERACTION WITH SUPPLEMENTARY CEMENTITIOUS MATERIALS IN CONCRETE

This chapter discusses the interactions of Type IL cement and supplementary cementitious materials (SCMs) and their effects on the performance of concrete. The SCMs used here were Class F fly ash, Class C fly ash, and ground granulated blast-furnace slag. The replacement rate of cement with fly ash was 15% by weight, while the replacement rate of cement with slag was 50% by weight. All concrete results reported in this chapter were for GDOT class AA concrete as described in Chapter 6.

8.1 SCM characterization

The SCMs used in this study are classified into two categories: pozzolanic and hydraulic. Pozzolanic SCMs contain reactive silicates which react with the calcium hydroxide produced from cement hydration to form additional calcium-silicate-hydrate (C-S-H), while hydraulic SCMs react with water and produce C-S-H. SCMs can have both pozzolanic and hydraulic properties, such as Class C fly ash which contains high amounts of calcium oxide. Class F fly ash contains low amounts of calcium oxide and is a pozzolanic material. Slag contains high amounts of calcium oxide and exhibits hydraulic behavior. Table 8.1 shows the chemical properties while Table 8.2 shows the physical properties of the SCMs used in this research.

Table 8.1: Chemical oxide analyses for SCMs
(LOI indicates loss on ignition at 1000°C) [50]

Component	Fly Ash (Class F)	Fly Ash (Class C)	Slag
SiO_2	51.30	34.57	38.77
Al_2O_3	23.32	18.78	7.62
Fe_2O_3	13.31	5.52	0.75
CaO	2.75	26.41	36.81
MgO	1.03	6.60	12.08
Na_2O	0.82	1.92	0.19
K_2O	2.43	0.47	0.48
TiO_2	1.25	1.39	0.26
SO_3	0.48	1.98	2.29
LOI	2.89	0.22	0.12

Table 8.2: Particle size distribution properties of SCMs [50]

Parameter	Cement A	Fly Ash (Class F)	Fly Ash (Class C)	Slag
D_{10}, μm	2.77	3.05	1.15	1.35
D_{50}, μm	10.0	15.3	8.08	7.38
D_{90}, μm	30.2	58.3	37.5	21.4
$D_{3,2}$, μm	6.28	6.67	3.58	3.79
$D_{4,3}$, μm	14.1	24.3	15.0	9.78
SSA, m^2/kg	288	337	627	566

8.2 Compressive strength

For this chapter, the following notation was used to label the concrete mixes as shown in Table 8.3.

Table 8.3: Notation of concrete mixes made with SCMs

Label	Cement source	Cement type	SCM type	SCM replacement of cement (% by weight)
A-F15	Plant A	Type I/II	Class F fly ash	15
AL-F15	Plant A	Type IL	Class F fly ash	15
A-C15	Plant A	Type I/II	Class C fly ash	15
AL-C15	Plant A	Type IL	Class C fly ash	15
A-S50	Plant A	Type I/II	Slag	50
AL-S50	Plant A	Type IL	Slag	50
C-F15	Plant C	Type I/II	Class F fly ash	15
CL-F15	Plant C	Type IL	Class F fly ash	15
C-C15	Plant C	Type I/II	Class C fly ash	15
CL-C15	Plant C	Type IL	Class C fly ash	15
C-S50	Plant C	Type I/II	Slag	50
CL-S50	Plant C	Type IL	Slag	50

Figure 8.1 shows the compressive strength values of Type I/II and Type IL cements from plant A with and without SCMs.

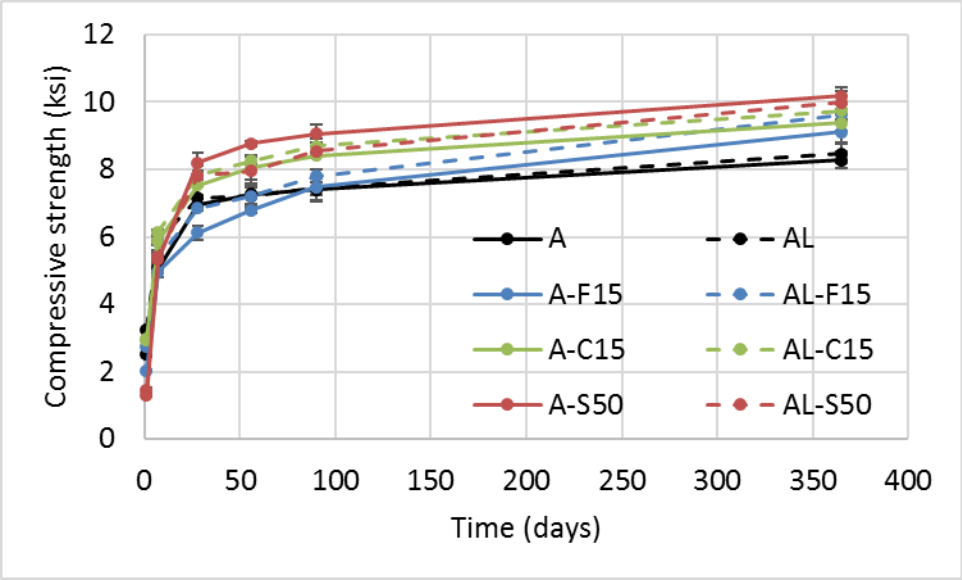

Figure 8.1: Compressive strength of Class AA concrete from plant A with SCMs

At one day, all SCM mixes showed lower compressive strength than the base mixes. The F-ash and C-ash mixes showed 10% to 20% lower strength than the base mixes, while the slag mixes showed ~50% lower strength than the base mixes. This was a result of the dilution of the cement by SCMs which may not participate in the compressive strength at early ages (due to the delay of the initiation of the pozzolanic reaction). Type IL showed higher strength than Type I/II with the F-ash and slag mixes, but similar strength for the C-ash mixes.

By 7 days, the strength of the SCM mixes caught up to and sometimes surpassed the base cement mixes; where the strength of the F-ash and slag mixes was less than 10% lower than the strength of the base mixes, while the C-ash mixes surpassed the strength of the base mixes which can be attributed to the hydraulic properties of C-ash and the lower replacement percentage compared to slag. AL-F15 showed higher strength than A-F15. Type I/II and Type IL showed similar values with C-ash and slag mixes.

By one year, all the SCM mixes resulted in strength values higher than the base mixes, with the slag mixes showing the highest strength. The compressive strength values of Type I/II with SCMs were similar to the values of Type IL with SCMs (no statistically significant differences).).

Figure 8.2 shows the compressive strength values of Type I/II and Type IL cements from plant C with and without SCMs.

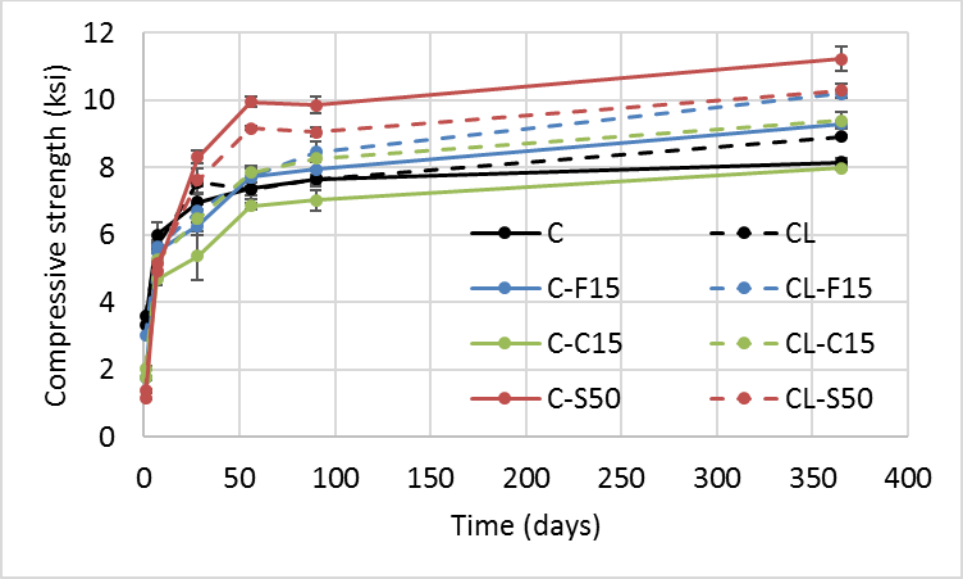

Figure 8.2: Compressive strength of Class AA concrete from plant C with SCMs

At one day, all SCM mixes showed lower compressive strength than the base mixes. The F-ash and C-ash mixes showed 50% lower strength than the base mixes (except for CL-F15 which showed 15% lower strength than CL), while the slag mixes showed 60% lower strength than the base mixes. This was a result of the dilution of the cement by SCMs which do not participate in the compressive strength at early ages (due to the delay of the initiation of the pozzolanic reaction). In general, at one day, the differences between the SCM mixes and the base mixes were larger for plant C than plant A as a result of the larger average particle size of the cement particles.

By 7 days, the F-ash mix strengths caught up to that of the base cement mixes; while C-ash and slag mixes showed lower values than the base mixes. For the C-ash and slag mixes, Type IL concretes showed strength values that were closer to the base mixes (10% lower than the base mixes) than Type I/II cement did (20% lower than the base

mixes). This indicates that limestone particles enhanced the nucleation effect with the SCM mixes.

By one year, all the SCM mixes resulted in strength values higher than the base mixes (except for CL-C15, which showed a similar strength to the base mix). The compressive strength of CL-F15 was higher than C-F15 (~15%). The C-C15 and CL-C15 mixes showed similar strength to the base mixes. For the slag mixes, the C-S50 and CL-S50 showed 35% and 15% higher compressive strength than the C and CL mixes, respectively. The difference was larger for Type I/II cement mainly due to the dilution effect as a result of the limestone replacement. All the SCM mixes showed either similar or higher strength than the base mixes, with the slag mixes showing the highest strength.

Figure 8.3 to Figure 8.5 show scatter plots of calcite content vs. the compressive strength of concrete at 1 day, 28 days, and 1 year for the F-ash, C-ash, and slag mixes, respectively. After applying a linear regression best fit line, it can be seen that the higher the calcite content, the larger the compressive strength for the fly ash mixes. However, the 1-year strength of the slag mixes is lower with higher calcite content. The nucleation effect was more dominant in the fly ash mixes, due to the larger particle size of the fly ash. However, the dilution effect was more dominant for the slag mixes due to the smaller particle size of the slag.

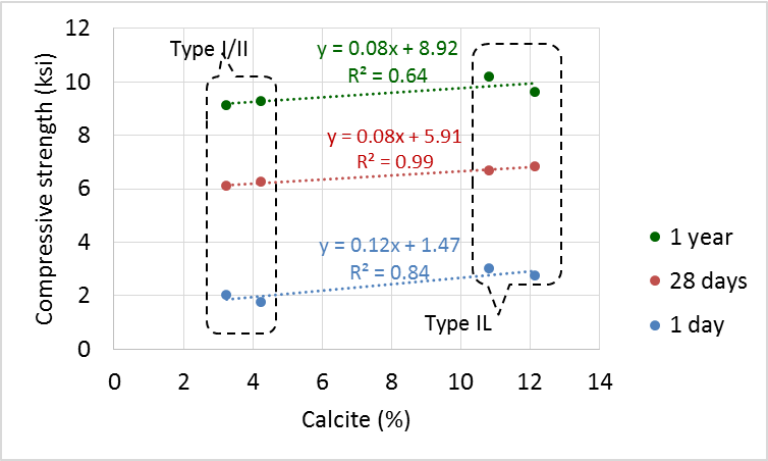

Figure 8.3: Effect of calcite content on compressive strength of concrete with class F fly ash

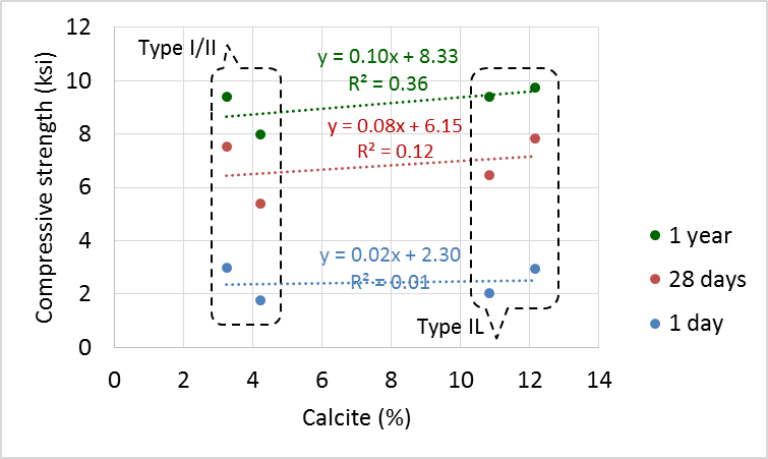

Figure 8.4: Effect of calcite content on compressive strength of concrete with class C fly ash

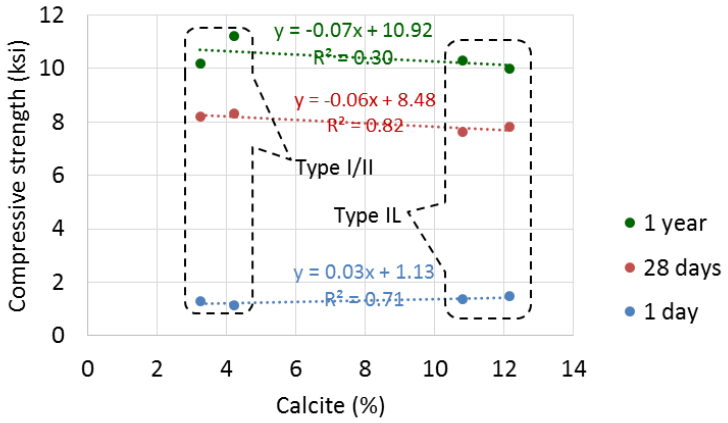

Figure 8.5: Effect of calcite content on compressive strength of concrete with slag

Analysis of variance (ANOVA) was conducted to investigate the statistical significance of the difference in values of the compressive strength of Type I/II and Type IL cement of plants A and C. A summary of the results for F-ash mixes is shown in Table 8.4. A positive percentage difference indicates concrete with Type IL showed a higher value than concrete made with Type I/II cement.

Table 8.4: ANOVA results for comparing Type I/II and Type IL from each plant for the compressive strength of the F-ash mixes

Time	Cement source and SCM			
	A/AL (no SCM)	A/AL + F-ash	C/CL (no SCM)	C/CL + F-ash
7 days	+16%	+9%	Similar	Similar
28 days	Similar	+12%	+8%	+7%
1 year	Similar	Similar	+9%	+10%

The results showed that for early-age strength, the F-ash mixes with finer Type IL cement (AL-F15) resulted in statistically higher strength when compared to the values of mix with the companion Type I/II (A-F15). The coarser Type IL cement, CL-F15, resulted in statistically higher strength at one year than C-F15. This indicates that for the F-ash mixes, the finer limestone resulted in higher strength at early age, while the coarser limestone resulted in higher strength at one year.

Table 8.5 shows the results of ANOVA for C-ash mixes, as well as the ANOVA results of the base mixes from plants A and C for comparison (discussed in Chapter 6). The results showed that the C-ash mixes with the finer Type IL cement (AL-C15) resulted in small differences that were not statistically significant when compared to the C-ash mixes with the companion Type I/II cement (A-C15). However, the C-ash mixes with the coarser Type IL cement (CL-C15) resulted in statistically higher strength when compared to the C-ash mixes with the companion Type I/II cement (C-C15). When compared to the base mixes (without SCMs), the main difference in behavior was observed at early age (7 days) where the C-ash decreased the differences between A and AL (finer) resulting in statistically similar strength, while it increased the differences between C and CL (similar fineness) where CL-C15 showed statistically higher strength. This can be due to Class C fly ash containing high amounts of calcium aluminosilicates, and De Weerdt at al. [61] reported chemical reactions occurring between the limestone and the aluminosilicates that resulted in increased volume of hydrates which subsequently led to increased compressive strength.

Table 8.5: ANOVA results for comparing Type I/II and Type IL from each plant for the compressive strength of the C-ash mixes

Time	Cement source and SCM			
	A/AL (no SCM)	A/AL + C-ash	C/CL (no SCM)	C/CL + C-ash
7 days	+16%	Similar	Similar	+12%
28 days	Similar	Similar	+8%	+20%
1 year	Similar	Similar	+9%	+18%

Table 8.6 shows the results of ANOVA for slag mixes, as well as the ANOVA results of the base mixes from plants A and C for comparison (discussed In Chapter 6). The results showed that the slag mixes with the finer Type IL cement (AL-S50) resulted in small differences that were not statistically significant when compared to the slag mixes with the companion Type I/II cement (A-S50). However, the slag mixes with the coarser Type IL cement (CL-S50) resulted in statistically lower strength than the mix with Type I/II cement (C-S50).

Table 8.6: ANOVA results for comparing Type I/II and Type IL from each plant for the compressive strength of the slag mixes

Time	Cement source and SCM			
	A/AL (no SCM)	A/AL + slag	C/CL (no SCM)	C/CL + slag
7 days	+16%	Similar	Similar	Similar
28 days	Similar	-5%	+8%	-8%
1 year	Similar	Similar	+9%	-8%

8.3 Elastic modulus

Elastic modulus was measured for concrete cylinders (6 in. x 12 in.) at 28 days of age (ASTM C469). Figure 8.6 and Figure 8.7 show the elastic moduli of cements from plant A and plant C, respectively, with SCMs. All mixes showed relatively similar values to the base mixes. The figures also show the elastic moduli compared to the values calculated using Equation 6.2 (from ACI 363R-10 section 6.3).

$$E = 40000\sqrt{f_c'} + 10^6 \qquad \text{Equation 6.2}$$

where:

- *E*: modulus of elasticity (psi)
- f_c': compressive strength (psi)

The values obtained using Equation 6.1 were higher than all of the experimental values indicating that the equation over estimates the 28-day elastic modulus of the concretes made with SCMs.

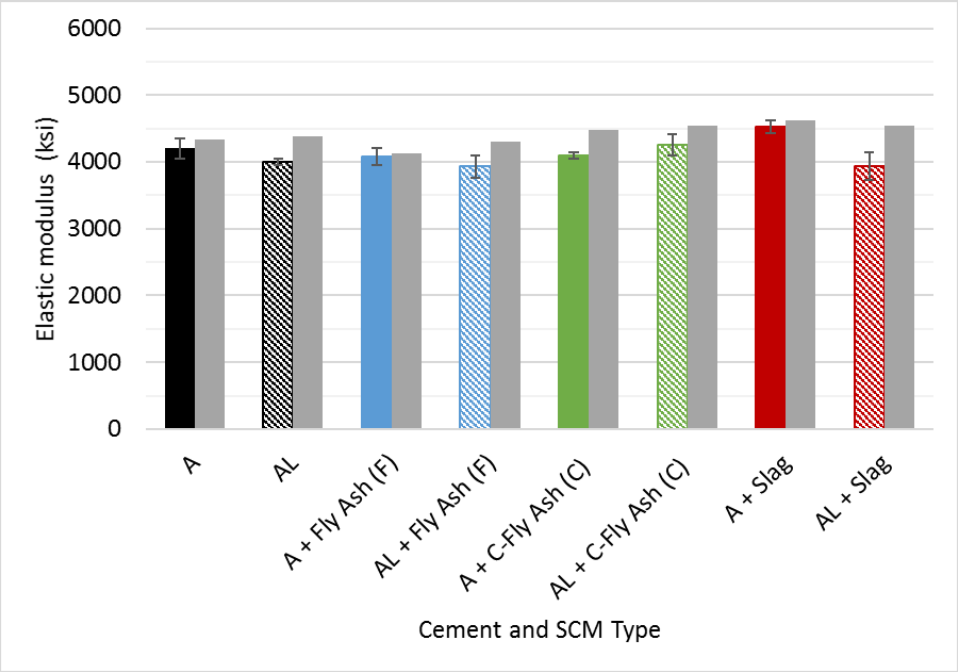

Figure 8.6: Comparison of elastic modulus values of plant A and SCMs with ACI 363R-10 predicted values in grey (Equation 6.2)

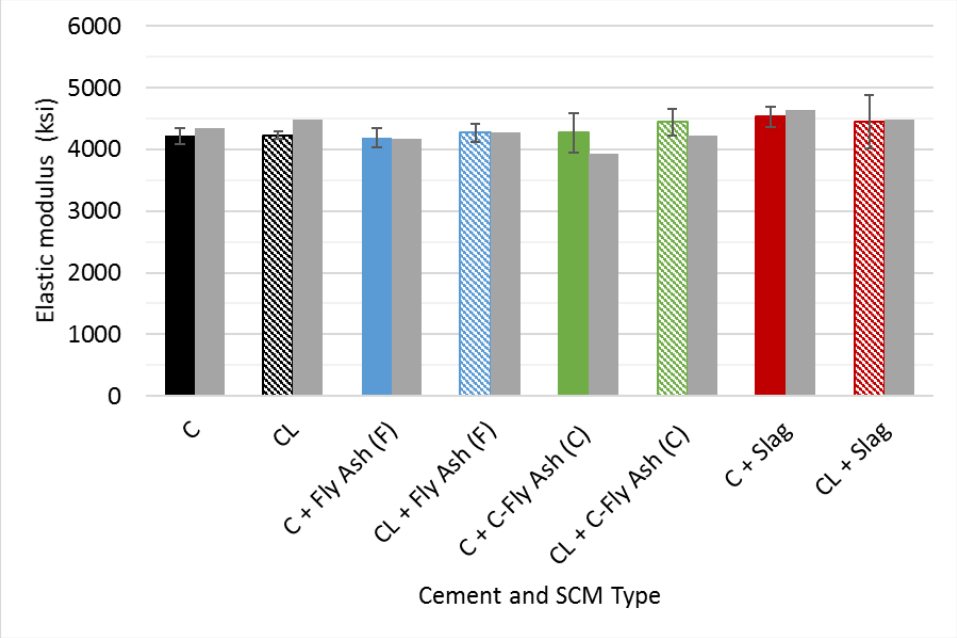

Figure 8.7: Comparison of elastic modulus values of plant C and SCMs with ACI 363R-10 predicted values

Figure 8.8 shows a scatter plot of calcite content vs. the elastic modulus of the SCM mixes and the base mixes of cements from plants A and C. After applying a linear regression best fit line, the general trend seen is that the higher the calcite content, the lower the elastic modulus. The exception to this trend was the mixes with the C-ash where higher calcite content corresponded with slightly higher elastic modulus. One possible reason for the behavior of the C-ash mixes is the hydraulic behavior of the C-ash. Class C fly ash contains high amounts of calcium oxide and reacts with water to produce C-S-H. The limestone particles have two effects related to surface area as well chemical interaction with the aluminosilicates [61]. Limestone particles increase the nucleation sites and, therefore, enhance the hydration reaction. A second explanation is related to the low fineness of C-ash, where the finer C-ash particles increased the nucleation sites and, therefore, enhanced the pozzolanic and hydration reactions of C-ash with higher limestone content.

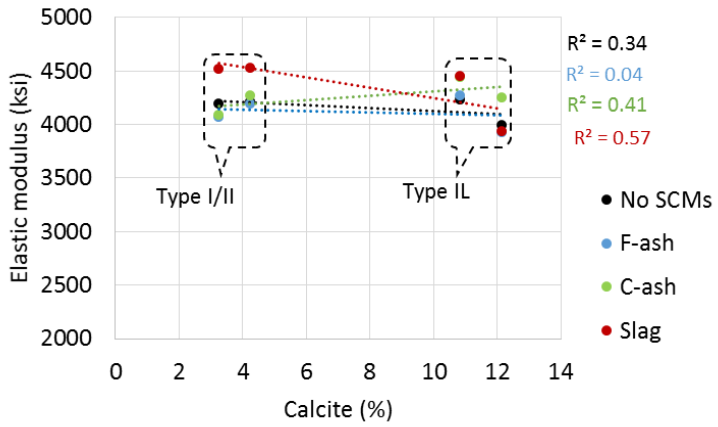

Figure 8.8: Effect of calcite content on elastic modulus of concrete with SCMs

8.4 Splitting tensile strength

Splitting tensile strength [ASTM C496, AASHTO T 198] was measured for concrete samples (4 in. x 8 in.) at 28 days of age. Figure 8.9 and Figure 8.10 show the splitting tensile strength values of cements from plant A and plant C, respectively, with SCMs. The figures also show the calculated values computed using ACI 363R-10 (equation 6-13 in ACI 363R-10 section 6.6) which was discussed in Chapter 6:

$$f_r = 7.4\sqrt{f'_c} \qquad \text{Equation 6.3}$$

where:

- f_{sp} = splitting tensile strength (psi)
- f_c' = compressive strength (psi)

For plant A (Figure 8.9), all SCM mixes showed lower splitting tensile strength than the base mixes. The F-ash mixes showed ~30% lower strength than the base mixes, and the C-ash mixes showed ~20% lower strength than the base mixes. For the fly ash mixes, Type I/II and Type IL showed relatively similar values. For the slag mixes, Type IL showed ~30% lower tensile strength than Type I/II. Cement AL as well as slag have small particle size. The small particle size of slag did not enhance the nucleation effect that was present due to the small limestone particles. The dilution effect was more dominant for the slag mix.

When comparing the measured values to the calculated values (Equation 6.3), the measured values of the SCM mixes with Type IL cement showed lower values than the calculated ones, suggesting that that such relations do not hold for SCM mixes with finer Type IL cement. As a reminder to the reader, for mixes without SCMs (discussed in Chapter 6), the measured values were equal to or slightly larger than the calculated values using Equation 6.3. The author hypothesizes that the partial replacement of cement with SCMs reduced the speed of hydration and therefore the tensile strength gain at 28 days (the age at which the test was conducted) did not match the values used to develop Equation 6.3.

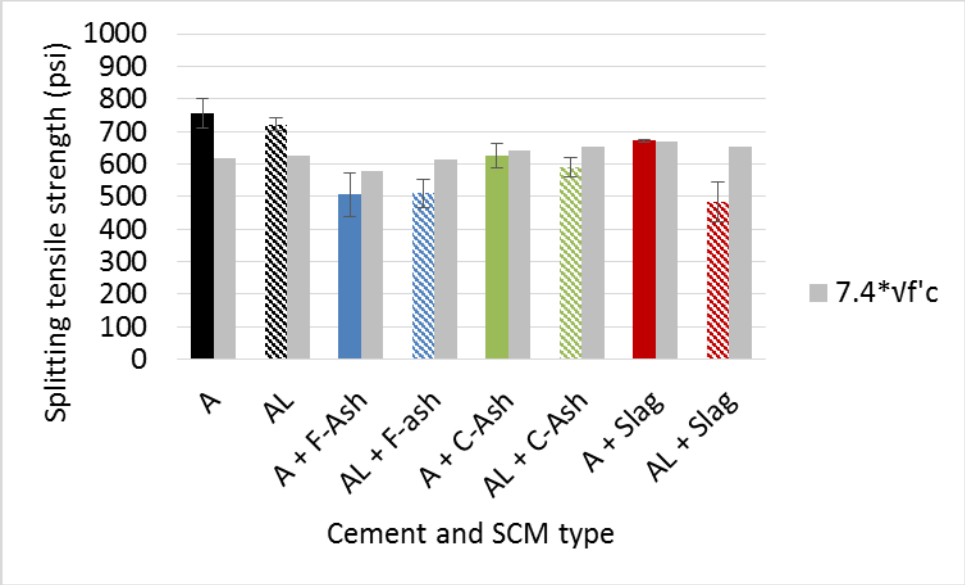

Figure 8.9: Splitting tensile strength of Type I/II and Type IL cements from plant A with SCMs.

For plant C (Figure 8.10), the fly ash mixes showed lower splitting tensile strength than the base mixes while the slag mixes showed relatively similar values to the base mixes. For F-ash and C-ash mixes, Type I/II cement with fly ash showed relatively similar values to the base mix while Type IL with fly ash showed ~15% lower strength than the base mix. This implies that the dilution effect is more dominant for the fly ash mixes with cements from plant C (due to the relatively larger size of cement C and CL). The slag mixes showed relatively similar values to the base mixes.

For plant C, the values obtained using Equation 6.3 were relatively similar to the experimental values. This indicates that Equation 6.3 was a good estimate of the tensile strength of concrete made with coarser limestone cement and SCMs.

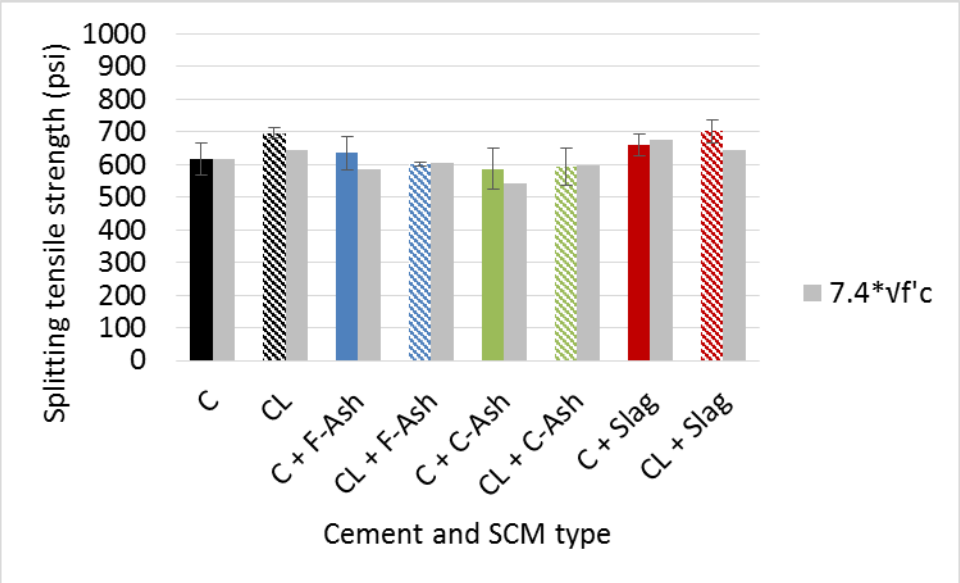

Figure 8.10: Splitting tensile strength of Type I/II and Type IL cements from plant C with SCMs

Figure 8.11 shows a scatter plot of calcite content vs. the splitting tensile strength of the SCM mixes and the base mixes of cements from plants A and C. After applying a linear regression best fit line, it can be seen that the scatter was large, but a trend can be observed where larger calcite content resulted in lower tensile strength.

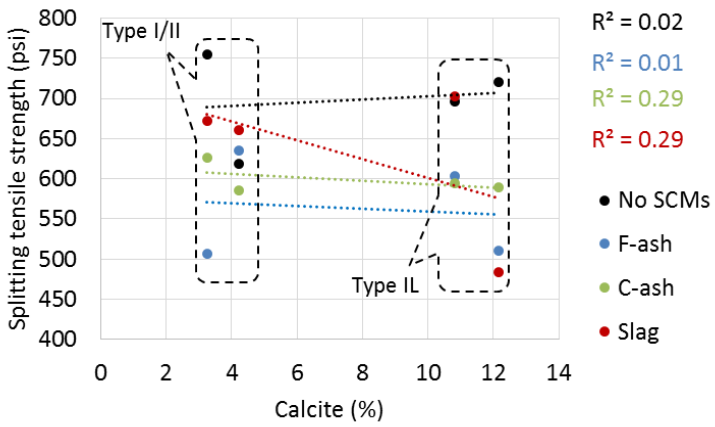

Figure 8.11: Effect of calcite content on the splitting tensile strength of concrete with SCMs

8.5 Drying shrinkage

The results of drying shrinkage (ASTM C157) measurements for the concrete mixes with SCMs are discussed below. All samples were cured for 28 days prior to the start of drying.

8.5.1 Class F fly ash

Figure 8.12 shows the drying shrinkage values of class AA concrete made with Type I/II and Type IL cements from plants A and C compared to mixes with 15% cement replacement (by weight) with class F fly ash.

For plant A, using 15% class F fly ash resulted in similar drying shrinkage values of Type I/II and Type IL concretes. When compared to the base mixes, using 15% class F fly ash reduced the drying shrinkage of Type I/II by 25% and Type IL by 15%.

For plant C, using class F fly ash resulted in relatively similar drying shrinkage values for Type I/II and Type IL concretes.

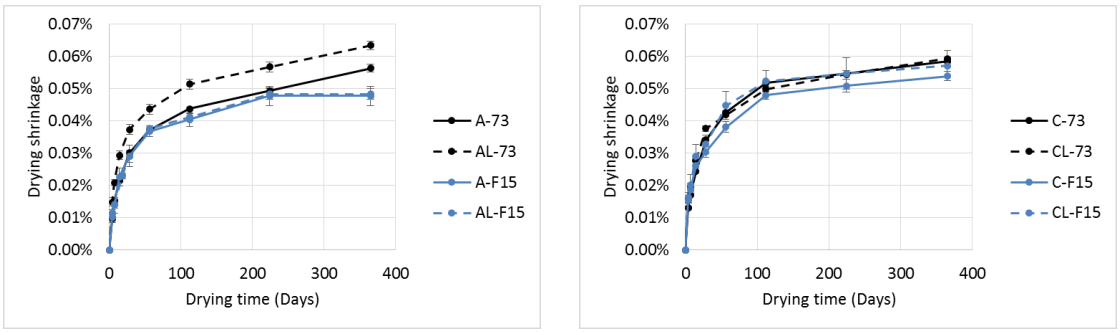

(a) Plant A (b) Plant C

Figure 8.12: Drying shrinkage of Type I/II and Type IL cements with 15% Class F fly ash replacement compared to base mixes

Analysis of variance (ANOVA) was conducted to investigate the statistical significance of the difference in values of the drying shrinkage of Type I/II and Type IL cement of plants A and C when used with class F fly ash in concrete. A summary of the results for the class F fly ash mixes is shown in Table 8.7. A positive percentage difference indicates concrete with Type IL showed a higher value than concrete made with Type I/II cement.

Table 8.7: ANOVA results for comparing Type I/II and Type IL from each plant for the drying shrinkage of class F fly ash mixes

Time	Concrete mixes compared	
	A-F15 and AL-F15	C-F15 and CL-F15
7 days	Similar	Similar
28 days	Similar	Similar
1 year	Similar	Similar

The results of ANOVA show that the difference in drying shrinkage between Type I/II and Type IL cements were not statistically significant at all ages.

8.5.2 Class C fly ash

Figure 8.13 shows the drying shrinkage values of class AA concrete made with Type I/II and Type IL cements from plants A and C compared to mixes with 15% cement replacement (by weight) with class C fly ash.

For plant A, using class C fly ash resulted in higher drying shrinkage of Type IL than Type I/II (~10% at 1 year). When compared to the base mixes, using 15% class C fly ash resulted in slightly lower drying shrinkage than the base mixes (~7% at 1 year).

For plant C, using 15% class C fly ash resulted in lower drying shrinkage of Type IL than Type I/II (~15%). When compared to the base mixes (i.e. without SCMs), using 15% class C fly ash resulted in higher drying shrinkage for Type I/II (~15%) than the base mix, while Type IL cement showed higher values during the first month (17% at 4

weeks) but then showed 7% lower shrinkage than the mix without the class C fly ash at 1 year.

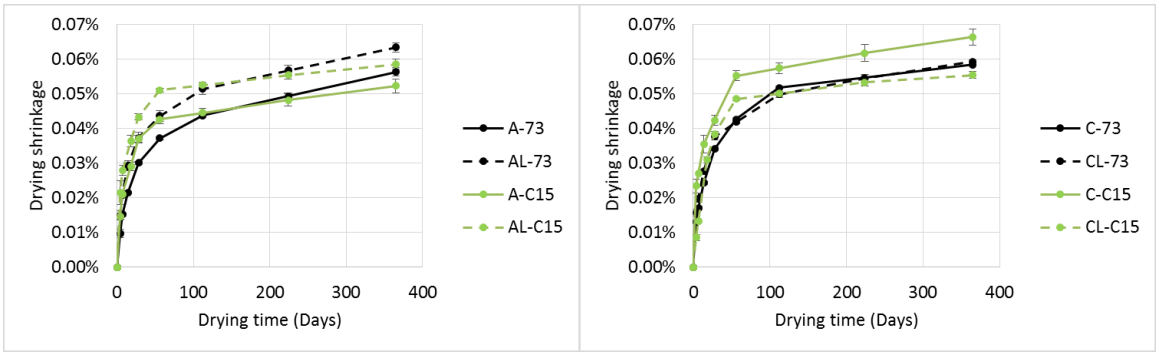

(a) Plant A (b) Plant C

Figure 8.13: Drying shrinkage of Type I/II and Type IL cements with 15% Class C fly ash replacement compared to base mixes

Comparing early age drying shrinkage behavior of the class C fly ash mixes with the class F-fly ash mixes (shown in Figure 8.14), the particle size seems to have a significant effect. At 7 days, cement A and AL with class C fly ash showed 35% higher drying shrinkage than the base mixes. Cement C with class C fly ash showed 60% higher drying shrinkage than the base mix, while cement CL with class C fly ash showed similar drying shrinkage to the base mix, indicating that the limestone in cement CL decreased the early age shrinkage when using class C fly ash.

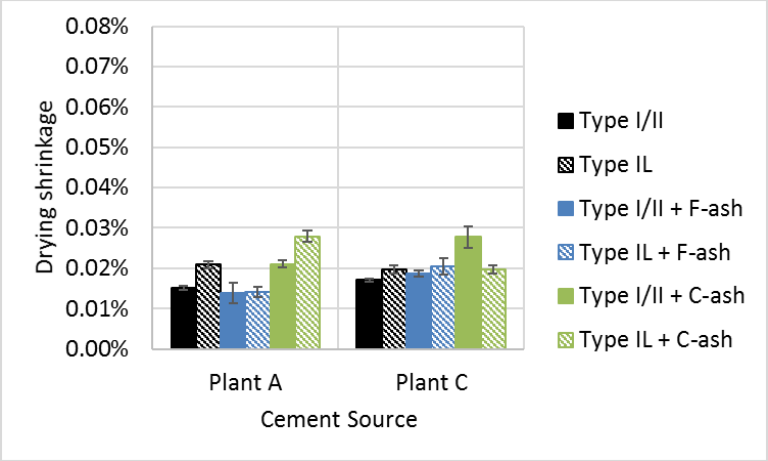

Figure 8.14: Drying shrinkage values at 7 days

Comparing the shrinkage at 1 year (shown in Figure 8.15), class F fly ash decreased the drying shrinkage for both cements. The difference when compared to the base mixes was higher for plant A than plan C (~20% and ~5%, respectively). Class C fly ash reduced the shrinkage for A, AL, and CL (~7%) but increased the 1-year shrinkage of cement C (~15%).

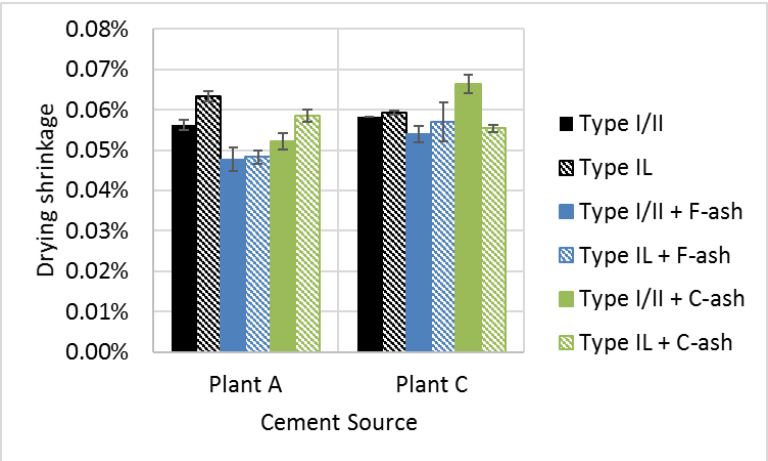

Figure 8.15: Drying shrinkage values at 365 days

Analysis of variance (ANOVA) was conducted to investigate the statistical significance of the difference in values of the drying shrinkage of Type I/II and Type IL cement of plants A and C when used with class C fly ash in concrete. A summary of the results for the class C fly ash mixes is shown in Table 8.8. If the p-value was lower than 0.05, the null hypothesis was rejected and the difference in the average values were considered statistically significant. A positive percentage difference indicates concrete with Type IL showed a higher value than concrete made with Type I/II cement.

Table 8.8: ANOVA results for comparing Type I/II and Type IL from each plant for the drying shrinkage of class C fly ash mixes

Time	Concrete mixes compared	
	A-C15 and AL-C15	C-C15 and CL-C15
7 days	+32%	-29%
28 days	+17%	-9%
1 year	+12%	-16%

The results of ANOVA show that the difference in drying shrinkage between Type I/II and Type IL cements were statistically significant at all ages. Concrete mix AL-C15 showed higher drying shrinkage than A-C15 while CL-C15 showed lower drying shrinkage than C-C15. The finer Type IL cement (AL) resulted in higher drying shrinkage which followed the same trend seen with the neat mixes. Therefore, finer Type IL cements blended with Class C fly ash are not recommended for applications were drying shrinkage is required to be minimized.

8.5.3 Slag

Figure 8.16 shows the drying shrinkage values of class AA concrete made with Type I/II and Type IL cements from plants A and C compared to mixes with 50% cement replacement (by weight) with slag.

For plant A, using 50% slag resulted in similar drying shrinkage values for A-S50 and AL-S50 mixes. When compared with base mixes, using 50% slag resulted in lower drying shrinkage values for Type I/II and Type IL (~20% and ~25%, respectively) at one year.

For plant C, using 50% slag resulted in 8% lower drying shrinkage values for CL-S50 when compared to C-50. When compared with base mixes, using 50% slag resulted in lower drying shrinkage values for Type I/II and Type IL (~5% and ~15%, respectively) at one year.

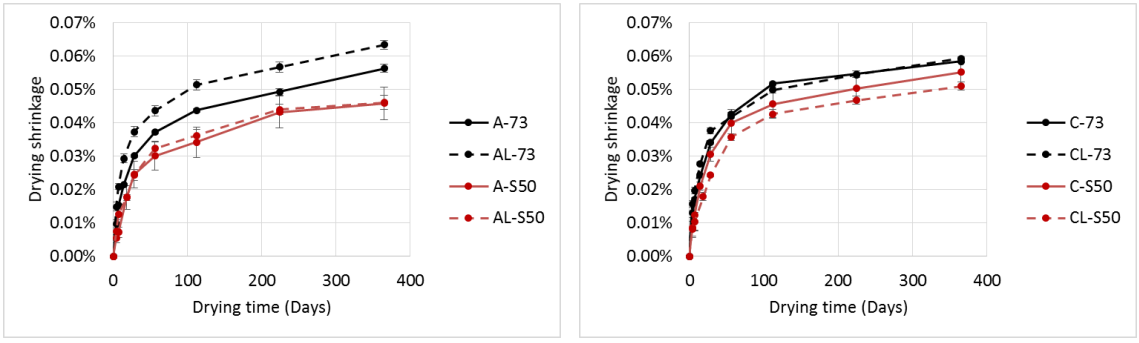

(a) Plant A (b) Plant C

Figure 8.16: Drying shrinkage of Type I/II and Type IL cements with 50% slag replacement compared to base mixes

Analysis of variance (ANOVA) was conducted to investigate the statistical significance of the difference in values of the drying shrinkage of Type I/II and Type IL

cement of plants A and C when used with class C fly ash in concrete. A summary of the results for the slag mixes is shown in Table 8.9. A positive percentage difference indicates concrete with Type IL showed a higher value than concrete made with Type I/II cement.

Table 8.9: ANOVA results for comparing Type I/II and Type IL from each plant for the drying shrinkage of slag mixes

Time	Concrete mixes compared	
	A-S50 and AL-S50	C-S50 and CL-S50
7 days	74%	Similar
28 days	Similar	-21%
1 year	Similar	Similar

The results of ANOVA show that when blended with slag, AL-S50 showed higher shrinkage than A-S50 at 7 days, while C-S50 and CL-S50 showed similar drying shrinkage. This indicates that when finer Type IL cement (AL) was blended with slag, the result was a larger drying shrinkage at early age which is not favorable, and therefore it is not recommended to use finer Type IL cement with slag for applications where low early age drying shrinkage is required. The ANOVA results showed similar shrinkage values of the slag mixes at 1 year.

8.6 Chapter discussion and conclusions

8.6.1 Mechanical properties

For finer Type IL cement (AL), the early-age concrete compressive strength was lower when blended with all SCMs in comparison to concrete made with Type IL (AL) without SCMs due to the dilution of the cement by SCMs and the delay of the initiation of the pozzolanic reaction. Also, Type IL showed higher strength than Type I/II for the F-ash and slag mixes indicating that the higher fineness enhanced early age strength development. At 1 year, Type IL concretes with SCMs resulted in similar strength to Type I/II concretes with SCMs, and all SCM mixes showed higher strength than the base mixes.

For Type IL cement of similar fineness to Type I/II (Plant C), the early-age concrete compressive strength was lower for all SCM mixes in comparison to concrete made with Type IL (CL) without SCMs, but the differences between the SCM mixes and the base mixes were larger for plant C than plant A as a result of the larger average particle size of the cement particles. At 1 year, Type IL with fly ash (both classes) resulted in higher strength than Type I/II with fly ash, while Type IL with slag resulted in lower strength than Type I/II with slag which indicates that the dilution effect was more dominant with coarser Type IL cement blended with slag. Nevertheless, all mixes with slag were stronger than the base mixes at one year.

When looking at the data from both plants, the higher the calcite content, the greater the compressive strength for the fly ash mixes. Slag mixes showed a similar trend

for the 1-day strength. However, the 1-year strength of the slag mixes was lower with higher calcite content due to the dilution effect which was enhanced by the higher cement replacement rate with slag (50%). The nucleation effect was more dominant in the fly ash mixes, due to the larger particle size of the fly ash.

Figure 8.17, Figure 8.18, and Figure 8.19 show previous compressive strength results for concrete and for mortar using Type I cement and class F fly ash [62], class C fly ash [62], and slag [63]. The fly ash mixes (Figure 8.17 and Figure 8.18) contained 75% cement and 25% fly ash by weight, while the slag mixes (Figure 8.19) contained 20% slag. The results showed reduced early age strength for all blends with SCMs due to the dilution of cement by SCMs and the delayed hydration and pozzolanic reactions of SCMs in relation to that of cement. Class C fly ash resulted in relatively higher strength due to its combined hydraulic and pozzolanic behaviour. Slag resulted in lower strength when blended with limestone in comparison to without limestone due to the dilution effect of limestone on the cementitious material of the blend. The trends seen were similar to the ones presented in this research. The results also show the compressive strength varied depending on the SCM composition and the mix designs.

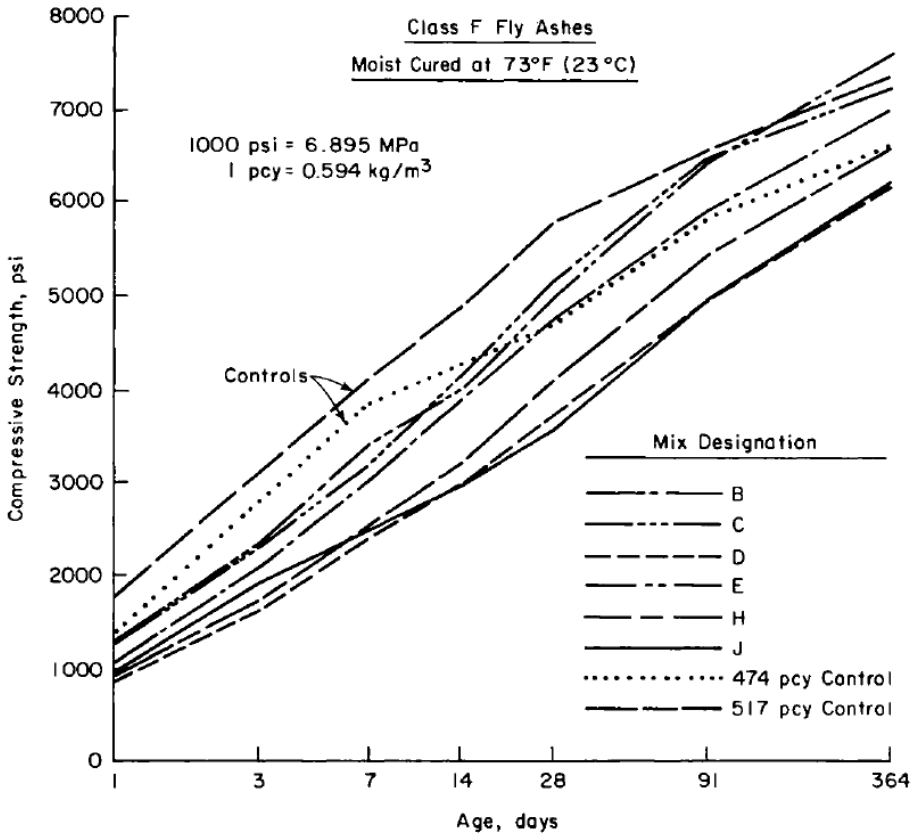

Figure 8.17: Compressive strength development of concrete with various Class F fly ashes. No mix had limestone addition

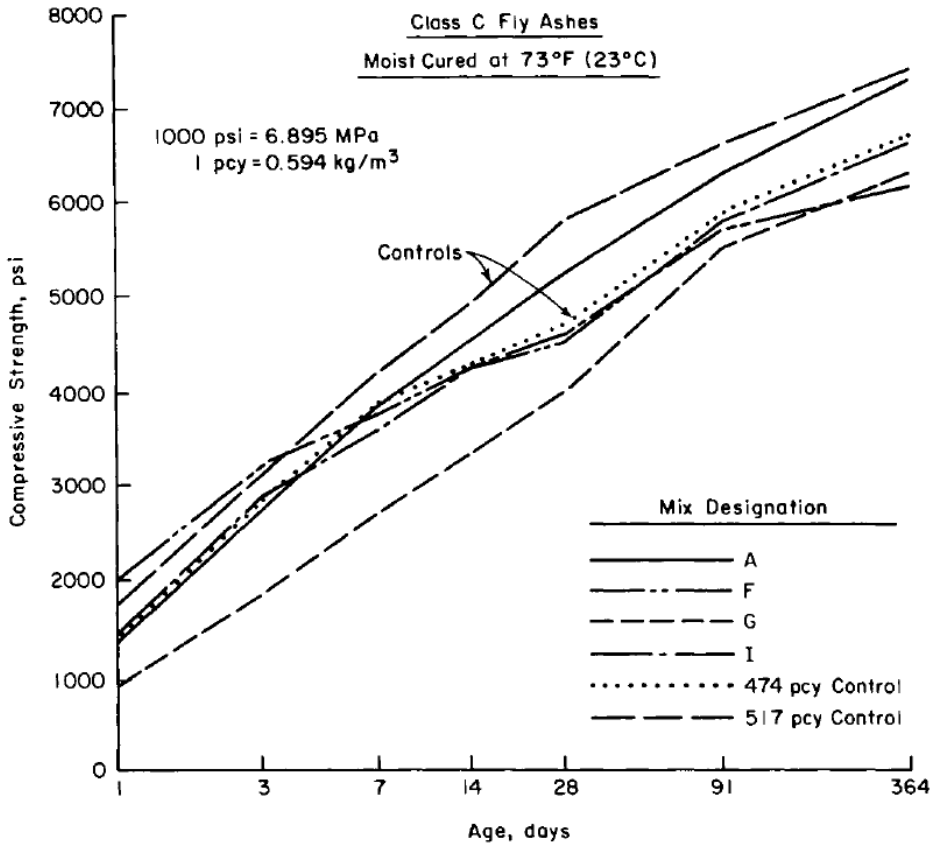

Figure 8.18: Compressive strength development of concrete with various Class C fly ashes. No mix had limestone addition

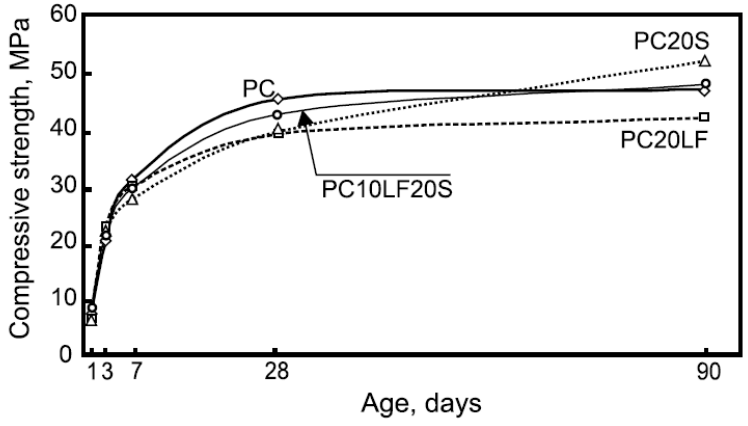

Figure 8.19: Compressive strength of mortar made various combinations of limestone filler and slag. "20LF" means a 20% replacement of cement with limestone while "10LF20S" means a 10% replacement of cement with limestone and 20% with slag.

Figure 8.20 and Figure 8.21 show the drying shrinkage (ASTM C157) values for concretes made with SCMs from plants A and C, respectively. The Class F fly ash mixes showed similar results when using Type IL and Type I/II. The class C fly ash mixes showed that finer Type IL (AL-F15) resulted in higher shrinkage than Type I/II (A-C15) while coarser Type IL (CL-C15) showed lower shrinkage than Type I/II (C-C15). At 7 days, the class F fly ash mixes showed similar or lower shrinkage than the base mixes while class C fly ash resulted in higher shrinkage than the base mixes. This indicates that Class F is better suited for lower early age shrinkage requirement when blended with Type IL cement. Finer Type IL cement with slag (AL-S50) showed similar shrinkage to Type I/II with slag (A-S50), while the coarser Type IL cement with slag (CL-S50) resulted in lower shrinkage than its companion Type I/II cement with slag (C-S50). At one year, all SCM blends showed similar or lower shrinkage than the base mixes.

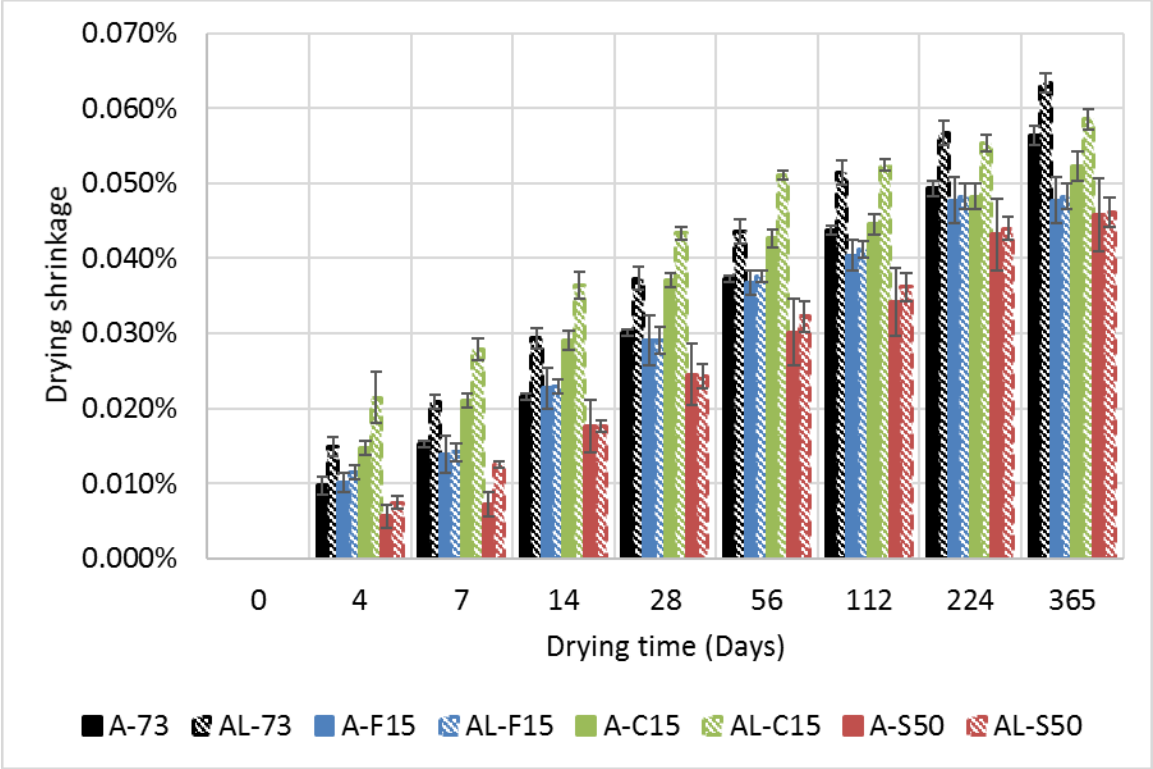

Figure 8.20: Drying shrinkage values (ASTM C157) of Type I/II and Type IL cement from plant A blended with various SCMs

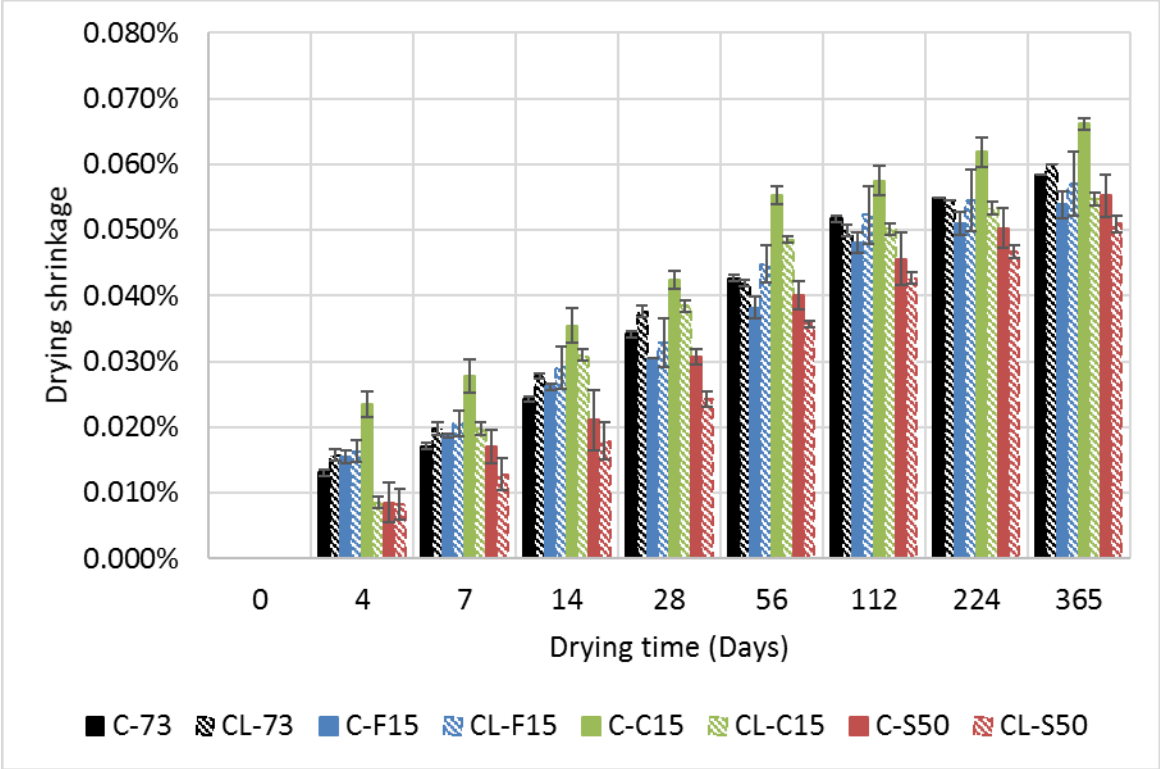

Figure 8.21: Drying shrinkage values (ASTM C157) of Type I/II and Type IL cement from plant C blended with various SCMs

CHAPTER 9: PRESTRESSED CONCRETE BEAM MATERIAL & STRUCTURAL PROPERTIES

This chapter compares the performance of Type I/II to Type IL cement in prestressed beam applications. The main objective was to determine if Type IL was applicable for use in bridge girders. Mustafa test-blocks [48] were constructed to investigate adequacy of bond between prestressing strand and the two concrete types. Prestressed beams were constructed to measure prestress losses, strand transfer length, strand development length, and beam flexural strength. GDOT's Class AAA concrete (Section 3.6 for mix design) with Type I/II and Type IL cements from plant C was used for block and beam construction because only C and CL were available from a local ready-mixed concrete plant.

9.1 Strand bond: Mustafa test for direct pull-out

Mustafa test for direct pull-out were performed to compare the direct bond strength of prestressing strands with concretes made with Type I/II and Type IL cement. The results showed that limestone cement performed similarly to Type I/II cement for bond development.

For ease of the reader, Figure 3.31 and Figure 3.32 are shown below to illustrate the specimen and the instrumentation used for the test. The load was measured using a load cell. The deflection was measured using a linear variable differential transformer (LVDT).

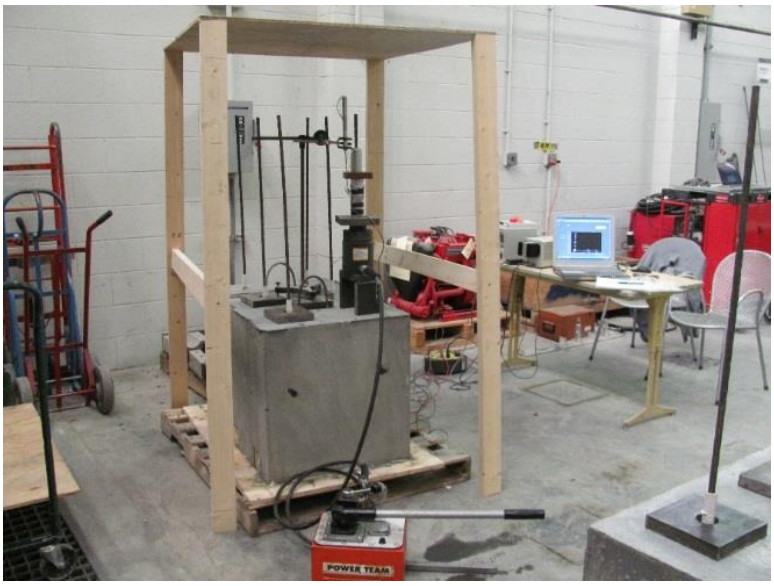

Figure 3.31: Specimen for the Mustafa test

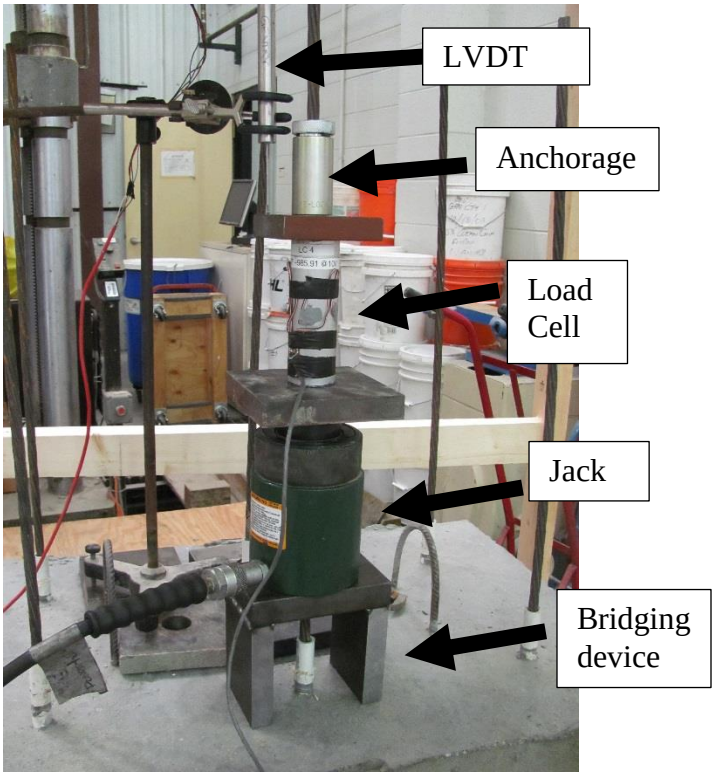

Figure 3.32: Instrumentation for the Mustafa test

The strands were pulled to a force beyond yielding with no observed slip. One of the wires in Strand 1 in the Type IL block broke after yielding, and no slip occurred in that case as well. The results showed similar behavior of the strands embedded in concrete with Type I/II to the strands embedded in concrete with Type IL cement as illustrated by the load-displacement plots in Figure 9.1. These Mustafa tests indicated that the strand-concrete bond was the same for concretes made with Type I/II and with Type IL cements.

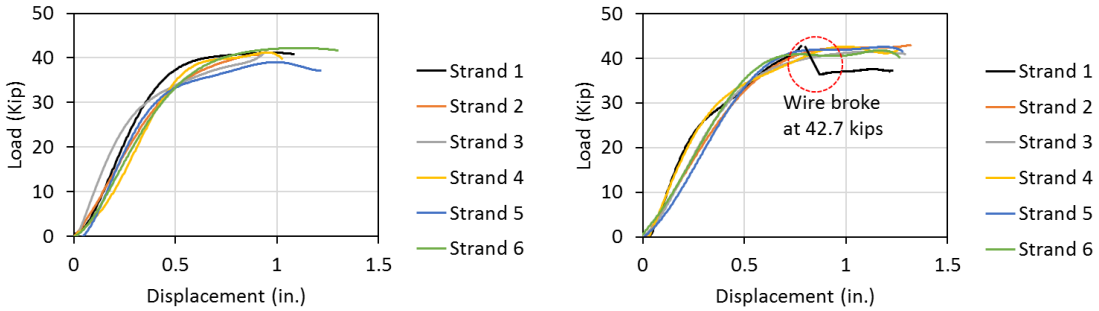

Figure 9.1: Mustafa pull-out test results, (a) Type I/II concrete, (b) Type IL concrete

9.2 Prestress losses in precast beams

To determine prestress losses in the four beams, strains were measured internally using vibrating wire strain gages located at the level of the strands, 2-in. above the bottom of each beam. Compression in concrete due to strand release caused the immediate measured strain values to increase (elastic shortening losses). The initial jacking force was 30.98 kips resulting in 202.5 ksi stress in the prestressing strands corresponding to 75% of the nominal strand strength which is the AASHTO stress limit

immediately prior to transfer for low relaxation strands. The measured compressive strain values continued to increase for the following 3 months due to time-dependent losses, drying shrinkage and creep. Relaxation losses were computed based on AASHTO refined equations for determining total losses; relaxation losses were computed as 1% of the jacking stress. Figure 9.2 shows beam 3 in its vertical position prior to testing.

Figure 9.2: Beam 3 in its vertical position prior to testing

Figure 9.3 shows the prestress losses over time for the four beams. Figure 9.4 shows the total loss in prestressing measured 3 months after strand release for the four beams (two made with Type I/II cement, B1 and B2, and the other two made with Type IL cement, B3 and B4) as well as the calculated losses using AASHTO LRFD [49] "refined" prestressing losses equations. The results show relatively similar total losses

among the 4 beams; total losses were also similar to those predicted using AASHTO LRFD. The average total prestress loss for beams made with Type IL were about 5% lower than the values calculated values using AASHTO equations, while the average total losses for beams made with Type I/II were about 6% less than the calculated values.

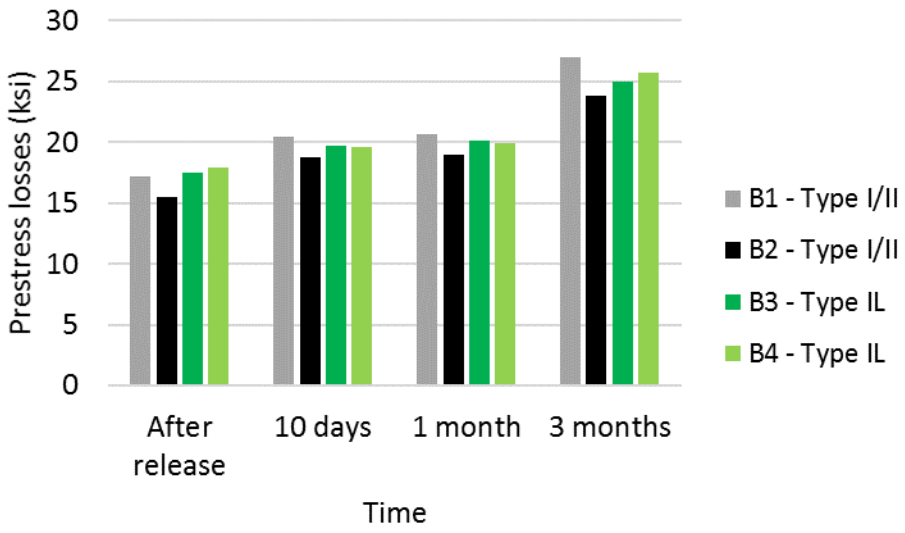

Figure 9.3: Prestress losses over time for the four beams

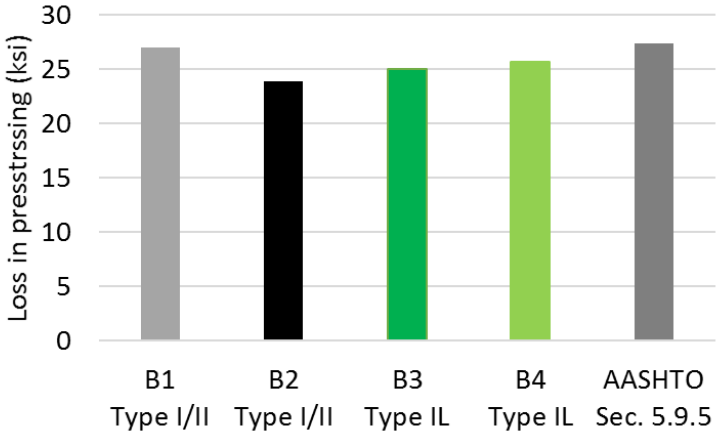

Figure 9.4: Total prestress losses in comparison to AASHTO "refined losses" calculations.

Figure 9.5 shows the distribution of prestress losses as a percent of initial prestressing force for beams made with Type I/II cement and beams made with Type IL cement. The results show that elastic shortening losses for concrete made with Type I/II cement (C) were 16% lower than concrete made with Type IL cement (CL). The main reason for the difference is that the compressive strength of concrete made with Type I/II cement was 16% higher than concrete made with Type IL cement with the Type IL concrete; the beams with Type IL cement had a modulus of elasticity about 5% less than that of the Type I/II concrete. The results also showed that the time-dependent losses of concrete made with Type I/II cement was 16% higher than that of concrete made with Type IL cement. The sustained prestressing load results in creep in the concrete. Concrete made with Type I/II cement resulted in higher amount of hydrates (C-S-H) than Type IL cement (due to the dilution effect of the limestone filler). Increasing the cement content increased creep as discussed by Nawy [64], and since the concrete made with Type I/II cement had more C-S-H, more creep resulted in concrete made with Type I/II cement than concrete made with Type IL cement. This resulted in higher time-dependent losses of concrete made with Type I/II cement than concrete made Type IL cement.

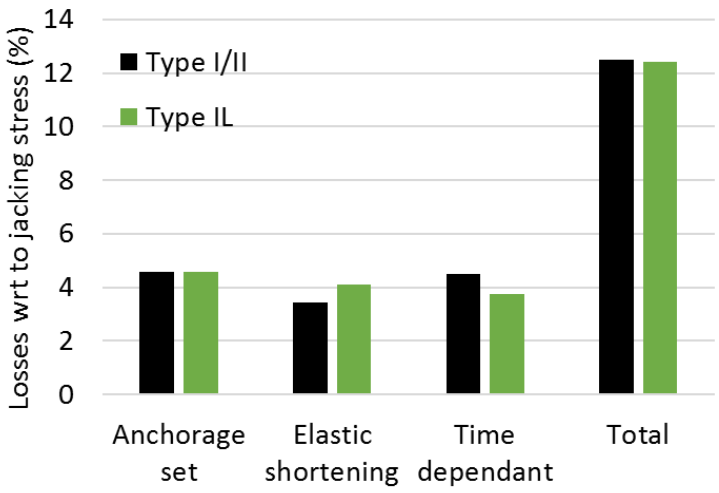

Figure 9.5: Average prestress losses of beams made with Type I/II and beams made with Type IL cement. Time dependent losses combine concrete creep and shrinkage plus strand relaxation

9.3 Transfer length

By use of the technique developed by Russell [65], the transfer length measurements were averaged and the transfer length (L_t) was determined as the intersection of the initial slope of the strain and 95% of the mean strain where the strain is constant, as shown in Figure 9.6. Table 9.1 presents the resulting transfer lengths. The experimental results were compared with those specified by AASHTO LRFD [49] and by ACI 318-14 [54]. The AASHTO value is determined as 60*d_b where d_b is the strand diameter. The ACI value is equal to (f_{se}/3000)*d_b where f_{se} is the effective stress in the prestressing strands after losses. The f_{se} value was determined using the measured initial and final strains in the strands as measured by the embedded vibrating wire strain gages and initial jacking forces. The results showed that transfer lengths were less than 30% of the AASHTO LRFD specified length for the beams made using Type IL cement. It is hypothesized that the longer transfer length found in the beams made with Type IL

cement was due to the lower modulus of elasticity of the Type IL concrete compared with the Type I/II concrete.

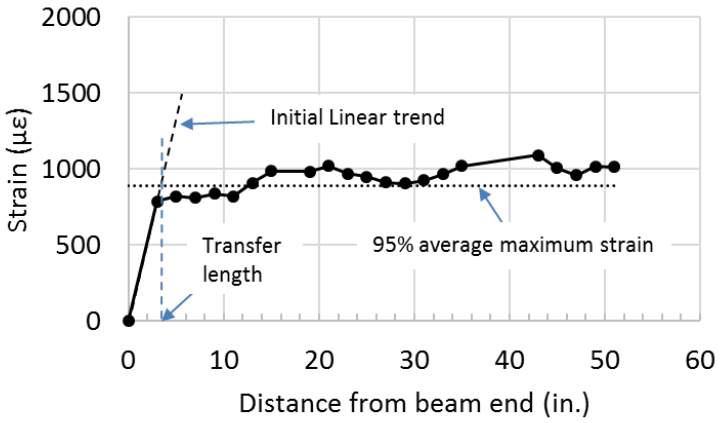

Figure 9.6: Determination of transfer length using Russell technique [65]

Table 9.1: Summary of transfer lengths of beams 1 to 4

Cement Type	Beam number	End of beam	Measured, L_t (in)	Average (in.)	AASHTO LRFD (in.)	ACI 318 (in.)	$\frac{\text{Measured } L_t}{\text{AASHTO } L_t}$
I/II	B1	Jacking	4	4	30	29.5	13%
I/II	B1	Dead	4				
I/II	B2	Jacking	4	4	30	30.0	13%
I/II	B2	Dead	4				
IL	B3	Jacking	8	8	30	29.8	27%
IL	B3	Dead	8				
IL	B4	Jacking	3	6	30	29.7	20%
IL	B4	Dead	9				

9.4 Development length

Figure 9.7 shows the load-deflection curves collected from the eight development length tests. The results show similar behavior for the prestressed concrete beams made with Type I/II and Type IL cements. No strand slip was observed in any of the tests, which demonstrated that the development length was less than 45% of the value calculated using the AASHTO LRFD [49] equations. It should be noted that for the last test of the beam with Type I/II cement (load applied at 45% of L_d), the beam was intentionally loaded until the section collapsed, as shown in Figure 9.8. At collapse, the prestressing strands ruptured, and the maximum concrete compressive strain was 0.001.

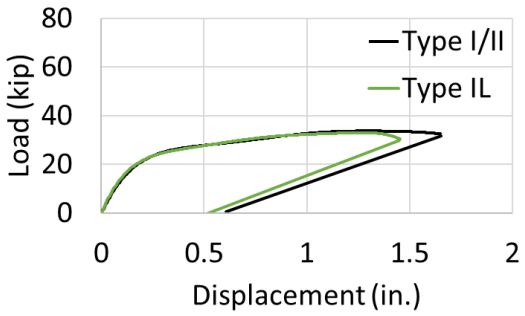

(a) Load applied at 90% of L_d

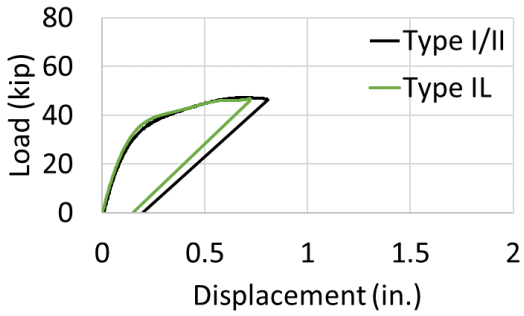

(b) Load applied at 65% of L_d

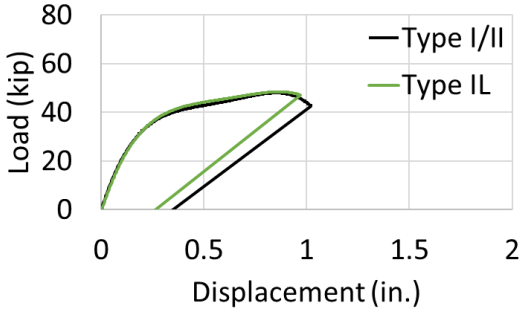

(c) Load applied at 50% of L_d

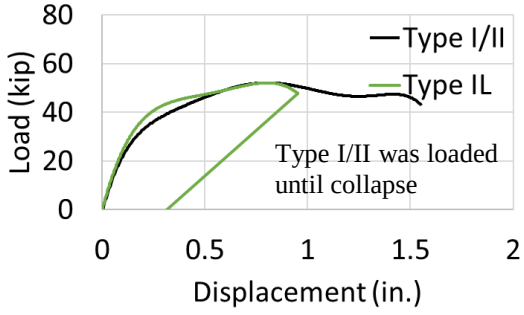

(d) Load applied at 45% of L_d

Figure 9.7: Load-deflection values of the development length tests

(a) Front view (b) Section view showing fractured strands

Figure 9.8: Collapse of Type I/II beam tested at 45% of L_d (53 in. from center of support) showing fractured strands

9.5 Flexural capacity

The experimental load-displacement results are shown in Figure 9.9. Beams made with Type I/II and those with Type IL cements behaved the same. The nominal ultimate moment capacity (M_n) of each beam was calculated using the rectangular stress block equations presented in AASHTO LRFD [49]. M_n was 2200 kip-in for all beams. The nominal computed flexural capacity was 8% lower than the maximum flexural moment

applied to the beams made with Type I/II cement as well as for beams made with Type IL cement.

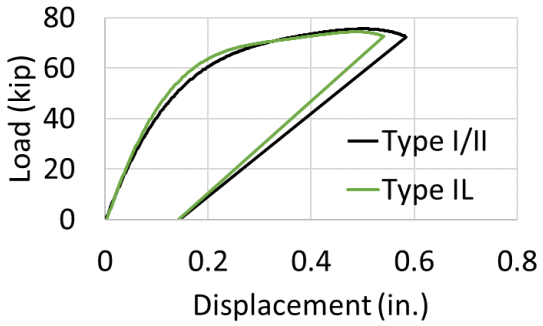

Figure 9.9: Average load-displacement results of the flexural tests

The points at which cracking occurred in the load-displacement curves were captured to calculate the measured cracking moment. Figure 9.10 shows a comparison of the measured cracking moment of the beams with made Type I/II cement and beams made with Type IL cement calculated from the flexural as well as the development length tests. The figure also shows the theoretical values calculated assuming a modulus of rupture equal to $0.2\sqrt{f'_c}$ (ksi) (approximately $6.3\sqrt{f'_c}$ (psi)) as per AASHTO [66]. The cracking-moment results show that Type I/II and Type IL cement resulted in similar behavior.

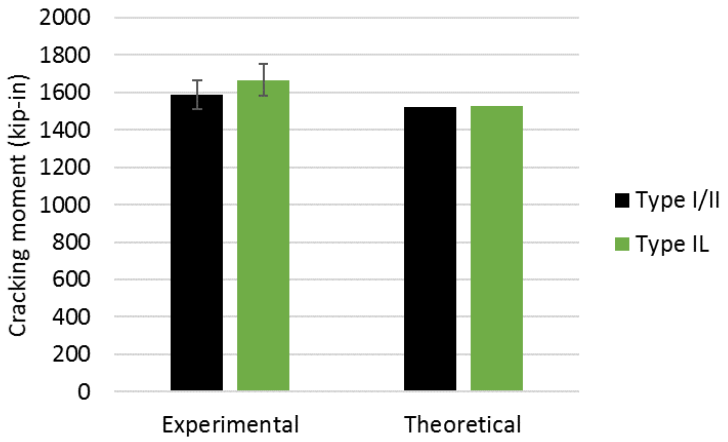

Figure 9.10:Cracking moment strength of beams made with Type I/II and Type IL cements

Figure 9.11 shows the load vs strain (measured at the level of the strand) curves collected from the eight development length tests. Strains were measured using dial gages attached to one side of the beam under point application of the load. The gauge length used was 23 in. Three gauges were attached for each test to measure the strain profile across the depth of the beam. The first gauge was attached at 1 in. from the top, the second at mid-depth, and the last at the level of the strand. The results show similar behavior for beams made with Type I/II and Type IL cements.

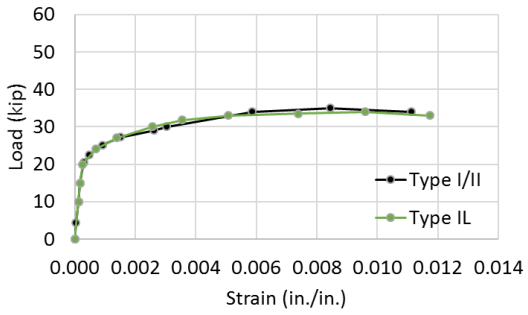

(a) 95% L_d test

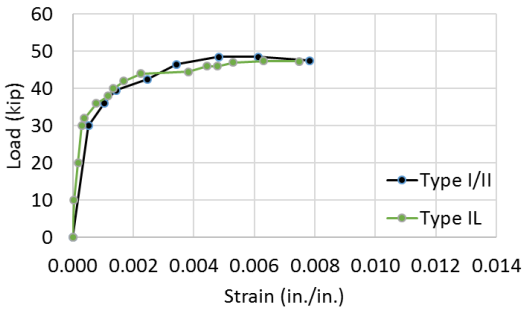

(b) 65% L_d test

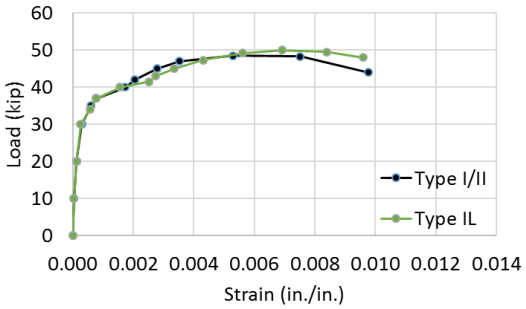

(c) 50% L_d test

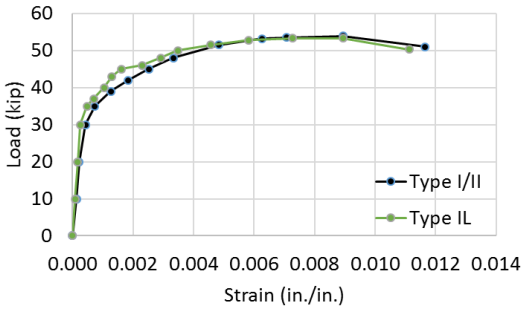

(d) 45% L_d test

Figure 9.11: Load vs strand-strain curves from the development length tests

The measured strains were also used to compute the curvature at each step of the load. Figure 9.12 shows the moment-curvature curves collected from the eight development length tests. The results show similar behavior for beams made with Type I/II and Type IL cements.

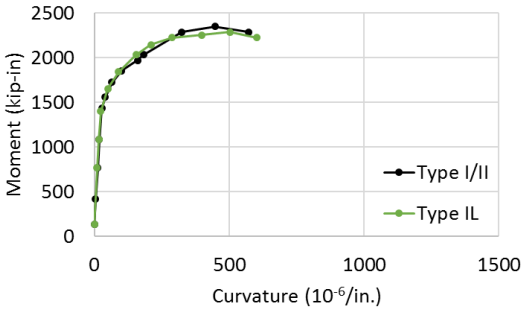

(a) 95% L_d test

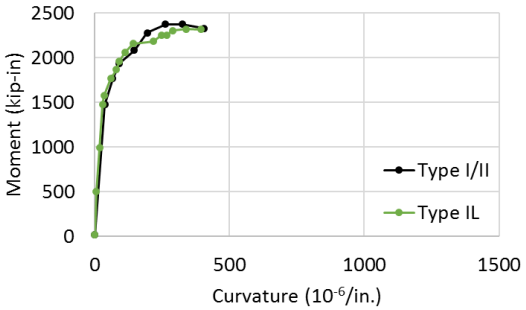

(b) 65% L_d test

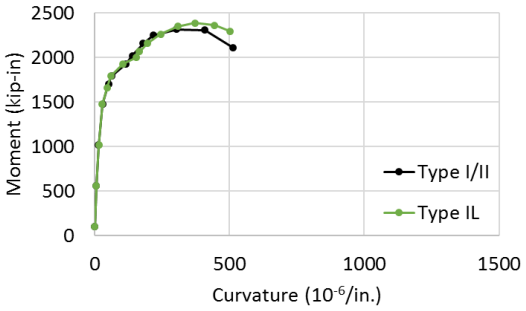

(c) 50% L_d test

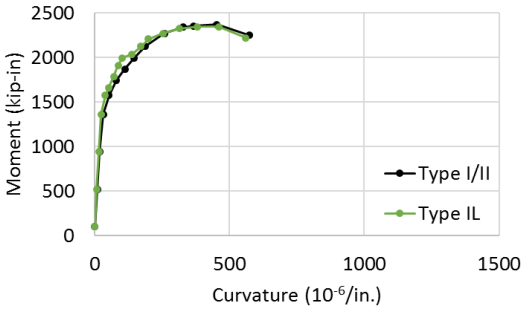

(d) 45% L_d test

Figure 9.12: Moment-curvature curves from the development length tests

9.6 Shear capacity

Loads were applied near the end of the beam to reduce the span-to-depth ratio and induce a shear failure. However, even with loads applied with distances as small as 45% of $L_{d,}$ which is equivalent to 2.24 of the beam depth, no shear failure was observed; the bond between the strands and concrete never failed. When one of the Type I/II beams tested at 45% of L_d was loaded until collapse, the failure was due to strand breaking as shown in Figure 9.8.

Therefore, actual shear capacity of the Type I/II and Type IL beams were never determined. Yet the maximum shear force in each beam, V_{exp}, was greater than the capacity calculated using AASHTO Equation 9.1 to Equation 9.5 given below. The experimental values are listed in Table 9.2and compared to the calculated capacities.

$$V_n = V_c + V_s \qquad \text{Equation 9.1}$$

$$V_c = min\begin{Bmatrix} V_{ci} \\ V_{cw} \end{Bmatrix}$$ Equation 9.2

$$V_{ci} = 0.02\sqrt{f'_c} \cdot b \cdot d_v + V_d + \frac{V_i M_{cre}}{M_{max}} \geq 0.06\sqrt{f'_c} \cdot b \cdot d_v$$ Equation 9.3

$$V_{cw} = \left(0.06\sqrt{f'_c} + 0.30 f_{pc}\right) b \cdot d_v$$ Equation 9.4

$$V_s = \frac{A_v f_y d_v}{s}$$ Equation 9.5

where:

b: Section width (in.)

V_d: Shear force at section due to unfactored dead load (kip)

V_i: Shear force at section due to externally applied loads occurring simultaneously with M_{max} (kip)

M_{cre}: Moment causing flexural cracking at section due to externally applied loads (kip-in).

M_{max}: Maximum moment at section due to externally applied loads (kip-in).

A_v: Area of shear reinforcement within a distance s (in2)

f_y: Specified minimum yield strength of reinforcing bars (ksi)

d_v: Effective shear depth (in.)

s: Spacing of transverse reinforcement measured in a direction parallel to the longitudinal reinforcement (in.)

Table 9.2: Maximum experimental shear load for beams made with Type I/II cement or Type IL cement compared to AASHTO theoretical capacity (kips)

Type I/II concrete	Type IL concrete	AASHTO
44.9	44.6	74.8

9.7 Chapter discussion and conclusions

Two 30-ft long precast pretensioned concrete beams were made using type IL cement from plant C and two were made using Type I/II cement from plant C. Both were reinforced with ½-in. diameter grade 270 low relaxation prestressing strand and were stressed identically. Tests examined strand bond, prestress losses, transfer and development length of the strand, and flexural strength. The following conclusions were made based on the performance of these prestressed concrete beams.

The bond capacity of the ½-in. strand found using Mostafa direct pull-out test [48] showed no difference in performance between Type IL and Type I/II cement. No strand slip was observed in any of the pull-out tests; yielding was developed in all strands.

The average total prestress losses found in beams made with Type IL cement was about 2% less than the average total loss found in beams made with Type I/II cement –

essentially no difference. These losses were about 5% less than those predicted using the "refined method" given in the AASHTO LRFD Bridge Design Specifications [49]. When looking at breakdown of prestress losses, concrete made with Type I/II cement showed lower elastic shortening losses and higher time-dependent losses than concrete made with Type IL cement.

Transfer length of the ½-in. diameter strands in the beams made with Type IL cement was less than 30% of the transfer length specified in AASHTO LRFD [49]. Development length of those strands was less than 45% of the development length specified in AASHTO LRFD [49], and was less than 71% of the development length specified in ACI 318 [54]

The flexural moment capacity of the prestressed concrete beams was about 5% greater than the nominal moment capacity calculated based on AASHTO LRFD [49]. AASHTO specifications provide a conservative flexural capacity for precast prestressed beams made using Type IL cements satisfying AASHTO M 240 [67] specifications.

CHAPTER 10: CONCLUSIONS AND RECOMMENDATIONS

10.1 Conclusions

The main objective of this research was to examine the performance of limestone-blended portland cement (Type IL) for structural applications and compare its performance to that of ordinary portland cement (Type I/II). As mentioned in Chapter 1, the specific objectives were:

1. Compare Type IL cements from several regional producers in terms of the particle size analysis and chemical composition.
2. Examine the effect of the limestone content and fineness on properties such as setting time, concrete mechanical properties, and dimensional stability.
3. Examine the effect of temperature on properties such as hydration kinetics, setting time, concrete mechanical properties, and dimensional stability when using Type IL cement.
4. Examine the effect of water/binder ratio and cement factor on concrete mechanical and durability properties when using Type IL cement.
5. Examine the effect of combining Type IL cement with supplementary cementitious materials such as fly ash (15% replacement) and slag (50% replacement) on properties such as hydration kinetics, setting time, concrete mechanical properties, and dimensional stability.
6. Assess and compare the structural properties of concrete made with Type IL cement to concrete made with Type I/II cement.

Cement characterization of samples obtained from five regional producers showed a variation in cement chemical phases as well fineness. The results showed that limestone content as well as cement fineness had significant effects on key properties such as hydration kinetics, setting time, mechanical properties, and dimensional stability.

Finer Type IL cements showed faster hydration and similar cumulative heat of hydration to Type I/II cements while coarser Type IL cements showed delayed heat peaks and lower cumulative heat of hydration than Type I/II cements. At 73 °F, finer Type IL cement showed higher cumulative heat of hydration than that of Type I/II cement and coarser Type IL cement showed similar cumulative heat of hydration to that of Type I/II cement. A different trend was observed at 140 °F: Finer Type IL showed similar cumulative heat of hydration as that of Type I/II and coarser Type IL showed a lower cumulative heat of hydration than Type I/II. This indicated that the dilution effect was exacerbated at higher temperature while the nucleation effect diminished.

For setting time, higher content of calcite reduced the setting time for Type IL cement at 40 ºF, 73 ºF, and 90 ºF. For Type I/II cement, higher calcite content increased the setting time at 40 ºF and 90 ºF. Larger particle size increased the setting time for Type IL cement. The same conclusion could not be made for Type I/II due to the lack of variation of mean particle size of the Type I/II samples. Finally, it was observed that higher C_3A content increased the setting time of Type IL cement at 40 ºF and 90 ºF, while higher C_3A content decreased the setting time at 73 °F; suggesting an interaction of limestone with C_3A at 40 ºF and 90 ºF.

The effect of *w/b* and cement factor in concrete on the mechanical properties of concrete was investigated. For the compressive strength, it was found that as the calcite content increased from about 4% to 12%, the greater the compressive strength. Also, it was found that higher fineness of Type IL cement led to greater strength. The effect of Type IL cement on the strength varied in concretes with different *w/b* ratios and cement factors (termed Classes A, AA, and AAA in this thesis).

The higher the concrete class (i.e., higher cement factor and lower *w/b* ratio), the greater the effect of Type IL cement on the strength. For class A concrete (higher *w/b* and lower cement factor), no statistically significant differences were found between use of Type I/II and Type IL cements. Also, for class A concrete, the difference in strength among cement producers was not statistically significant.

For class AA concrete (moderate *w/b* ratio and cement factor), the difference in strength of fine-grade Type IL cement and Type I/II cement was significant, while the difference in strength between coarse-grade Type IL cement and Type I/II was not significant. Also, for class AA concrete, the difference in strength among cement producers was statistically significant.

For class AAA concrete (lower *w/b* and higher cement factor), the effect of Type IL cement was more significant than the other two classes. Type IL cement led to lower strength (when having similar fineness to Type I/II). Higher fineness of Type IL cement increased the strength and resulted in statistically insignificant differences with Type I/II

cement. For the elastic modulus and splitting tensile strength, the results in general followed similar trends to those of the compressive strength.

One significant observation was that the effect of nucleation was more dominant for class A (lower cement factor and higher *w/b* ratio) while the dilution effect was more dominant for class AAA concrete (higher cement factor and lower *w/b*). Another observation was that in several cases the results showed that the source of the Type IL cement had a more significant effect on mechanical properties than the type of cement.

Regarding the effect concrete class on drying shrinkage, it was found that the higher calcite content, the greater the drying shrinkage. Also, the higher fineness of Type IL cement led to higher shrinkage for moderate *w/b* and cement factor. At early age, Type I/II and Type IL cements showed conflicting relationships with the average particle size where finer Type I/II cements resulted in lower shrinkage while finer Type IL cements showed higher shrinkage values. The effect of Type IL cement on the drying shrinkage varied in different concrete classes. Type IL cement in class AAA concrete showed lower shrinkage than Type IL in class AA concrete. For class A concrete (i.e. higher *w/b*), no statistically significant differences in shrinkage were found between Type I/II and Type IL cement at 7 days. However, finer limestone cement (AL) decreased the long-term drying shrinkage of this class A concrete.

For class AAA concrete (i.e. lower *w/b*), no statistically significant differences in drying shrinkage were found between Type I/II and Type IL cement at 1 year. However,

finer limestone cement decreased the early age drying shrinkage of this class AAA concrete.

When used with supplementary cementitious materials (SCMs), higher calcite content (greater amount of limestone) resulted in higher compressive strength for the fly ash Class C and Class F mixes but lower compressive strength for the slag mixes. This indicated that 15% fly ash mixes are more suitable SCM to be blended with Type IL cements than 50% slag mixes. Also, experimental values of the modulus of elasticity and splitting tensile strength showed lower values than those computed using equations from ACI 363R-10 for both Type I/II and Type IL concretes [1].

The drying shrinkage results varied among the three SCMs investigated in this research. The Class F fly ash mixes showed similar results when using Type IL and Type I/II cements. The class C fly ash mixes showed that finer Type IL resulted in higher shrinkage than Type I/II, while use of coarser Type IL cement resulted in lower shrinkage than Type I/II mixtures. When compared to mixes without SCMs, the class F fly ash mixes showed similar or lower shrinkage than the base mixes without SCMs, while class C fly ash resulted in higher shrinkage than the base mixes. This indicated that Class F was better suited for lower early age shrinkage requirements.

Concrete cylinders were cured at the following temperatures for Class AA concretes: 40°F, 73°F, 90°F for Class AA concrete. Results showed that concretes with the finer Type IL cement are more sensitive to effects of higher curing temperature. When curing at 90 °F, the finer Type IL cement showed significant (30%) increase in

compressive strength development at early age as well as 1 year when compared with Type I/II cement. When curing at 40 °F, finer Type IL cement (AL) showed higher early strength but similar strength at later age. For coarser Type IL, curing at 90 °F showed similar concrete compressive strengths for concretes using Type I/II and Type IL cements. Curing at 40 °F showed higher early age compressive strength of coarser Type IL cement than Type I/II but similar strength at 1 year.

The use of Type I/II cement and Type IL cements were compared for use in prestressed precast concrete beams by constructing two 30-ft beams with each cement type. Each concrete was class AAA (high cement factor and low *w/b*, with compressive strengths of about 12.5 ksi for Type I/II beams and 11 ksi for Type IL beams at time of beam tests). Most important was the comparison of bond between the prestressing reinforcement and the concrete using the different cements. The bond capacity of the unstressed ½-in. strand found using Mostafa direct pull-out test [48] showed no difference in performance between concrete with Type IL and Type I/II cement. No strand slip was observed in any of the pull-out tests; yielding was developed in all strands.

For the prestressed beams, Type IL resulted in a slightly greater average total prestress losses (2%) than Type I/II; this difference was considered negligible. These losses were about 5% less than those predicted using the "refined method" given in the AASHTO LRFD Bridge Design Specifications [49]. When looking at breakdown of prestress losses, concrete made with Type I/II cement showed lower elastic shortening losses and greater time-dependent losses than concrete made with Type IL cement.

Regarding the transfer length, use of Type IL cement resulted in longer transfer length; yet, the experimental transfer lengths were less than 30% of the AASHTO LRFD specified length (60 d_s). It is hypothesized that the longer transfer length found in the beams made with Type IL cement was due to the lower modulus of elasticity of that concrete compared with the Type I/II concrete. Development length of those strands was less than 45% of the development length computed using AASHTO LRFD [49].

The flexural moment capacity of the prestressed concrete beams was about 5% greater than the nominal moment capacity calculated based on AASHTO LRFD [49]. AASHTO specifications provide a conservative flexural capacity for precast prestressed beams made using Type IL cements satisfying AASHTO M 240 [67] specifications.

Overall, concretes using Type IL cement performed the same as concretes using Type I/II concrete. AASHTO LRFD specifications [49]can be used for the structural design of prestressed concrete beams constructed using Type IL cements satisfying AASHTO M 240 [67] specifications.

10.2 Recommendations

The following recommendations are concluded based on the scope and results of this research:

- For applications where faster setting time and faster strength development are needed, finer Type IL cement is recommended. Also, higher calcite content (up to 15% as per this research) increased the rate of strength

development and decreased the setting time. However, the increased fineness may result in higher heat of hydration that could lead to cracking.

- Type IL cement with higher C_3A content resulted in slower setting time when conducted at 40 °F and at 90 °F. This requires further research.
- For applications where lower drying shrinkage is required, lower calcite content and lower fineness are recommended. Also, to reduce shrinkage when using Type IL, it was found that using a lower *w/b* and higher cement factor reduced drying shrinkage of concrete.
- When blended with supplementary cementitious materials, Type IL cement showed the better performance with 15% fly ash than 50% slag. Blending with class F fly ash showed the best performance.
- The equations in ACI363R-10 [1] overestimated the elastic modulus and splitting tensile strength values for concrete made with Type IL cement blended with SCMs. More research is needed to develop better regression models.
- Type IL cement showed higher early strength of concrete when cured at high and low temperatures.
- Type IL cement showed equivalent performance to Type I/II cement for structural applications. Type IL showed slightly higher prestress losses and transfer length than Type I/II cement which should be taken into account by the designer.

- Development length of the prestressing strands was less than 45% of the development length specified in AASHTO LRFD [49]. More research is needed to develop better regression models.

REFERENCES

1. ACI 363R-10, *Report on High-Strength Concrete*.

2. Bonavetti, V., et al., *Limestone filler cement in low w/c concrete: a rational use of energy.* Cement and Concrete Research, 2003. 33(6): p. 865-871.

3. Hawkins, P., P.D. Tennis, and R.J. Detwiler, *The use of limestone in Portland cement: a state-of-the-art review*. 2003: Portland Cement Association Skokie.

4. Hooton, R., M. Nokken, and M. Thomas, *Portland-limestone cement: state-of-the-art report and gap analysis for CSA A 3000.* Cement Association of Canada. University of Toronto, 2007.

5. Tennis, P.D., M.D.A. Thomas, and W.J. Weiss, *State-of-the-art report on use of limestone in cements at levels of up to 15%*. 2011, Portland Cement Association: Skokie, Illinois. p. 78.

6. European Standard EN 197-1, *Cement - Part 1: Composition, specifications, and conformity criteria for common cements*. 2011: European Committee for Standardization, Brussels, Belgium.

7. CSA Standard A3001, *Cementitious materials for use in concrete*. 2013, Canadian Standards Association: Mississauga, Ontario, Canada.

8. ASTM C150, *Standard Specification for Portland Cement*. 2004, ASTM International: West Conshohocken, PA.

9. AASHTO M85, *Standard Specification For Portland Cement*. 2009, American Association of State Highway and Transportation Officials.

10. ASTM C595, *Standard Specification for Blended Hydraulic Cements*. 2012, ASTM International: West Conshohocken, PA.

11. Boden, T.A., G. Marland, and R.J. Andres, *Global, regional, and national fossil fuel CO_2 emissions*. 2010, Carbon Dioxide Information Analysis Center, Oak Ridge National Laboratory, U.S. Department of Energy, Oak Ridge, Tenn., U.S.A.

12. Worrell, E., et al., *Carbon dioxide emissions from the global cement industry 1.* Annual Review of Energy and the Environment, 2001. 26(1): p. 303-329.

13. Kelly, T.D. and G.R. Matos, *Historical statistics for mineral and material commodities in the United States (2016 version).* 2016, U.S. Geological Survey Data Series 140.

14. Van Oss, H.G., *Background facts and issues concerning cement and cement data*. 2005.

15. Soroka, I. and N. Stern, *Calcareous fillers and the compressive strength of Portland cement.* Cement and Concrete Research, 1976. 6(3): p. 367-376.

16. Feldman, R., V.S. Ramachandran, and P.J. Sereda, *Influence of CaCO3 on the Hydration of 3CaO· Al2O3.* Journal of the American Ceramic Society, 1965. 48(1): p. 25-30.

17. Soroka, I. and N. Setter, *The effect of fillers on strength of cement mortars.* Cement and Concrete Research, 1977. **7**(4): p. 449-456.

18. Matschei, T., B. Lothenbach, and F.P. Glasser, *The role of calcium carbonate in cement hydration.* Cement and Concrete Research, 2007. 37(4): p. 551-558.

19. Lothenbach, B., et al., *Influence of limestone on the hydration of Portland cements.* Cement and Concrete Research, 2008. 38(6): p. 848-860.

20. Ramachandran, V.S., *Thermal analyses of cement components hydrated in the presence of calcium carbonate.* Thermochimica Acta, 1988. 127: p. 385-394.

21. Kakali, G., et al., *Hydration products of C 3 A, C 3 S and Portland cement in the presence of CaCO 3.* Cement and Concrete Research, 2000. 30(7): p. 1073-1077.

22. Tsivilis, S., et al., *A study on the parameters affecting the properties of Portland limestone cements.* Cement and Concrete Composites, 1999. 21(2): p. 107-116.

23. Nocuń-Wczelik, W., B. Trybalska, and E. Żugaj, *Application of calorimetry as a main tool in evaluation of the effect of carbonate additives on cement hydration.* Journal of Thermal Analysis and Calorimetry, 2013. 113(1): p. 351-356.

24. Dhir, R., et al., *Evaluation of Portland limestone cements for use in concrete construction.* Materials and Structures, 2007. 40(5): p. 459-473.

25. El-Didamony, H., et al., *Limestone as a retarder and filler in limestone blended cement.* Ceramics, 1995. 39(1): p. 15-19.

26. Al-Khaiat, H. and M.N. Haque, *Effect of initial curing on early strength and physical properties of a lightweight concrete.* Cement and Concrete Research, 1998. 28(6): p. 859-866.

27. D.P. Bentz, E.F.I.B.E.B. and W.J. Weiss, *Limestone Fillers Conserve Cement; Part 2: Durability issues and the effects of limestone fineness on mixtures.* Concrete International. 31(12).

28. Alunno-Rosetti, V. and F. Curcio. *A contribution to the knowledge of the properties of portland-limestone cement concretes, with respect to the requirements of european and Italian*. in *Proceedings of the 10th International Congress on the Chemistry of Cement*. 1997.

29. Detwiler, R.J., *Properties of Concretes made with Fly Ash and Cements Containing Limestone*. 1996: Portland Cement Association.

30. ASTM C157, *Standard Test Method for Length Change of Hardened Hydraulic-Cement Mortar and Concrete*. 2014: Pennsylvania, UnitedStates.

31. Gonzalez, M. and E. Irassar, *Effect of limestone filler on the sulfate resistance of low C 3 A Portland cement.* Cement and Concrete Research, 1998. 28(11): p. 1655-1667.

32. ASTM C1012, *Standard Test Method for Length Change of Hydraulic-Cement Mortars Exposed to a Sulfate Solution*. 2015, ASTM International.

33. Batic, O., et al., *Rebar corrosion in mortars with high limestone filler content.* Anti-Corrosion Methods and Materials, 2013. 60(1): p. 3-13.

34. ASTM C33, *Standard Specification for Concrete Aggregates*. 2016, ASTM International.

35. Georgia Department of Transportation, *Standard Specifications for Construction of Transportation Systems, Section 500 - Concrete Structures*. 2015, Georgia Department of Transportation.

36. ASTM C192, *Standard Practice for Making and Curing Concrete Test Specimens in the Laboratory*. 2016, ASTM International.

37. ASTM C618, *Standard Specification for Coal Fly Ash and Raw or Calcined Natural Pozzolan for Use in Concrete*. 2015, ASTM International: West Conshohocken, PA.

38. AlabamaDOT, *Standard Specifications for Highway Construction - Section 501*. 2012.

39. ASTM C191, *Standard Test Methods for Time of Setting of Hydraulic Cement by Vicat Needle*. 2013, ASTM International: West Conshohocken, PA.

40. Georgia Department of Transportation, *Standard Specifications for Construction of Transportation Systems, Section 500 Concrete Structures*. 2015: Georgia Department of Transportation.

41. ASTM C39, *Standard Test Method for Compressive Strength of Cylindrical Concrete Specimens*. 2016, ASTM International, West Conshohocken, PA.

42. AASHTO T 22, *Compressive Strength of Cylindrical Concrete Specimens*, in *Standard Specifications for Transportation Materials and Methods of Sampling and Testing and AASHTO Provisional Standards*. 2016, American Association of State Highway and Transportation Officials.

43. ASTM C469, *Standard Test Method for Static Modulus of Elasticity and Poisson’s Ratio of Concrete in Compression*. 2014, ASTM International.

44. ASTM C496, *Standard Test Method for Splitting Tensile Strength of Cylindrical Concrete Specimens*. 2011, ASTM International.

45. AASHTO T 198-15, *Splitting Tensile Strength of Cylindrical Concrete Specimens*, in *Standard Specifications for Transportation Materials and Methods of Sampling and Testing and AASHTO Provisional Standards*. 2016, American Association of State Highway and Transportation Officials (AASHTO).

46. AASHTO T 160, *Length Change of Hardened Hydraulic Cement Mortar and Concrete*, in *Standard Specifications for Transportation Materials and Methods of Sampling and Testing and AASHTO Provisional Standards*. 2016, American Association of State Highway and Transportation Officials (AASHTO).

47. ASTM C512, *Standard Test Method for Creep of Concrete in Compression*. 2015, ASTM International.

48. Logan, D.R., *Acceptance criteria for bond quality of strand for pretensioned prestressed concrete applications.* PCI journal, 1997. 42(2): p. 52-90.

49. AASHTO, *LRFD Bridge Design Specifications*. 2016, American Association of State Highway and Transportation Officials: Washington, D.C.

50. Kurtis, K., et al., *Assessment of limestone blended cements for transportation applications*, Georgia Department of Transportation, 2017. Report Number: FHWA-GA-17-13-09

51. Mehta, P.K. and P.J.M. Monteiro, *Concrete: Microstructure, Properties, and Materials*. 2013: McGraw-Hill Education.

52. Cornell, J. and R. Berger, *Factors that influence the value of the coefficient of determination in simple linear and nonlinear regression models.* Phytopathology, 1987. **77**(1): p. 63-70.

53. Hooton, R.D., *Effects of carbonate additions on heat of hydration and sulfate resistance of Portland cements*, in *Carbonate additions to cement*. 1990, ASTM International.

54. ACI 318, *Building Code Requirements for Structural Concrete* 2014, American Concrete Institute.

55. Carrasquillo, R.L., *Microcracking and engineering properties of high-strength concrete.* 1980.

56. Adams, L.D. and R.M. Race, *Effect of limestone additions upon drying shrinkage of Portland cement mortar*, in *Carbonate additions to cement*. 1990, ASTM International.

57. Tsivilis, S., et al., *Properties and behavior of limestone cement concrete and mortar.* Cement and Concrete Research, 2000. 30(10): p. 1679-1683.

58. Vuk, T., et al., *The effects of limestone addition, clinker type and fineness on properties of Portland cement.* Cement and concrete Research, 2001. 31(1): p. 135-139.

59. FHWA, *Section 718- 47 High Performance Concrete For Precast And Prestressed Bridge Elements*. https://www.fhwa.dot.gov/resourcecenter/teams/structures/hpm_3.cfm.

60. Higginson, E., *The effect of cement fineness on concrete*, in *Fineness of Cement*. 1970, ASTM International.

61. De Weerdt, K., et al., *Hydration mechanisms of ternary Portland cements containing limestone powder and fly ash.* Cement and Concrete Research, 2011. **41**(3): p. 279-291.

62. Gebler, S.H. and P. Klieger, *Effect of fly ash on physical properties of concrete.* Special Publication, 1986. 91: p. 1-50.

63. Menendez, G., V. Bonavetti, and E.F. Irassar, *Strength development of ternary blended cement with limestone filler and blast-furnace slag.* Cement & Concrete Composites, 2003. 25(1): p. 61-67.

64. Nawy, E.G., *Prestressed Concrete: A Fundamental Approach*. 2010: Prentice Hall.

65. Russell, B.W., *Design guidelines for transfer, development and debonding of large diameter seven wire strands in pretensioned concrete girders*. 1992, University of Texas at Austin.

66. AASHTO, *LRFD Bridge Design Specifications*. 2012, American Association of State Highway and Transportation Officials: Washington, D.C.

67. AASHTO M240, *Standard Specification For Blended Hydraulic Ccement*. 2015.